Diagnosis of the Failure of Ultrafiltration Membranes Used in the Dairy Industry

A thesis submitted in fulfilment of the requirements

for the degree of Doctor of Philosophy

in Chemical and Process Engineering

at the University of Canterbury

Kuldeep Yadav

May 2009

“When I asked God for strength
he gave me difficult situations to face

when I asked God for brain & brown
he gave me puzzles in life to solve

when I asked God for happiness
he showed me some unhappy people

when I asked God for wealth
he showed me how to work hard

when I asked God for favours
he showed me opportunities to work hard

when I asked God for peace
he showed me how to help others

God gave me nothing I wanted
he gave me everything I needed.”

- Swami Vivekananda

Summary

The long term degradation of polyethersulfone (PES) based ultrafiltration membranes used in the dairy industry has been investigated. The main aim of the study was to identify characterisation techniques which could give an indication of the condition and performance of ultrafiltration membranes after long term exposure to sodium hypochlorite solution. Membranes were degraded using sodium hypochlorite solution at pH 9, 10, 11 and 12, and with 5000 ppm-days to 25,000 ppm-days of exposure at 55°C. The degraded membranes were studied using the following characterisation techniques: dynamic mechanical analysis (DMA), thermogravimetric analysis (TGA), tensile testing, field emission scanning electron microscopy with energy dispersive x-ray spectroscopy (FESEM-EDS), Fourier transform infrared-attenuated total reflectance spectroscopy (FTIR-ATR), contact angle, drop absorption, zeta potential, liquid-liquid displacement porosimetery (LLDP), protein separation, and colour measurement. The protein separation test included membrane throughput measurements (using casein-whey as feed), with size exclusion chromatography and gel electrophoresis to analyse the feed, permeate and retentate. Also a membrane disinfection experiment was performed to study the effect of sodium hypochlorite pH on disinfection of mixed dairy culture.

DMA, TGA and tensile testing showed that the membrane degradation reaction is a surface reaction with very little effect on bulk properties of the membrane, though TGA indicated a possible decrease in molecular mass of PES with degradation. FESEM imaging showed pit formation and surface cracking on the PES layer with hypochlorite degradation of membrane. The pit formation was only noticed in pH 9 and 10 hypochlorite degradation but FTIR-ATR analysis confirmed that the PES surface was affected at all the four hypochlorite pH values used. Both FESEM and FTIR-ATR indicated that the degradation increased with decrease in hypochlorite pH and increase in exposure time. A new peak formed at 1034 cm^{-1} was identified in the FTIR-ATR spectra of all the hypochlorite degraded membranes. EDS analysis indicated the presence of chlorine on the surface of membrane without any traces of sodium. Contact

angle, liquid absorption, and water-alcohol-water flux tests indicated that the liquid-PES surface interactions changed with degradation. An increase in fouling of the degraded membranes was found in the membrane throughput test. UV absorption (permeate stream), SEC chromatography and gel electrophoresis confirmed α-lactalbumin and β-lactoglobulin protein leakage through the hypochlorite degraded membrane. The amount of leakage increased with decrease in hypochlorite pH and increase in exposure time.

It is proposed that the hypochlorite degradation occurred with a chain scission of the PES polymeric backbone at phenyl-SO_2 linkage leading to formation of two parts with one end terminating with sulfonic acid and other end terminates with phenyl chloride group. The chain scission leads to surface roughness, pitting and changes in the surface-liquid interaction, all of which caused the results obtained. The membrane disinfection test showed equal reduction in microbial load at all the hypochlorite pH values. Further studies are necessary to fully understand the role of hypochlorite pH in disinfection.

This research has used a wide range of techniques to gain a full understanding of the mechanisms of PES degradation by sodium hypochlorite solution. Accordingly, characterisation regimes for autopsy analysis and in-line monitoring of membrane condition are proposed with an aim of efficient judging of the degradation condition of membrane.

Acknowledgements

I would like to express my sincere thanks to my supervisor, Associate Professor Ken Morison, for his vision and support throughout this research work. His support and guidance helped to shape me into an independent thinker and researcher. I also thank him for his patience during thesis editing especially with my Indian English. Working under his supervision was a learning experience with excitement and fun.

I would also like to thank my co-supervisor, Dr. Mark P. Staiger, for his enthusiasm, support, and guidance throughout this research. His level of energy always surprised me.

The financial assistance from Fonterra Co-operative Group Ltd. is gratefully acknowledged; without it I would never have been here. Thanks to Mike Toplis for showing his support to this research. Thanks also to Terry Killoran for his useful inputs throughout the project.

I would like to acknowledge the CAPE technical staff of Leigh Richardson, Bob Gordon, Rayleen Fredericks-Short, Peter Jones, Tony Allen and Trevor Berry. Thanks to Clyde McCready, for his support during fabrication of LLDP equipment. I thank them all for always listening to me whenever I rushed to them with a problem.

I would like to acknowledge my friends in CAPE who were always willing to have a cup of tea with me. I would also like to thank my family and friends for their support.

Finally, I would like to thank Almighty for giving me opportunity, challenges and strength to be a human.

Table of Contents

APPENDICES

Nomenclature

Abbreviations

Abbreviation	Explanation
AFM	Atomic force microscopy
APC	Aerobic plate count
CV	Column volume
DF	Diafiltration
DMA	Dynamic mechanical analysis
DMF	di-methyl-formamide
ED	Electrodialysis
EDS	Energy dispersive x-ray spectroscopy
EDTA	Ethylenediamine tetraacetic acid
FESEM	Field emission scanning electron microscopy
FTIR-ATR	Fourier transformed infrared attenuated total reflectance spectroscopy
GMP	Glyco-macro-peptides
GPC	Gel permeation chromatography
HPLC	High-performance liquid chromatography
IE	Ion exchange
IPN	Interpenetrating polymer network
LLDP	Liquid-liquid porosimetery
MF	Microfiltration
MMV	Maubois, Mocquot and Vassal cheese making process
MOPS	3-(n-morpholino) propanesulfonic acid
MWCO	Molecular weight cut off
NF	Nanofiltration
NMP	n-methyl-2-pyrrolidone
PAN	Poly acrylonitirile
PEG	Poly ethylene glycol
PES	Polyethersulfone
Pluronic®	Poly(ethylene oxide)-*b*-poly(propylene oxide)-*b*-poly(ethylene oxide)

PSU	Polysulfone
PVP	Poly vinyl pyrrolidone
RO	Reverse osmosis
RCF	Relative centrifugal force
SDS	Sodium dodecyl sulphate
SDS-PAGE	Sodium dodecyl sulphate-polyacrylamide gel electrophoresis
SEM	Scanning electron microscope
TGA	Thermal gravimetric analysis
TMP	Trans membrane pressure
UF	Ultrafiltration
UV	Ultra violet
WPC	Whey protein concentrate
WPI	Whey protein isolates
XPS	X ray photoelectron spectroscopy

Symbols

Symbol	Explanation
$+\Delta L$	Sample is lighter than the control sample
$+\Delta a$	Sample is redder than the control sample
$+\Delta b$	Sample is yellower than the control sample
$-\Delta a$	Sample is greener than the control sample
$-\Delta b$	Sample is bluer than the control sample
$-\Delta L$	Sample is darker than the control sample
A	Cross section area of sample
B	Desired whole radius, mm
b	Sample geometry term
D	O-ring groove depth, mm
E	Efficiency of joint
E'	Storage modulus
E''	Loss modulus
E_{ab}	Total change in sample colour as compared to the control sample
f_o	Force applied at the peak of sine wave
G_d	O-ring Groove diameter, mm
$ID_{o\text{-}ring}$	Internal diameter of O-ring, mm
k	Sample displacement at the peak of sine wave
K_L	Conductivity of the dispersion medium
L	Length of sample
P	Pressure
Q	Internal pressure, Pa
R	Radius
S	Maximum allowable stress, Pa
t	Desired plate/shell thickness, mm
$tan\delta$	Loss factor
T_g	Glass transition temperature, °C
T_{onset}	Weight loss onset temperature in TGA experiment, °C
V_S	Streaming potential
W	O-ring groove width, mm
x	Constant related to the surface tensions of foulants

y	Constant are related to the surface tensions of water
ΔG_f	Total free energy change
Δp	Applied pressure difference
γ_S^d	Surface energy arising from non-polar dispersion
v	Poison ratio
δ	Phase angle, °
ε	Strain
ε^*	Complex strain
ε'	In phase strain
ε''	Out of phase strain
ε_o	Strain at maximum stress
ζ	Zeta potential
η	Dynamic viscosity of dispersion medium
σ_b	Maximum bending stress, Pa
σ_m	Maximum Allowable Stress for plates (below 38ºC), Pa
ψ	Relative permittivity of dispersion medium
ψ^o	Permittivity of Vacuum
ω	Frequency, Hz

Chapter 1 Introduction

1.1 Statement of Problem and Opportunities

Milk production in New Zealand has expanded steadily at a rate of 4% per annum since 1990 and is expected to reach a record 16.3 million tons in 2009 (New Zealand Dairy and Products Annual Dairy Industry Report, 2008). New Zealand is a major dairy exporter and accounts for a significant percentage of global trade in dairy products. Whole milk powder is the leading dairy export accounting for just over one-third of total exports followed by butter, cheese, and non fat dry milk. With exports revenue of $NZ 13.5 billion for the 2008-09 year (Annual Review 2008, Fonterra Co-operative Group Ltd) Fonterra is not only New Zealand biggest dairy company but also the biggest export earner. New Zealand accounts for about two percent of world dairy production but exports more than 95 percent of all its products making it the world's largest dairy product exporter.

Membrane technology is a well established separation technique in the New Zealand dairy industry. New Zealand, Australia and Europe are leading players in development and application of membrane technologies in the dairy industry (Siebert et al., 2001). Membrane processes are extensively used by the dairy industry for ultrafiltration and reverse osmosis of milk products to produce whey protein concentrate, and concentrated milk which is further utilised in cheese vat, ice cream, cultured dairy products and fluid milk protein fortification. Also dairy farmers in remote regions are using reverse osmosis to remove water from milk near the farms or at processing plants to reduce raw milk transportation costs.

Membranes technologies have brought about a significant change in the dairy industry and, with emerging markets for functional foods, membrane technology provides a capability of creating entirely new, more functional food products, for example, high-

protein low-lactose fluid milk, high-protein low-lactose ice cream, non fat yogurt, and high protein sports drink.

There is lot of research going on to develop new polymeric synthetic membranes. The choice of a given polymer as a membrane material is based on very specific properties, originating from structural factors and the final application of the membrane. Sulfone polymers, especially polyethersulfone (PES) and polysulfone (PSU), are very commonly used as membrane material for food and dairy processes. They have very good chemical, mechanical, thermal, and hydrolytic stability. Polysulfone is commonly used to form ultrafiltration and microfiltration membranes. They are also used to form the porous support/backing layer of many reverse osmosis membranes. Due to its wide range of acid and alkali tolerance, it is easy to clean polysulfone membranes or support layers.

Polyethersulfone is used as a membrane material for both ultrafiltration and microfiltration membranes. The ultrafiltration membranes used in the dairy industry generally have a PES barrier (filtration) layer on a non woven polyester fibre backing/ support. PES has very high thermal stability, with an upper operating temperature of 125 ºC. It is a stable polymer which can perform under a broad pH and temperature range which makes it possible to sterilize membranes in some applications by either steam or autoclaving. Polyethersulfone membranes are low protein binding membranes as compared to other commercial polymers, and give excellent flux rates with batch to batch and within batch consistency in performance. They are also compatible with a variety of sealing methods, and membrane regeneration can be accomplished by using sodium hydroxide even at elevated temperatures.

Although membranes show great potential for dairy usage, fouling problems limit their application. Fouling is caused by the deposition of suspended or dissolved solids on the external membrane surface, on the membrane pores, or within the membrane pores. Fouling results in a decrease in performance of a membrane, in term of membrane flux and may alter separation characteristics. Membrane fouling is removed to an extent by a multi-step cleaning regime followed by a sanitisation process to disinfect the membrane.

Cleaning and sanitisation are very important operations in the dairy industry and have to be performed regularly to maintain the desired separation qualities and hygiene of the membranes.

The cleaning chemicals generally used in the dairy industry are acid, alkali, detergents and sanitizers like sodium hypochlorite or hydrogen peroxide. There are many commercial premixed cleaning and sanitizing mixes available depending on the type of fouling to be removed and type of feed solution. Generally to maintain the high levels of hygiene strong disinfection regimes are followed which leads to a significant exposure of membrane surface to these potentially harsh chemicals.

The cleaning and disinfectant solutions employed to clean membranes, can also be responsible for changes in membrane properties which generally cause two type of failure. The functional properties of the membrane can gradually change which can be seen as an increase in pressure drop across the membrane, or a decrease in flux values, so the production can no longer meet requirements in terms of volume or quality. Secondly the membrane layer can crack causing a leak of the feed/retentate stream into the permeate stream and the required separation can no longer be maintained. In either case the plant has to be shut down for membrane replacement. Bégoin et al. (2006) studied the effects of cleaning solutions, i.e. nitric acid, sodium hydroxide solution, a formulated detergent Ultrasil 10, and sodium hypochlorite solution on PES ultrafiltration membranes. They found that the acid, base and detergents at the concentrations used in industry had no significant effect on membrane properties as compared to disinfectants like sodium hypochlorite. Bleach produced many cracks in the active layer and the membrane lost its separating properties. Rouaix et al. (2006) investigated the effect of disinfectants on physical properties of polysulfone membranes and concluded that chemical changes leading to defects are obscure and need further investigative research. The current life of an ultrafiltration membrane in industry is only 2-3 years depending on the severity of usage. The exact chemical mechanism of the disinfectant-polymer interaction and subsequent membrane failure is not, as yet, clearly understood.

1.2 Objectives and Outcomes

There is a substantial investment by the dairy industry in polysulfone and polyethersulfone membranes. A short operating life and frequent failure leads to direct expenditure in purchase and installation of new membranes. This effect is coupled by the fact that an ultrafiltration system has to be shut down during maintenance and installation, which can directly affect the production rate of the industry.

The main objective of this study was to improve the understanding of the effect of disinfectant chemicals especially sodium hypochlorite and consequently of the degradation mechanism of membranes. Various characterisation techniques available were studied and applied in an effort to indentify the techniques which could detect these chemical changes in the membrane and differentiate between degraded and non-degraded membranes. Also emphasis was given to the techniques which can be sensitive to the extent of the damage in terms of ppm-days of exposure to disinfectant solution and help in estimating the age of the membrane in terms of chemical exposure. Accordingly effort was made to propose a cleaning regime with an aim of extending the lifetime of the membranes. The proposed study may benefit the dairy industry in terms of increased membrane operating life. A new set of disinfection conditions based on this study may result in a decrease in membrane failure rates, which can lead to low installation and maintenance cost and less plant shutdowns. The overall result may be an increase in flexibility of the working systems with better profit for the industry.

The following points were within the scope of the study:

- An in depth study of various membrane characterisation techniques with an aim to detect and understand degradation of membranes.,
- The design and set up of experiments to chemically damage the membranes and characterize changes,
- The study of disinfectant and membrane interaction at various points of contact and measurement of changes in surface chemistry and morphology of the membrane,

- Determination of a characterisation regime that gives a good indication of membrane condition in terms of chemical degradation.

The following points were out of the scope of the study

- Fouling and fouling mechanisms,
- Effect of cleaning agents on fouling of membrane.

1.3 Outline of Thesis

Chapter 2 begins with a general literature review of membrane processes used in the dairy industry, cleaning and sanitisation of ultrafiltration membrane. This is followed by review of various properties of membranes which are helpful in monitoring cleaning of membranes. This chapter also includes a brief review of polysulfone family polymers which are common polymers used for making food and dairy grade membranes.

Chapter 3 starts with details of the various types of material sample tested. It is followed by a section on cleaning process used for virgin and sodium hypochlorite degraded membranes. It also includes the method followed for studying the stability of hypochlorite solutions at various pH conditions followed by the procedure applied for hypochlorite exposure and control. This chapter also includes a section on methods used for sample preparation and characterisation of bulk, surface and separation properties of new and hypochlorite degraded samples. This includes tensile testing, and thermo gravimetric analysis and dynamic mechanical analysis for measuring bulk properties mainly mechanical and thermal properties of membrane. Surface characterisation techniques includes field emission scanning electron microscopy (FESEM) coupled with energy dispersive X-ray spectroscopy or EDS, Fourier transform infrared - attenuated total reflectance (FTIR-ATR) spectroscopy, liquid-liquid displacement porosimetery (LLDP), surface zeta potential measurement, contact angle measurement, liquid absorption test. The section on LLDP also includes details of designing, fabrication and testing of in-house built LLDP equipment. Separation properties characterisation includes cross-flow flux measurement and protein separation test. The chapter ends with method

details of hypochlorite disinfection test on dairy microbial culture. The step by step procedures followed for various characterisation techniques are covered in Appendix 1.

Chapter 4 elaborates the main results and discusses the various characterisation techniques used to characterize bulk, surface and separation properties of new and hypochlorite degraded samples. A collection of extended results is presented in Appendix 2.

Chapter 5 discusses the relationship between various characterisation techniques and how they can be used together to give a better understanding of the chemical-polymer interactions and mechanisms of degradation during the hypochlorite treatment. It also includes the recommended characterisation regimes for failure/autopsy analysis and online determination of membrane condition in industry. Finally in Chapter 6, conclusions are drawn on effect of hypochlorite on ultrafiltration membranes. It also includes the future research work possible in continuation of this study.

Chapter 2 Review of Literature

Introduction

In general, membrane separation aims at partial separation of a feed containing a mixture of two or more components by use of a semi-permeable barrier (the membrane) through which one or more of the species are able to pass. The driving force for membrane separation process can be gradients in pressure, concentration, electrical potential or temperature. An overview of various membrane processes and driving forces is given in Table 2.1.

Table 2.1 Membrane processes and driving force (Mulder, 1997)

Driving Force	Membrane process
Pressure	Microfiltration, Ultrafiltration, Nanofiltration, Reverse osmosis, Piezodialysis, Gas separation Vapour permeation, Pervaporation
Electrical Potential	Electrodialysis, Membrane electrolysis
Concentration	Dialysis, Diffusion dialysis
Temperature/pressure	Thermo-osmosis, Membrane distillation

Membranes have many advantages in comparison to other separation techniques, which fall in two main categories (Ionics Inc, 2004)

(a) Improved production process, i.e.

- Consistent and high quality of permeate and retentate
- Reduced production costs
- Low energy costs
- Low maintenance
- Chemical and temperature resistance
- Long membrane operating life

(b) Recovery of valuable products that previously would have been lost to waste.

Membranes can usually handle a wide variety of feed liquids, which allows elimination of several steps in the process and hence, can reduce the total footprint of the plant and the consumption of chemicals. Membrane processes have a very low operating cost, which other conventional systems do not.

Some colloidal solids can permanently foul the membrane surface. Surface fouling is a major issue in dairy and food-based membrane separation system operation. Therefore cleaning and sanitization of membrane becomes a very important step in food and dairy processing to maintain required product flux, separation quality and a high level of hygiene. It is done by a multi-step cleaning regime followed by a sanitization process to disinfect the membrane. The use of harsh chemicals for cleaning and sanitization can contribute to long term degradation of membrane and ultimately leading to loss of mechanical integrity and membrane failure. Therefore immense care is taken while selecting a membrane system for a specific application.

2.1 History of Membrane Processes

In the early 20th century membranes were used mainly for studying barrier properties, diffusion studies and related phenomena. They were never considered as an industrial level separation technique due to its high cost, low reliability and unselective nature (Mulder, 1997). In early 1960, the development of the asymmetric cellulose acetate reverse osmosis membrane by Loeb and Sourirrajan (1963) led to a breakthrough in the industrial application of membranes. 1960 to 1980 was a period of considerable change in the development of the membrane technology as a commercially viable separation technique (Baker, 2004). New membrane modules to increase the membrane surface area , e.g., spiral wound, hollow fibre, and plate and frame, were developed which led to rapid commercialization of membrane processes. The research work by Henis and Tripodi (1981) led to the emergence of industrial membrane gas separation processes. By the end of the 20th century, advanced development of process specific ceramic membranes increased the scope of membrane applications in a wide variety of industry due to their incredible properties. Technological advances in the last 25 years have led to establishment of membrane technology as a major separation industry but there is also continuous need for improved membranes and new concepts

are regularly introduced to develop membranes with enhanced performance and prolonged operating life.

2.2 Membrane Processes

The key pressure driven membrane processes used in dairy industry (depending on size and nature of particle to be separated) are microfiltration (MF), ultrafiltration (UF), nanofiltration (NF) and reverse osmosis (RO).

Microfiltration is a low-pressure cross-flow membrane process for separating colloidal and suspended particles in the range of 0.1 to 5 microns (Cheryan, 1998). Reverse osmosis is generally viewed as a dewatering process as water is the only substance that permeates while the membrane retains almost all the dissolved solids (Dairy Management Inc, 2000). The method of dissolved salt removal is not just a physical process based on size difference as in MF but is mainly influenced by the osmotic pressure. Nanofiltration is applied in the area between the separation capabilities of reverse osmosis membranes and ultrafiltration membranes. NF separation is governed by mass transfer phenomena consisting of diffusion and flow through pores and involves the use of membranes that are tight enough to retain lactose (Rosenberg, 1995).

Ultrafiltration is a membrane separation process where the high molecular weight components, e.g., protein, and suspended solids are rejected. Low molecular weight components pass through the membrane freely. There is consequently very little rejection of mono- and disaccharides, salts, amino acids, organic and inorganic acids (Wagner, 2001). The UF membrane pore size spans from 1 nm to 0.1 μm (Zeman and Zydney, 1996). Osmotic effects in UF membranes are small and applied pressure of 1-10 bar is used mainly to overcome the viscous resistance of liquid permeation through the porous membrane structure. Commercial UF membranes are asymmetric, with a thin barrier layer of 0.1-1 μm thick exposed to feed side. The barrier layer is supported by a highly porous layer some 50-250 μm thick (Scott, 1995). The separation mechanism of UF membrane is mainly sieving where an increase in pressure increases the flux rates. The wide variety of applications of UF includes

- Treatment of water and effluents

- Clarifications of juices and wines
- Milk protein concentration and sterile filtration.

2.3 Membrane Elements

An important component of the separation system is the actual equipment, within which membrane is housed. The device is referred as a membrane element or module. The hydrodynamic conditions within an element depend on type of membrane as well as specific element design (Ghosh, 2003). An optimal element configuration should have the following characteristics (Wang et al., 2007)

- A high membrane area to module bulk volume ratio
- A high level of turbulence for efficient mass transfer and low accumulation of solids on the membrane surface
- Ease of cleaning
- A low energy expenditure per unit permeate volume.

The type of element is generally selected according to feed type and required production volume. The elements are based on either cylindrical or planar geometry and are constructed by potting or sealing the membrane material into a corresponding assembly. Commercial elements are designed for long term use over the course of a number of years. The four main types currently used in membrane processes are as follows:

2.3.1 Plate and Frame

These systems consist of membrane sandwiched between membrane support plates. The membrane, feed spacer and product spacer are layered together between the two end plates (Sutherland, 2008). The membranes in this module are easy to clean and replace but low membrane area per volume reduces its application in high pressure application.

2.3.2 Spiral-Wound

A variation of the basic plate and frame concept is the spiral-wound module which is widely used in RO, UF and gas separation. Its basic design is illustrated in Figure 2.1. A spiral-wound element contains one or more membrane envelopes each of which contains two membranes separated by a porous permeate spacer (Wagner, 2001). The permeate spacer allows a free flow of permeate out of the envelope. The membrane envelopes are separated with each other by a highly porous feed spacer, which provides uniform flow of feed and retentate across the membrane surface. The membrane envelope is glued on the three sides but is open at its fourth side where it is connected to a porous central tube that collects permeate. This module is wound into a spiral and placed in an outer cylindrical cell. A multi-envelope system not only increases the membrane area significantly but also minimize the pressure drop encountered by the permeate travelling towards the central pipe. In this module it is easy and inexpensive to adjust hydrodynamics by changing the feed spacer thickness to overcome fouling and concentration polarization. Bypassing of feed may occur due to non-uniform wrapping of the module spiral.

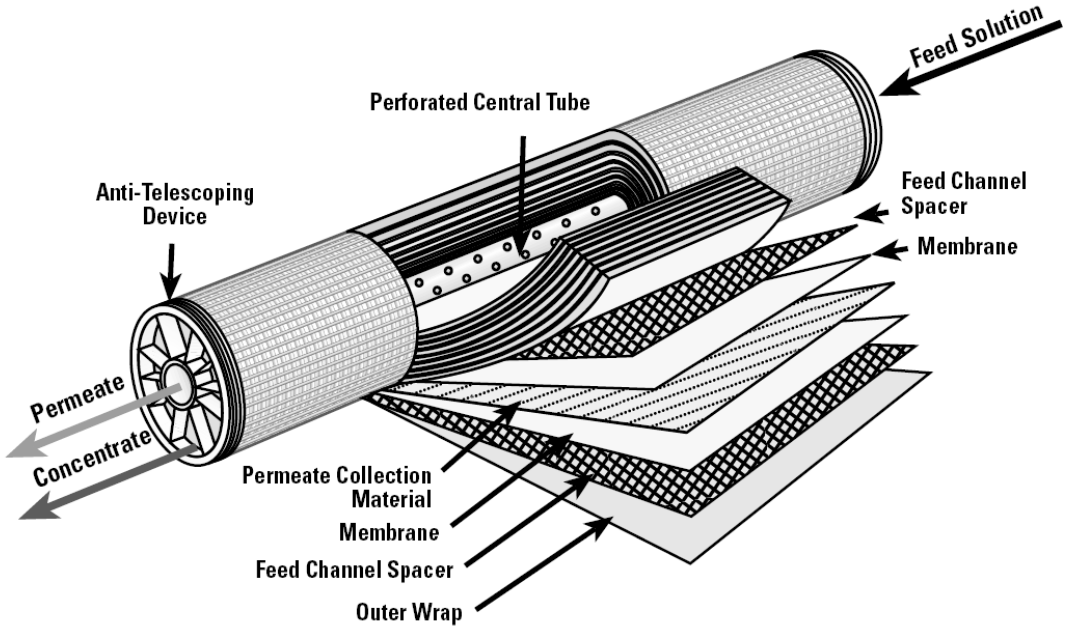

Figure 2.1 Basic design of spiral-wound module (Wagner, 2001)

2.3.2 Tubular

Tubular membranes have good fluid hydrodynamics and are quite resistant to fouling and can handle high amounts of suspended solids and even fibres. Polymeric tubular membranes are made by casting a membrane onto the inside of a pre-formed highly porous tube (Porter, 1990). Tubular membranes are also available with ceramic membranes. Ceramic membranes are corrosion resistant and have excellent high pressure and temperature. It allows a regular chemical washing of the membranes without losing their performance over several years (Scott, 1995).

2.3.4 Hollow Fibre

A hollow fibre membrane consists of a bundle of polymeric hollow fibres usually less than 1 mm in diameter and unlike other membrane systems does not have any support layer (Baker, 2004). Uniformity of fibre diameter and permeability is very important for consistent performance. Lemanski and Lipscomb (2000) showed that for a counter-current hollow fiber gas separator, a 10% variation in inner diameter of fibre can produce large variation in module performance.

2.4 Membrane Processes in the Dairy Industry

In the dairy industry, membrane separation is significantly associated with pressure driven separation techniques, i.e. MF, UF, NF and RO (Rosenberg, 1995). The dairy industry has benefitted enormously by recent advances in membrane technology. This can be demonstrated in processing of whey. Thirty years ago whey was seen as waste product from the cheese making process and had to be disposed of as effluent or used as animal feed. However, by using membrane processes, whey is being used to produce whey protein isolates that are used in health drinks and infant formulas.

Microfiltration is used for cheese whey clarification, reduction of microbial load from skim milk and whey and de-fatting whey intended for whey protein concentrate and protein fractionation. MF can also be used to produce a pasteurized milk beverage as shown in Figure 2.2. Ultrafiltration is ideal for fractionation of milk for cheese

production, i.e. the retentate contains proteins, fat and certain insoluble and bound salts, while permeate contains mainly lactose and soluble salts. Another application of UF is in speciality milk-based beverages, e.g., UF concentration of skimmed milk to produce a product that has a high calcium and protein content. Standardization of milk and milk products can be done using UF permeate (Puhan, 1991). UF is also used in production of whey protein concentrates and isolates which can be further used in health and sports drinks.

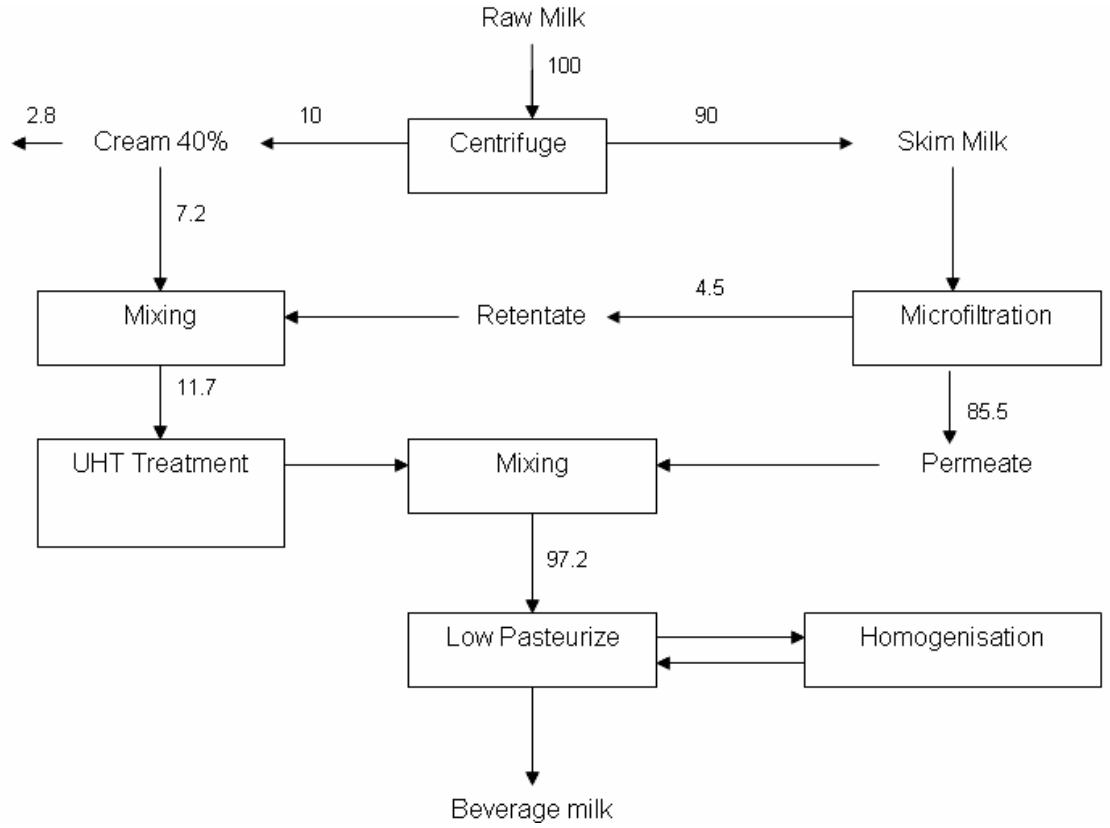

Figure 2.2 Manufacturing process for a pasteurized beverage milk using microfiltration (Walstra, 2006)

Nanofiltration is used for partial desalination as well as concentration of whey (van der Horst et al., 1995), which converts acid and salted whey into a valuable by-product which had become worthless due to addition of salts or acids during manufacturing of cheese. Reverse osmosis is used for concentration of milk (Zall, 1987b) and whey by removal of water. The application of membrane processes in the dairy industry can be classified into three main areas as described by Pouliot (2008) (Table 2.2)

Table 2.2 Membrane processes classification in dairy industry (Pouliot, 2008)

Classification	Application
Alternative to unit operations	Water removal (evaporation) Control over microbial load (sterilization) Fat removal (skimming)
Process enhancement	Removing casein micelles from milk Extracting whey proteins Separating proteins and peptides Recycling brine De-fatting whey
Creating new products	UF-cheese Extended shelf like milk Milk based beverages (UF permeates) Textured milk products Fermented milk

2.4.1 Application of Membranes in Cheese Production

MF is used is used as a pre-step in protein extraction processes for making micellar casein products and whey protein isolates. When skim milk is passed through a ZrO_2, TiO_2 ceramic MF membrane with a pore size of 0.1 μm a clear and sterile micro-filtrate similar to sweet whey is obtained (Daufin et al., 2001). The possibility of using UF to pre-concentrate milk before cheese making was very attractive in terms of total volume of milk handled and to solve the problem of large waste disposal. The first example of UF based cheese making process was MMV process, named after the developers Maubois, Mocquot and Vassal (Maubois et al., 1980). In this process the whole or skim milk is concentrated three to five fold to produce a pre-cheese concentrate with 20-30% solids, which can be directly used for cheese making. The process resulted in an increase in milk protein utilization which increased cheese production by 10%. This fact made the MMV process widely used for cheese making. The MMV process is more suited to soft cheese production (Camembert, Mozzarella and Feta) but cannot be used directly for hard cheeses (Cheddar and Swiss) for which a 25% protein level is required. Figure 2.3 shows the simplified flow diagram for traditional cheese making and MMV process. New advances in membrane technology have resulted into extensive application of membranes for various varieties of cheeses manufacturing with different technological variations (Henning et al., 2006).

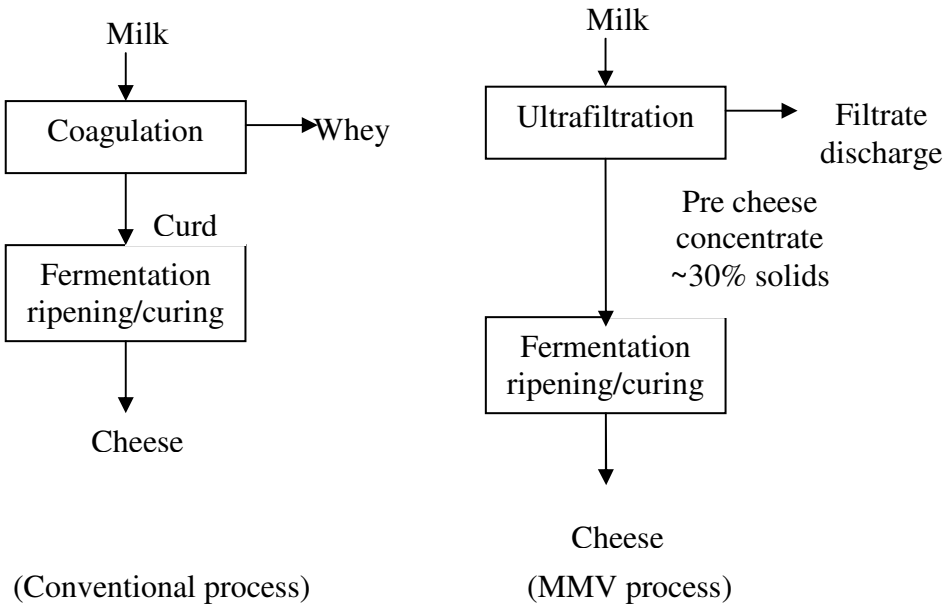

Figure 2.3 Flow schematic for traditional and MMV cheese making processes

2.4.2 Application of Membranes in Whey Processing

Due to advances in membrane technology, whey is now considered to be a nutritious protein source instead of a waste product from cheese manufacturing. Today whey protein concentrate production by ultrafiltration is well established in the dairy industry. Several technological advances and variation for concentrating whey and isolating serum proteins have been extensively studied (Mehra and Kelly, 2004; Zydney, 1998; Hobman, 1992). A typical process train for processing cheese whey is shown in Figure 2.4. The goal of the whey separation process is to separate the whey into three streams: whey protein concentrate (WPC), lactose concentrate and filtrate water. The most valuable of these is the WPC fraction depleted in salts and lactose. Whey has a high lactose concentration and low protein content, so before whey protein can be used as a concentrate, the protein concentration should be increased to a minimum of 60-70% on dry basis and the lactose content reduced by 95%.

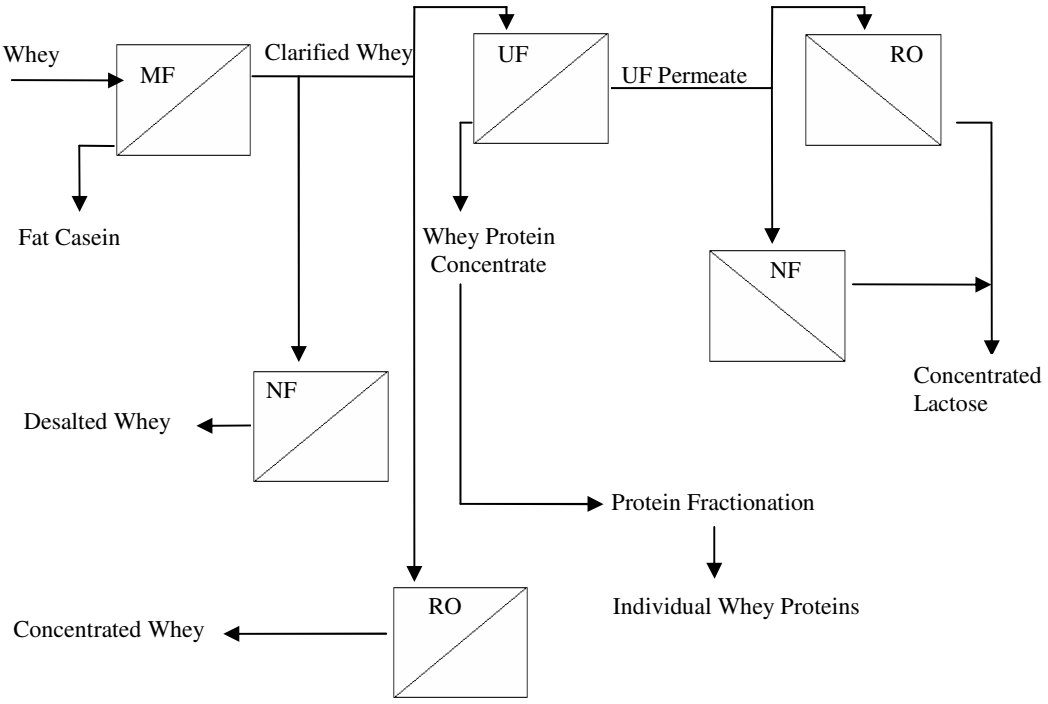

Figure 2.4 Membrane processing of cheese whey (adapted from Cheryan, 1998)

A high salt content of 8-20% dry basis in salt containing whey creates a number of processing problems like nutritional imbalance of salt in final protein concentrates which makes it inappropriate for various human and infant food products. It can also cause high fouling of UF and MF membrane used in processing of whey and slow lactose crystallization rate during lactose recovery. Desalting of whey with NF becomes a useful option to retain the product quality of the end products (Kelly et al., 1992).

2.4.3 Fractionation of Whey

WPC can further be fractionated into α-lactalbumin, and β-lactoglobulin and glyco-macro-peptides (GMP) that may have pharmaceutical value (Horton, 1998). Purified α–lactalbumin has important applications in advanced baby food formulae (Maubois and Oliver, 1992). Maillart and Ribadeau-Dumas suggested a process of fractionating whey proteins from whey protein isolate (WPI) by a UF process which yielded more than 83% of the β-lactoglobulin in the WPI. Tanimoto *et al.* (1990) suggested a process to prepare purified GMP, which exploits the tendency of GMP to exist as monomer at pH 3-4 and to go under aggregation at pH >4, with a combination of membrane separation techniques. Higher molecular whey proteins (immunoglobulin,

bovine serum albumin and lactoferrin) can be isolated from low molecular weight fractions (mainly α–lactalbumin and β-lactoglobulin) by using hydrophilic cellulose membrane (Mehra, and Donnely, 1993). Membrane processes are now acknowledged as a resourceful tool to separate minor compounds like bioactive peptides, growth factors etc. which can be used in development of new value added products. Membrane processes like UF, NF can be selectively used to fractionate peptide mixture and amino acids (Groleau et al., 2004). Application of membranes in extraction of growth factor from colostrum and milk is being actively studied and membranes have been successfully applied to recover growth factor from whey (Gauthier et al., 2006).

2.5 Cleaning and Disinfection of Membrane

2.5.1 Membrane Fouling

Membrane process systems are now an integral part of the dairy industry. These systems are operated in a series of stages with a step increase in concentration level at each stage. The pressure driven membrane processing of dairy fluids is accompanied by a decrease in flux due to fouling causing an increase in processing time. Initially a rapid fall in flux is observed, mainly due to concentration polarization. The retained solutes can accumulate at the membrane surface where their concentration will gradually increase. Such a concentration build-up will generate a diffusive flow back to the bulk of the feed, but after a given period of time steady-state condition will be established (Mulder, 1997). This concentration polarization can be decreased by increasing the turbulence in the flow.

Also during the process it is possible that, under high pressures, the membrane undergo a “creep” or “compaction” phenomenon, which may change the permeability of the membrane (Zeman and Zydney, 1996). This usually happens in polymeric membrane under very high pressure and is usually not seen in MF or UF. Initially the decline in flux is rapid and then it slows down to reach a quasi-state flux, generally after 1-2 h after the start. After the initial sharp decline, flux still continues to decrease slowly with filtration time, and the flux may be considerably lower than the initial

flux values after several hours of operation (D'Souza and Mawson, 2005). The main reason for this flux decline is fouling. Fouling is a limiting factor in consistent and efficient performance of membrane processes in dairy industry. Membrane fouling is caused by pore blocking due to foulants such as organics, minerals, colloids, microbial contaminants, and particles on the membrane surface, or by cake formation (Song, 1998). In the dairy industry, membrane surfaces and its pores are fouled with organic and inorganic components from milk so membranes are cleaned on a regular basis to ensure hygienic operations and maintain membrane performance (Barlett et al., 1995). Removal of the fouling layer by thorough cleaning is essential to maintain desired membrane performance.

2.5.2 Membrane Surface and Solute Interactions

Membrane fouling is caused by the interaction between membranes and solutes such as organic matter, colloidal particles, and inorganic crystals present in solution. Membrane fouling has usually been explained by the following known mechanisms: pore blocking, cake formation, ligand exchange reaction, charge interaction, or hydrophobic interaction (Belfort et al., 1996; Choo and Lee, 1996; Fane, 1994). The interaction between membrane surfaces and solutes in solution plays an important role in determining the extent of membrane fouling. Surface properties like surface charge, hydrophobicity and surface roughness can affect the severity of fouling and cleaning of membrane surface. Evans and Bird (2006) studied the solute-membrane fouling interactions during ultrafiltration of black tea liquor. They found fluoropolymer membrane became fouled with hydrophilic tea species. Cleaning was not able to remove these particles fully and the deposits modified the membrane surface to give fluxes similar to those seen with more hydrophilic materials. Weis *et al.* (2003) suggested a strong relationship between the fouling and cleaning history, the surface charge and the performance of the PES and PSU membranes in terms of flux recovery. Persson *et al.* (2003) found that electrostatic interactions between the protein and the membrane affected the transmission of protein during crossflow microfiltration (PES and nylon microfiltration membranes). They showed that at high ionic strength the charged protein molecules are shielded from the membrane resulting in an increase in protein transmission. Kim *et al.* (2009) suggested that

cationic surfactant pre-coating on the membrane surface can reduce hydrophobic organic fouling during desalination of waste water with a relatively high salt content.

Choo and Lee (2000) tested the severity of fouling for three membrane materials, polysulfone, cellulose and fluoropolymer in terms of surface free energy changes calculated from measured contact angle. They found that the fouling severity was in the sequence of polysulfone (worst), cellulosics, and fluoropolymer (least). They also developed a fouling model which related surface free energy change to fouling as:

$$\Delta G_f = a + b\sqrt{\gamma_S^d} \tag{2.1}$$

where ΔG_f is the total free energy change, γ_S^d is the surface energy arising from non-polar dispersion and the terms a and b are related to the surface tensions of foulants and water, respectively, and they can be regarded as constants for a particular feed solution.

Weis *et al.* (2005) found that for membranes of a similar hydrophobicity but different surface roughness (PSU and PES), flux decline over multiple fouling and cleaning cycles was found to be more significant for rougher surfaces (PSU). Their experiment also indicated that both the degree of fouling and the type of fouling were determined by the hydrophobicity of membrane. Boussu *et al.* (2006) found that the hydrophobicity of nanofiltration membranes was the most influential factor in colloidal fouling, independent of colloid size or colloid charge. They also found that during filtration of small colloids by rough membranes, "valley clogging" played an additional secondary role in membrane fouling. They suggested that the optimal membrane choice to minimize fouling is a membrane with a hydrophilic, smooth surface.

Lindau *et al.* (1995) investigated the affect of a low-molecular hydrophobic solute, i.e. octanoic acid on the flux of polysulphone ultrafiltration membranes. They found that octanoic acid decreased the clean water flux for the membranes significantly but that change depended on the MWCO of the membrane. Octanoic acid was detected even after through cleaning of the membrane. They suggested that the solute particles adsorbed on membrane surface reduced the effective pore radii resulting in a decrease

of water flux. This experiments shows that the solute membrane interaction is also important for flux characteristics of the membrane.

2.5.3 Membrane Cleaning

Cleaning can be defined as "a process where material which is not an integral part of membrane is relieved of it" (Trägårdh, 1989). The main aim of the cleaning is to remove any chemical, organic or microbial residues left after the filtration which may hinder the flow of permeate through the membrane, or is not desirable to maintain the required product quality. To achieve the above aim, an aggressive, optimised cleaning procedure is used. The cleaning procedure and frequency of the cleaning process is optimised based on the type of process fluids, type of membrane and cleanliness and disinfection level required. A faulty approach to cleaning can increase the total cost of the filtration process significantly (Hall, 1992). In order to clean a membrane, three types of energy inputs are needed (Cheryan, 1998): chemical energy, in the form of cleaning chemicals, thermal energy, in the form of heat, to increase the efficiency of the cleaner, and mechanical energy, in the form of increased turbulence and high velocities. Cleaning chemicals should have properties that are well suited to the filtration system (Luss, 1984). It should have good solubility and buffering when in contact with the fouling material and should easily be rinsed away with water.

Water is used for both making up cleaning solutions and for rinsing. The quality of water is very important for an efficient cleaning process. Tran-Ha and Wiley (1998) found that impurities such as particulates and dissolved salts present in cleaning water affected the efficiency of cleaning of polysulfone membranes. Depending on the fouling composition, single component cleaners like sodium hydroxide or a multi-component cleaner which contains a variety of chemicals, each with specific function to perform, can be used. Generally commercially available cleaning chemicals are mixtures of alkalis, surfactants, sequestering agents and buffering agents. Fouled membranes are generally cleaned with an initial hot water flush followed by acid cycle, then alkali cycle and lastly sanitization cycle with intermittent hot water rinses. Generally the temperature during the whole cleaning process is kept at 50-55ºC to

increase the efficiency of cleaning. A typical cleaning regime for cleaning polysulfone UF membranes fouled with cheddar cheese whey was given by Bohner and Bradley (1992) as follows:

Step 1: Rinsing the membrane system for 2 min with water initially

Step 2: Sodium hydroxide solution at pH 11.0, with 0.l% of a non-ionic surfactant added, circulated for 20 min.

Step 3: 2-min rinse with water,

Step 4: A 1: l mixture of nitric and phosphoric acids at pH 2 circulated for 20 min

Step 4: 2-min rinse with water,

Step 5: Finally, sodium hydroxide solution at pH 11.0, with 200 ppm of sodium hypochlorite added, circulated for 20 min and rinsed.

All cleaning solutions and all rinse waters were at 54ºC.

Most common cleaning chemical used for membrane cleaning are as follows:

2.5.3.1 Acids

Generally nitric acid, phosphoric acid, citric acid or a combination thereof (pH 1.5-2.8) is used to clean inorganic matter and oxide films, e.g., calcium based scales in dairy membranes. Phosphoric acid is the least aggressive to membranes and has a detergent action because of the phosphate group (Zeman and Zydney, 1996). Nitric acid is effective but corrosive and is undesirable as the effluent stream will contain nitrates. Citric acid is good for iron deposits. Sulphuric and hydrochloric acids are avoided due to the corrosive effect on steel.

2.5.1.2 Alkalis

Alkalis are generally more suited for organic based fouling (Cheryan, 1998) and are very effective against many biological/organic foulants, silica and inorganic colloids. They are generally used up to pH 12, if compatible with the membrane. 0.2% caustic solution at 50ºC allowed the recovery of most of the membrane flux of WPC fouled ultrafiltration membranes (Nigam et al., 2008). There are a large number of alkaline cleaning chemicals available including hydroxides, carbonates, silicates. Every chemical has its own advantage and disadvantage. Sodium hydroxide is the simplest alkaline cleaner but does not have good buffering capacity. Phosphates, e.g., sodium tripolyphosphate, tri sodium phosphate etc., act as water softeners and are very effective at dispersing large colloids. Sodium hypochlorite can be used as a cleaning

agent for oxidising organic fouling matter. Silicates are particularly effective at sequestering magnesium (Zeman and Zydney, 1996).

2.5.1.3 Surfactants

The effectiveness of alkali cleaning cycle can be increased by adding surfactants to cleaning solution. Kazemimoghadam and Mohammadi (2007) found that a combination of sodium dodecyl sulphate (SDS), ethylenediamine tetraacetic acid (EDTA) and sodium hydroxide was a better cleaning agent as compared to sodium hydroxide alone for cleaning and flux recovery of ultrafiltration membranes used for the dairy industry. Surfactants act as efficient cleaning agents by (1) displacing foulants from membrane due to their strong adsorption, (2) emulsifying oils and fats and (3) solubilising hydrophobic foulants. Surfactants are available with a wide range of chemical structure and can be neutral, negatively charged (anionic) and positively charge (cationic). Physico-chemical interaction between the membrane surface and the solute can be controlled by using proper surfactants. Morel *et al.* (1997) found that even a small concentration of cationic surfactant can radically modify membrane properties. Chen *et al.* (1992) found that initial water flux of polysulfone ultrafiltration was reduced but protein fouling on membranes was significantly diminished by use of anionic surfactants.

2.5.1.4 Sequestrants/ Chelating Agents

Sequestrants contain two or more electron donor atoms that can form coordinate bonds to a single metal atom to form a complex. These complexes are much more soluble in water, thereby effectively removing the metal cations like Ca^{2+} and Mg^{2+} from the solution. The most common chelating agents are EDTA, citrates and sodium tripolyphosphate.

2.5.1.5 Enzymes

Enzymatic cleaning is generally done for the sensitive membrane which can not withstand harsh temperatures, pH conditions and strong chemicals. Different types of enzymes or a mixture can be used depending on the type of foulants. Enzymes are available that can degrade material such as proteins (protease), starch (amylase) and fats and oils (lipases). Usage of enzymes is gaining popularity due to the long-term degradation effect of chemicals even on strong membranes like of polyethersulfone.

Proteases are the most common enzymes used due to the prevalence of protein fouling in various membrane assisted processes. Allie *et al.* (2003) showed that enzyme based cleaning agents can be successfully used in removing biological fouling (mainly proteins and lipids) in biological streams, like abattoir effluents. Mufioz-Aguado *et al.* (1996) studied the effectiveness of enzyme and detergent cleaning of a polysulfone ultrafiltration membrane and found that in cleaning of foulants containing proteinaceous components (like foulants from whey separation), enzymatic cleaners play a vital role in scissioning specific points in the protein strands. Detergent cleaners also interact with the protein strands at specific points and also rapidly solubilise any small loose protein fragments. Both cleaning agents can be used in a two step cleaning process, with enzyme followed by detergent cleaning.

Other cleaning methods can be in used in combination with chemical cleaning to enhance the cleaning efficiency. Use of ultrasonics in combination with cleaning solution can improve the flux recovery of membrane used in the dairy industry without damaging the membrane structure itself in long term use (Muthukumaran et al., 2004). It may be due to increase in turbulence within the cleaning solution by ultrasonic energy. Fouling can be effectively decreased by membrane surface pre-treatment (Maartens et al., 2000) or by pre-treatment of the feed (Maartens et al., 1999).

2.5.1.6 Cleaning Efficiency

Cleaning efficiency can be judged on basis of composition, appearance or measurement of microbial count of the final rinse water. However the application of these tests is limited in real time industrial processes. In industry, cleaning efficiency is generally measured as restoration of initial water flux or initial feed flux through the membrane. This may or may not indicate the condition of the membrane surface and many times, even after restoration of flux, the membrane can act differently and can foul quickly or show different separation properties. Therefore it may be hard to decide when the optimal separation conditions are achieved. Many surface analysis techniques like Fourier transformed infrared - attenuated total reflectance spectroscopy (FTIR-ATR), zeta potential measurements (Zhu and Nystrom, 1998), X-ray photoelectron spectroscopy (XPS) (Daufine et al., 1992) have been used in combination with flux recovery tests for better analysis of membrane cleanliness.

Most of the surface analysis methods are destructive because the membrane has to be taken out of the module and cut open which limits the application of these tests in industry. Flux recovery test still remains the routine test to judge the efficiency of the cleaning process.

2.5.2 Disinfection/Sanitization

Though detergents have some disinfection ability, a sanitization step is done to ensure required reduction of microbial load and to maintain the high hygiene standards required in dairy industry. Disinfection should destroy all living pathogenic microorganisms (Zeman and Zydney, 1996). It also decreases the load of spoilage microorganism significantly, which is necessary to maintain consistent and high level of product quality. However, it should be remembered that sanitising without prior cleaning is of no value (Cheryan, 1998). All the sides of membranes and other surfaces which are in contact with dairy fluids should be accessible and must be sanitized properly (McDonough and Hargrove, 1972). If microbial levels are not controlled, they will eventually form biofilms. The size, complexity, and resistance to sanitization of the colony increases within this biofilm and eventually it becomes difficult for sanitizer to penetrate. They also become a source of recontamination when sanitizing steps do not completely remove the biofilm. A single routine sanitization usually only affects the top layer of the biofilm, so viable bacteria deep in the biofilm will quickly contaminate the system again and high bacteria levels will be seen again within a few days. To destroy an established biofilm repetitive sanitizing cycles are required (Mueller and Paulson, 1997). A good sanitizer should posses following qualities (Boufford, 1996):

- Should be a broad spectrum disinfectant (kill large varieties of microorganisms)
- Be effective at low concentration
- Be effective even for very high microbial loads
- Should not be corrosive to membrane system, within the limits of usage
- Easy to clean and flush away
- Should not leave any toxic or harmful residues
- Should be stable and effective during the whole sanitization cycle

The most commonly used sanitizing agents used in dairy membrane processes are sodium hypochlorite, hydrogen peroxide and sodium metabisulphite. Hypochlorite is very corrosive at low pH so sodium hypochlorite disinfection is generally done in the pH range of 10-11 (Ricketts et al., 1985). It is broad spectrum disinfectant but its stability and effectiveness is governed by pH and temperature of the solution. It is highly unstable in presence of organic compounds, and residual chlorine can affect the food odour and flavour. Metabisulphite, at slightly acidic pH releases SO_2 which acts as a disinfectant. It is not aggressive to membranes like hypochlorite and leaves no harmful residues. However it has a slow mode of action which means a long sanitization cycle and increase in time before the membrane can be reused (Krack, 1995). A study by Pavlova (2005) showed that 0.25 % metabusulphite is not sufficient to prevent biological fouling in ultrafiltration spiral wound membranes. Generally metabisulfite is used for storage of the membranes or for membranes which are sensitive to hypochlorite. Hydrogen peroxide is also a broad spectrum sanitizer and leaves no harmful residue as it decomposes into water and oxygen. It is slow acting and is not generally compatible with polyamide membranes. Per acetic acid is used extensively in cleaning and disinfection of membrane for biological and medical application due its quick-acting ability and decomposition into nontoxic acetic acid. Steam sterilization is also used for membrane systems used in pharmaceutical industries where very high level of sterility is required. Table 2.3 shows the dose and disinfection time needed for various sanitizers for removal of biological fouling in purified-water system.

Table 2.3 Typical biocide dosage levels, (Mittelman, 1986)

Chemical	Dosage Level ppm	Contact Time (hours)
Chlorine	50-100	1-2
Ozone	10-50*	<1
Chlorine dioxide	50-100	1-2
Hydrogen peroxide	10% (v/v)	2-3
Iodine	100-200	1-2
Quaternary ammonium compounds.	300-1000	2-3
Formaldehyde	1-2% (v/v)	2-3
Anionic & non-ionic surfactants	300-500	3-4

* Ozone dosage is 10-50 mg/l, but the residual levels in water were 1-2 ppm.

2.6 The Sulfone Family Polymers

A variety of polymers are studied and applied for making membranes. A polymer should posses qualities as below which qualifies it to be used as membrane:

- Exhibit a wide range thermal stability
- Exhibit chemical stability over a wide range of pH
- Should be able to form thin defect free films or hollow filaments
- Should have good mechanical strength to withstand high pressure during operation.

Sulfone family polymers are one of the most common polymers used in membrane processes in the food and dairy industry. The sulfone family polymers include polysulfone, polyethersulfone and polyphenylsulfone. These polymers are characterized by $-SO_2-$ as a constituent in the largely aromatic group polymer structure (Cheryan, 1998). The first commercial sulfone polymer was Udel, (Union Carbide, now Amoco), followed by Astrel 360 (Minnestosa Mining and Manufacturing), which was termed as polyarylsulfone and Victrex (ICI), a polyethersulfone (Brydson, 1995). The various sulfone polymers differ in the spacing between the aromatic groups, which in turn affects their glass transition temperatures, (T_g)which ranges from 180 to 250ºC. This allows a continuous use of the polymer even at 200ºC (Harper, 2002). Sulfone polymers have good creep behaviour, and are generally transparent. They have good chemical resistance (Harper, 2003) and are approved for food contact and potable water. However they can be dissolved in polar solvents like n-methyl-2-pyrrolidone (NMP) or di-methyl-formamide (DMF) and solvent attack may cause environmental stress cracking (Black and Hastings, 1998). Aliphatic polysulfones do not have the same resistance to light and heat as the aromatic polysulfones, so they have limited usage and cannot be used as working materials. The simplest aromatic polysulfone is poly (*p*-phenylene sulfone) (Figure 2.5).

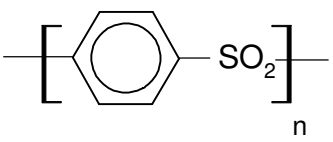

Figure 2.5 Chemical structure of *p*-phenylene sulfone

It does not show thermoplastic behaviour, melting and decomposition even at 500ºC. To make polysulfone mouldable in conventional machines, the polymer chain is made flexible by incorporating ether linkages in the polymer backbone. Generally commercial sulfone polymers are synthesized by Friedel-Crafts reaction and nucleophilic reactions (Kricheldorf et al., 2004). Despite being costly, sulfone family polymers are used in wide range of application due to there high thermal stability, high glass transition temperature and good mechanical properties. They are amorphous and have good dielectric properties and hydrolytic resistance and can withstand hot water and steam (Kroschwitz, 1990). They are suitable for use in engineering parts, electrical components, utensil coatings and filtration membrane systems. The two important members of sulfone family polymers are polysulfone and polyethersulfone. Both of them are widely used in membrane based separation processes in the food and dairy industry

2.6.1 Polysulfone (PSU)

The chemical structure of polysulfone is shown Figure 2.6.

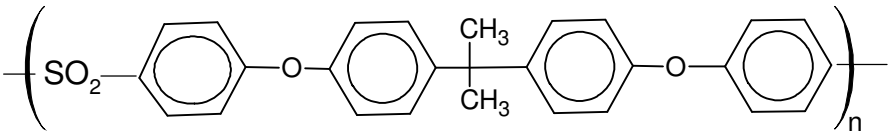

Figure 2.6 Chemical structure of polysulfone

Polysulfone is a transparent thermoplastic and is prepared by the reaction between the sodium salt of 2, 2- bis (4-hydroxyphenol) propane and 4, 4- dichlorodiphenyl sulfone (Harper and Petrie, 2003). Figure 2.7 shows a “textbook” example of a condensation or step-growth polymerization (Robert, 1995).

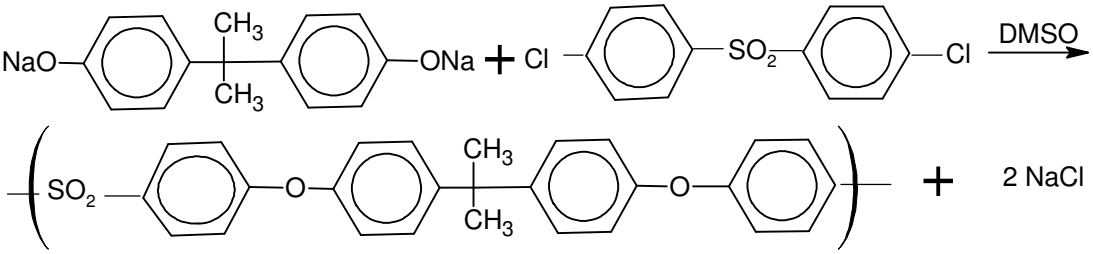

Figure 2.7 Chemical reaction to produce PSU, DMSO: dimethyl sulfoxide

The sulphur in the oxidised state gives polysulfone affinity for water. This discourages adsorption of organic substances which makes it a good material for making membranes. The linkages connecting the benzene rings are hydrolytically stable. Polysulfone is self extinguishing and has a T_g of 180ºC. PSU has an operating temperature range of -101 to 149ºC. Polysulfone has high impact strength and good electrical properties. It has high melt stability which allows production of thin films and sheets. Polysulfone has good weatherability and it is not degraded by UV radiation. However it experiences mild degradation of its physical properties, and slight yellowing on prolonged exposure to sunlight. Polysulfone is used in applications requiring high-temperature resistance, e.g., coffee carafes, piping, sterilizing equipments. Polysulfone is also used in electrical applications for connectors, switches and in manufacturing of membrane and membrane supports.

Polysulfone as a Membrane Material

The first development of PSU membranes appeared in the 1960s as an alternative to cellulosic membranes. Polysulfone membranes are widely used as a support for the fabrication of thin-film composite membranes. The majority of today's RO membrane consists of a PSU support covered by a thin selective layer of aromatic polyamide (Salamone, 1998). It is also used to form ultrafiltration and microfiltration membranes. Owing to its wide range of acid and alkali tolerance, it is easy to clean polysulfone membrane or supports. Due to its chemical, mechanical, thermal, and hydrolytic stability, polysulfone is commonly used as a membrane materials for a wide variety of membrane applications (Zeman and Zydney, 1996). Some of them are mentioned below:

- Dairy industry for protein separation and whey protein recovery
- Pharmaceuticals
- Beverage filtration and concentration
- Haemodialysis
- Drinking and ultra-pure water
- Gas separation
- Bacteria and particulate removal.

2.6.2 Polyethersulfone (PES)

Polyethersulfone is characterized by $–SO_2-$ as a constituent in the largely aromatic group polymer structure and has an ether-diphenylsulfone repeat unit as shown in Figure 2.8. PES lacks the $–CH_3$ group which alters the property of the membrane. Polyethersulfone can be synthesized by an electrophilic substitution which gives a *p*-substituted product as Figure 2.9 (Elias, 1984).

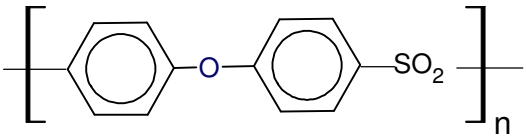

Figure 2.8 Chemical structure of PES

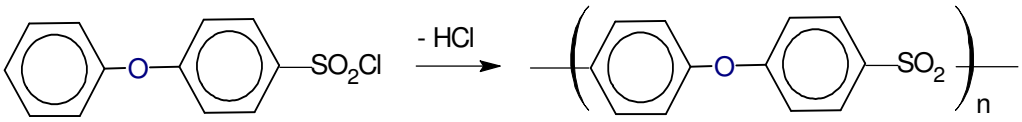

Figure 2.9 Chemical reaction to produce PES

PES is also a transparent polymer with high temperature resistance and self-extinguishing properties. PES is rigid, strong and has very low creep over a range of temperature reaching over 150ºC (Charrier, 1991) due to its high T_g ~250ºC. Since PES is an aromatic highly polar polymer it is resistant to aqueous acids, bases, salts, and hydrocarbons including petrol and grease even at high temperature. However it can be dissolved in polar solvents like n-methyl-2-pyrrolidone (NMP) or di-methyl-formamide (DMF). Also it has poor weathering or ultra-violet resistance so outdoor uses are limited. However, resistance to ionizing radiation is good in the temperature range of 20-200ºC. Table 2.4 lists some of the important properties of PES as a polymer. PES has ability to be shaped to fine tolerances which makes it a suitable material as an integrated circuit carrier (Birley and Scott, 1982). PES is used in electrical appliances like switches and battery parts. The ability of PES to withstand repeated sterilization, allows it to be used in variety of medical applications.

Table 2.4 Important properties of polyethersulfone

Property	Range
Processing temperature	357-351ºC
Glass transition temperature	227-238ºC
Continous service temperature	177-199ºC
Tensile strength at break,	0.82-1.63 x 10^2 MPa
Tensile strength, yield	0.89-1.45 x 10^2 MPa
Tensile modulus	0.40-0.93 x 10^4 MPa
Water absorption, 24 hr	0.29-0.41%

(Taken from, Henkel Corporation, 2005)

Property	Range
Contact angle with water (for PES flakes)	80º
MW (light scattering in NMP)	46-55,000 g/mol

(Taken from Ultrason E and S, Luvitec, Versatile materials for the production of tailor-made membranes, BASF Aktiengesellschaft, 2004)

Thermal Stability (Thermo gravimetric analysis)				
Weight Loss %	1	2	5	10
Temperature, °C	472	487	511	530

(Taken from Radel, Resins Design Guide, 2004)

Polyethersulfone as a Membrane Materials

Polyethersulfone is a well established membrane filtration polymer in the dairy, food, biotechnological, and pharmaceutical industries. PES membranes are used in both ultrafiltration and microfiltration membranes. These membranes demonstrate very high thermal stability, with an upper operating temperature of 125°C. It is a stable polymer which can perform under a broad pH and temperature range. Its wide temperature range makes it possible to sterilize the membranes by either steam or autoclaving. PES membrane has reduced membrane thickness as compared to polyamide and polysulfone membranes (30 μm as compared to 40-50 μm) which results in higher hydraulic permeability in water (Somasundaram, 2006).

Polyethersulfone is a low protein binding material as compared to other commercial polymers and gives excellent flow rate with batch to batch and within batch consistency in performance. Membrane regeneration, storage and depyrogenation can be accomplished by using NaOH even at elevated temperatures.

Polyethersulfone has the highest proportion of sulfone moieties in the polymer repeat unit among all the sulfone polymers. This polar part makes PES more hydrophilic and as a result PES has the highest water absorption of the commercial sulfone family

polymers. Since polyethersulfone membrane can work at high temperature and a broad pH range and is resistant to most of the cleaning chemicals, cleaning and sanitising PES membrane is not a daunting task. PES membrane's high strength and durability is advantageous during usage that involves aggressive handling or automated equipment. Its superior burst strength protects the integrity of the membrane under high pressure. Also PES is well-suited to various membrane preparation methods and is compatible with a variety of sealing methods which makes it easy to use it as membrane material in various module configurations. PES is commonly used as membrane materials for a wide variety of ultrafiltration and reverse osmosis applications as mentioned below:

- Dairy industry for protein separation and whey protein recovery
- Pharmaceuticals
- Beverage filtration and concentration
- Haemodialysis
- Drinking and ultra-pure waters
- Gas separation
- Bacteria and particulate removal.

Although both PSU and PES show excellent compatibility with acids and alkalis, they are highly soluble in polar solvents like DMF, NMP and chloroform which eliminates the use of PSU/PES base membrane processes for solvent-based feed solutions. It also becomes difficult to coat the PSU supports with polymers, that are soluble in organic solvents.

Also these membranes do not have great affinity for water which prevents spontaneous wetting with aqueous media. Therefore the membrane must be kept soaked in water or glycerol to prevent it from drying out (Nunes and Peinemann, 2006). Hydrophilicity of PSU/PES membrane can be increased by surface modification of the polymer by incorporating hydrophilic groups in the polymer (Zuwei et al., 2006 and Roux et al., 2005).

Due to their non-crystalline nature, PSU and PES are susceptible to environmental stress cracking. Possibly, PES and PSU should not be used in contact with polar

solvents. Even in contact with even mildly polar liquids, the object in use should be free from external and internal stresses at the surface to avoid stress cracking. The parts can be stress relieved by annealing them at a temperature below the melting temperature of polymer (Ratner et al., 2004).

2.7 Membrane Life

Membrane life can be defined as the time duration the membrane can perform profitably in terms of acceptable flux and product concentration (can be concentration in permeate or retentate depending on the aim of the separation), under a given set of separation and cleaning conditions. Generally the performance of membrane is monitored by the clean membrane water flux. A gradual decrease in clean water permeability of membrane occurs as a function of the number of cleaning cycles (Wenten, 1994). Under continuous use of the membrane, with time, a gradual increase in the pressure drop to an unacceptable level or physical cracking of the membrane can occur (Rouaix et al., 2006). In either case the membrane may be said to be finished its working life and needs to be replaced.

2.7.1 Factors affecting Membrane Life

There are number of factors which can directly or indirectly affect membrane life.

Membrane material

Ceramic membranes can withstand harsher conditions of temperature pH and pressure as compared to polymeric membranes. They can withstand many thousands of back flushing operations for membrane cleaning (Scott, 1995) which enables them to have a superior membrane life as compared to polymeric membranes. However even if ceramic membranes themselves are very resistant to extremes of operating conditions it is the non-inorganic parts like seals, gaskets, o-rings etc. which limit their performance (Cheryan, 1998)

Type of Feed

Viscosity of feed, solid concentration and type of solids present in the feed governs the fouling type and rate, which influence the cleaning strategy and frequency of cleaning cycles needed (Scott, 1995). Because of the challenging environment in which ultrafiltration membranes are operated and the regular cleaning cycles, membrane lifetime is significantly shorter than that of RO membranes (Baker, 2004).

Cleaning Strategy

The type of cleaning chemicals, frequency of cleaning cycle, and time duration for each cleaning cycle, directly influence the exposure of membrane to strong chemicals. Also sometimes special cleaning cycles with very harsh cleaning conditions are performed in addition to routine cleaning cycles to improve the performance level of the membrane. Good rinsing or flushing after each cleaning step is important to minimize the prolonged exposure of harsh chemicals to the membrane. Periodical cleaning is a necessity of membranes, but it should only be performed when necessary, due to adverse effect of chemicals on membrane life (Wagner, 2001).

2.7.2 Effect of Sodium Hypochlorite as Disinfectant on PES and PSU membranes life

The oxidative nature of hypochlorite, which is one of the most commonly used disinfectants, may have detrimental effects on the mechanical properties, surface morphology and overall integrity of PSU and PES membranes. In recent years a few studies have been done on the effect of sodium hypochlorite on PES membranes. Bégoin *et al.* (2006) studied the effect of ageing in alkaline, acid, alkaline chlorine oxidant and a commercial alkaline cleaning solution (Ultrasil 10) at 50°C on spiral wound PES ultrafiltration membrane. They found that the membrane appeared stable in all solutions except those containing chlorine. The long term exposure of alkaline bleach led to surface cracking of the PES layer in ultrafiltration membranes. The degradation was linked to breakage of the C–S bond in PES (phenol–SO_2–phenol) and the formation of a Cl–S bond after long-term exposure to bleach.

Arkhangelsky *et al.* (2007) also found that long term exposure of PES-based membranes led to a possible chain scission at the ether-sulfone linkage which may result in loss of membrane integrity. A similar study by Thominette *et al.* (2006) showed that the PES embrittlement rate was four times faster in PES membrane fibres than in PES films and concluded further research was required on the mechanical properties and failure of membranes.

A similar effect has been observed in polysulfone membranes when exposed to hypochlorite solution. Gaudichet-Maurin and Thominette (2006) studied the long term behaviour of polysulfone membranes with focus on chemical structure–mechanical properties relationships. They immersed the polysulfone membranes in bleach solutions with various pH values. They observed that degradation, which causes an embrittlement of the fibre, occurs by chain scission with the hydroxyl radical $OH^{\bullet}$ formed in the bleach solution. The lifetime of the fibre depended on the total chlorine concentration and pH of the hypochlorite solution.

Causserand *et al.* (2008) found that the exposure of polysulfone membrane to sodium hypochlorite produced chain breakage leading to loss in the membrane's mechanical properties. They suggested that, with sodium hypochlorite exposure polysulfone may degrade by radical oxidation catalyzed by the presence of metallic ions such as Fe^{2+} and Cu^{2+} changing the membrane structure at the microscopic level.

Generally polyethersulfone and polysulfone based membranes are modified by adding polymeric additives to improve its hydrophilicity and flux properties. Numerous studies (Wolff and Zydney, 2004; Qin et al., 2003; Qin et al., 2005; Rouaix et al., 2006) have affirmed that hypochlorite has a major effect on additive polymers rather than the main polymer. This makes modifying the membranes a difficult choice for improving fouling characteristics of the membranes.

2.8 Ultrafiltration Membrane Characterization

Characterization of ultrafiltration membrane can be classified into two major divisions (1) characterization of membrane as a polymer, i.e. bulk properties of membranes, and (2) characterization of membrane as a porous surface, i.e. surface properties of the membranes. The techniques generally used to characterize bulk properties of membrane are mainly destructive type methods or can only be applied off-line. A characterization methodology that is non-destructive and could provide real-time measurements would be of significant value to the membrane industry (Ramaswamy, 2006). The destructive techniques are mainly useful for research or failure analysis. Only few of the techniques used to characterize surface of the membrane are non-destructive, and can be applied in industry for judging the health of membranes. Table 2.5 shows various membrane characterization techniques applied in this study.

Table 2.5 Classification of membrane characterization techniques studied

Bulk properties of membrane	DMA (dynamic mechanical analysis) TGA (thermal gravimetric analysis) Tensile strength and tensile modulus X-ray diffraction
Surface properties of membrane	FESEM (field emission scanning electron microscopy) EDS (energy dispersive x-ray spectroscopy) FTIR-ATR (Fourier transform infrared - attenuated total reflectance) spectroscopy Contact angle and surface energy and liquid dispersion test Streaming potential measurement Liquid-liquid displacement porosimetery Protein rejection Water flux test and membrane throughput test Surface colour measurement

2.8.1 Dynamic Mechanical Analysis (DMA)

Dynamic Mechanical Analysis (DMA) is a thermal analysis technique used to measure changes in the visco-elastic response of a material, by applying oscillating sinusoidal stress, as a function of temperature, time or deformation frequency. For DMA a low amplitude stress is applied so that the sample is always within the elastic region of strain-curve. Under an applied force the material may deform elastically or may flow. For a perfectly elastic material the applied stress and the resultant strain are perfectly in phase as shown in Figure 2.10.

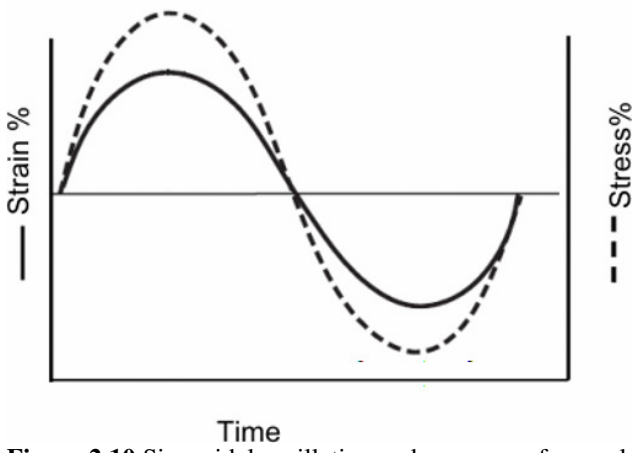

Figure 2.10 Sinusoidal oscillation and response of a purely elastic material (Ehrenstein et al., 2004)

In case of visco-elastic material like polymer the stress strain curve is out of phase as shown in Figure 2.11.

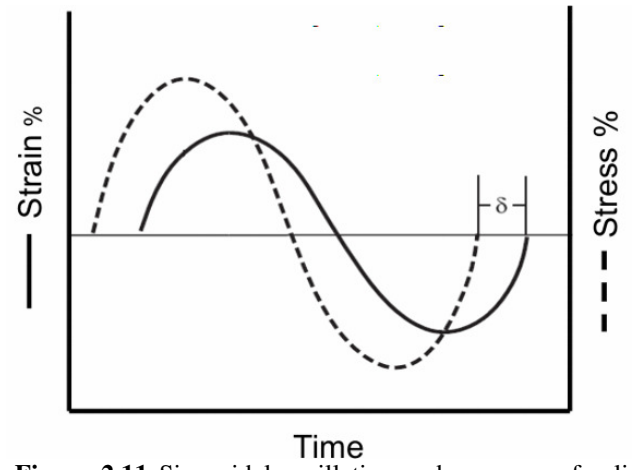

Figure 2.11 Sinusoidal oscillation and response of a linear visco-elastic material; δ = phase angle (Ehrenstein et al., 2004)

DMA measures the amplitude of the stress and strain and the phase angle between them, which becomes the primary inputs for calculating various dynamic properties. In the case of an elastic response the strain at any time can be written as (Menard, 2008)

$$\varepsilon(t) = \varepsilon_o \sin \omega t \tag{2.2}$$

where $\varepsilon(t)$ is the strain at time t, ε_o is the strain at maximum stress and ω is the frequency. For a material like a polymer which is in between the two limits, i.e. elastic and viscous, the elastic response at any time, t can be given by

$$\varepsilon(t) = \varepsilon_o \sin(\omega t + \delta) \tag{2.3}$$

where δ is the phase angle/lag between applied stress and resultant strain. Equation (2.3) can be written as

$$\varepsilon(t) = \varepsilon_o \left[\sin(\omega t)\cos\delta + \cos(\omega t)\sin\delta\right] \tag{2.4}$$

Equation (2.4) can be broken into in phase and out of phase strain components.

$$\varepsilon'(t) = \varepsilon_o \sin\delta \tag{2.5}$$

$$\varepsilon''(t) = \varepsilon_o \cos\delta \tag{2.6}$$

The vector sum of the two components gives the overall or complex strain.

$$\varepsilon^* = \varepsilon' + \varepsilon'' \tag{2.7}$$

Dynamic properties measured by DMA

The **storage modulus *E'*** represents the stiffness of a elastic material and is proportional to the energy stored during the loading cycle and is calculated as (Menard, 2008)

$$E' = (f_o / bk)\cos\delta \tag{2.8}$$

where δ is the phase angle b is the sample geometry term, f_o is the force applied at the peak of sine wave, and k is the sample displacement at the peak.

The **loss modulus *E"*** is defined as being proportional to the energy dissipated during one loading cycle and is a measure of vibrational energy that has been converted during vibration and can not be recovered at a given frequency ω. E'' is given by

$$E'' = (f_o / bk)\sin\delta \tag{2.9}$$

The **loss factor tan *δ*** is the ratio of loss modulus to storage modulus and is given by

$$\tan\delta = (E''/E') = \varepsilon''/\varepsilon' \tag{2.10}$$

It represents the mechanical damping or internal friction in a viscoelastic sample. A high tan δ indicates that material has high non-elastic strain, whereas a low value indicates a high elastic strain component.

DMA can be a useful technique for identifying polymers, doing glass transition studies and checking polymer compatibility in laminates. Faria *et al.* (2007) studied dynamic mechanical analysis for polymer identification. They used the technique to classify both amorphous and semi-crystalline polymers. They showed the possibility of identifying polymers and developing an automated approach for polymer analysis. Ferández-Blázquez *et al.* (2005) performed DMA on thermotropic poly(ether)ester and found that DMA can easily differentiate between various mesophases of the polymer, i.e. from quenched to annealed. Cohen *et al.* (2000) were able to differentiate between aged and new parchment sample by studying shrinkage behaviour of the samples under static load when completely immersed in water, using a dynamic mechanical thermal analyzer. Keusch and Haessler (1999) studied interfacial bonding of differently treated glass fiber in epoxy resin composites. They found that the storage modulus increase with increase in interfacial bonding. Decreases in the loss modulus and tanδ values were also linked to improvement in adhesion in the samples. Raghi *et al.* (2000) studied the compatibility of un-plasticized poly vinyl chloride and indulin lignin before and after an artificial weathering process. They observed that the tan δ curve had only one peak in both cases which confirmed that the two polymers were compatible in both cases.

2.8.2 Thermogravimetric analysis (TGA)

Thermogravimetric analysis (TGA) has proved to be a highly successful technique for determining the thermal stability of polymeric systems by monitoring the weight change that occurs as a specimen is heated (Sandler *et al.* 1998). In this technique the change in sample weight is measured while the sample is heated at a constant rate (or at constant temperature), under an air (oxidative) or nitrogen (inert) atmosphere. The maximum temperature limit for the experiment is selected such that there is no more loss in specimen weight at the end of the experiment, implying that all chemical reactions are completed (i.e., all of the carbon is burnt off leaving behind inorganic

ash). Thermogravimetric curves are typical feature for a given polymer or compound because of the unique sequence of the physicochemical reaction that occurs over specific temperature ranges and heating rates and are a function of the molecular structure. The changes in mass are a result of the rupture and/or formation of various chemical and physical bonds at elevated temperatures that lead to the evolution of volatile products or the formation of heavier reaction products.

Knowledge of degradation and the mode of decomposition under the influence of heat gives useful information which can be useful for polymer processing and fabrication procedures. Mathew *et al.* (2001) studied the thermal stability of natural rubber/polystyrene interpenetrating polymer networks (IPNs) with help of TGA and found that the full-IPNs have better stability than semi-IPNs which was due to higher entanglement density of full-IPNs. Riga et al., 1998 investigated the oxidative behaviour of crystalline and non crystalline polymers with TGA and found that polycarbonates and polysulfones were the most stable among the non crystalline polymers studied. Marcilla *et al.* (2008) characterised the blend of vacuum gas oil and low density polyethylene by TGA to explore the possibility of using commercial fluid catalytic cracking units or similar processes for recycling plastic wastes.

2.8.3 Tensile Properties

A tensile test is probably the most fundamental type of mechanical test that can be performed on a material. Although tensile testing is not the best way to characterize the engineering behaviour of polymers, it is simple, relatively inexpensive, and fully standardized. The morphology of a polymer directly influences the tensile properties of polymer; tensile properties of a polymer directly depend on molecular weight or degree of polymerization of a polymer. Also polymer chain orientation and degree of crystallinity affects the tensile properties of a polymer (Sperling, 2006). An increase in the crystalline component may increase the tensile strength of the polymer. Therefore a change in tensile properties of a polymer is a good indication of a change in morphology of that polymer (Chung and Teoh, 1999). For example, the tensile strength of the polymer is one of the most sensitive measures of the degree of ageing

of insulating materials. Although it does not measure the functional property directly, it gives an indication of the progression of ageing (Bartnikas, 1987).

A decrease in mechanical strength of membranes and support layers can cause a loss in membrane integrity leading to complete breakdown of membranes. This makes study of mechanical strength of new (Lin and Chung, 1994), modified (Zu *et al.* 2007) or aged membrane (Arkhangelsky et al., 2007; Sasuga et al.. 1999) material essential in relation to practical application of polymer materials in the membrane industry.

2.8.4 FESEM-EDS

FESEM coupled with an EDS system is a powerful tool to study the surface of membranes. It not only provides a realistic view of the membrane surface but also with EDS system the elemental surface composition of the membrane can be successfully mapped. This technique is an important tool for studying surface change and deformities and changes in surface chemical composition with chemical or physical ageing of the membranes. Many researchers have successfully used this technique for studying chemical ageing, fouling and cleaning efficiency on polysulfone and polyethersulfone membrane surfaces (Bégoin *et al.* 2006a, 2006b; Rabiller-Baudry *et al.* 2002; Lindau and Johnson, 1994). Although FESEM imaging is widely used in studies of polymeric membranes, there are some limitations. Artifacts may be formed by specimen charging that occurs in the FESEM when the subject is non-conductive and by structural damage caused by the high energy electron beam when it contacts the surface. Also the sample has to be in a completely dry state during analysis which does not allow microscopic imaging of the membrane in its original wet state.

2.8.5 FTIR-ATR

FTIR gives a fingerprint of a polymer sample with absorption peaks (which correspond to the frequencies of vibrations between the bonds of the atoms making up the material) at a very quick scanning rate. The physical properties of polymers are very dependent on their molecular structure. The FTIR microscopy can identify

polymers, additives, and determine presence of impurities (Robinson and Frame, 2005). The nature of absorption is related to type of atoms presents and their arrangement in the molecule. Because each different material is a unique combination of atoms, no two compounds produce the exact same infrared spectrum. Therefore, infrared spectroscopy can result in a positive identification of different kinds of materials. With modern software algorithms, infrared spectroscopy is an excellent tool for quantitative analysis. For analysing the surface of thin film and polymeric membrane a special accessory attenuated total reflectance (ATR) cell is required in combination with FTIR to enable samples to be examined directly in the solid or liquid state without further preparation (Mossoba, 1999). This advantage makes this technique a useful tool in studying the surface chemistry of membranes. In this technique a beam of infrared light is passed through the ATR crystal in such a way that it reflects at least once off the internal surface in contact with the sample. This reflection forms the evanescent wave (it is a near-field standing wave having an intensity which decays exponentially with distance from the interface at which it is formed) which extends into the sample, typically by a few micrometres. The beam is then collected by a detector as it exits the crystal. A number of researchers have used this technique to study the surface chemistry of new or modified PES membranes (Bolong et al., 2009; Zhu et al., 2007; Susanto et al., 2007; Pieracci et al., 1999). Also it has been applied to characterize membrane fouling, cleaning process and chemical degradation of PES membranes (Bégoin et al., 2006a, 2006b; Rabiller-Baudry et al., 2002; Belfer et al., 2000).

2.8.6 Contact Angle

The contact angle is a measure of the tendency for the liquid to wet the solid surface. The lower the contact angle, the greater is the tendency for water to wet the solid and the higher the hydrophilicity of the surface (Kwon et al., 2006). Contact angle is an index of the hydrophobicity of membrane surface, which can be measured by captive bubble and sensile drop methods (Jucker and Clark, 1994). Contact angle θ can be defined as “the angle formed by a liquid at the three-phase boundary, where a liquid, gas and solid intersect” (Hubbard, 2002). It can be seen in the Figure 2.12 that low

values of θ indicate that the liquid spreads, or wets well, while high values indicate poor wetting.

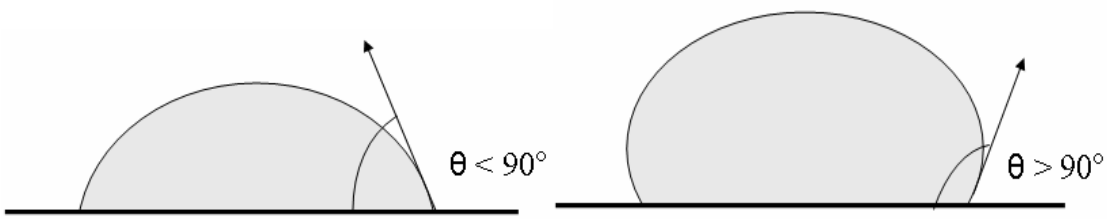

Figure 2.12 (a) Wetting liquid drop (b) Non-wetting liquid drop

If the angle θ is less than 90° the liquid is said to wet the solid. If it is greater than 90° it is said to be non-wetting. A zero contact angle represents complete wetting.

Susanto and Ulbricht (2009) applied sessile drops static contact angle to characterize PES ultrafiltration membranes prepared by non-solvent-induced phase separation method using different macromolecular additives poly ethylene glycol (PEG), poly vinyl pyrolidone (PVP) and poly(ethylene oxide)-*b*-poly(propylene oxide)-*b*-poly(ethylene oxide) (Pluronic®) and found that PES–PEG membrane had significantly lower contact angle compared to other membranes indicating that it was the most hydrophilic membrane, while PES–PVP and PES– Pluronic® membranes showed similar value. Reddy and Patel (2007) studied the hydrophilicity of modified PES membranes by measuring advancing contact angle and concluded that a decrease in contact angle with increase of PAN (poly acrylonitirile) in the polymeric casting solution clearly indicated an increase in hydrophilicity with the modification. Boussu *et al.* (2006) compared the commercial nanofiltration membranes with in-house casted PES membrane and concluded that, out of the group all PES membranes, it had the most hydrophobic membrane surface and that casted and commercial PES membranes were similar in nature. Susanto *et al.* (2007) studied the fouling of dextran and myoglobin on non-porous PES surfaces and found that the contact angle decreased significantly by 4.5° and 8.9° for dextran and myoglobin exposed films in comparison to unexposed PES film, which confirmed a strong adsorption of the macromolecules on the film surface. A similar effect was also observed when the same experiment was conducted on PES membranes (Susanto and Ulbricht, 2005). Guan *et al.* (2005) affirmed that hydrophilicity of PES membranes can be increased by sulfonation with chlorosulfonic acid because the contact angle of water with membrane surface decreased after the modification.

Contact angle is not easy to measure for membranes because of their membranes porous nature and uneven surface. Contact angle measurements should be taken at different locations of the membrane sample and the effect of the membrane pore size and surface roughness must be considered to determine the true contact angle of membrane (Li et al., 2008).

2.8.7 Zeta Potential and Streaming Potential

Zeta potential gives insight of the surface charge and adsorption properties of membrane surface. Zeta potential for membrane surfaces can be calculated by measuring streaming potential values (Amy and Cho, 2001). In this method a liquid is forced through a narrow slit under a pressure gradient. The excess charges near the wall are carried along by the liquid and their accumulation down-stream causes the build-up of an electric field which drives an electric current back (by ionic conduction through the liquid) against the direction of the liquid flow. A steady state is quickly established, and the measured potential difference across the capillary or plug is called the streaming potential. It is related to the driving pressure and to the potential in the neighbourhood of the wall. Zeta potential can be calculated from streaming potential as (Delgado et al., 2007)

$$\zeta = V_S \left(\frac{\eta K_L}{\psi \psi^o \Delta p} \right) \tag{2.11}$$

where V_S is the streaming potential, Δp the applied pressure difference, η dynamic viscosity of the dispersion medium, ψ is the relative permittivity of the dispersion medium, ψ^o is the electric permittivity of vacuum, and K_L conductivity of the dispersion medium

The magnitude of the zeta potential is directly related to the magnitude of the surface charge and so the zeta potential measurement reflects surface charge properties very well. The rate of adsorption and fouling is correlated to changes in surface charge of the membrane during ultrafiltration processes (Nyström et al., 1994) so zeta potential is an important characterization technique to study the behaviour of membrane surfaces for fouling and cleaning. Zeta potential can be measured as a function different electrolyte pH to gives charge behaviour of PES membrane surfaces for a

wide range of pH and to find the iso-electric point, i.e. where no net charge exists (Susanto et al., 2007; Susanto and Ulbricht, 2005). Zularisam *et al.* (2007) used zeta potential measurement for foulant analysis on PSU membranes fouled by natural organic matter foulant and found the foulants were mainly neutral or positively charged. Wang *et al.* (2006) used zeta potential measurement to study the change in surface charge of modified PES ultrafiltration membranes. Rick *et al.* (1997) used this technique for measuring zeta potential of polyethersulfone UF membranes and found that the PES membranes have an iso-electric point around pH 2.2 to 2.4 and the specific adsorption of divalent ions lead to a decrease in the streaming potential for a given ionic strength and pH. Kwon and Leckie (2006) used this technique to study the hypochlorite degradation of cross linked polyamide membranes and found that exposed membranes were more hydrophilic and had a slightly more negative zeta potential.

2.8.8 Liquid-Liquid Displacement Porosimetery (LLDP)

LLDP is a porosimetric characterization technique generally applied for ultrafiltration and microfiltration membranes. In this technique a membrane is wetted by a wetting liquid and another immiscible liquid (displacement liquid) is forced through the pores under pressure. The second liquid needs to overcome the pressure due to interfacial tension within the membrane pores and hence the measured flux depends on the applied transmembrane pressure and the pore size distribution. The wetting liquid and the displacement liquid are chosen such that the interfacial tension is minimal. This technique is also referred to as "permoporometry" by Munari *et al.* (1989), biliquid permporometry by Kim *et al.* (1994), and liquid-liquid porosimetry by Zeman and Zydney (1996). This technique was developed by Erbe (1931) and presented by Kesting (1971). Following this work, the technique was greatly developed into further stages by Capannelli *et al.* (1983) who studied and tested the method various asymmetric UF membranes. These authors further developed the LLDP method by implementation of the models proposed by various others in the literature to successfully develop equipment for the flux and pressures measurements with a good reliability for evaluating the pore size distribution (Capannelli et al., 1988).

Abaticchino *et al.* (1990) reviewed and discussed various techniques used for characterization of polymeric UF membranes, with special emphasis on the problem of evaluating porosity. They concluded that none of the methods individually supply an exhaustive answer to membrane characterization problems, mainly because the "active pore" radius changes with the working conditions and the investigated system. But among the available methods, LLDP seemed to offer the best benefits.
Wienk *et al.* (1994) analysed critical factors involved in the determination of the pore size distribution of UF membranes using LLDP method which should be considered to avoid erroneous results. This included instabilities in pressure measurement, pressure dependent permeability and repeatability of reruns on the same membranes.

A study by Gijsbertsen-Abrahamse *et al.* (2004) indicated that the assumption that the pores of the membrane are not interconnected could lead to erroneous results. Determining the pore size distribution with membrane characterization methods using liquid displacement is incorrect if the pores are connected to each other or if there is a resistance against flow in the membrane sub-layer or in the measurement apparatus. As a result of the additional resistance, the estimated pore size distribution shifts toward smaller pores and a larger number of pores. Calvo *et al.* (2004) applied LLDP technique for characterizing track etched UF membranes with nominal mean pore diameter of 50 nm and the results were compared with those obtained using SEM. Comparison gave a good agreement between both results. Calvo *et al.* (2008) used LLDP successfully to characterize pore size distribution of ceramic tubular membranes with nominal molecular weight cut off (MWCO) of 50, 150 and 300 kDa. Their results showed a good accuracy and reproducibility of LLDP measurements.
Morison (2008) reviewed and numerically tested methods for the determination of pore size distribution of liquid membranes by liquid–liquid porosimetery and found that all methods were very sensitive to measurement noise as low as ±0.1%, and that some form of data smoothing was required to obtain a satisfactory distribution. He also proposed a method based on the ratio of flux liquids with and without a liquid–liquid interface to reduce the error due to elastic and permanent membrane compression.

Although a few researchers have used LLDP for calculating the pore size distribution of membranes but no too much research work has been done on this technique in past

years due to difficulties in an appropriate design of the experimental protocol and scope for development exists.

2.8.9 Water Flux Test

Water flux measurement is the most common and widely used technique to examine the efficacy of membrane cleaning (Cheryan, 1998). During filtration the permeate flow rate through the membrane goes down due to fouling. The target of membrane cleaning is to clean off the fouling and to regenerate the flux to the initial water flux value. The initial water flux through a membrane at a given trans-membrane pressure is measured and at the end of the cleaning cycle the water flux is again measured and if both the values lie within an acceptable range the membrane is said to be clean and regenerated. Many researchers have used clean membrane water flux as a criterion for checking the efficacy of membrane cleaning processes (Zator et al., 2008; Jung et al., 2006; Sandy te Poele and van der Graaf, 2005; Nyström and Zhu, 1995).

A water flux test on a new membrane gives an initial glance about what realistic product flow can be expected from the new membrane (Cheryan, 1998). However care should be taken while making such inferences from water flux data as the flow of product through the membrane is very complex and depends on various factors such as feed constituents, membrane-feed surface interaction, fouling rate, ionic strength and type of membrane module.

2.8.10 Protein Separation

Protein separation analysis is a non-destructive technique which not only provides valuable information about the separation properties of the membrane but also is more realistic test which can be used by the industry on a regular basis to monitor the health of membranes. It can be performed with a series of tests depending on the information required from the analysis.

The simplest tests are membrane flux and protein retention measurement. For an aqueous solution containing protein, both protein retention and membrane flux values

are measured simultaneously, which gives a better overview of membrane separation behaviour. This technique is used to study protein adsorption and fouling on a membrane surface (Clark et al., 1991; Matthiasson et al., 1983).

Nakatsuka and Michaels (1992) studied the separation of proteins by ultrafiltration through sorptive and non-sorptive polysulfone membranes and found that proteins interact differently with both the membranes, and flux and protein rejection was a function of the solution ionic strength, protein concentration, pH, and the prior history of membrane exposure to protein solutions. Blanpain-Avet *et al.* (1999) investigated fouling mechanisms and protein retention at laboratory scale for the microfiltration of a clarified beer and found that protein retention level throughout the filtration was found to be closely related to the nature of fouling. Almécija *et al.* (2007) studied the effect of pH on whey protein fractionation by ceramic ultrafiltration membranes. The authors noted that pH had a significant effect on protein retention. Retentate yield for α-lactalbumin ranged from 43% at pH 9 to 100% at pH 4, while β-lactoglobulin, ranged from 67% at pH 3 to 100% at pH 4. Atra *et al.* (2005) verified the applicability of ultra and nano filtration membranes for whey protein and lactose utilization with help of membrane flux and protein retention values.

For crude protein solutions identifying individual proteins is difficult and requires a series of isolation and purification techniques. Neyestani *et al.* (2003) used a series of separation and purification techniques which included gel filtration and anion exchange chromatography to isolate α-lactalbumin and β-lactoglobulin from whey samples. The isolated proteins can further be verified by their molecular weights using gel electrophoresis. Liang *et al.* (2005) isolated whey proteins from raw milk by serial defatting, casein elimination, lactose removing, and separating by gel filtration chromatography. They used SDS-PAGE electrophoresis to measure the molecular weight range of the isolated proteins.

Chapter 3 Materials and Methods

3.1 Membranes and Their Preparation

3.1.1 Commercial Ultrafiltration Membrane

The ultrafiltration membrane used for the study was an industrial PES membrane with a low molecular weight cut off of 10 kDa (HYT membrane, Koch Membrane Systems, Massachusetts, USA) used in food and dairy industry. The membrane element consisted of a number of membrane envelopes wound together around a central tube as shown in Figure 3.1 Each envelope consisted of two membranes (0.18 ± 0.01 mm thick) glued back to back at the ends and separated by a permeate spacer.

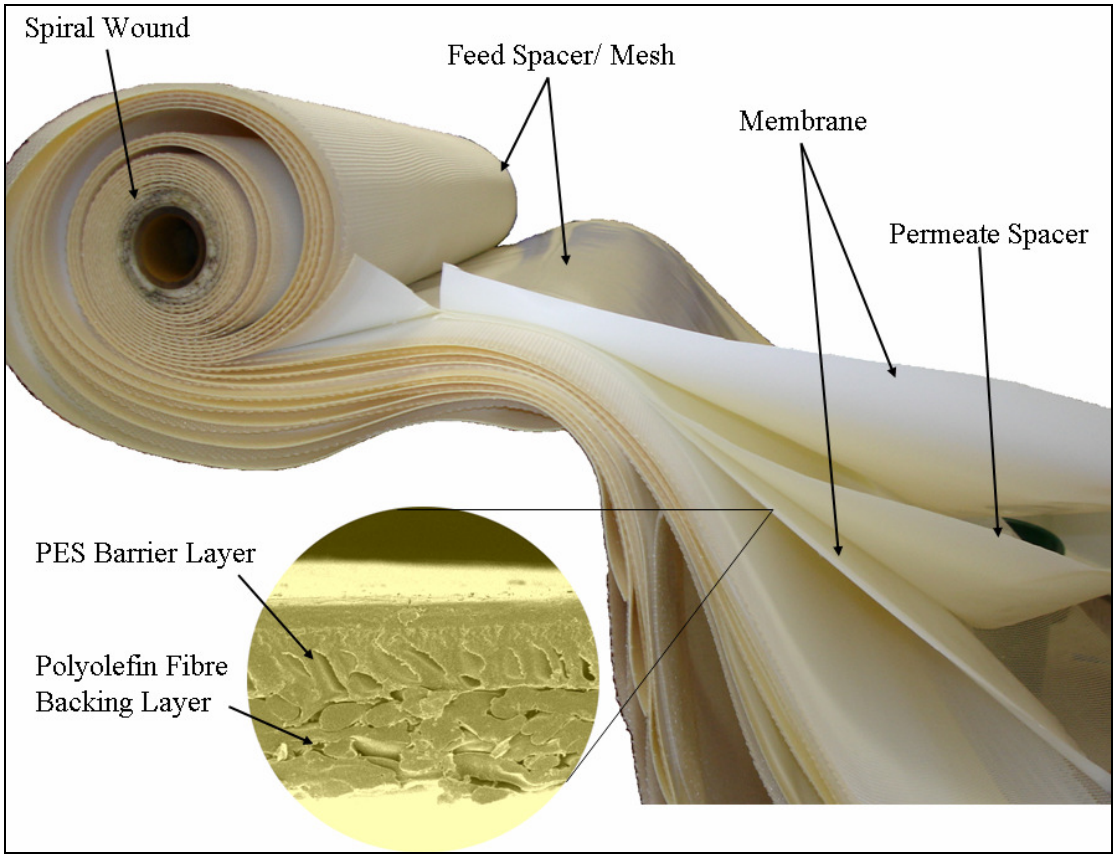

Figure 3.1 Details of PES ultrafiltration membrane (HYT membrane, Koch membrane system)

Each envelope was separated by a feed spacer. The spiral was cut open and flat membrane sheets were cut out for analysis. The flat sheet consisted of a semi-

permeable PES barrier layer on a backing made of non-woven polyolefin fibres. The purpose of backing was to provide mechanical support to barrier layer. The new membrane element came stored in glycerine to prevent membrane pores from drying out. A thorough cleaning of membrane was necessary to wash out glycerine from the membrane pores before any further experimentation.

Cleaning of Membrane

The membranes were thoroughly washed under running water for 5 minutes to remove all the surface glycerine. Then they were cut into a size suitable to fit in the lab scale ultrafiltration unit (Sepa CF Membrane cell, Osmonics, MN, USA). A single membrane was placed inside the ultrafiltration unit and was sealed inside the cell with a hydraulic pressure of 5 bar gauge. Figure 3.2 shows the details of the membrane cleaning system used. Water was passed through the membrane at 1 bar gauge for 20 minutes to flush out glycerine from the membrane pores. The clean membranes were then stored in purified water from a Millipore water purification system (Elix-5, Millipore, USA) for 24 hrs in an effort to diffuse out traces of any remaining glycerine.

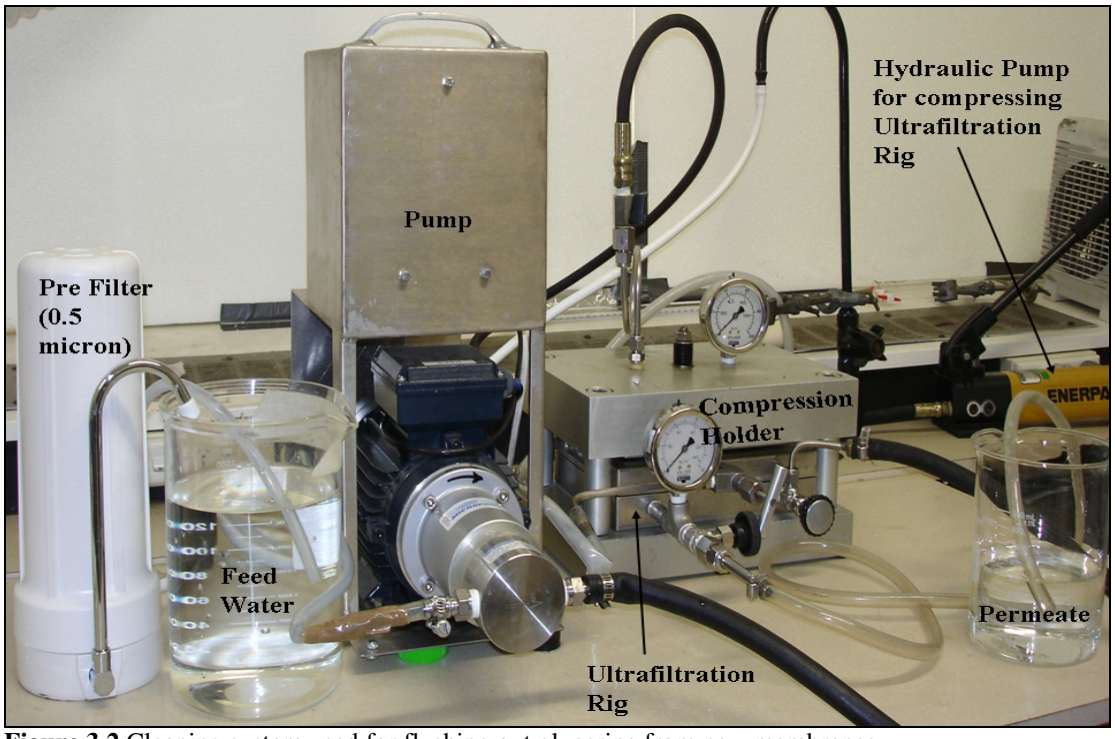

Figure 3.2 Cleaning system used for flushing out glycerine from new membranes

3.1.2 PES Sheet/Foil

Since ultrafiltration membrane is a porous material, it was important to know the effect of porosity of membrane on variation in thermo-mechanical and surface properties measurements. It was decided to measure the dynamic mechanical properties, streaming potential and contact angle on non-porous PES sheet and compare the results with the properties measured for the commercial ultrafiltration membrane. A thin PES film was also tested for dynamic-mechanical properties.

The PES sheet (Ultrason E 6020P, BASF, Ludwigshafen, Germany) obtained was non-porous with a thickness of 0.25 ± 0.002 mm.

The thin PES film (SU301025, Polyethersulphone Film, Good Fellow Cambridge Ltd., Huntington, England) was non-porous, clear amber in colour with a thickness of 0.03 ± 0.005 mm. PES film was tested to examine the effect of thickness on the DMA response.

Cleaning of the Sheet and Foil

Sheets and foils were washed under running water and were soaked in household detergents to remove any surface oil and dirt. They were then thoroughly washed and stored in purified water till further used. PES foils were very thin and care was taken not to wrinkle them as this might affect DMA results.

3.1.3 Commercial Ultrafiltration Membrane Backing Layer

Due to the double structure of the commercial ultrafiltration membrane (Koch, International), any of the bulk properties measured was a combined property of the double layer. Due to this it was difficult to detect changes in the properties of individual layers with hypochlorite degradation. For a better understanding of degradation of the membrane, it became essential to study the bulk properties of each layer separately in addition to the properties of membrane as a whole.

Initially, efforts were made to manually peel off the PES layer from the backing layer, but this could not be done easily. A new method of selectively dissolving out the PES layer in a solvent was developed to obtain the backing layer.

- Clean ultrafiltration membrane was soaked for 15 min in excess anhydrous 1-methyl-2-pyrrolidinone (NMP) to selectively dissolve the PES layer of the membrane. After 15 minutes the solvent was discarded and PES depleted membrane was again soaked in excess NMP for 15 minutes to obtain PES free backing layer.
- It was not possible to wash out NMP from the backing layer using water as water acts as a coagulating agent for NMP-dissolved PES. Any dissolved PES in residual NMP (entrapped in the backing layer) would re-coagulate when it comes in contact with water. Therefore the backing was centrifuged (Heraeus, Multifuge 3L, Kendro Laboratory Products, Germany) at room temperature at 2500 rpm for 15 minutes in specially made cage type centrifuge cell as shown in Figure 3.3.
- After centrifugation the backing layer was kept in a vacuum oven at 60ºC over night to remove any traces of solvent left. The backing was microscopically examined (Leica Stereoscan S440, Scanning Electron Microscope) for any traces of PES on the backing surface and then stored in a polyethylene bag in a desiccator.

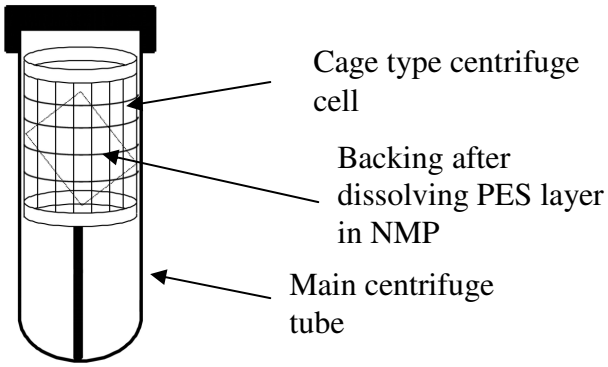

Figure 3.3 Centrifuge cell made for removing solvent from backing layer

3.1.4 PES Microfiltration Membrane

To analyse the effect of hypochlorite on the mechanical properties of the PES layer only, a PES 0.2 μm, microfiltration membrane (PES membrane filters, PES 029025, from Sterlitech Corporation, USA) was also tested. It was a flat sheet circular disk membrane and had a single semi-permeable PES layer with no backing material. The membranes were obtained in a dry state and were soaked in water for 24 hrs before further experimentation.

3.2 Hypochlorite Decay Experiment

Before starting the sodium hypochlorite exposure experiment it was essential to know about the chlorine decay rate with varying pH at the sanitization temperature (55ºC). A better knowledge of chlorine decay would result in a better control and less fluctuation in chlorine concentration of the solution during the hypochlorite exposure experiment. It was decided to check chlorine stability at five different pH values as shown in Table 3.1.

Table 3.1 Control conditions for hypochlorite decay experiment

Solution pH	7, 8, 9, 10, 11 and 12
Chlorine, ppm	600 ± 50
Solution temperature	55ºC
Amount of solution	1.5 L

Sodium hypochlorite solutions were prepared from dilution of a concentrated sodium hypochlorite solution (13.5% NaClO solution, Ian Coombes Ltd, NZ). The chlorine concentration was measured as "mg Cl as Cl_2 /L " as per an iodometric titration method (Clescerl *et al.*, 1999; method 4500-Cl B) and pH was measured with a pH 510, Bench pH meter (Eutech instruments Pte. Ltd., Singapore). The pH was adjusted using concentrated HCl (36%) and NaOH (saturated) solutions. Glass jars with air tight lids were selected for the experiment. The glass jars were pre-treated by exposing them to 1000 ppm sodium hypochlorite solutions overnight to remove chlorine demand of glass jar if any, which could interfere with experimental results. The solution were filled into the glass jars and kept in constant temperature water bath at 55ºC. The experiment was continued for maximum of 12 days to obtain decay

curves. The chlorine concentration and the pH of solution were measured periodically depending on the initial pH of the solution.

3.3 Hypochlorite Exposure Experiment

The cleaned membranes were soaked in sodium hypochlorite for four different exposure times ranging between 10,000 ppm-days to 25,000 ppm-days at 55°C. The conditions for hypochlorite exposure experiment are given in Table 3.2

Table 3.2 Control conditions for hypochlorite exposure experiment (all batches at 55°C solution temperature)

Batch 1 (June 2007)	
Solution pH	9, 10, 11 and 12
Exposure, ppm-days	10000, 15000, 20000 and 25000 (in 700 ± 50 ppm hypochlorite solution)
Batch 2 (May 2008)	
Solution pH	9, 12
Exposure, ppm-days	10000 (in 700 ± 50 ppm hypochlorite solution)
Batch 3 (Dec 2008)	
Solution pH	9, 10, 11 and 12
Exposure, ppm-days	10000, 15000 and 20000 (in 700 ± 50 ppm hypochlorite solution)

The solutions were made 750 ppm initial concentration and replenished again when concentration decreased to ~ 650 ppm so that the average concentration for every replenishment remained around 700 ppm. The solution preparation and condition control was the same as for the hypochlorite decay test (Section 3.2). After exposure the membrane was taken out carefully and rinsed with running tap water for 5 minutes and then soaked in purified water overnight to leach out any residual chlorine entrapped in the membrane. All the prepared membrane samples were then stored in oxygen depleted water in an air tight container. The oxygen depleted water was obtained by purging nitrogen gas in pre-boiled water under partial vacuum for 1 hour.

3.4 Characterization Techniques

The bulk properties of the membranes were measured with DMA, TGA, and tensile testing. Surface chemistry of the samples was analysed by FTIR-ATR and FESEM-

EDS. Contact angle and liquid absorption measurements were used to study surface-liquid interaction changes. Zeta potential measurement was used to study changes in surface charge of the membranes. A unique surface colour measurement test was used to analyse the change in colour of the various sample surface after high temperature treatment and to correlate colour change with the hypochlorite exposure of the membrane. Liquid-liquid porosimetery, protein separation test (using casein whey as feed), cross-flow flux test were done to analyse the change in separation properties of the membrane with exposure to hypochlorite solution at various conditions.

3.4.1 Dynamic Mechanical Analysis (DMA)

Viscoelastic properties of the membranes were examined using a Diamond DMA, Dynamic Mechanical Analyzer (Perkin Elmer, USA). The tensile storage modulus, E', the tensile loss modulus, E" and the ratio of the loss and storage modulus, tan δ, were measured under tensile mode. The temperatures at the tan δ peaks were assigned as the glass transition temperatures for polymers in the membranes (Menard, 2008).

3.4.1.1 Samples

Commercial ultrafiltration membrane (Koch), backing layer, PES sheet, PES film and PES microfiltration membrane (Sterlitech), each untreated and with 10,000 ppm-days hypochlorite exposure at pH 9 and 12 were tested to detect any change in dynamic mechanical properties. Also Koch membranes with 25000 ppm-days hypochlorite exposure at pH 9 and 12 were tested and results were compared with Koch membrane pH 9 and 12, 10,000 ppm-days exposed samples. All the samples were cleaned as per Section 3.1 and then dried in a vacuum oven at 60°C overnight before testing.

3.4.2.2 Procedure

All the samples were analyzed under tensile mode. DMA test conditions for various samples are summarized in Table 3.3.

Table 3.3 DMA test conditions for PES membrane and PES sheet/film samples

	Commercial Ultrafiltration membrane, HYT, Koch	**Backing Layer**	**Microfiltration Membrane, Sterlitech**	**PES Sheet, Ultrason E 6020P, BASF**	**PES Film, GoodFellow**
Exposure conditions tested					
Hypochlorite Exposure pH (for 10,000 ppm-days exposed samples)	New, 9 and 12	New, 9 and 12	New, 9 and 12	New, 9 and 12	New, 9 and 12
DMA testing conditions					
Specimen geometry (length, mm x width, mm)	20 x 7	20 x 7	10 x 7	20 x 7	10 x 7
Load Setting	Force amplitude default value = 2000 mN Tension force minimum = 10 mN Tension force gain = 1.5 Distance (L) amplitude μm = 10	Force amplitude default value = 400 mN Tension force minimum = 10 mN Tension force gain = 1.5 Distance (L) amplitude μm = 5	Force amplitude default value = 2000 mN Tension force minimum = 10 mN Tension force gain = 1.5 Distance (L) amplitude μm = 10	Force amplitude default value = 2000 mN Tension force minimum = 10 mN Tension force gain = 1.5 Distance (L) amplitude μm = 10	Force amplitude default value = 400 mN Tension force minimum = 10 mN Tension force gain = 1.5 Distance (L) amplitude μm = 5
Tightening torque, N cm	30	30	20	30	20

Temperature Program

The temperature program selected for measurement is given in Table 3.4. The starting cell temperature was fixed to 30°C to avoid any fluctuation in room temperature. The maximum temperature limit for the program was selected as 255°C, since after this temperature the sample became sticky and it was hard to remove off the tension chuck and clamp. The temperature increase rate was 2 °C/min, without holding.

Table 3.4 Temperature program used for DMA of membrane sample

S. No	Cell Temperature, Initial, °C	Cell Temperature Final, °C	Rate, °C/min	Holding Time, minutes
1	30	60	2	0
2	60	90	2	0
3	90	120	2	0
4	120	150	2	0
5	150	180	2	0
6	180	210	2	0
7	210	240	2	0
8	240	255	2	0
Temperature Program Mode			Ramp Mode	
Measured Frequency, Hz			1, 2, 5, 10	

Direction of Measurement

The direction of polymer orientation is important in determining its dynamic-mechanical properties. It can vary with the direction of sample cut from the membrane sheet. Therefore all the samples from commercial ultrafiltration membranes were cut in the direction perpendicular to the direction in which membrane curled (if there is no external stretching force applied on the membrane). The same care was taken while cutting backing layer samples. This precaution was not necessary in case of the PES microfiltration membrane (Sterlitech), PES sheet or film samples.

Tightening Torque

A uniform tightening torque was necessary on all the four screws in chuck and clamp of tension assembly, while positioning the sample in the tension attachment. This was important to prevent slippage and to have uniform clamping stress on the sample. A torque screw driver (Model: Quick Set Minor by Torque Leader, M.H.H. Engineering Company Ltd. England) was used to apply specified tightening torque as shown in Table 3.3.

The samples were carefully cut with a fine blade to produce smooth, defect free edges. The sample was then placed in the DMA tension probe and clamps were tightened uniformly. The standard DMA measurement procedure was followed according to Perkin Elmer (2002). For the step by step procedure please refer to Appendix 1.1.

3.4.2 Thermogravimetric Analysis (TGA)

Thermogravimeteric analysis was carried out using a TGA, SDT-Q600 (TA Instruments, USA). In most cases, TGA analysis is performed in an oxidative atmosphere (air or oxygen) with a linear temperature ramp.

3.4.2.1 Samples

Commercial ultrafiltration membrane (Koch): new, pH 9 and pH 12 (10,000 ppm-days and 25,000 ppm-days hypochlorite exposure) were tested to study the effect of exposure time on the thermal degradation of membranes. Microfiltration membranes (Sterlitech): new, pH 9 and pH 12 were tested for 10,000 ppm-days exposure to study the thermal degradation of PES without any backing polymer. All the samples were cleaned as per Section 3.1 and then dried in vacuum oven at 60°C overnight before testing. The samples were then cut into small pieces to fit in the TGA instrument pan.

3.4.2.2 Procedure

The samples were analysed from room temperature to 700°C at a heating rate of 10°C/min, under an atmosphere of dry air with a flow of 100 ml/min. The sample size for the experiments was 10 mg. In the initial stage of each run, the sample was kept isothermally at 120ºC for 2 hours in the TGA machine to remove any traces of moisture from the sample. It was assumed that any loss in weight during the isothermal stage was due to removal of moisture. The weight obtained at the end of isothermal stage was considered as the initial weight of the sample for analysis.

Ceramic pans were chosen for the experiment as they were easy to clean with a hot flame. Clean empty pans were placed on each of the two arms of TGA microbalance

(outer arm: sample pan; inner arm: reference pan). The furnace was closed and weight was tared. The sample pan was carefully taken out and filled with shredded sample pieces. Care was taken to avoid overfilling the sample as this would give errors in degradation behaviour curve due to non-uniform heating of the sample. The pan filled with sample was carefully placed back on the microbalance arm and the furnace was started according to the specified temperature program. A TGA curve (weight loss versus temperature) was generated automatically and saved by the TGA instrument. For details of the experimental procedure refer to Appendix 1.2.

3.4.3 Tensile Testing

The Koch membrane and the polyolefin backing samples were tested with a MTS, 858 table top system (MTS Systems Corp., USA). Sterlitech membranes had very low tensile strength so the samples were tested by Diamond DMA under static testing mode.

3.4.3.1 Samples

Commercial ultrafiltration membrane (Koch), backing layer, and microfiltration membrane (Sterlitech): new, pH 9 and pH 12 (10,000 ppm-day hypochlorite exposed) samples were tested to examine any change in the tensile properties of the sample with hypochlorite exposure. All the samples were cleaned as per Section 3.1 and then dried in a vacuum oven at 60°C overnight before testing.

3.4.3.2 Procedure

For tensile testing of the commercial ultrafiltration membrane and backing layer, the MTS, 858 table top system was used. A load cell of 2.5 kN with an axial displacement of 2 mm/min was applied. Testing was done at 25ºC and a sample size of 10x30 mm was used for testing. Five measurements were performed for each sample. Since microfiltration membranes had no backing, they were very soft and fragile and hence Diamond DMA under static testing mode was used with a load cell of 1 N and an axial displacement rate of 1 μm/s. Testing was done at 25ºC and a sample size of 10x7 mm was used for testing. Five measurements were performed for each sample.

The samples were carefully cut with a fine blade to produce smooth defect free edges. The width of each sample was measured at several points along the length. The thickness of the sample was measured at several points by screw micrometer and the average value was used for calculations. The set load and axial displacement rate was selected and the test specimen was placed in the grips of the testing machine. Care was taken to align the long axis of the specimen with an imaginary line joining the points of attachment of the grips to the machine. The grips were carefully tightened with a uniform load on both the grips to a degree essential to minimize slipping of the sample during testing. After each run the load versus extension data was automatically recorded by the testing machine.

Offset yield strength (with 0.02 strain value offset), tensile strength and elastic modulus were calculated as per ASTM standard D 882-02.

3.4.4 FESEM-EDS

The surface of new and hypochlorite treated membranes was carefully examined for any surface defect produced by exposure of the membrane to hypochlorite. Surface microscopy was performed with a high resolution FESEM, JEOL JSM 7000F (JEOL Ltd., Japan). Identification of elements on the membrane surface was done with an EDS microanalysis system (JED 2300) coupled with the FESEM.

3.4.4.1 Samples

Commercial ultrafiltration membrane (Koch): new, pH 9, 10, 11 and 12 (10,000, 15,000, 20,000 and 25,000 ppm-days hypochlorite exposure) were tested to study the effect of pH and exposure time on the surface of the membranes. Microfiltration membrane (Sterlitech): new, pH 9 and pH 12 (10,000 ppm-days hypochlorite exposure) were also tested. New and pH 9, 25,000 ppm-day degraded PES foil (Good Fellow) were also analysed. In house casted PES ultrafiltration membrane was analysed to study the microscopic structure of membrane layer (For detailed casting process please refer to Appendix 1.3). All the samples were cleaned as per Section 3.1. After cleaning, samples were immersed in methanol for 15 minutes to remove any residual surface debris and then dried in vacuum oven at 60°C overnight. The

dried samples were then coated with carbon by a K975X, Turbo coater (Emitech, UK) at a pressure of 5.0 x 10^{-4} Pa and coating thickness of 20 nm. For EDS analysis an accelerating voltage of 12 kV and probe current of 0.59008 nA, 50X magnification was used. The mass fraction of each element present on the surface was recorded.

3.4.4.2 Procedure

Sticky carbon tape was fixed on a clean FESEM stage and then clean dried membrane samples were pasted on the top carbon tape. To prevent sample contamination, care was taken not to touch the sample or FESEM stage with bare hands. Air was blown on the surface of the samples to remove any dirt or impurities. The samples were than placed in carbon coater and carbon coating was done. Carbon coated samples were than placed inside the FESEM stage cell and a step by step procedure according to operating instruction for FESEM, JEOL JSM 7000F and JED 2300, EDS system was followed to take the pictures of membrane surface and to perform EDS analysis. For details refer to Appendix 1.4. For EDS data analysis the procedure described by Rabiller-Baudry *et al.* (2002) was used. The atomic composition was expressed as the ratio of each element to sulphur. The carbon peaks were not considered due to excess carbon present on the surface from carbon coating.

3.4.5 FTIR-ATR

Functional groups on the surface of new and treated membranes were identified by FTIR-ATR. The spectra was recorded by a Digilab, FT 4000, Excalibur series (Cambridge USA).

3.4.5.1 Samples

Commercial ultrafiltration membrane (Koch): new, pH 9 and pH12 (10,000 ppm-days and 25,000 ppm-days hypochlorite exposure) were tested to study the effect of exposure time on the changes of surface chemistry of the membranes. Both the PES side and backing side were tested for any change in the functional groups on the surfaces. Microfiltration membranes (Sterlitech): new, pH 9 and pH12 (10,000 ppm-days exposure) were also tested, and the change in absorption was compared with that of the Koch membrane samples. All the samples were cleaned as per Section 3.1. After cleaning, samples were immersed in methanol for 15 minutes to remove any

residual surface debris and then dried in vacuum oven at 60°C overnight before testing.

3.4.5.2 Procedure

The FTIR-ATR test parameters settings are given in Table 3.5.

Table 3.5 FTIR-ATR test condition used

Number of scans	64
Resolution	2 cm^{-1}
Sensitivity	1
Filter	1.2
Speed	kHz

The ATR cell contained a ZnSe crystal at a nominal incident angle of 45º and single internal reflection on the membrane surface. The samples were carefully placed on the crystal of ATR cell, with the side to be tested facing the crystal. The sample was fixed onto the ATR cell with a mechanical press system. The ATR cell was then placed in the FTIR instrument and whole system was closed. Then dry air was blown for 30-45 minutes under the ATR cell to remove any trace moisture which can produce artefacts in the FTIR spectra. The spectra were collected as per the standard procedure for the Digilab, FT 4000 instrument.

3.4.6 Contact Angle Measurement

A visiting research intern Gareth Thomas (Thomas, 2008) carried out many tests on contact angle and surface energy of the membranes treated as a part this research work. The drop absorption method (Section 3.4.7) was developed based on the recommendation from Thomas in his report.

Contact angle and surface energy measurements were done by an optical contact angle and surface tension meter (CAM 200, KSV Instruments, FL). The main parts of the instrument are shown in Figure 3.4. The most important part of the instrument was a high performance digital CCD fire-wire (IEEE 1394) camera and optimized background illumination. If an image is out of focus the camera can be moved forward or backwards of rail for adjustment. The instrument was connected to a computer and CAM contact angle software was used to calculate contact angle of the

drop. The drop delivery system consisted of a syringe mounted into a micrometer which was connected to a drop needle by flexible tubing. Also the instrument had a height adjustment mechanism to adjust the height of the drop needle. The drop needle system was mounted on a clamp stand on the instrument and the height of the needle could be adjusted accordingly.

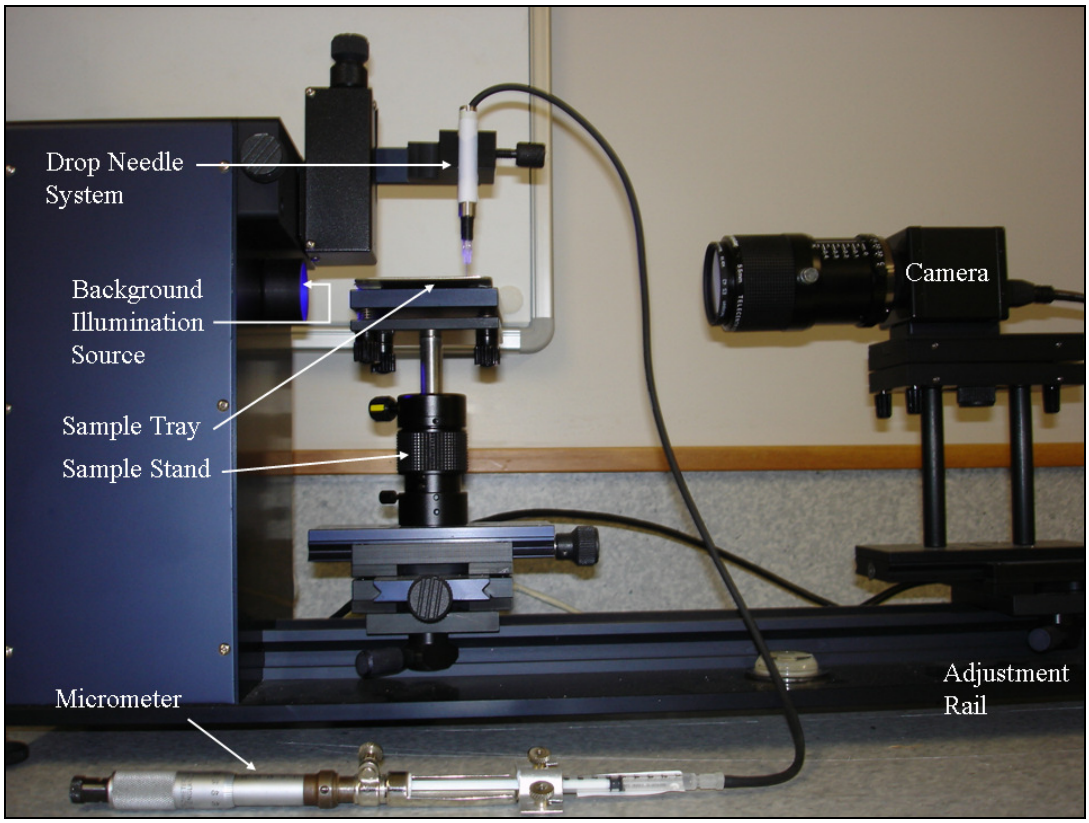

Figure 3.4 Details of contact angle measurement apparatus

3.4.6.1 Samples

Following samples were analysed for contact angle measurements

- PES sheet: new pH 9 and pH 12 (10,000 ppm-days sodium hypochlorite exposed samples),
- PES film: new pH 9 and pH 12 (10,000 ppm-days sodium hypochlorite exposed samples),
- Commercial ultrafiltration membrane, (Koch): new pH 9 and pH 12 (10000 and 25,000 ppm-days sodium hypochlorite exposed samples)

Test Liquids

The test liquids used were:

- Purified water (Millipore water purification system, Elix-5, Millipore, USA)

- Formamide (BDH Chemical, 99.5%)
- Glycerol (BDH Chemical, 99.5%)
- Methylene iodide (BDH Chemical, 99.5%)

All the samples were cleaned as per Section 3.1. After cleaning sample were immersed in 1% sodium hydroxide for 15 minutes and rinsed by purified water. Then the samples were immersed in methanol for 15 minutes and again washed with purified water. This extra cleaning step was done in an attempt to remove any residual surface debris. The samples were then dried in vacuum oven at 60°C overnight. The commercial membrane samples had a tendency to curl during drying so extra weight was put on the corners of the membrane during drying to keep the membrane flat. The dried samples were pasted on a sample tray which was a steel plate, with help of double sided sticky tape. Extreme care was taken not to contaminate the surface of the membrane during pasting or applying pressure on the surface to get better adhesion. The membrane edges which were not sticking properly were carefully cut with scalpel to leave behind a flat surface.

3.4.6.2 Procedure

The sample tray was mounted on the instrument analysis platform. The liquid transfer system was screwed into the position as in Figure 3.4. The relevant variables, i.e. liquid used and its properties, were selected from the software database. As soon as experiment was initiated, the camera was switched on and the image of needle and the surface appeared on the computer screen. The camera focus was adjusted to see a clear drop and the height of the needle was adjusted. A liquid drop was carefully dropped on the surface and instantly contact angle of the liquid drop was measured with help of CAM software. The contact angle measurements were done at room temperature, i.e. 20 ± 1°C and drop size for each run was ~ 8μL

3.4.7 Drop Absorption Test

A liquid drop absorption test was performed on new and hypochlorite treated commercial ultrafiltration membranes. As soon as the test liquid drop touched the membrane surface, the membrane started absorbing the liquid, resulting in a change in

contact angle with time which was measured by an optical contact angle as per previous section.

3.4.7.1 Samples

Commercial ultrafiltration membrane (Koch) samples with the following exposure conditions were tested: new, pH 9, pH 10, pH 11 and pH 12 (5,000, 10,000, 15,000 and 20,000 ppm-days sodium hypochlorite exposed sample for each pH). The test liquid used for the test was 20% (w/w) methanol solution.

All the samples were cleaned as per Section 3.1. After cleaning, samples were immersed in methanol for 15 minutes and stuck on a glass plate using double sided sticky tape. The surface was covered with lint free tissue paper to prevent any surface contamination. Samples where then dried in vacuum oven at 60°C overnight. The apparatus setup for the experiment and the precautions followed during sample preparation were same as for Section 3.4.6.

3.4.7.2 Procedure

The procedure followed for the test was same as for Section 3.4.6.2 with only one change. Instead of recording a single frame, the camera was set to record multiple frames at fixed time interval of 10-60 seconds till the test liquid drop was completely absorbed in the surface or the contact angle became too small (< 10°, depending on background resolution) to be measured by the CAM 200 software.

3.4.8 Zeta Potential

The zeta potential of the membrane surface was determined using an electro-kinetic analyzer (EKA, Anton Paar, Austria), which adopted the streaming potential method for surface charge analysis. This instrument, which was situated in Department of Chemical Science and Engineering, UNSW, Sydney, included an analyzer, a measuring cell, electrodes, and a data control system. The analyser controlled a mechanical drive unit which produced and measured the pressure needed to pump the electrolyte solution from a reservoir into and through the measuring cell. The temperature and conductivity of the solution were automatically measured by in-built

sensors and pH was measured externally. The measuring unit consists of a rectangular cell in which the solution passes along a channel formed by two layers of the sample separated by an inert spacer as shown in Figure 3.5.

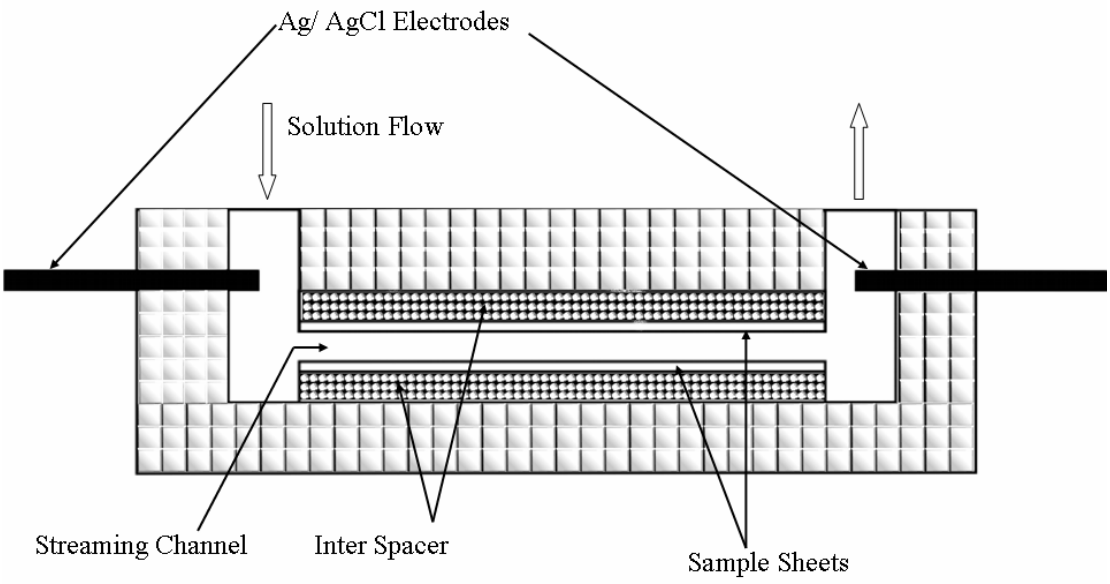

Figure 3.5 Schematic diagram of streaming potential measuring cell (EKA, Anton-Paar)

Ag/AgCl electrodes at each end of the channel were used to determine the potential generated by the flow. Additionally, the electrodes were stored in 0.01 M KC1 solution overnight to prevent any build-up of charge. The zeta potential measurement was carried out using a solution of 1 mM KCl at pH values ranging from 2 to 10 and at temperature close to 25°C.

3.4.8.1 Samples

Following samples were analysed for zeta potential measurements

- PES sheet: new, pH 9, pH 10, pH 11 and pH 12 (25,000 ppm-days sodium hypochlorite exposed samples)
- Commercial ultrafiltration membrane (Koch): new, pH 9, pH 10, pH 11 and pH 12 (25,000 ppm-days sodium hypochlorite exposed samples)

The samples were soaked in 50% ethanol solution for 15 minutes to remove any surface deposits which may interfere with zeta potential measurements. Samples were then thoroughly washed with purified water and soaked in 1 mM KCl solution overnight at 10°C to stabilise the surface charge of the samples before any further testing.

3.4.8.2 Procedure

The internal flow system of the instrument along with the tubing was rinsed with purified water with two rinse cycles each for the bypass system (for 20 s) and for the cell side (for 50 s). The pH electrode was calibrated every day before starting any run on the machine. The sample was carefully placed in measuring cell and clamped tightly to prevent any leakage. Care was taken not to touch the samples with bare hands. Once the measuring cell was fitted back in the system and the Ag/AgCl electrodes connected to the cell, the streaming channel was rinsed again with purified water to remove any surface contamination. After rinsing, the solution was changed to 1 mM KCl, rinsed again and then measurements were performed. The pH of solution was increased and decreased step by step and zeta potential measurements were taken. At the end of run the whole system was rinsed with purified water 5 times and the electrodes were stored in 1 mM KCl solution.

3.4.9 Liquid-Liquid Displacement Porosimetery (LLDP)

LLDP experiments were performed using an in-house designed and fabricated LLDP apparatus. Hence a part of LLDP characterization techniques was to design and fabricate LLDP apparatus which can work on wide range of pressure conditions and give stable flux reading even for very small volumes of fluid handled. It was decided to design a membrane holder that could handle pressure of 1-50 bar, and the fluid sample cylinder with maximum fluid volume of 500 ml. The small ultrafiltration rig would benefit by handling small volumetric flow rates, which was essential to decrease the test fluid volumes needed for each experimental run.

3.4.9.1 Design Consideration

The membrane holder and the sample cylinders were considered as pressure vessels. The membrane holder plates were designed by considering them as flat circular plates of constant thickness and the sample cylinders were considered as shells under internal pressure. Designing was done according to ASME Boiler and Pressure Vessel Code, 2004. All design calculations were done with a minimum safety factor of 2.9. The design drawings were made in Solid Works 2006 SP5.1 software package. To

cross check the safety factor, a stress analysis was also performed on both the plates of the ultrafiltration rig using "COSMOSXpress" stress analysis tool present in Solid Works package. All the valves and fitting used in apparatus were Swagelok stainless steel pressure fittings (Swagelok Fluid System Technologies, New Zealand). For details of design calculations and apparatus detailed diagrams please refer to Appendix 1.5.

Apparatus

Figure 3.6 shows details of the equipment setup for LLDP experiment. The main parts of the apparatus were as follows

- Membrane holder
- Pressure source
- Sample cylinders
- Bubble removal system
- Data acquisition system
- Weighing system

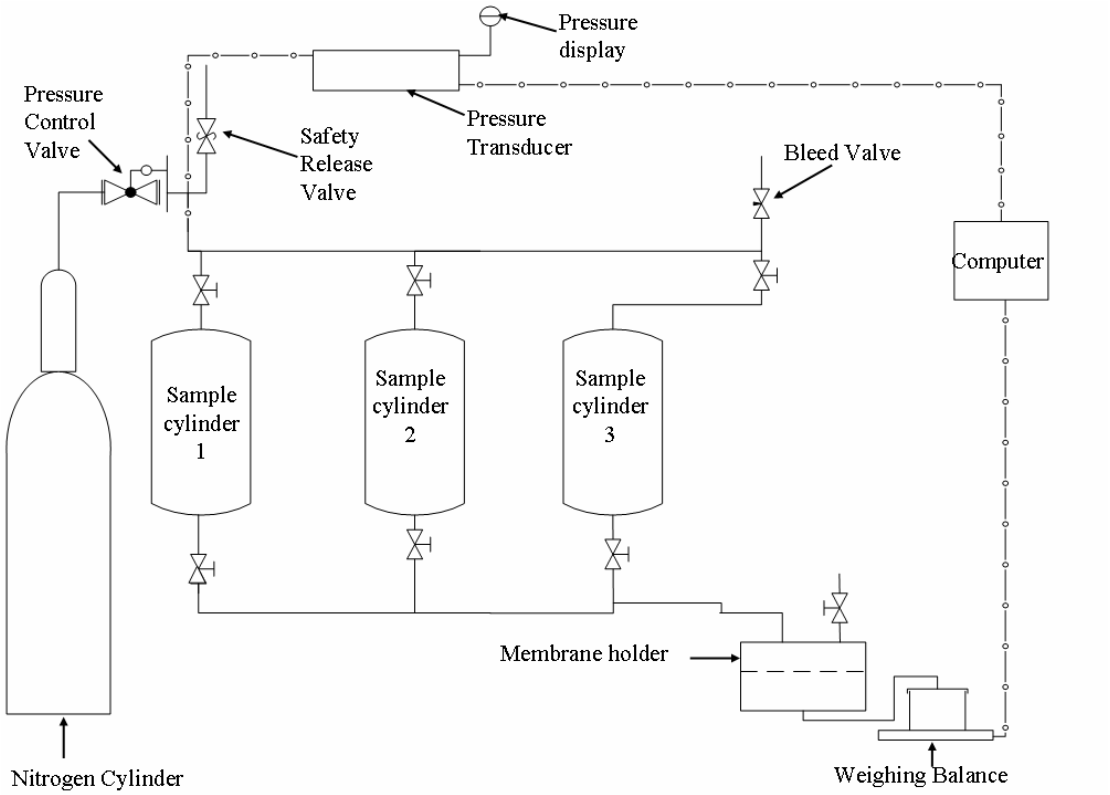

Figure 3.6 Process flow diagram of LLDP apparatus

Membrane Holder

The holder consisted of two stainless steel plates and the membrane was placed in between the plates. Each plate had a 50 mm (diameter) internal circular slot to accommodate the membrane and to provide the fluid volume necessary for flow to pass through the membrane. Each plate had six equi-distance holes for the bolts. The two plates were sealed with an o-ring and the force, necessary for sealing was applied by tightening six bolts with the help of a torque wrench. The feed side plate had two holes (2 mm in diameter) drilled near the circumference of the circular slot, one as inlet for liquid and the second hole for liquid by pass used only for removing air bubbles (Figure 3.7a). During the LLDP runs the liquid bypass outlet was always closed and system acted as a dead end filtration system. The permeate side disc had a single hole (2 mm in diameter) bored in the centre for permeate outlet. A sintered stainless steel disc was fitted on the permeate side plate, which provided support to the membrane and uniform flow of permeate to the permeate outlet (Figure 3.7b).

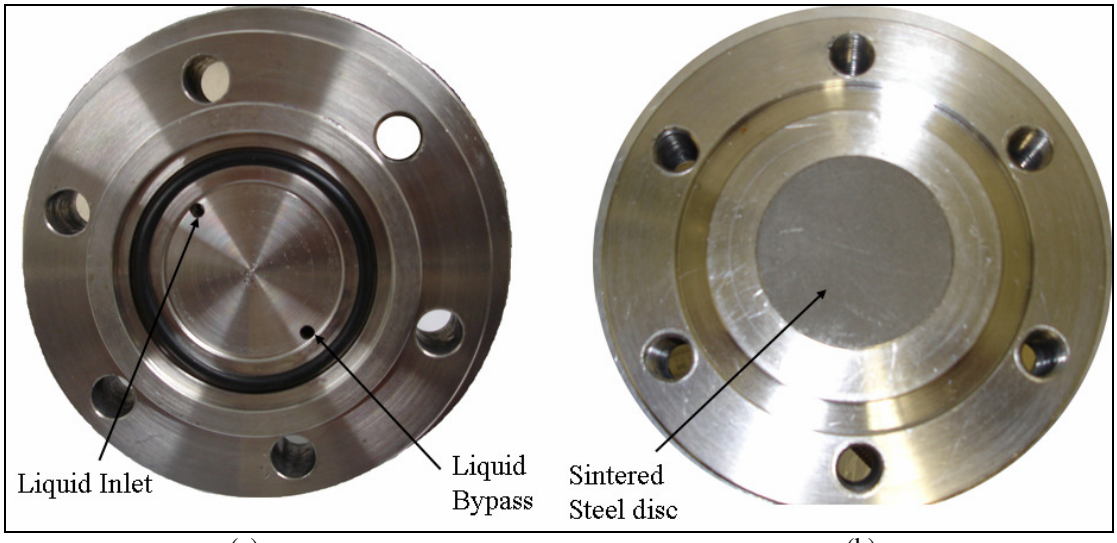

Figure 3.7 Membrane holder plates (a) Feed side plate (b) Permeate side plate

Pressure Source

Pressurised nitrogen was used to provide high pressure necessary for flow through the membrane. Nitrogen had the benefit of providing instantaneous pulse free pressure. The nitrogen gas pressure was controlled by a precise needle valve and simultaneously the pressure signal was transmitted to a computer by a pressure transducer (Model: 1001K-06, Paroscientific Inc, USA). Also a digital pressure

display was attached to pressure transducer for ease of opertaion. For safety purposes a safety release valve (50-100 bar) was installed in the main incoming nitrogen line.

Sample Cylinders

Three stainless steel sample cylinders with internal volume of 300-500 ml were connected to the main liquid line to ultrafiltration rig. The first cylinder was allocated for cleaning liquids, i.e. purified water or methanol. The second cylinder (500 ml internal volume) was allocated to wetting liquid and the third cylinder (300 ml internal volume) was allocated to displacement liquid. All the cylinders were also connected to a gas bleed valve to release the pressure inside the cylinder after every run.

Weighing System

The permeate line from the membrane holder was connected to a collector which was placed on weighing balance with measuring capacity ranging from 0.1 mg to 320 g (Model no: CP324S, Saratorius AG, Germany). The weight signals were simultaneously sent to the computer with a sampling time of 5 s.

Air Removal System

Entrapped air in the empty volume of the membrane holder can hinder the accurate recording of the permeate flow values by pushing air bubbles through the membrane pores. At the start of each run, once the membrane was fitted inside the cell it was necessary to remove this entrapped air before the start of flow measurement. For this the membrane holder was fitted on a special frame, which could be rotated 90° on either side to facilitate removal of air bubbles as shown in Figure 3.8. The frame was tightened to the main shaft by a screw type frame tightner, which will tighten the frame at any rotation angle needed. Also a simple angle measurement scale was placed behind the frame to measure the specific position of rotation of membrane holder. The liquid bypass outlet of the rig was connected to a valve which could be opened for the liquid to bypass the system without passing through the membrane. Flexible steel tubing was attached from the main line to membrane cell to allow membrane holder to rotate.

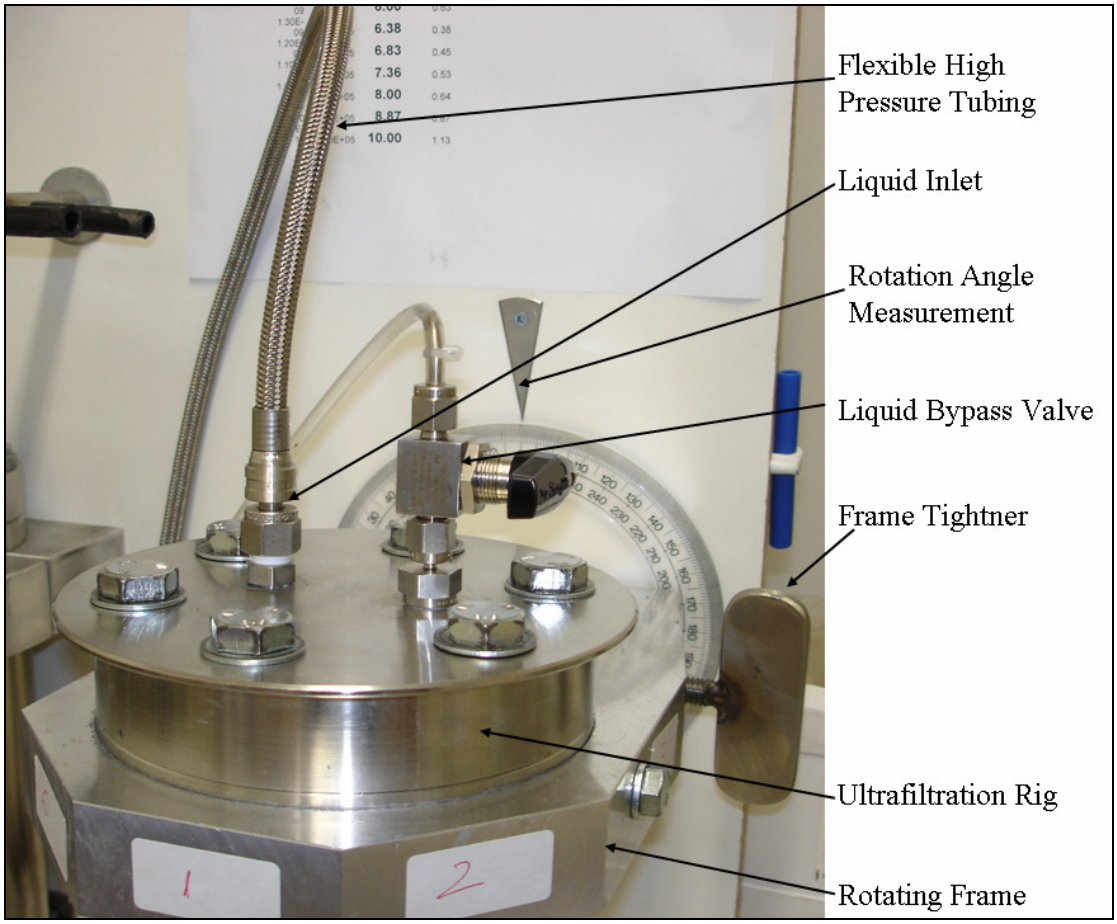

Figure 3.8 Close view of air bubble removal system

Data Acquisition

Signals from pressure transducer and weighing balance were simultaneously logged in the computer via a Visual Basic program. The sampling time for data acquisition was fixed to 5 s. The program calculated and displayed time, weight, pressure, and flux for each sampling point. It also simultaneously saved the data in a text file.

Figure 3.9 shows the LLDP apparatus installed in laboratory. The whole laboratory was insulated and the temperature of the room was maintained at 20±1°C.

3.4.9.2 Samples

Commercial ultrafiltration membrane (Koch): new, pH 9 10,000 ppm-days hypochlorite exposed samples were tested to analyse the validity of the LLDP test with these membranes.

Liquid Used

- Water used for the experiments was purified water, from the Millipore purification system (Elix 5)
- Mixture of isobutanol/methanol/water (15:7:25) (v/v/v)

The alcohol mixture was prepared and poured into a separating funnel, shaken vigorously, and left to stand overnight. The alcohol rich phase is lighter than water rich phase so the two phases separated out and water rich phase was extracted by draining it out from the stopcock at the bottom of separating funnel. One phase was used as the wetting liquid and other as the displacement liquid.

Prior to each experiment methanol was passed through the membrane at 2 bar absolute for 15 minutes. This step was necessary to negate the effect of alcohol on flux values during LLDP experiment. Membrane surface was rinsed with water and then water was passed for 30 minutes at 2 bar absolute to remove methanol from membrane pores.

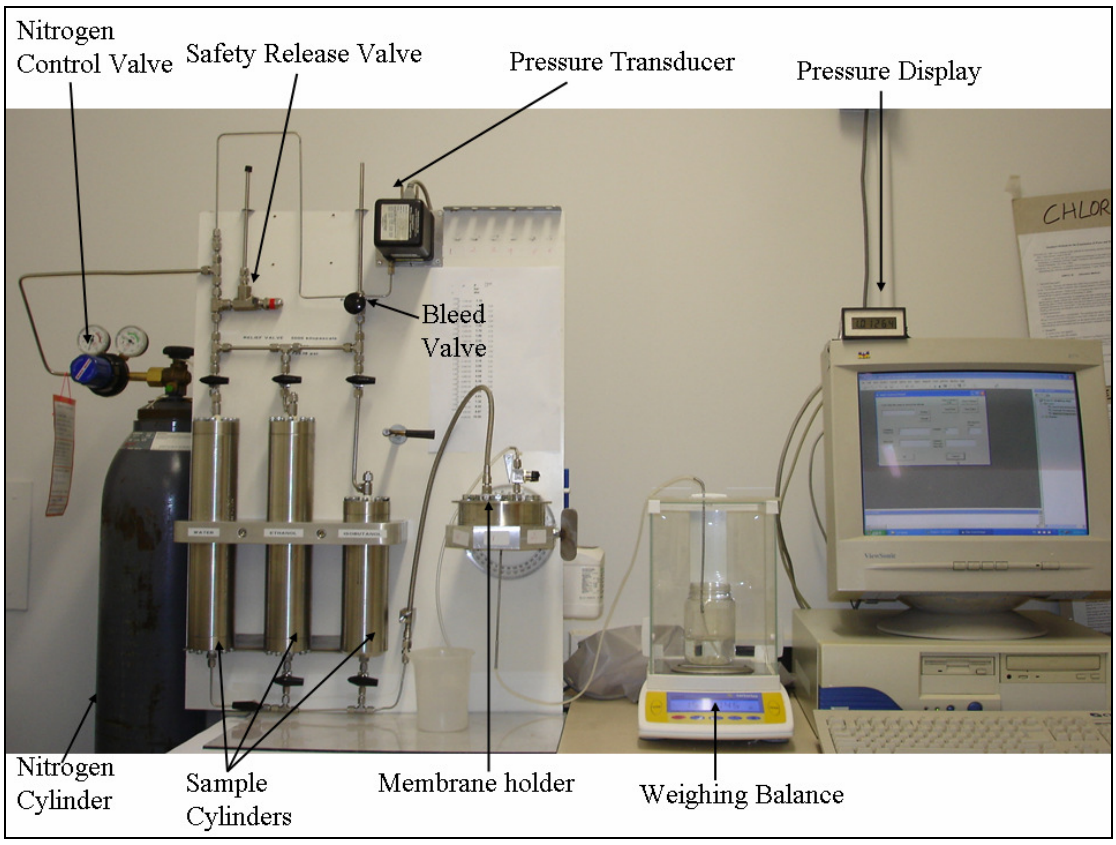

Figure 3.9 LLDP apparatus installed

3.4.9.3 Procedure

The membrane was cut into circular disc of 60 mm in diameter and placed on the permeate side plate. The feed side plate was carefully placed on the top and bolted together with permeate side plate, with a uniform pressure applied by a torque wrench (54 N-m). Once the membrane was fitted inside the membrane holder the first step was to remove the air bubbles.

Air Bubble Removal

The membrane holder was rotated by 90° clockwise, so that bypass outlet was toward the top and feed inlet at the bottom. The rig was tightened at this position. The bypass valve was opened and slowly the pressure was applied to have a flow through the bypass line. The air bubbles present in the system were pushed out with bypass liquid stream. The liquid was allowed to flow till no more air bubbles were detected in the bypass line. The bypass valve was closed and the pressure was reduced to normal atmospheric pressure to stop the flow. The membrane holder was loosened and rotated back to 0° position and tightened firmly. This procedure was followed only once, at the start of each run.

Compression Testing

During LLDP runs the membranes tended to compress under high applied pressure so it was essential to study the effect of compression on membrane permeance (flux/pressure) which may affect the LLDP results. To analyse this compression, a run was performed on a new ultrafiltration membrane. The membrane was subjected to a pressure of 2 to 10 bar absolute and relative flux values for purified water were measured. Once the run was finished the pressure was released and a second repeat run was performed.

LLDP Measurement

The methanol treated flat membrane pieces were cut into circular disc 60 mm above in diameter and placed in LLDP filtration cell. The surface of the membrane was again rinsed with purified water. The membrane was wetted with the “wetting liquid” by passing it through the membrane at 2 bar absolute for 20 minutes to make sure that all membrane pores are in a wetted state. The flow was then changed from wetting

liquid to displacement liquid and a run was done using a sequence of pressures 1.18 to 10 bar abs to obtain a broad spectrum of flux versus pressure measurements. At the end of each run, the pressure was released via bleed valve and membrane holder was opened. The membrane was taken out and the system was closed back for cleaning. The whole system was cleaned by passing 100% methanol for 10 minutes and then purified water for 10 minutes. Data obtained was further evaluated for calculating pore size distribution according to method described by Morison (2008).

3.4.10 Cross-flow Flux Measurement

A variety of salt solutions and alcohols were passed through the new and hypochlorite exposed commercial ultrafiltration (Koch) membranes and respective flux was measured by the AKTA Crossflow® (GE Healthcare Biosciences AB, Sweden). The AKTA Crossflow® was a fully automatic membrane filtration system. It provided uniform trans-membrane pressure (TMP) and simultaneously measured retentate, permeate and feed flow rates. At the same time it also measured the pH and UV absorption values for the permeate stream. A special perspex ultrafiltration rig was made for the experiment. The rig had 100 mm x50 mm active area for membrane filtration. Figure 3.10 shows the details of the apparatus setup used for the flux test. All flux values were measured at 20°C, TMP of 1 bar and a feed flow of 50 ml/min. All the membrane samples were cleaned as per Section 3.1 and stored in purified water before testing.

3.4.10.1 Sample

Water flux test was performed on commercial ultrafiltration membranes (Koch): new, pH 9 and pH 12 (10,000 ppm-days hypochlorite exposed) samples. New membrane samples were exposed to 0.1% NaCl, 0.1% $MgCl_2$ and 0.1% Al_2Cl_3 by passing these test liquids through the membrane at 1 bar TMP for 30 minutes. Simultaneously the flux value for each test liquid was measured. A similar experiment was performed with methanol, ethanol and iso-propanol as test liquids. Clean water flux was measured before and after each exposure and the values were compared to analyse the effect of cations and alcohol on water flux values. The idea behind this study was that the ions may alter the surface charge of the membrane and hence may change the

water flux values for the membrane. On the other hand alcohol may affect the water flux values by forming hydrogen bonds with water with the membrane.

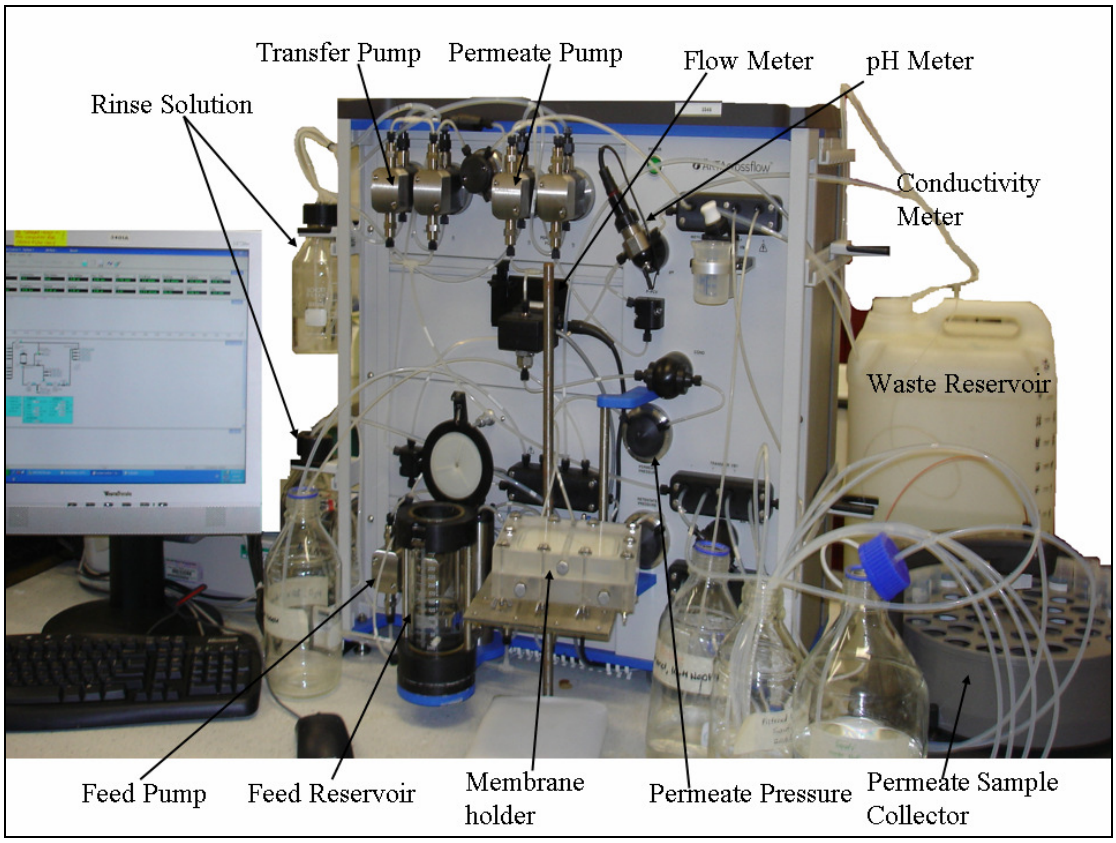

Figure 3.10 Fully automatic membrane filtration systems, Akta Crossflow, GE Healthcare

3.4.10.2 Procedure

Before any testing, the AKTA Crossflow system was rinsed with 0.01M NaOH and 20% ethanol solution and the level sensor was calibrated. The transfer, feed and permeate pumps were made active (switched on) and respective valves were opened. The TMP was set to 1 bar and the feed flow was set to 50 ml/min. A clean wet membrane was cut into a 110 mm x 60 mm rectangular piece and placed inside the membrane holder. The membrane holder was connected to the system by connecting corresponding permeate, feed and retentate ports. The reservoir was filled with water and the run was started. Although the system started collecting the flux values immediately, the flux after 15 minutes of running was used for analysis, because the system took around 5-10 minutes to attain the desired TMP value. After measuring the water flux values the run was stopped and the running liquid was changed to the test liquid (i.e. salt solution or alcohols) and the run was started again. At the end of

an exposure time of 30 minutes, the remaining test liquid was discarded to the waste reservoir and whole system was thoroughly rinsed with water at least four times to wash of the test liquid from the surface of the membrane and reservoir. The reservoir was refilled with water and the system was allowed to run for 30 minutes to remove test liquid from the pores. The clean water flux was measured again. Once the run was finished the test liquid was discarded and the system was rinsed four times with water. After the water rinse the system was rinsed once with 30% ethanol and at the end of the rinse the feed reservoir was emptied and system was shutdown.

3.4.11 Protein Separation Test

Whey protein separation was studied to check the separation performance of new and hypochlorite exposed membranes. The membrane studied is mainly used for whey protein separation from cheese whey in industry so the following test was a more realistic approach to membrane characterization in industry. α-lactalbumin and β-lactoglobulin were selected as the target protein for the study. The whey was passed through the membrane using Akta Crossflow (for details of the instrument please refer to Section 3.4.10) and the corresponding permeate flux was recorded to study membrane throughput. The feed, permeate and retentate were collected and further analysed for protein identification by size exclusion chromatography (Akta Explorer, 10, GE Healthcare Biosciences AB, Sweden). Also standard whey proteins (α-lactalbumin and β-lactoglobulin) were run on the Akta Explorer as comparison reference. Molecular weights of the whey proteins in the permeate, feed, and retentate were analysed by sodium dodecyl sulfate polyacrylamide (SDS-PAGE) gel electrophoresis. Gel electrophoresis was performed in a vertical mini-gel system (XCell SureLock Mini-Cell, Invitrogen, USA).

3.4.11.1 Samples

Protein separation analysis was performed on commercial ultrafiltration membranes (Koch): new, pH 9, pH 10, pH 11 and pH 12 hypochlorite exposed samples. Samples from all the four exposures, i.e., 5,000, 10,000, 15,000 and 20,000 ppm-days were analysed. The membrane samples were cleaned as per Section 3.1 and stored in purified water till further testing.

Whey

The milk "Meadow Fresh, Trim" for whey preparation was procured from a local supermarket. The composition of the milk used is given in Table 3.6.

Table 3.6 Composition of milk used for whey making (as per milk bottle label)

Content	Amount g/100 ml
Protein	3.7
Fat	0.4
Sugar	4.9
Sodium	0.09
Calcium	0.260

The milk was heated to 45ºC with continuous stirring and then the pH was reduced to 4.5 using 5M HCl. The casein aggregated out leaving behind clear light green whey. The whey was decanted and then centrifuged at 3200 rpm (Multifuge 3L, Heraeus Kendro Lab Products, Germany) for 30 minutes at 20ºC. Centrifuged whey was kept in a refrigerated condition at 5ºC overnight which allowed the smaller casein particles to aggregate and settle down. The next morning the pH of whey was adjusted to 7.4 at 20ºC causing calcium phosphate to precipitate. Therefore the whey was again centrifuged at 3200 rpm for 30 minutes at 20ºC. The clear whey obtained was used as the feed for membrane throughput test.

The membrane throughput test was performed using the Akta Crossflow system. The test was performed at 3 bar TMP, feed flow of 200 ml/min and feed temperature at 20ºC. The initial feed volume for each run was 150 ml and the retentate was recirculated to the feed reservoir.

Size exclusion chromatography was done using a Superdex-200 HR 10/30 column which had a molecular weight cut off range of 10 to 600 kDa. The test conditions applied are given in Table 3.7.

Gel electrophoresis was done using NUPAGE 4-12% Bis-Tris gel having 1mm x 10 wells. 3-(n-morpholino) propanesulfonic acid (MOPS) buffer was used as the running buffer and the test was carried out with a fixed voltage of 200±1 V for 30 minutes.

The loading dye used contained β-mercaptoethanol, SDS, glycerol and stain, bromophenol blue.

Table 3.7 Test conditions used for size exclusion chromatography test

Column	Superdex-200-HR-10/30
Flow Rate	0.50 (ml/min)
Column pressure limit	1.5 (MPa)
Wavelength	280 nm, 215 nm
Buffer	Phosphate buffered saline (PBS) at 7.4 pH. Recipe: NaCl 8g, KCl 0.2 g, Na_2HPO_5 1.44g and KH_2PO_4 in 1000 ml of solution)
Injection volumes	50 (µl)
Length of Elution	1.2 (column volume ,CV)

The recipe for MOPS buffer stock solution is given in Table 3.8. The MOPS running buffer was made by diluting one part of stock solution with 19 parts of water. The identification of protein was done by protein ladder made of pre-stained SDS-PAGE markers (Precision plus protein standards, All blue, Bio-Rad Laboratories, USA).

Table 3.8 Composition of MOPS stock buffer used for gel electrophoresis experiment

Chemical	Amount, g/L of solution
50mM MOPS	209.2
50 mM Tris base	121.2
0.1% SDS	20
1mM EDTA (ethylenediamineteraacetic acid)	6

3.4.11.2 Procedure

Membrane Throughput Test

The reservoir was filled with 150 ml of whey sample, and the run was started. The permeate flux, pH and UV absorption values were automatically recorded by the Akta Crossflow system. After 30 minutes of running 5-8 ml retentate was collected and simultaneously 5-8 ml of permeate was collected for further analysis. Before the start of each run 5-8 ml of feed sample was also collected for analysis. The samples collected were instantly frozen to prevent any deterioration for whey proteins. The permeate flux data was further analysed for time dependent effects on membrane throughput with the whey filtration process.

Size Exclusion Chromatography

The test conditions according to Table 3.7 were set in the Akta Explorer system and standard procedure for the Akta Explorer was followed to obtain chromatograms. An

auto-sampler (A900, GE Healthcare Biosciences AB, Sweden) was used for injecting the samples in the system. Known amounts of α–lactalbumin (from bovine milk, SIGMA, USA ≥85%) and β-lactoglobulin (from bovine milk, Sigma, USA, ≥90%), i.e. 3 mg/ml and 1 mg/ml respectively, were tested to obtain standard chromatograms for the target proteins. Identification of individual protein peaks for α-lactalbumin and β-lactoglobulin was done according to Liang *et al.* (2005). The area under the curve for each chromatograph was calculated and compared to the standard curve generated to find the amount of α-lactalbumin and β-lactoglobulin for each sample.

Gel Electrophoresis

The samples (5-10 µl) were well-mixed with the loading dye and centrifuged at 4°C and 12000 rpm for 30 s (Eppendorf Centrigue 5415R, Eppendorf AG, Hamburg, Germany) and heated at 100°C in Dry-Bath (Grant Instruments Cambridge Ltd., Cambridge, England) for 5-10 minutes. The samples were again centrifuged for 30 s at 13000 rpm (Mini Spin, Eppendorf AG, Hamburg, Germany) prior to being loaded on to the gels. The running buffer was filled into the electrophoresis cell and the gel was placed inside the cell. The gel contained 10 wells and loading sequence followed is given in Table 3.9

Table 3.9 Loading sequence followed in gel electrophoresis experiment

Slot/Well sequence in Gel	Sample
1	Protein ladder
2	Standarad β-lactoglobulin (1mg/mL)
3	Standarad α-lactalbumin (3 mg/mL)
4	Retentate, pH 9 20000 ppmdays
5	Permeate, pH 9 20000 ppmdays
6	Permeate, pH 11 20000 ppmdays
7	Permeate, pH 11 20000 ppmdays
8	Permeate, pH 11 20000 ppmdays
9	Retentate, new membrane
10	Permeate, new membrane

The power supply was set to 200 V and switched on. After 30 minutes the power supply was switched off and the gel was carefully taken out from the cell. The gel was taken out from the plastic cover and washed with water. Washed gel was stained with 0.25% coomassie brilliant blue solution containing 12.5% trichloroacetic acid, 20% methanol, and 7.0% acetic acid for 1 hr and de-stained with a solution of 20% methanol and 7.0% acetic acid overnight. The de-stained gel was again washed and digitally scanned to get an image of the gel.

3.4.12 Colour Measurement

A unique colour measurement test was developed to measure the colour of new and degraded commercial ultrafiltration (Koch) membranes. All the colour measurements were done for the PES surface layer only, i.e. no colour measurement was done on the backing layer. The colour measurement was done by a colorimeter/ spectrophotometer (Minolta CM2500D) in hunter labs colour space. The colorimeter was connected to a computer and operated via company software, "SpectraMagic". A new membrane was used for comparison of the colour measurement results.

3.4.12.1 Sample

The colour test was performed on commercial ultrafiltration membrane (Koch): new, pH 9, 10, 11 and pH 12 (25,000 ppm-days hypochlorite exposed) samples. All the membrane samples were cleaned as per Section 3.1. Wet membrane samples were washed with methanol to remove any surface contamination. The membrane was cut into square piece of 5 cm x 5 cm and clamped in square frame stand with an exposed surface of 4 cm x 4 cm as shown in Figure 3.11. This was done to prevent curling of the membrane during drying process. The membrane samples were than dried in a vacuum oven.

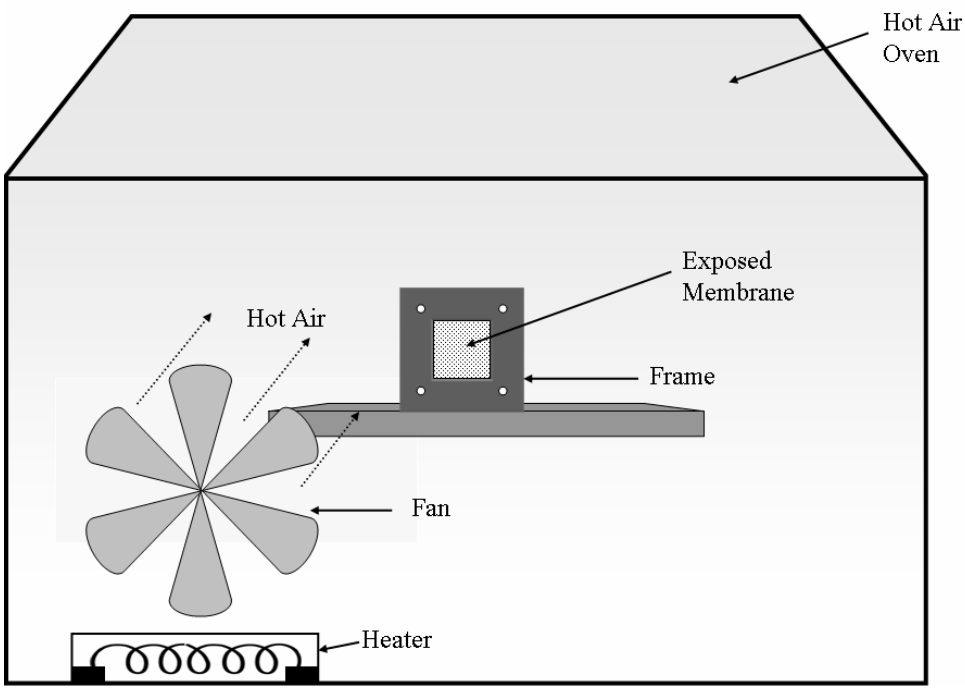

Figure 3.11 Schematic of hot air exposure to dried membrane samples

Each dried membrane sample (still clamped in frame) was exposed to hot air in a precisely controlled hot air oven at 233±2°C. After high temperature exposure the sample was immediately cooled down to room temperature. The sample was taken out from the frame and stored in desiccator. Also simultaneously a new membrane sample (without heat exposure) was dried in vacuum oven which was used as a reference sample for colour measurement.

3.4.12.2 Procedure

The "Spectra Magic" software was activated and the colorimeter was switched on. The corresponding communication port (CM2500D) was activated. The Colorimeter was then calibrated against standard white and black colour discs. Hunters lab colour space was selected from a list provided in the software. The colour test was run first on the reference sample and then on the test sample. Colour coordinate values collected for each sample were then saved as Excel file.

3.4.13 Hypochlorite Disinfection Test

It was necessary to study the disinfection efficiency of the hypochlorite solution at various pH values. Microbe (from raw cheese whey) loaded membranes were treated with 10.5 to 12 pH solutions and disinfection efficacy was checked by measuring areobic plate count, i.e. APC/mL, before and after the treatment. Also another test was conducted by suspending an extracted microbial culture directly in hypochlorite solution at various pH and extracting out culture again after treatment and process further for microbial count.

3.4.13.1 Samples

Microbial Load

The raw cheese whey for the test was procured from a local milk processing plant (Fonterra's Clandeboye, NZ, milk processing unit). The cheese whey was kept at 20°C for 7 days incubation to increase the microbial load in the whey.

Membrane Samples

New commercial ultrafiltration membrane samples (Koch) thoroughly cleaned (as per Section 3.1) were used for this test. The membrane was placed in a lab scale ultrafiltration unit (Sepa CF Membrane cell, Osmonics, MN, USA) and cheese whey was passed through the membrane at 1 bar trans membrane pressure, 20°C for 12 hr. Permeate and retentate were mixed back to the feed to maintain the level of whey in feed tank. The whey was passed through membrane at a flow rate of 3 ml/s. For hypochlorite treatment the membrane was cut into five equal pieces (one as control and four for hypochlorite treatment at various pH).

Extracted Microbial Culture

For each direct hypochlorite exposure test a microbial culture sample was prepared by centrifuging 200 ml of cheese whey at 500 RCF (relative centrifugal force), 4°C for 10 minutes. After centrifugation the clear whey was decanted and the microbial culture settled in the bottom was used for hypochlorite disinfection test. To prevent any water shock to microbial culture the treated and control samples were rinsed with a sterilised peptone saline solution (i.e. peptone 1 g, sodium chloride 8.5 g in 1L of water) instead of sterilised water.

Test conditions

Following test conditions were used for hypochlorite disinfection test

Hypochlorite Solution pH: 10.5, 11, 11.5 and 12

Chlorine strength: 200 ppm

Solution temperature: 55°C

Exposure time: 20 minutes

3.4.13.2 Procedure

Disinfection Test on Membrane Surface

At the start, one cut out piece from microbial loaded membrane sample was taken out as a control which was soaked in sterilised water for 20 minutes at 55°C instead of hypochlorite solution. The other membrane samples were soaked in hypochlorite solutions (pH: 10.5, 11, 11.5 and 12) for 20 minutes at 55°C. After the exposure was complete the membrane samples were taken out and were rinsed by soaking in

sterilised water four times, each at 55°C for 10 minutes. The rinsed samples were then packed in sterilised bags and sent to a local microbial testing company (New Zealand Laboratory Services Ltd., Christchurch) for aerobic plate count (APC). The membrane samples were rinsed in 10 ml letheen broth to suspend the micro organism from membrane surface into the broth. The incubation was done at 35±1°C for 48±3 hr. The results were expressed as total APC/ml.

Disinfection Test on Microbial Culture

For the alternate test, the extracted microbial culture samples were re-suspended in hypochlorite solution at various pH at 55°C for 20 minutes. The control sample for comparison was an extracted microbial culture suspended in peptone saline instead of hypochlorite solution. The suspended culture samples were than centrifuged out at 500 RCF, 4°C for 10 minutes. The hypochlorite solution was then decanted and the separated culture was again suspended in peptone saline solution and centrifuged. The saline rinsing and centrifugation cycle was done twice to eliminate any further hypochlorite exposure. The microbial culture samples extracted after final centrifugation were sent to the New Zealand Laboratory Services Ltd., Christchurch for APC. All extracted cultures were diluted in 10 ml letheen broth before proceeding for APC. The incubation was done at 35±1°C for 48±3 hr. The results were expressed as total APC/ml.

Chapter 4 Results and Discussion

4.1 Hypochlorite Decay Experiment

The hypochlorite decay experiment was conducted at 55ºC from pH 7 to 12, to study the stability of sodium hypochlorite solution with time at a given temperature. This aimed at defining an optimum time period required for maintaining pH and chlorine levels of hypochlorite during hypochlorite assisted membrane degradation experiments. Figure 4.1 shows the drop in pH and Figure 4.2 shows fall of chlorine concentration in the hypochlorite solution with time at 55ºC for a specific hypochlorite solution pH.

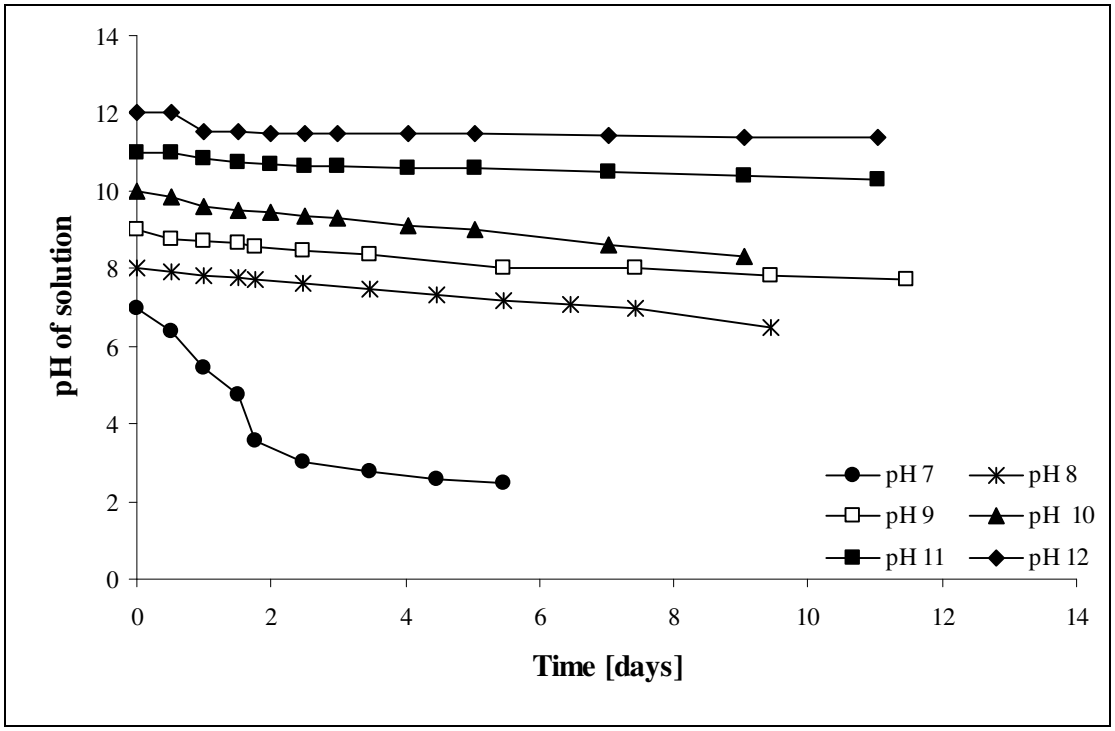

Figure 4.1 Change in pH of the sodium hypochlorite solution with time at 55°C

It was observed that the pH stability of hypochlorite solution increased with the increase in initial pH of the solution. Hypochlorite solution with an initial pH of 12 exhibited the least fall in pH with time; the pH of the solution decreased from 12 to 11 in 12 days. The hypochlorite solution with initial pH 7 proved to be highly unstable and experienced a rapid fall in pH from 7 to 5.4 within 1 day. A similar trend was observed for the decrease of chlorine concentration of the solutions with time. Solutions with an initial pH of 12 proved to be the most stable in terms of chlorine

decay and again the pH 7 hypochlorite solution was most unstable and experienced a fall of more than 300 ppm (from initial concentration of 600 ppm) in less than two days.

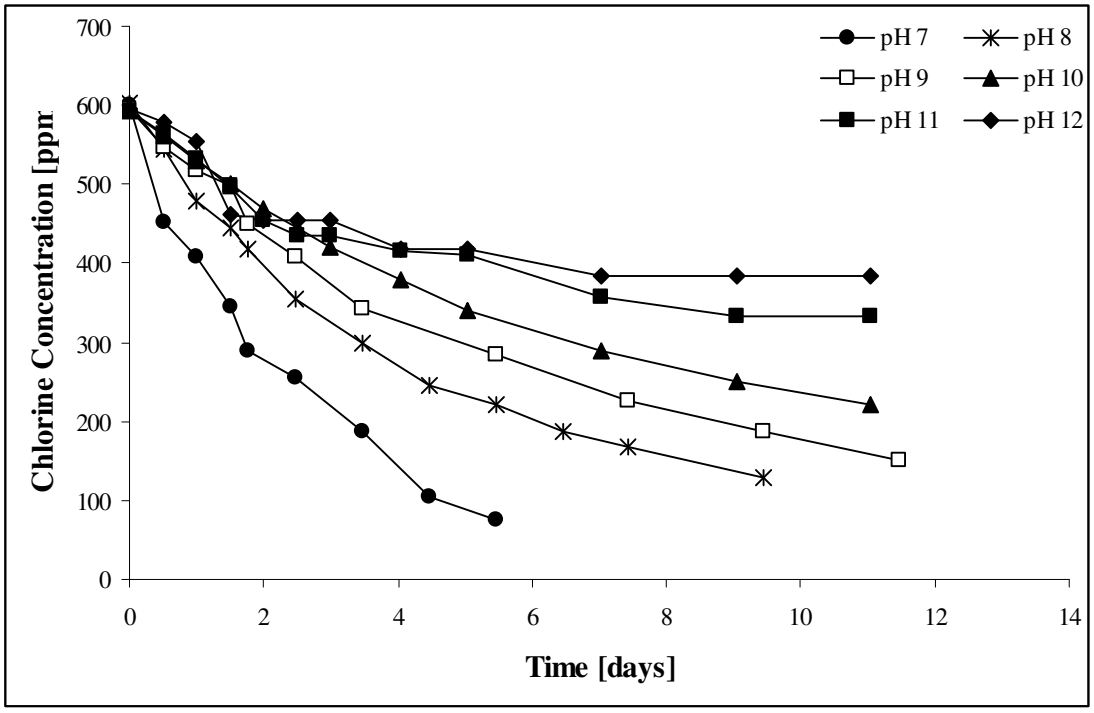

Figure 4.2 Change in chlorine concentration of the sodium hypochlorite solution with time

Also it was noted that all the solutions experienced a rapid fall in pH and chlorine concentration initially for the first few days and then a slower fall occurred. It was because part of free chlorine was used up in fulfilling the chlorine demand of the system (i.e. glass jar, lid, seals etc) and once that chlorine demand decreased the degradation of hypochlorite was slower for the rest of the time period. It was concluded that the stability of hypochlorite solutions both in terms of pH and chlorine concentration was greater with a higher initial pH of the solution. Also it would be difficult to maintain a steady pH and chlorine concentration of pH 7 and pH 8 solution even if the chlorine concentration replenishment and pH maintenance is done every day. It was decided to conduct the hypochlorite exposed membrane degradation experiment at pH 9, 10, 11 and 12. This pH range included the industrial working hypochlorite pH range of 10.5 from 11.0 (as per membrane manufacturer, Koch International) but also gave a flexibility of realistic maintenance of steady pH and chlorine concentration for a long exposure time (i.e. 35 days at 700 ppm for a total exposure of 25,000 ppm-days)

4.2 Dynamic Mechanical Analysis (DMA)

Commercial ultrafiltration membranes (in a dry state) were tested for dynamic mechanical properties (method in Section 3.4.1). Five individual samples were tested as repeats for membrane from each exposure condition. Figure 4.3 shows the E' curves for new membranes over the temperature range of 30 to 260°C. Figure 4.4 shows change in E" with temperature and Figure 4.5 shows the change in tan δ with temperature for a new membrane sample.

The double layered structure of the membrane can be clearly detected by double peaks (for E" and tan δ) or double slopes (for E') in the curves. For example, in the case of the new membrane, the loss modulus curve showed the first peak around 105ºC which corresponded to dampening in the polyolefin backing layer. The second peak produced at 229°C corresponded to the PES layer of the membrane (Figure 4.4).

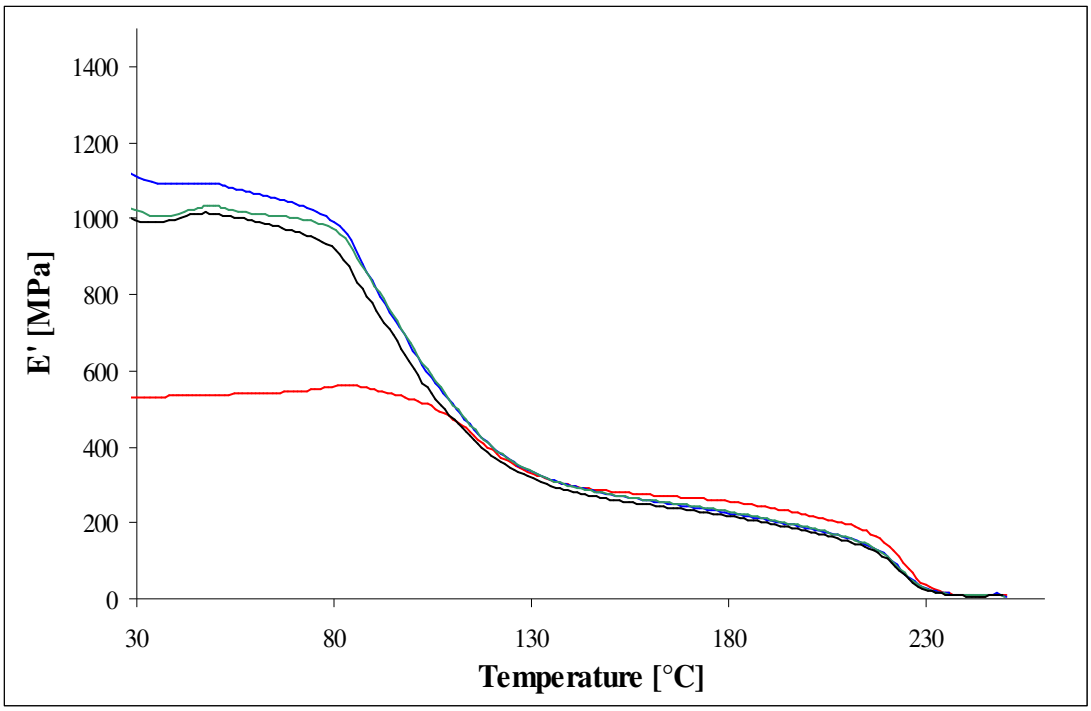

Figure 4.3 E' curve for Koch new membrane repeats at 1 Hz

Similarly for new membrane samples the first peak around 113ºC in the tan δ curve (Figure 4.5) corresponded to the glass transition temperature (T_g) of the backing layer material and the second peak around 236ºC corresponded to the T_g of the PES layer.

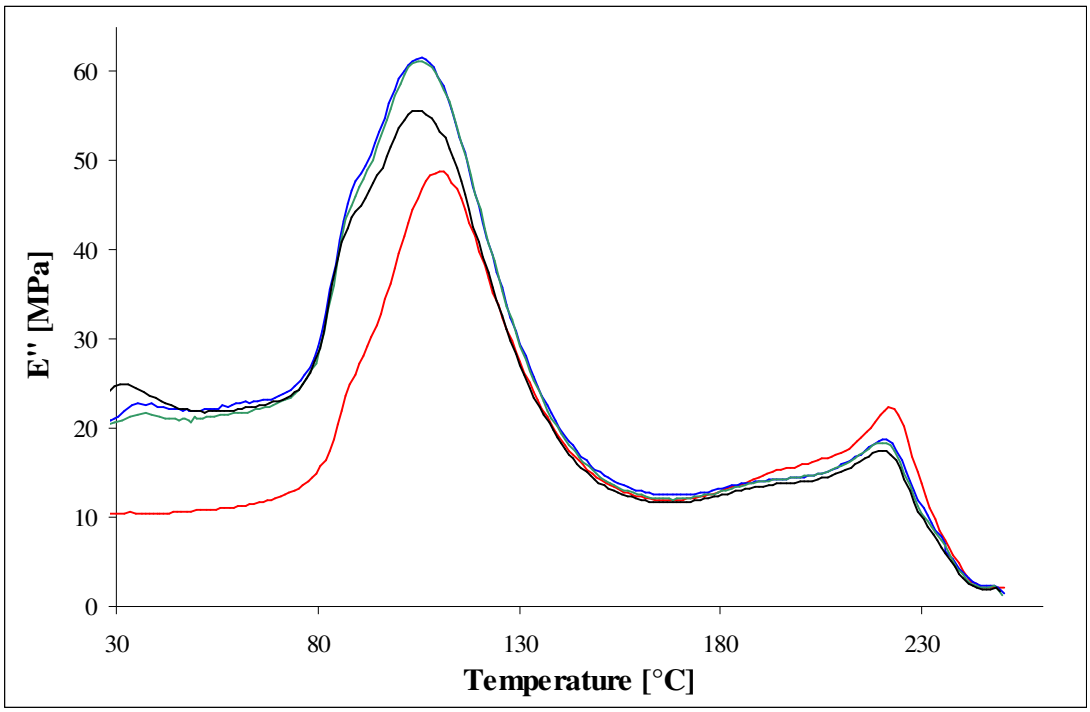

Figure 4.4 E" curve for Koch new membrane repeats, at 1 Hz

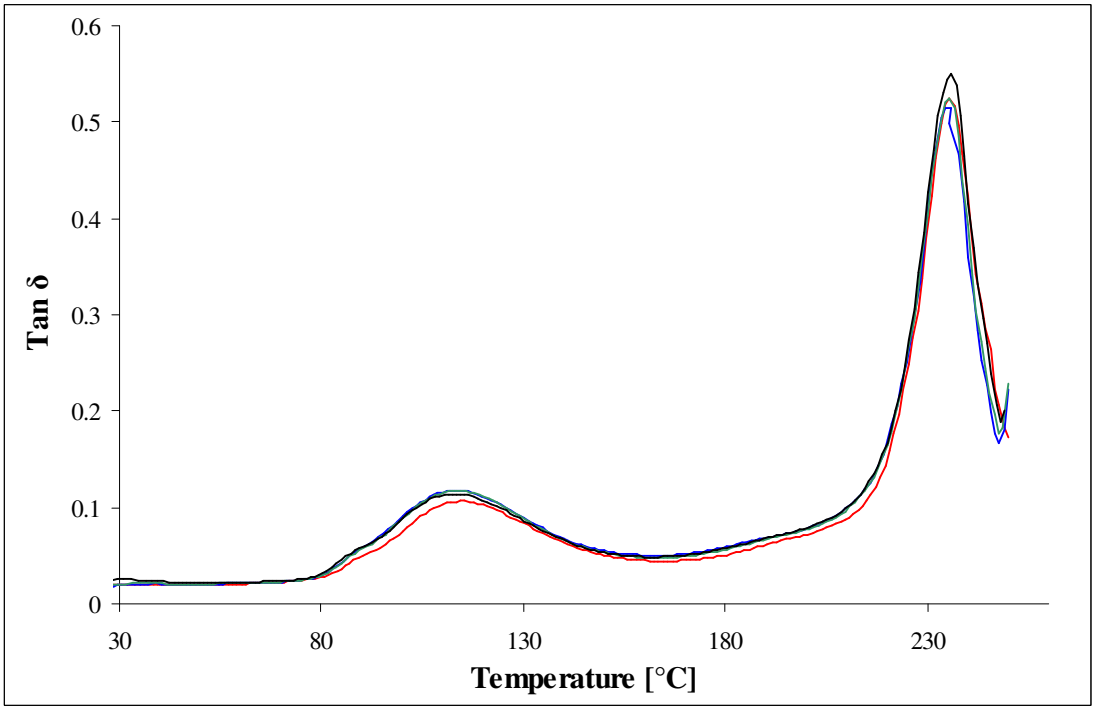

Figure 4.5 Tan δ curve for Koch new membrane repeats, at 1 Hz

It was observed that the initial stiffness (initial E' value) varied from 550 to 1100 MPa for different repeats on new membranes. This large variation (±14.5% standard deviation from mean) in initial stiffness may be due to the fact the membrane samples are anisotropic porous structure and the stiffness may vary from sample to sample. In

addition to this, commercial ultrafiltration membranes have a double layer structure and the amount of polymer in the double layer may vary from sample to sample even if the samples have the same thickness. This high uncertainty in sample structure and composition may result in different initial E' values for the same type of samples. Another reason may be sample loading conditions. Although the absolute values of storage values had large uncertainty, the trends of the E' curves, i.e. slope and peak positions, were similar and repeatable irrespective of the repeats. The slope of the curve gives an indication of T_g, which is a property of the material and may not depend on the porosity or irregularity in sample physical structure.

A similar observation was also made for loss modulus curves (Figure 4.4). The initial loss modulus values showed a large variation (±14% standard deviation from mean) and the peak heights varied with repeats. Variation in peak heights can be due to variation in the amount of each polymer (i.e. PES in membrane layer and polyolefin for backing) in samples tested. However the curve trend or peak positions were repeatable. Since tan δ is the ratio of storage modulus to loss modulus, only a negligible uncertainty (±0.13% standard deviation from mean) was observed and the curves were repeatable for all the repeats for new membranes (Figure 4.5). Similar observations were made for pH 9 10,000 ppm-days and pH 12 10,000 ppm-days hypochlorite exposed samples. It was inferred that absolute values of moduli had large uncertainty so it was appropriate to follow trends of the curves rather than absolute values of moduli.

The peaks of the tan δ curves were assigned as glass transition temperatures of the different layers in the membrane. Since tan δ curves were very repeatable an effort was made to detect any change in glass transition of the samples with hypochlorite degradation (detected as change in position of peak in tan δ curve). The repeats on pH 9 and pH 12 10,000 ppm-days exposed samples showed an uncertainty of ± 4°C (from mean T_g) for the glass transition temperature of PES layer. For detailed E', E" and tan δ curves please refer to Appendix 2.1.1. Figure 4.6 shows the change in tan δ for 10,000 ppm-days exposure. No change in the T_g of the backing layer (around 113°C) was observed for any of the exposures at various pH values. Any change in the T_g of the PES layer as compared to new membranes was within the uncertainty in measurements (±4°C) and was considered insignificant. Similarly no significant

change in storage modulus curve slope and loss modulus peak position was observed for any degraded sample as compared to new membranes (Figure 4.7 and 4.8).

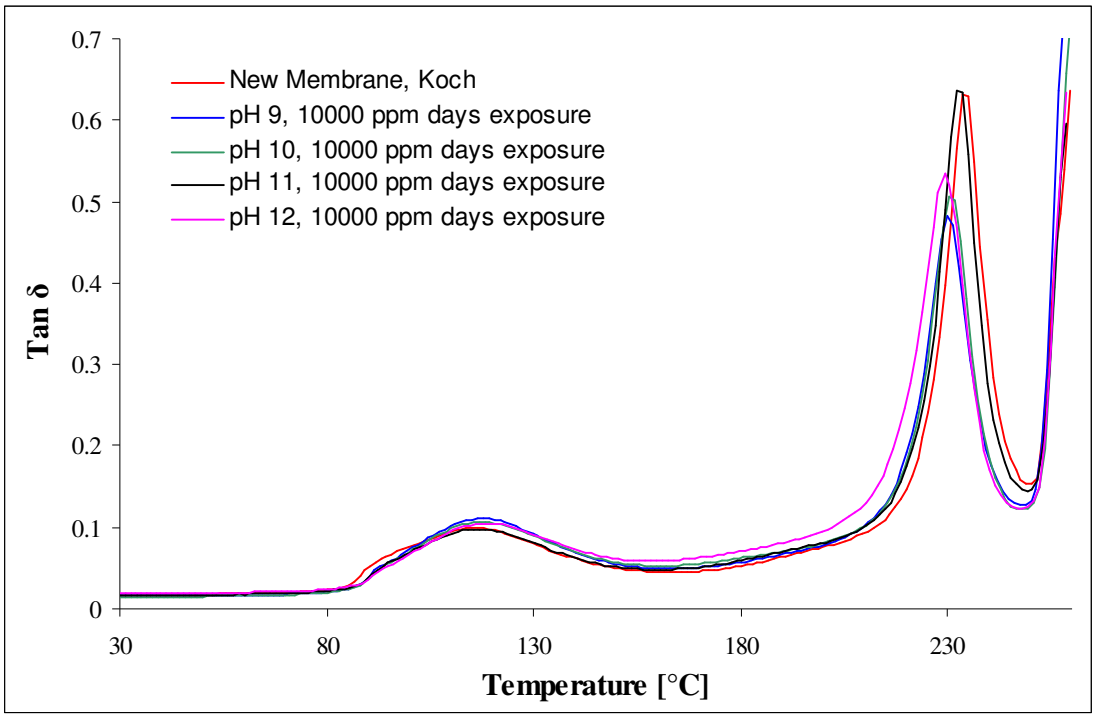

Figure 4.6 Tan δ curve for new and hypochlorite degraded Koch membranes (pH 9-12, 10,000 ppm-days exposure), at 1 Hz

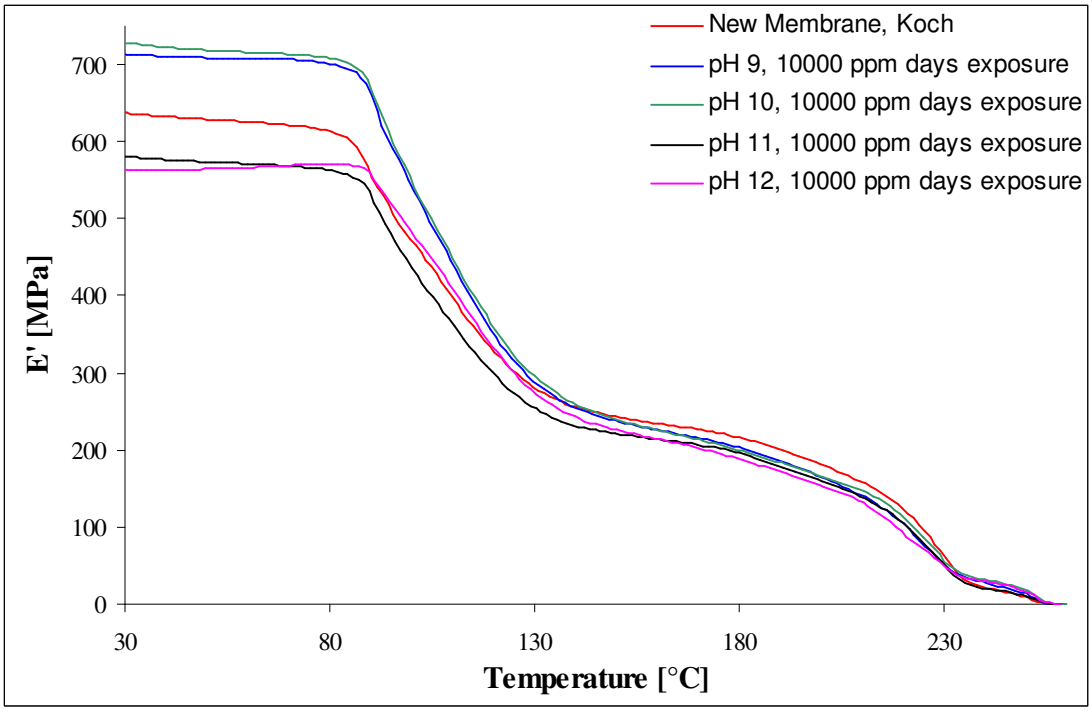

Figure 4.7 E' curve for new and hypochlorite degraded Koch membranes (pH 9-12, 10,000 ppm-days exposure), at 1 Hz

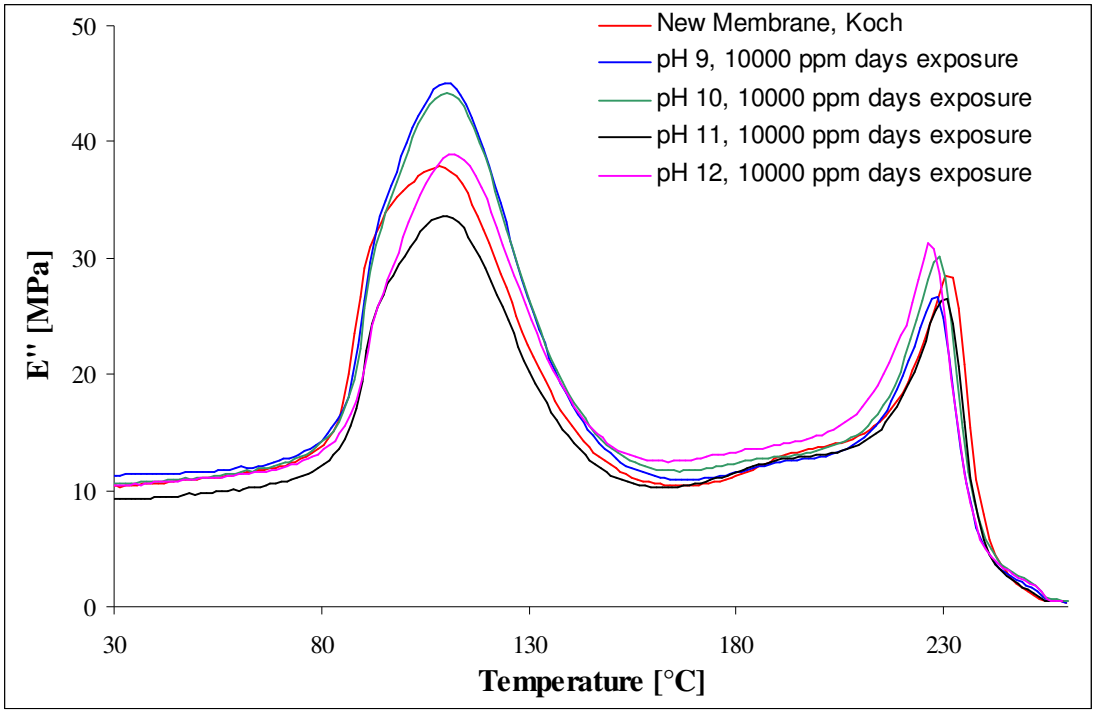

Figure 4.8 E" curve new and hypochlorite degraded Koch membranes (pH 9-12, 10,000 ppm-days exposure), at 1 Hz

Two main conclusions were drawn from this experiment. First, that 10,000 ppm-days may not be enough exposure to produce a change in membranes which can be detected by DMA. It is likely that hypochlorite degradation is a surface degradation that does not affect bulk properties like glass transition temperature significantly, within exposure conditions applied. To study the effect of high exposure time, it was decided to measure the dynamic mechanical properties of membrane degraded with a very high hypochlorite exposure time of 25,000 ppm-day. Second, conventionally DMA is normally done on non-porous films or sheets so it was possible that porous nature of PES layer or fibrous backing layer may have resulted in high uncertainties masking the effect of hypochlorite, if any, on the membrane. To study the effect of the porous nature of the PES layer or the backing on DMA response, non-porous PES sheet and foil (10000 ppm-days exposure) were tested for any change in dynamic mechanical properties with hypochlorite exposure.

Figure 4.9 shows the tan δ curve for new and hypochlorite degraded membrane (Koch) samples for hypochlorite pH 9 to 12 at 25,000 ppm-days exposure. No significant change in T_g was observed for either PES or backing layer. Similarly no significant changes in loss modulus peaks or storage modulus slopes were observed

even at a high exposure of 25,000 ppm-days. It was concluded that even 25,000 ppm-day exposure is not enough to make any change in the glass transition of the polymers in membranes. For storage and loss modulus curves for Koch membrane degraded for 25,000 ppm-days exposure please refer to Appendix 2.1.2.

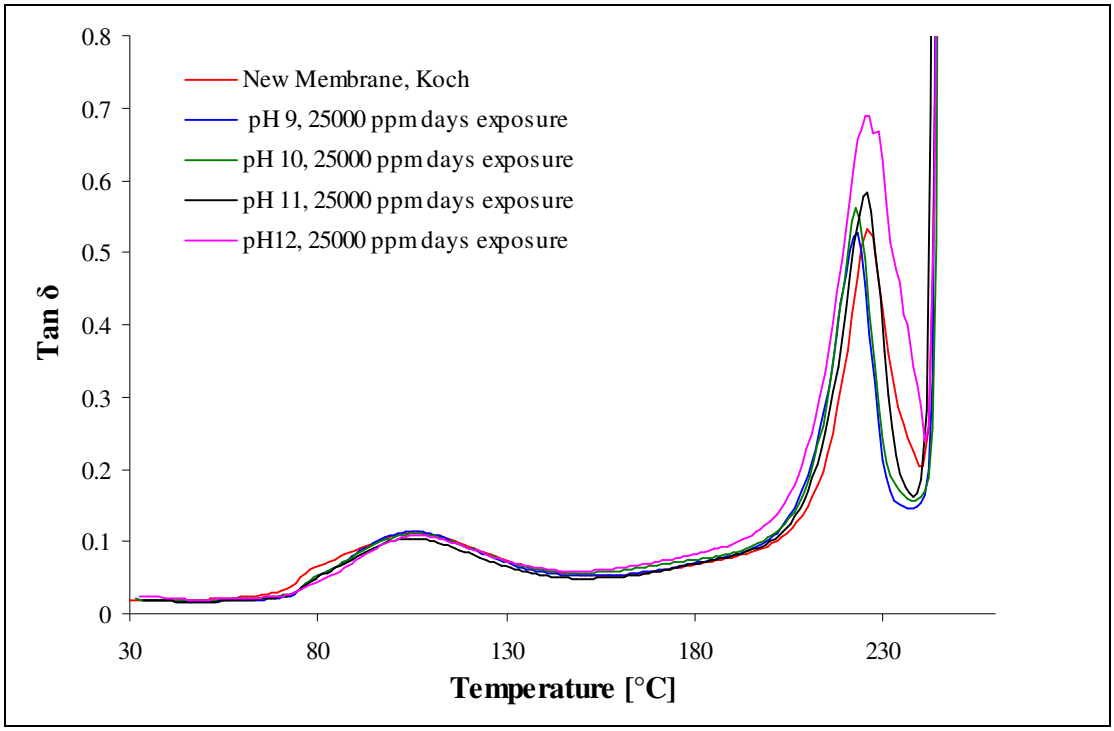

Figure 4.9 Tan δ curve for new and hypochlorite degraded Koch membranes (pH 9-12, 25,000 ppm-days exposure), at 1 Hz

Figure 4.10 shows the change in tan δ values with temperature for samples of the backing layer degraded at various pH values for 10,000 ppm-days hypochlorite exposure. All the samples showed a single peak at 121±2°C corresponding to the T_g of the backing layer. Another small secondary peak was observed at 63±2°C which was hidden in case of ultrafiltration membrane testing. No peak was observed for PES which indicated that the backing layer was free from PES. Moreover an increase of 9°C in the T_g for backing layer was observed as compared to new commercial ultrafiltration membranes. This shows that the double layer structure interferes with the T_g measurement of individual polymers in the layers. No significant change in T_g was observed which could be related with the pH of the hypochlorite exposure. No significant trends were observed which could link the DMA response to the pH of hypochlorite exposure for either the storage or the loss modulus curve. For detailed E' and E" curves for the backing layer please refer to Appendix 2.1.3.

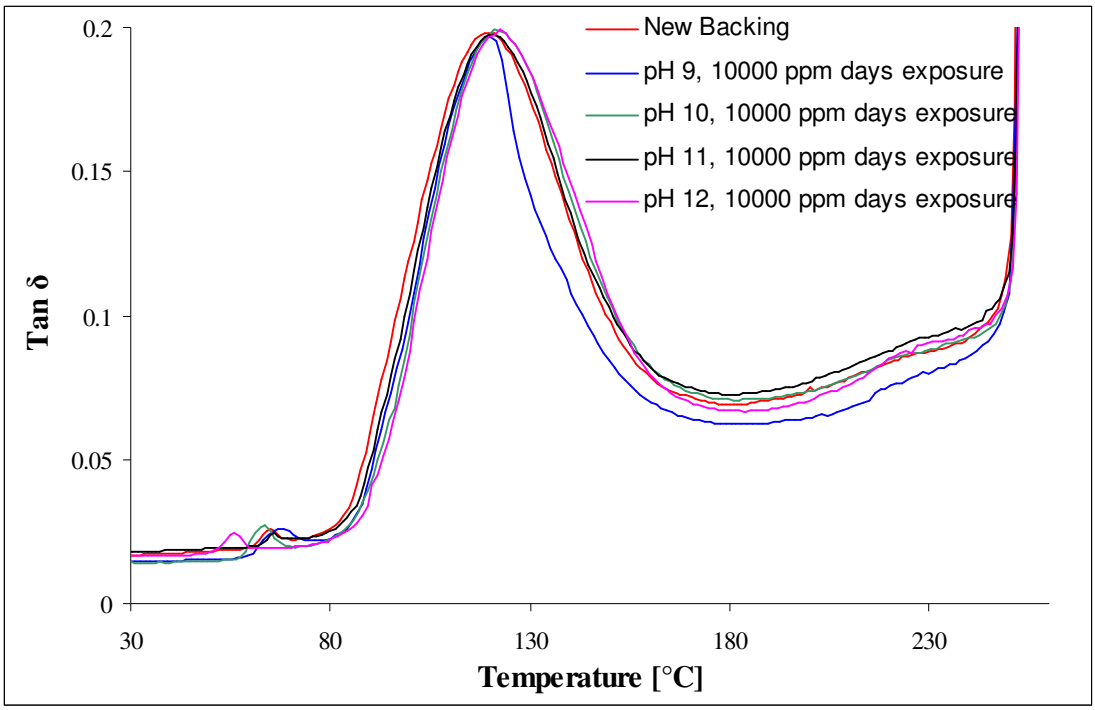

Figure 4.10 Tan δ curve for new and hypochlorite degraded backing from Koch membranes (pH 9-12, 10,000 ppm-days exposure), at 1 Hz

The DMA response of the membranes was a compound effect of both PES and the backing layer which made it difficult to study the effect of degradation on the properties of an individual layer. To resolve this DMA testing was done on a PES free backing layer and PES membrane, supplied by Sterlitech which does not have any backing layer. It was hoped that the Sterlitech membrane would experience the same effect with hypochlorite exposure as expected from the PES layer of a commercial ultrafiltration membrane.

Figure 4.11 shows tan δ curve for Sterlitech membranes for new and hypochlorite degraded samples (pH 9 and pH 12, 10,000 ppm-day exposure). A single peak at 241±1°C was observed for all the exposures, which corresponded to the T_g of PES. Since the Sterlitech PES membrane does not have a backing, it was very soft and fragile and registered initial stiffness 10 times lower than commercial ultrafiltration membranes which shows that the stiffness of commercial ultrafiltration membrane was dominated by backing layer. No change in the loss and storage modulus curves for degraded membranes (in comparison to new membrane) was observed. For detailed E' and E" curves for the Sterlitech membrane please refer to Appendix 2.1.4.

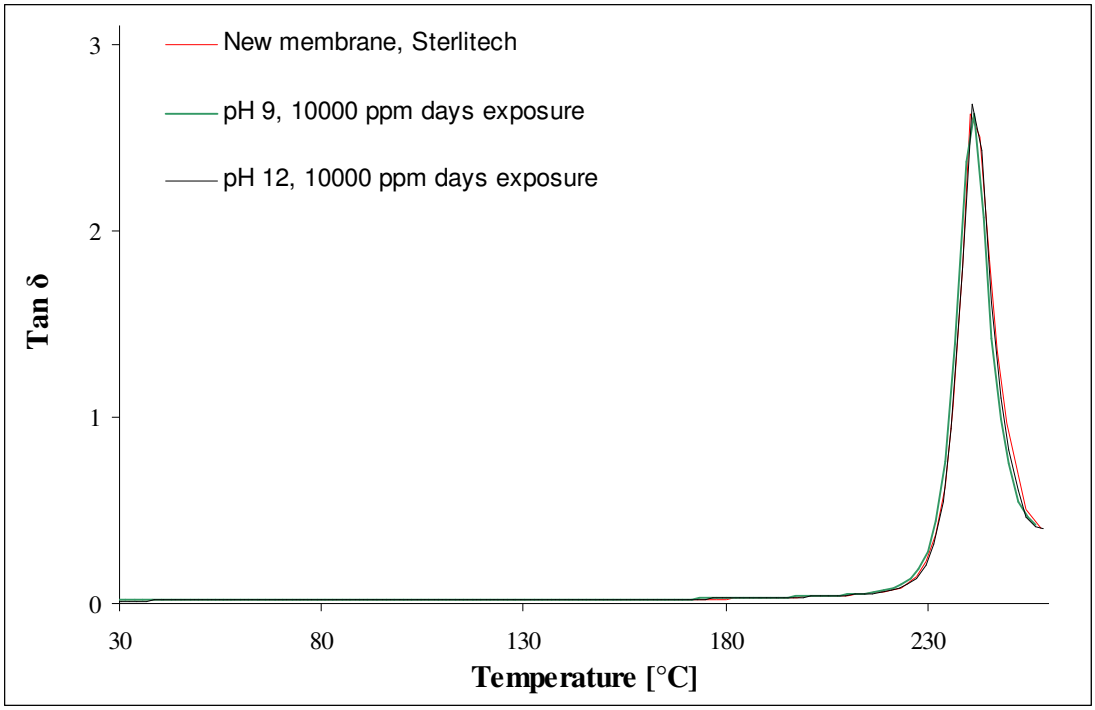

Figure 4.11 Tan δ curve for new and hypochlorite degraded Sterlitech membrane (pH 9-12, 10,000 ppm-days exposure), at 1 Hz

Tan δ curves for PES foil (Good Fellow) and PES sheet (BASF) also showed a single peak 232±2°C and 225±2°C respectively. No significant change in glass transition temperature of PES was observed even at higher exposures of 25,000 ppm-days (Figure 4.12 and 4.13). Absence of any significant trend in initial stiffness values for both in PES foil and sheet confirmed that porosity of membrane was not masking the hypochlorite effect on the dynamic mechanical properties. Similarly no significant change in the loss modulus curve was detected for either PES foil or sheet. For detailed E' and E" curves for PES foil and PES sheet please refer to Appendices 2.1.5 and 2.1.6 respectively.

It was concluded that DMA gave good measurements of T_g and the dynamic mechanical behaviour of ultrafiltration membranes but no significant change in dynamic mechanical properties of membrane and PES sheet samples was detected for all the exposure conditions tested. It was observed that the backing layer of commercial ultrafiltration membrane had a very high initial stiffness values as compared to PES layer and dominated the E' response of DMA. It was concluded that hypochlorite degradation is a surface phenomena and very harsh exposure conditions, i.e. a very low pH of hypochlorite solution and a long exposure time period, may be

required to have a significant effect on bulk properties like glass transition temperature of the polymer in the membrane.

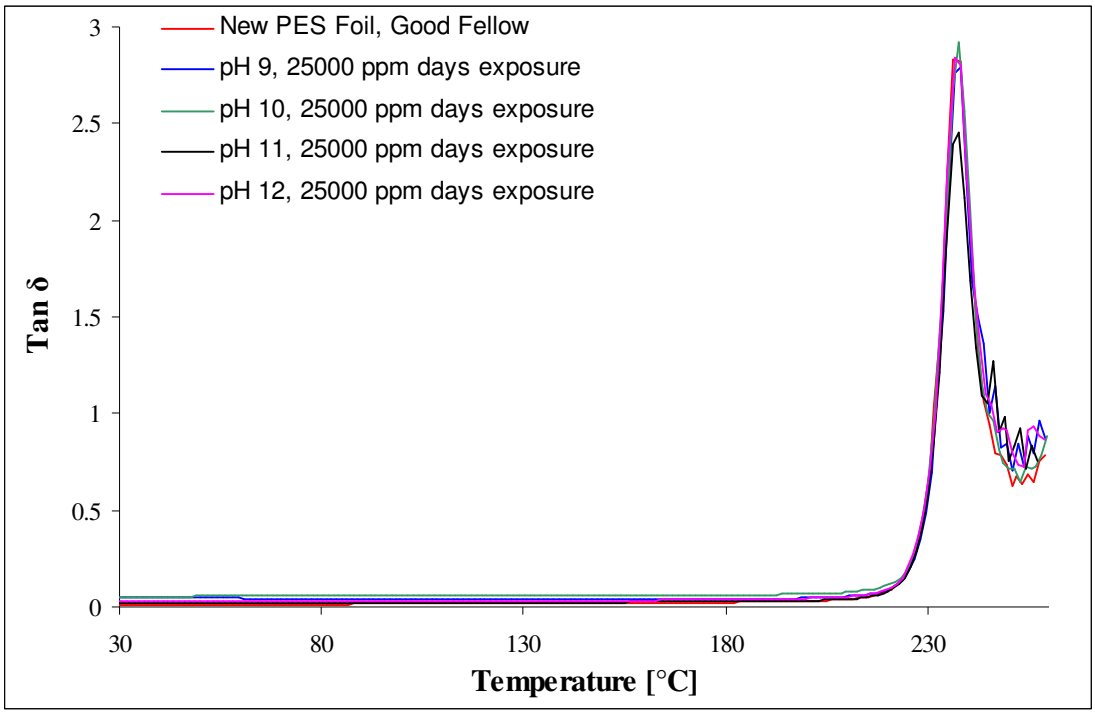

Figure 4.12 Tan δ curve for new and hypochlorite degraded PES foil (Good Fellow) (pH 9-12, 25,000 ppm-days exposure), at 1 Hz

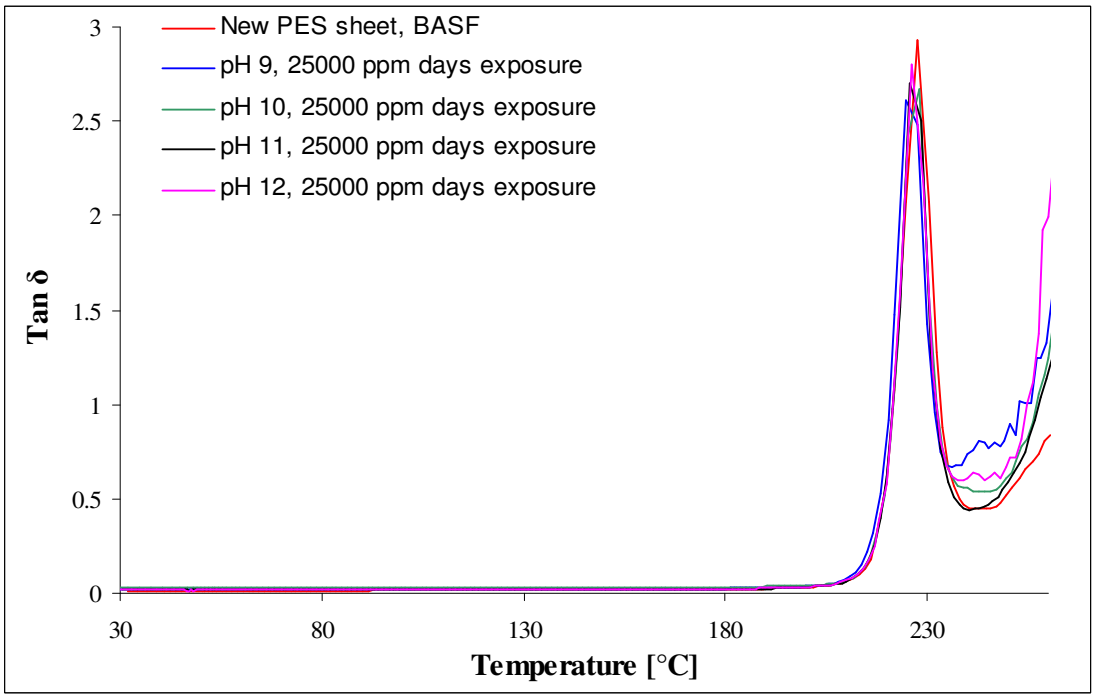

Figure 4.13 Tan δ curve for new and hypochlorite degraded PES sheet (BASF) (pH 9-12, 25,000 ppm-days exposure), at 1 Hz

4.3 Thermo Gravimetric Analysis (TGA)

The thermal stability of both the commercial UF membrane (Koch) and the Sterlitech membranes was determined by TGA (method in Section 3.4.2). Koch membranes showed two transitions of loss in weight in two separate temperature ranges due to their double layered structure and Sterlitech membrane showed only one transition as it is had no backing layer (Figure 4.14). In the case of the new Koch membrane the first transition, around 398°C, was related to the decomposition of backing layer. The second one occurred around 462°C which was assumed to be the onset of thermal degradation of PES layer in the membrane.

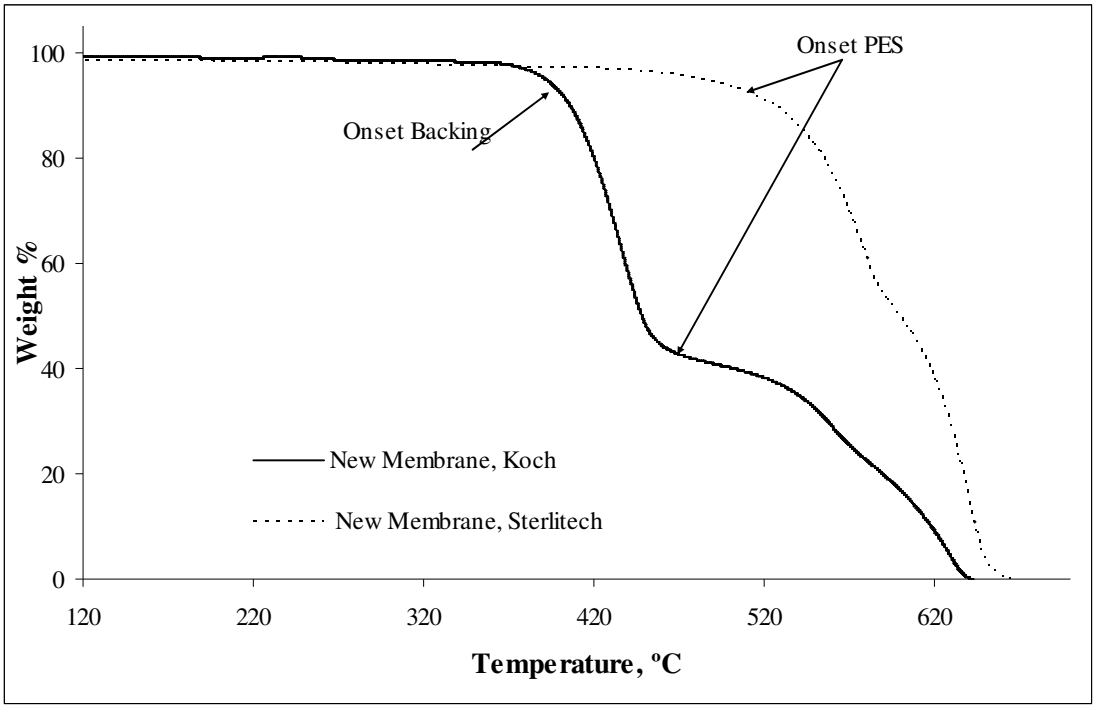

Figure 4.14 TGA curves for new Koch and Sterlitech membranes

Due to the double layer structure of the membrane it was hard to observe the true onset of degradation for the PES layer and hence an inclined plateau was observed during the initial degradation stage of PES layer. The Sterlitech membrane demonstrated only a single transition, i.e. degradation of PES onset around 470°C as it had no backing layer.

Figure 4.15 shows the TGA results for new and degraded Koch membranes for pH 9 and 12 10,000 ppm-day hypochlorite exposure. No significant change in degradation

behaviour was noticed for either pH 9 or pH 12 degraded membrane samples. The slopes for both backing and PES thermal degradation curves remained unchanged, i.e. no change in thermal degradation rate occurred with hypochlorite treatment samples. It was concluded that 10,000 ppm-day exposure was too low for TGA to detect any change in thermal degradation behaviour. Therefore it was decided to test 25,000 ppm-day hypochlorite exposed samples.

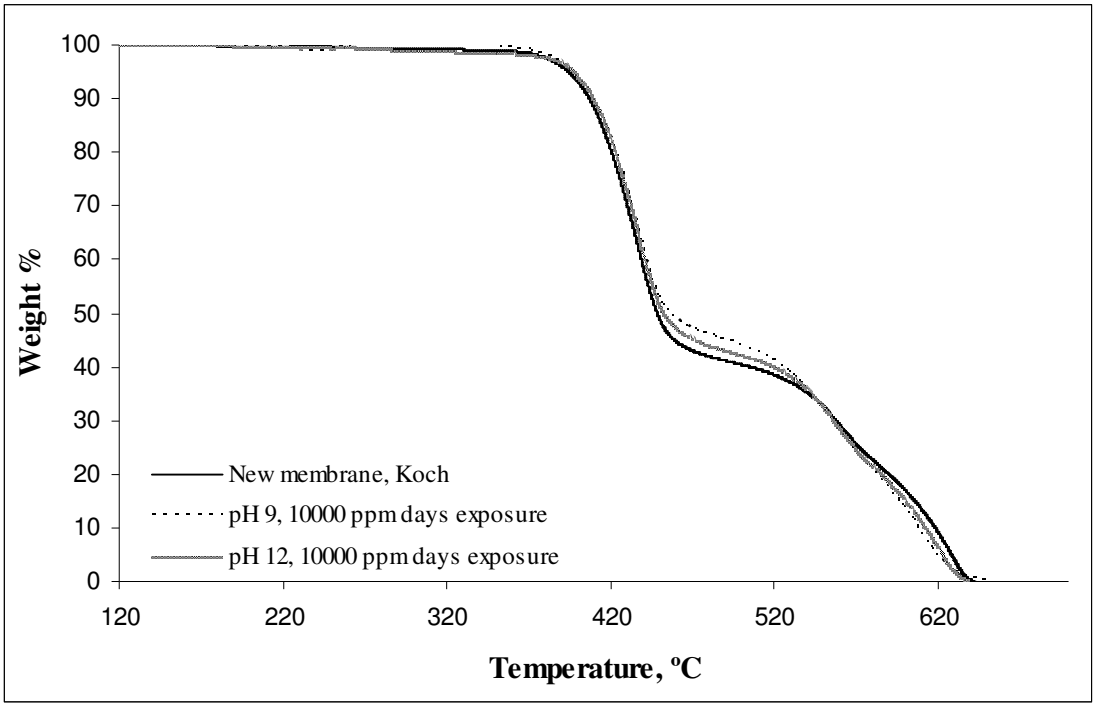

Figure 4.15 TGA curve for new and hypochlorite aged Koch membranes for various pH of hypochlorite solution for 10000 ppm-days of hypochlorite exposure

Figure 4.16 shows TGA curves for new and degraded Koch membrane for 25,000 ppm-day exposure. It can be noticed that the backing layer degradation onset was similar for all the exposures but pH 9 exposed samples showed a decrease in PES thermal degradation onset temperature as compared to new and pH 12 exposed samples. Table 4.1 shows further details of thermal degradation sequence as the temperatures of different weight fraction loss.

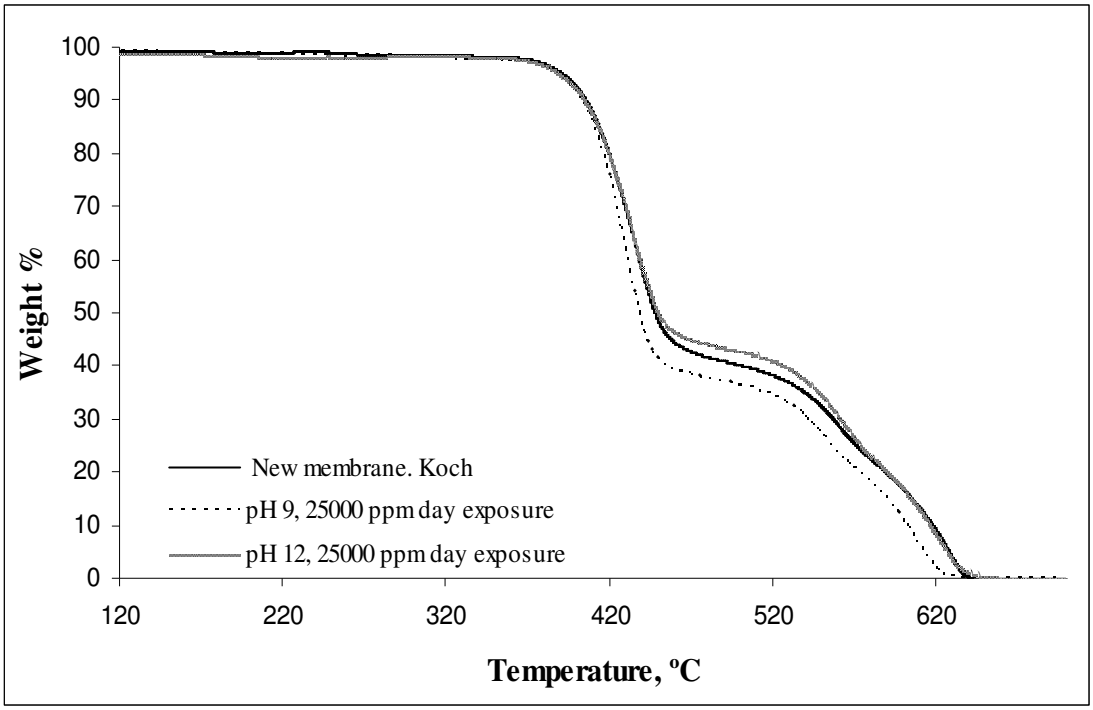

Figure 4.16 TGA curve for new and hypochlorite aged Koch membranes for various pH of ageing solution for 25000 ppm-days of hypochlorite exposure

Table 4.1 Characteristic temperatures from TGA analysis for new and hypochlorite aged Koch membrane 25000 ppm-days hypochlorite aged samples

Sample	Degradation onset (backing)	5% Weight loss, backing	Degradation onset (PES layer)	95% Weight loss, total
New	398°C	410°C	460°C	629°C
pH 9 treated	400°C	409°C	451°C	614°C
pH 12 treated	400°C	410°C	458°C	628°C

Hypochlorite ageing did not affect the thermal degradation behaviour of the backing layer at any pH of the hypochlorite solution used which can be noticed by similar thermal degradation onset temperatures or 5% weight loss temperatures. However thermal stability of the PES layer was lowered by ageing at pH 9. There was a lower thermal degradation onset temperature of PES layer for pH 9 treated samples as compared to pH 12 treated or new samples. Also it can be observed from the slope of the curves (Figure 4.16) that thermal degradation rate was higher in case of pH 9 treated samples, i.e., it will reach to zero weight at a lower temperature than the other two samples which is shown by 95% weight loss temperature in Table 4.1. Figure 4.17 shows the TGA curve for the Sterlitech membrane at pH 9 and 12 hypochlorite exposure for 10,000 ppm-days and Table 4.2 shows the details of degradation sequence for the same.

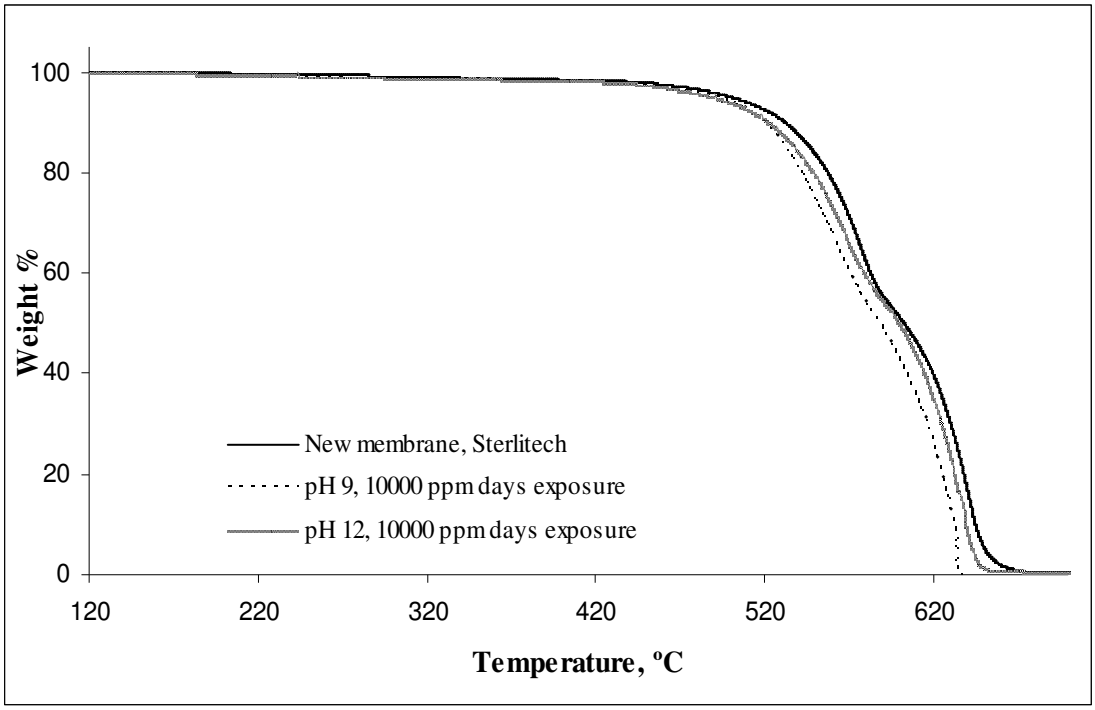

Figure 4.17 TGA curve for new and hypochlorite aged Sterlitech membranes for pH 9 and 12 hypochlorite solution for 10000 ppm-days of exposure

Table 4.2 Weight loss temperatures from TGA analysis for new and hypochlorite aged Sterlitech membrane 10000 ppm-days hypochlorite aged samples

Sample	5% Weight loss PES layer	95% weight loss Total
New	450°C	650°C
pH 9 treated	493°C	634°C
pH 12 treated	496°C	643°C

The Sterlitech membrane exposed at pH 9 showed a lower 5% and 95% weight loss temperature as compared to new or pH 12 treated samples which is in agreement with thermal degradation results for the PES layer in Koch membranes.

TGA analysis of Koch and Sterlitech membranes confirmed that the hypochlorite affects the thermal degradation properties of PES in both the membranes. Thermal degradation properties of the backing layer were not affected by hypochlorite exposure. The lowering of the thermal degradation temperature of the PES layer may be due to a decrease in the molecular mass of PES by chain scission during the ageing process. pH 12 hypochlorite treated membranes had a smaller change in thermal degradation behaviour as compared to pH 9 hypochlorite treated samples which

shows that pH plays an important role in hypochlorite degradation behaviour of membranes.

4.4 Tensile Testing

Tensile testing was done on the Koch ultrafiltration membrane, backing and Sterlitech microfiltration membrane, pH 9 and 12, 10,000 ppm-days hypochlorite exposed samples, to analyse the effect of hypochlorite treatment on the membrane as a whole and on the different layers of the membrane.

Figure 4.18 shows a representative stress-strain curve for new and degraded Koch membrane samples. Clearly pH 9 exposed samples showed a lower stress values at the break point as compared to both pH 12 exposed samples and new membrane. A similar trend was noticed in tensile testing done on the backing layer (Figure 4.19) and the Sterlitech membranes (Figure 4.20).

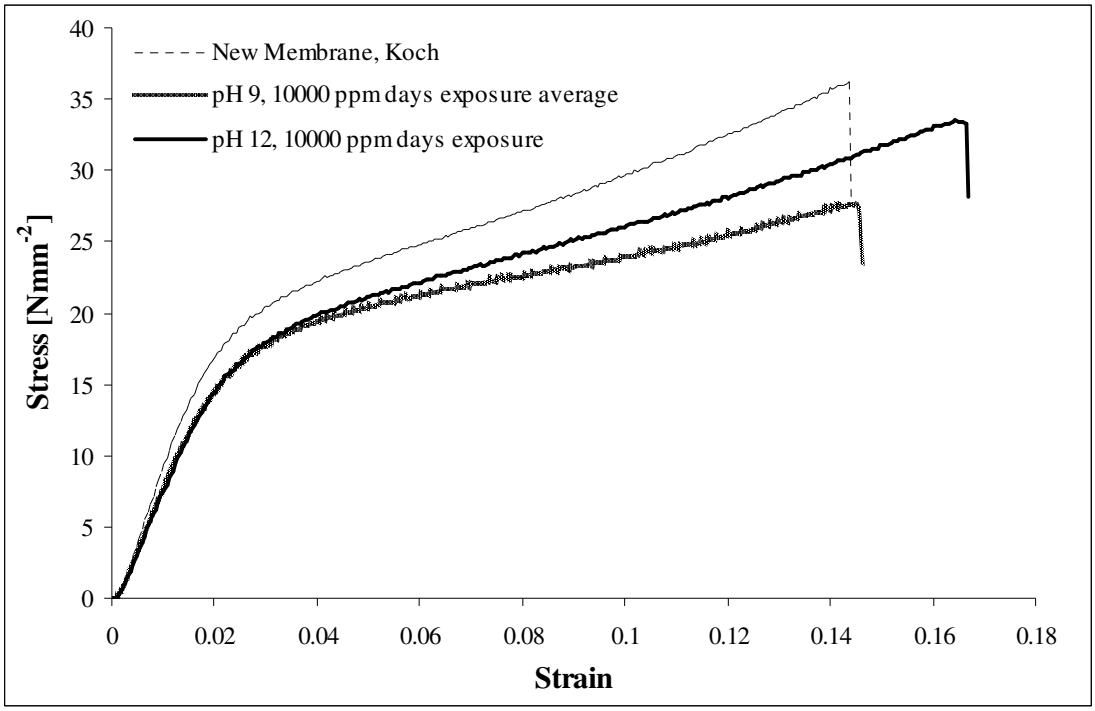

Figure 4.18 Representative stress strain curve for new and hypochlorite exposed Koch membranes (pH 9 and 12, 10,000 ppm-days)

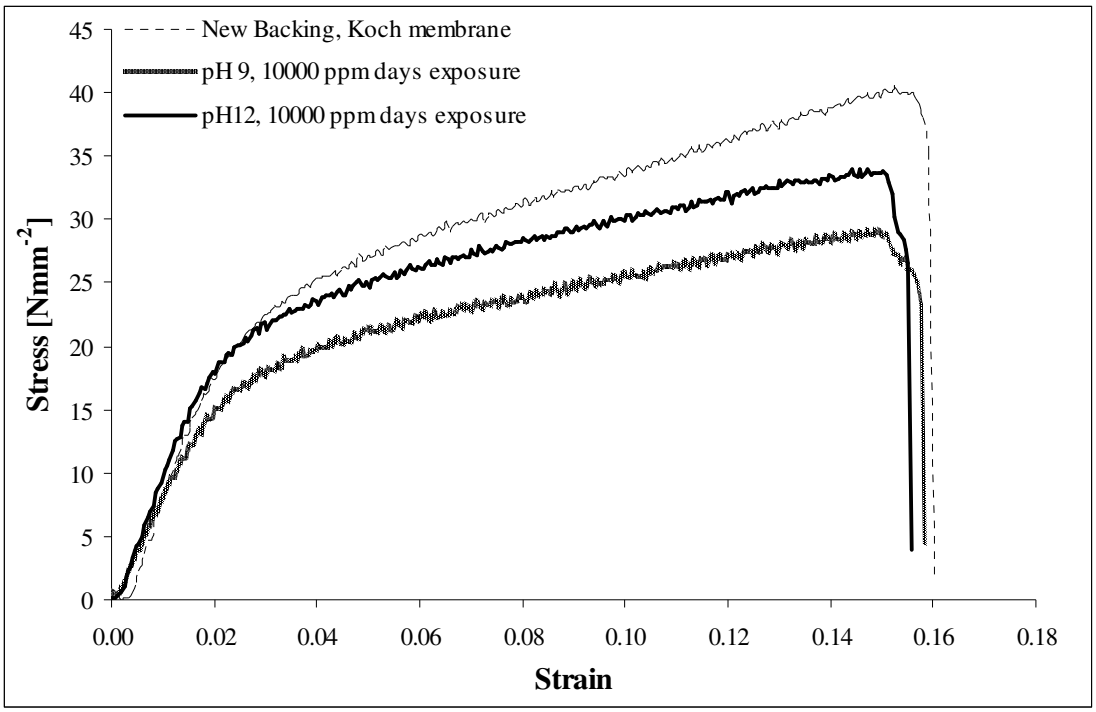

Figure 4.19 Representative stress strain curve for new and hypochlorite exposed backing layer of the Koch membrane (pH 9 and 12, 10,000 ppm-days)

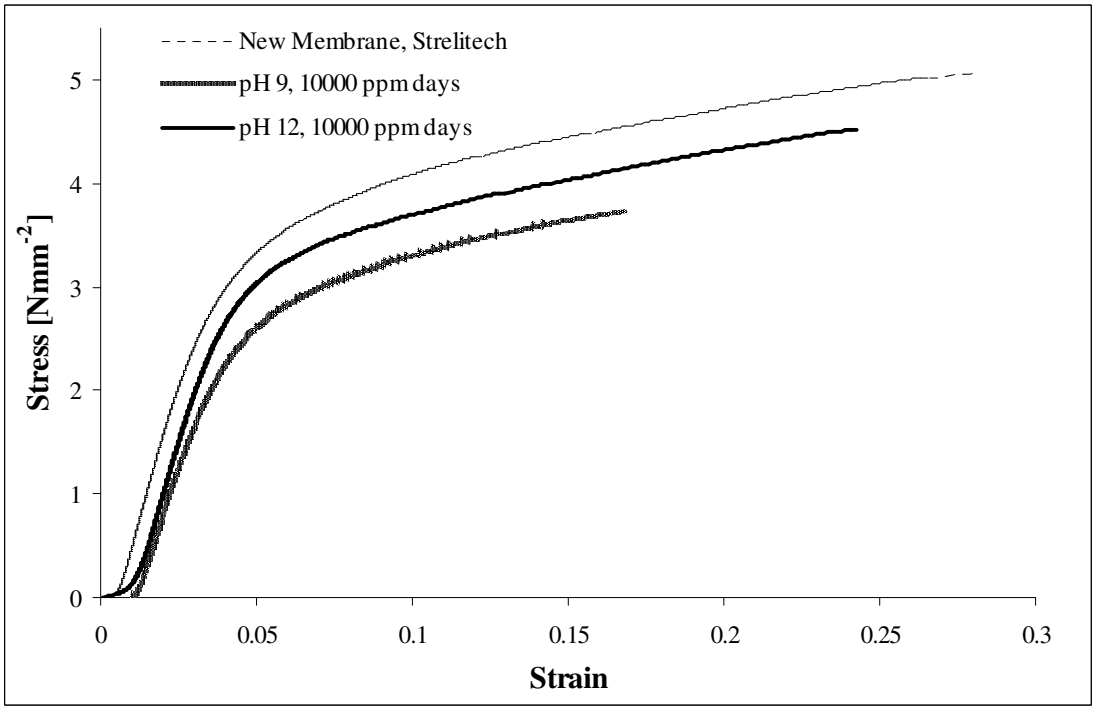

Figure 4.20 Representative stress strain curve for new and hypochlorite exposed Sterlitech membrane, (pH 9 and 12, 10,000 ppm-day)

Further analysis was done to calculate the tensile strength, yield strength and elastic modulus for each sample tested. Figure 4.21 shows the tensile strength (calculated by dividing the maximum load by the original minimum cross-sectional area of sample) of the tested samples. Clearly the pH 9 treated samples showed a significant decrease

in tensile strength for both types of membrane sample. A similar effect was noticed for the tensile strength of the backing layer. Figure 4.22 shows the offset yield strength (0.02 strains offset) (calculated by dividing the load at yield point by the original minimum cross-sectional area of sample) and Figure 4.23 shows the elastic modulus of new and treated samples. Elastic modulus was calculated by drawing a tangent to the initial linear portion of the stress-strain curve, and calculating the slope of the line.

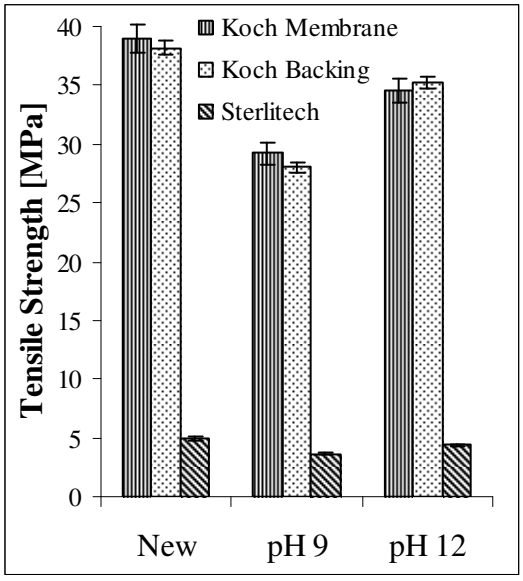

Figure 4.21 Tensile strength for new and hypochlorite aged Koch membrane 10000 ppm-days hypochlorite aged sample

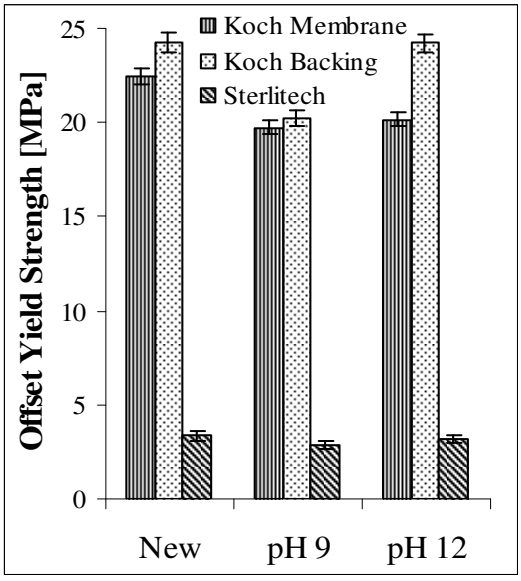

Figure 4.22 Offset yield strength for new and hypochlorite aged Koch membrane 10000 ppm day hypochlorite aged sample

A general trend was observed for all the calculated properties, i.e., a decrease in all property values for pH 9 treated samples as compared to new and pH 12 treated samples. It was noted that for same pH values the tensile properties were quite similar for both the backing layer and Koch membrane samples. It can be inferred that the tensile properties of membrane, as a whole, were mainly governed by the backing layer with very small or negligible contribution from the top PES layer. This may be attributed to a huge difference in strength of the two polymers which is obvious by looking at Sterlitech membrane tensile properties. Sterlitech membranes, which had no backing, showed a significant decrease of 26% and 11% in tensile strength both pH 9 and pH 12 treated samples respectively as shown in Table 4.3, (For details of analysis on Koch membranes and backing samples please refer to Appendix 2.2).

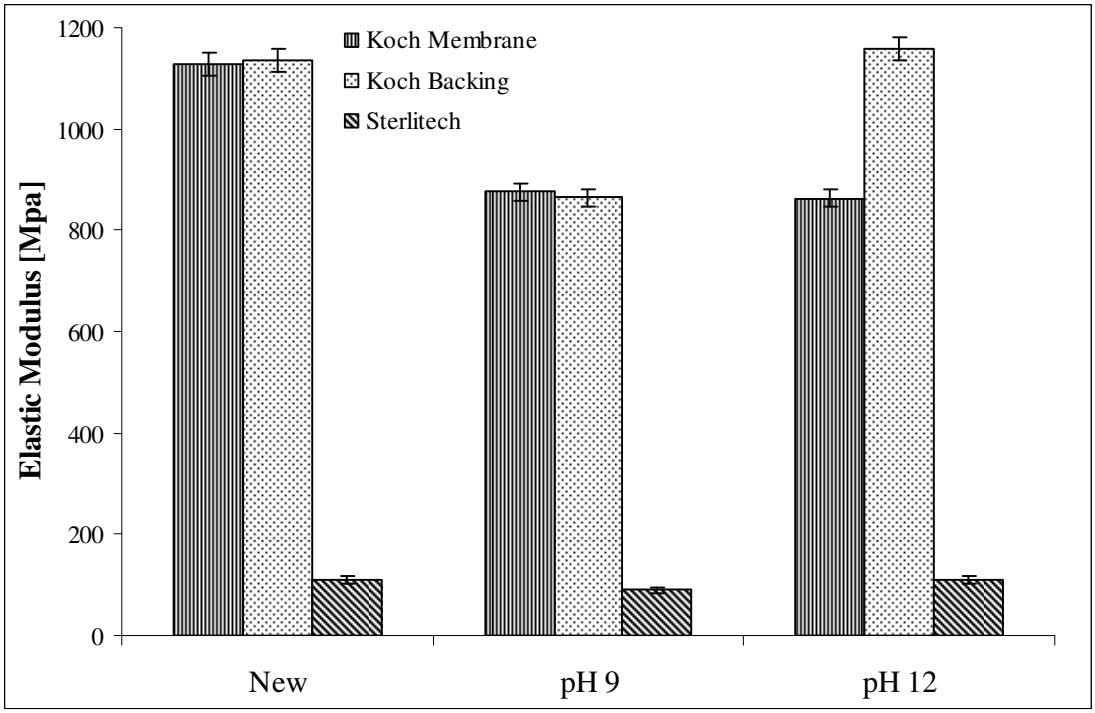

Figure 4.23 Elastic modulus for new and hypochlorite aged Koch membrane 10000 ppm-days hypochlorite aged sample

Table 4.3 Tensile properties of Sterlitech membrane new and 10,000 ppm-days hypochlorite exposed samples

Property	Sample		% Decrease
Tensile Strength MPa	Sterlitech New	4.9	0
	Sterlitech pH 9	3.7	25.9
	Sterlitech pH 12	4.4	11.2
Yield Strength MPa	Sterlitech New	3.4	0
	Sterlitech pH 9	2.9	14.45
	Sterlitech pH 12	3.2	6.0
Elastic Modulus MPa	Sterlitech New	108.8	0
	Sterlitech pH 9	89.4	17.8
	Sterlitech pH 12	110.2	-1.30

A similar effect was observed for offset yield strength values but elastic modulus did not change significantly for pH 12 treated samples. The tensile tests confirmed that hypochlorite treatment at both pH changed the tensile properties of membranes though the severity of degradation was more obvious for pH 9 degraded samples.

4.5 FESEM Imaging and EDS Analysis

New and hypochlorite exposed membrane samples were microscopically analysed for any signs of surface erosion or cracks by high resolution FESEM. Before preparing

samples for FESEM imaging the test specimen were physically observed to detect any change visible to the naked eyes.

4.5.1 Physical Observations

Two distinctive surface-defects, crack formation and loss in surface gloss, were observed on the PES layer of membranes.

4.5.1.1. Crack Formation

For samples degraded by hypochlorite exposure at pH 9 it was observed that the membrane surface PES layer was weak and easily formed cracks with simple twisting and bending of the membrane. This defect was observed in all the exposures from 10,000 ppm-days to 25,000 ppm-days exposed samples, though the ease in cracking increased with exposure time. pH 10 hypochlorite exposed membrane also showed surface cracking on twisting and bending but to a lesser extent than the pH 9 treated membranes. pH 11 treated membrane showed cracking only after extreme twisting and folding of the membrane while this defect was absent in new or samples treated at pH 12 hypochlorite (for all the exposure times).

4.5.1.2 Surface Gloss

The PES layer of the new membrane samples had a surface gloss. Irrespective of pH of hypochlorite treatment, a loss in the surface gloss was observed in all the hypochlorite degraded samples. The decrease in surface gloss was more prominent in pH 9 and 10 treated samples as compared to pH 11 and 12 treated samples. The decrease in surface gloss was more obvious in 25,000 ppm-days aged samples as compared to 10,000 ppm-days aged samples. The loss in surface gloss may be due to the increase in surface roughness with hypochlorite ageing. The decrease in surface gloss was directly related to pH and exposure time.

4.5.2 FESEM Imaging

4.5.2.1 Structure of Different Membranes

The commercial membrane is a double layer structure so it was essential to understand the detailed structure of the membrane microscopically. FESEM imaging was done on new commercial ultrafiltration membrane (Koch), in-house cast PES membranes and new Sterlitech microfiltration membranes to have a better understanding of the membrane structure. Figure 4.24 shows the cross-sectional view of the Koch commercial UF membrane. The double layer structure of the membrane is clearly visible with the PES membrane layer cast on top of a polyolefin backing layer. Figure 4.25 and 4.26 shows the cross-sectional and front view of the backing layer respectively. It can be noticed that the backing is made of non-woven fibres compressed together to make a highly porous sheet. The fibres are compressed randomly without any particular orientation. This randomness in backing structure probably contributed to uncertainty in measured mechanical properties of membrane especially DMA and tensile strength.

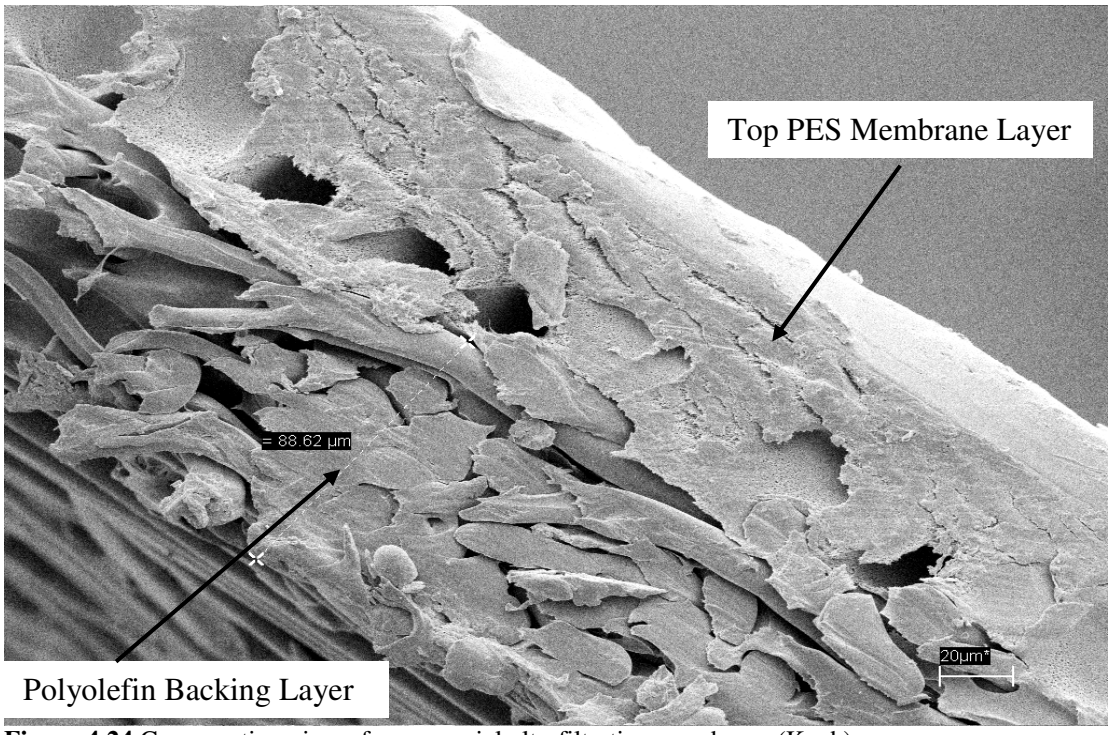

Figure 4.24 Cross section view of commercial ultrafiltration membrane (Koch)

Figure 4.25 Cross section view of backing layer, membrane, new membrane (Koch)

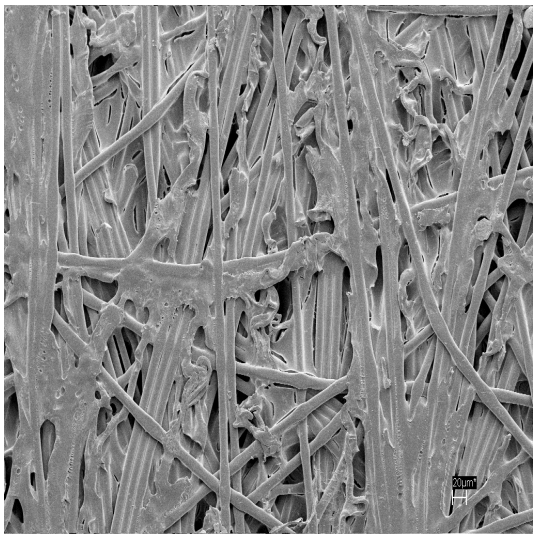

Figure 4.26 Front view of backing side of new new membrane (Koch)

To study the structure of the PES membrane layer, the PES ultrafiltration membrane was cast in house, using a phase inversion method and imaged under SEM for microscopic study. Figure 4.27 shows the cross-sectional view of an in-house cast PES ultrafiltration membrane. It shows that the actual active separation area is a thin barrier skin at top. The pore size increases going down from the skin ending up in big porous channels which forms a highly porous PES membrane back. The thick membrane back provides mechanical strength to the thin barrier skin.

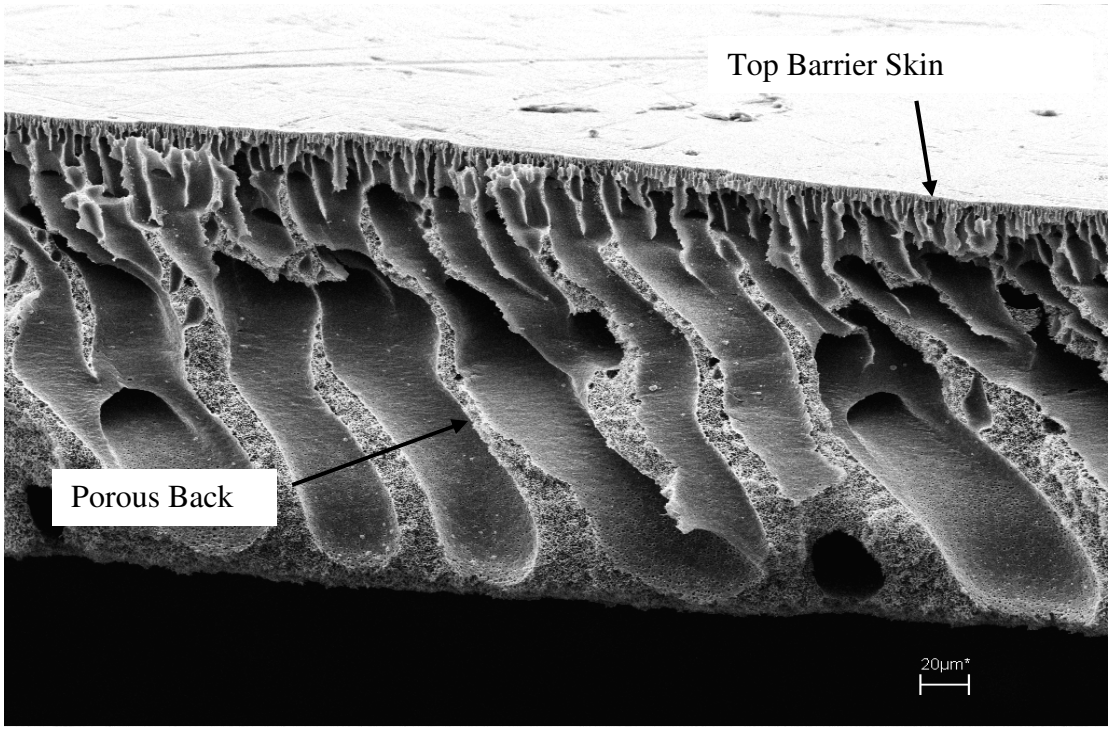

Figure 4.27 Cross section view of an in-house cast PES ultrafiltration membrane

In the case of commercial ultrafiltration membranes the casting is done on polyolefin backing which increases the mechanical strength of the membranes. It allows the usage of membrane under high or fluctuating operating pressure conditions. Efforts were made to visualise the pores of the Koch UF membranes, but owing to their low MWCO of 10 kDa, no pores were visible even under a very high magnification of 20,000X. Beyond 20,000X surface charging of the membrane became a problem and produced artefacts which limited any further increase in magnification. Figure 4.28 shows the front view of a Sterlitech microfiltration membrane. Since it had a significantly larger pore size of 0.2 μm, the porous structure of the surface was easily visible under FESEM. It can be observed that even the microfiltration membrane had a thin skin layer with smaller pores as compared to the layer just under beneath it. It was also observed that the membrane had a random distribution of pores with a wide range of pore size.

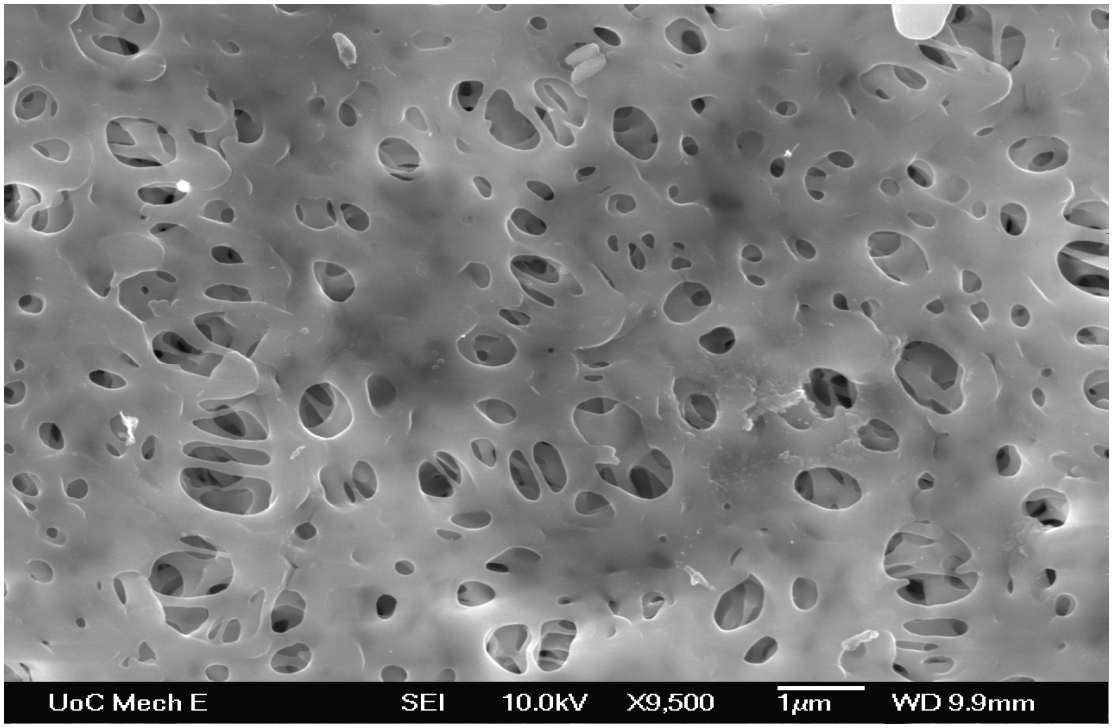

Figure 4.28 Front view of new Sterlitech membrane

4.5.2.2 FESEM Analysis of Hypochlorite Exposed Membrane Samples

Koch Ultrafiltration Membrane

Microscopic imaging was done to analyse the surface of the commercial ultrafiltration membrane for any change in surface structure that could be detected by FESEM.

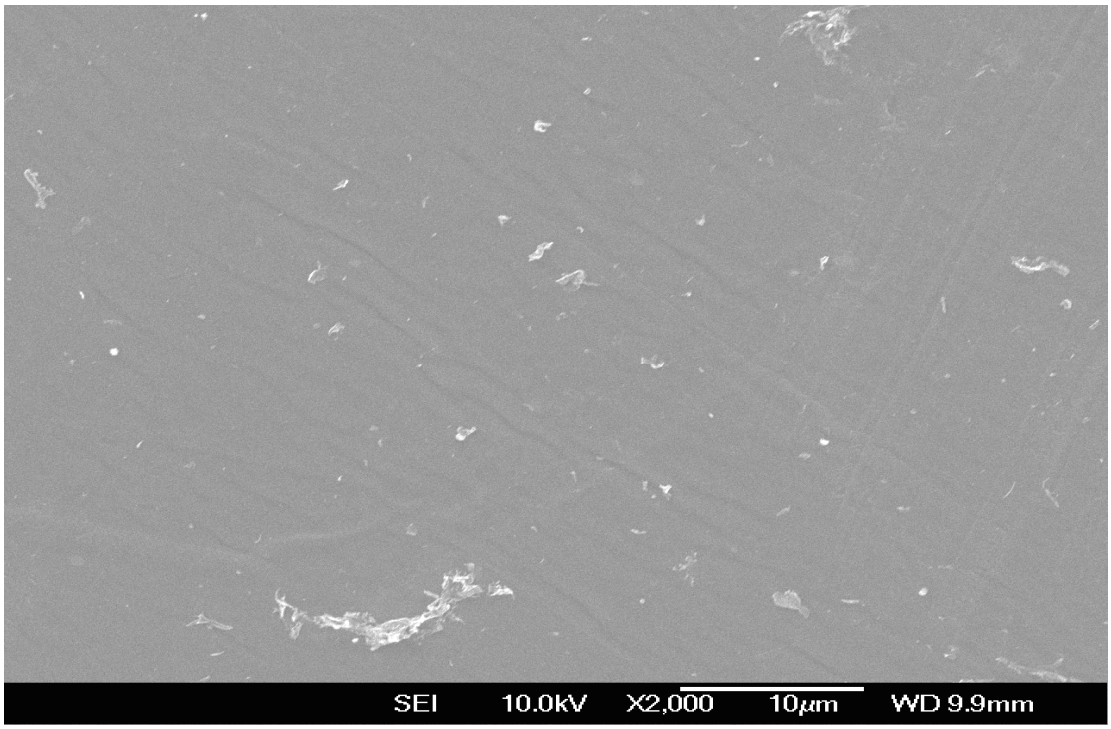

Figure 4.29 New Koch Membrane at X2000 magnification

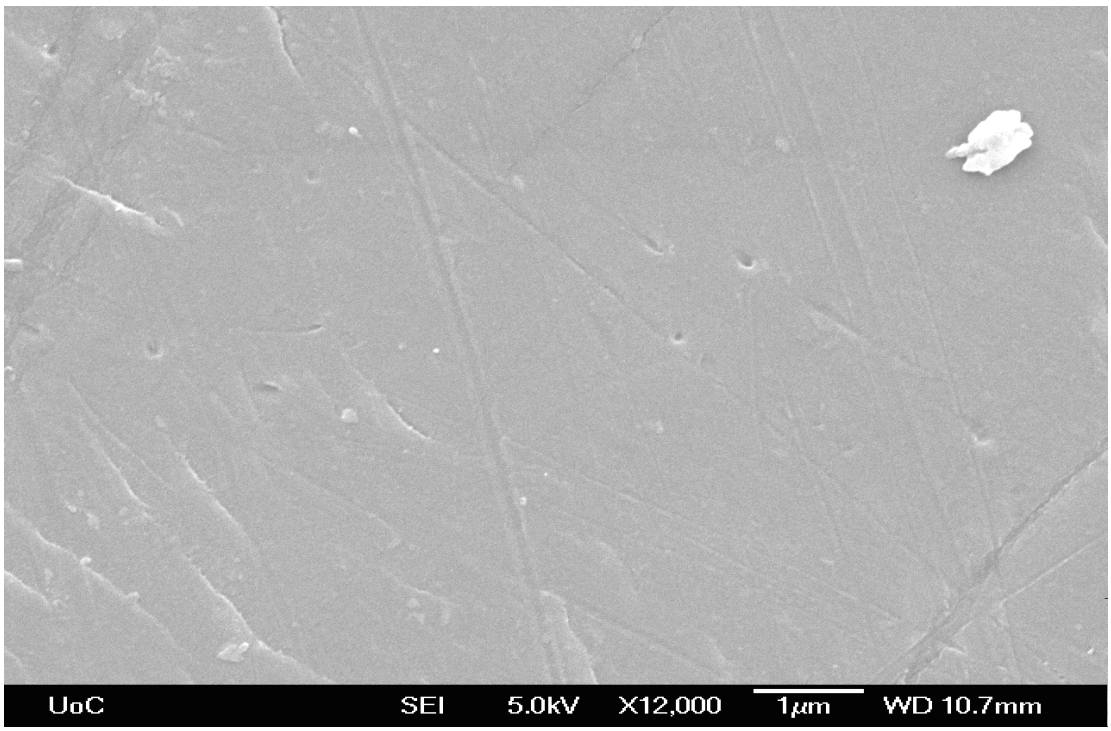

Figure 4.30 New Koch Membrane at X12000 magnification

Figures 4.29 and 4.30 show the PES side of a Koch membrane at X2000 and X12000 magnifications. A clean smooth surface without any surface cracks pitting was observed even at very high magnification of X12000. Surface blemishes were observed at X12000 which were highly localised and were spotted only at a few

places on the membrane surface (Figure 4.30). The PES membrane layer was a very porous and soft material so some surface abrasion and blemishes were expected. pH 12 hypochlorite (25,000 ppm-day) exposed membranes also showed no signs of surface cracking, pitting or any other defect as compared to new membrane even at a high magnification of X13000 (Figure 4.31). Localised surface blemishes similar to new membrane were also observed. It was concluded that even at a very high exposure of 25,000 ppm-days at pH 12, the PES membrane layer surface was similar to the new membrane and no surface defects was detected that could be linked to hypochlorite degradation of membrane (even at magnification of X13000).

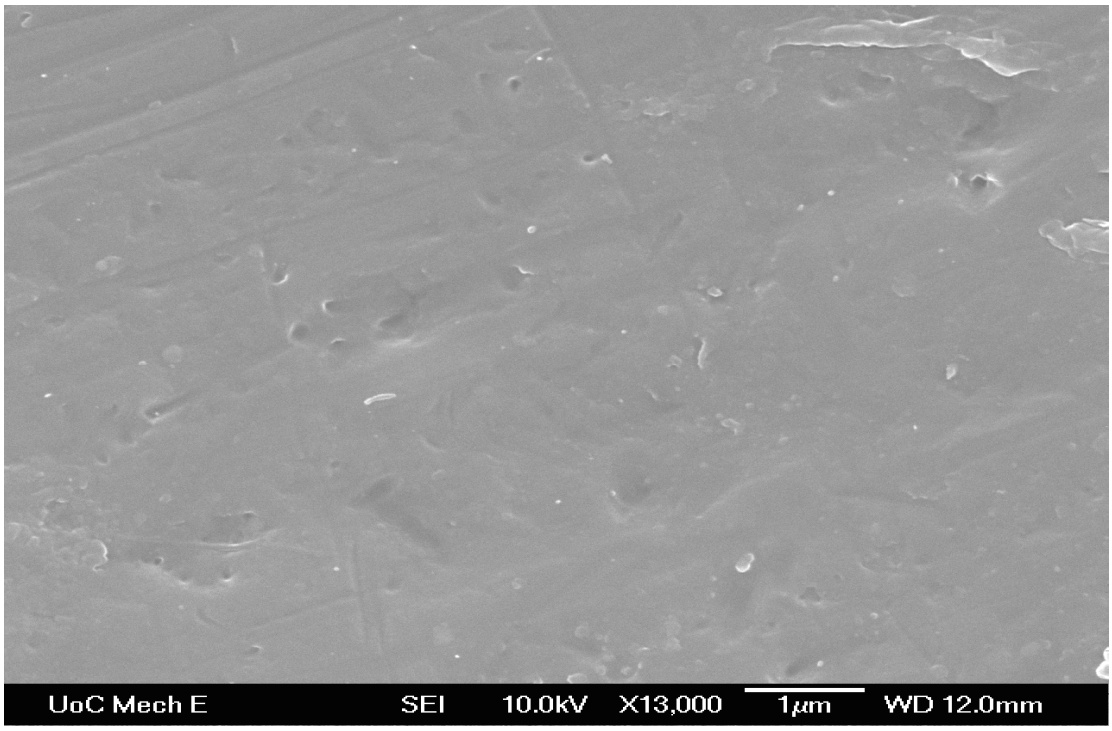

Figure 4.31 Hypochlorite degraded membrane (Koch) (pH 12, 25,000 ppm-day exposure)

Figure 4.32 shows the PES membrane side of pH 11, 25,000 ppm-days hypochlorite degraded membrane. Although the membrane did not show any signs of surface pitting, some small surface cracks were detected. Surface cracking of PES layer showed an indication of degradation of PES with hypochlorite treatment which led to a decrease in PES strength leading to surface cracking of membrane. Figures 4.33 to Figure 4.36 shows the FESEM images of the PES layer surface for pH 10 hypochlorite exposed membranes (from 10,000 to 25,000 ppm-days exposure time). The surface of pH 10, 10,000 ppm-days treated membrane showed no surface cracking or surface defects that can be linked with hypochlorite exposure and the surface appeared to be similar to the surface of new membrane (Figure 4.33). At

15,000 ppm-days of exposure the surface appeared to be uneven and rough as compared to the new membrane (Figure 4.34), which gave an indication of hypochlorite degradation of the membrane.

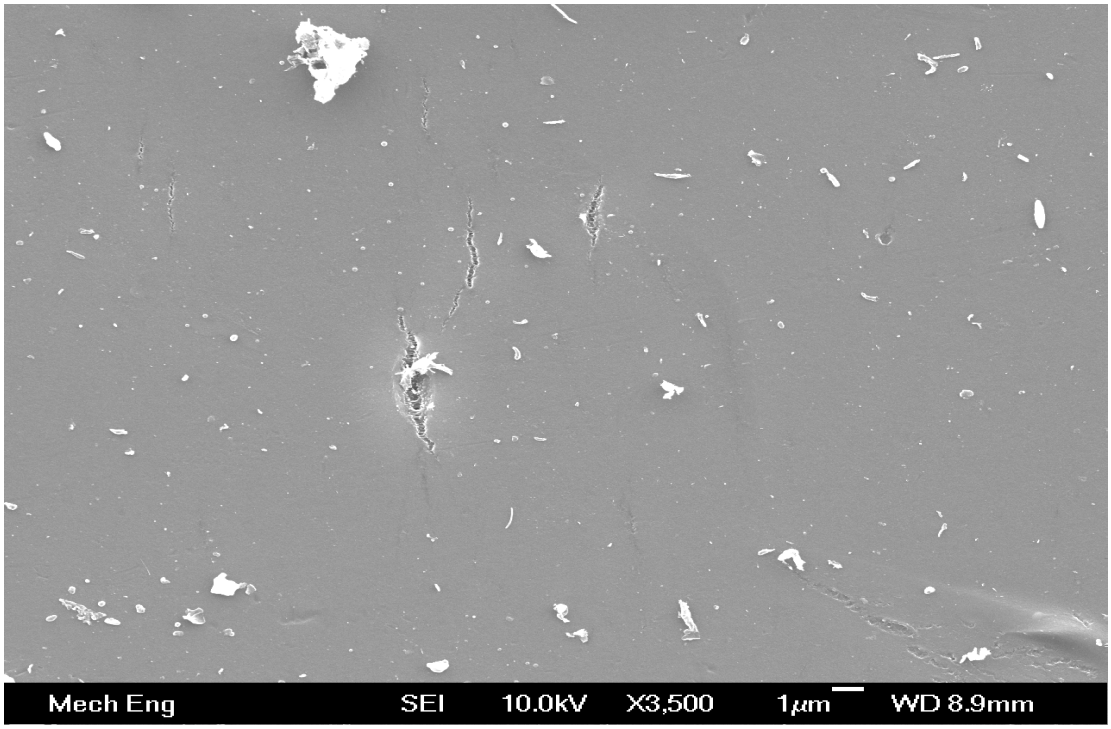

Figure 4.32 Hypochlorite degraded membrane (Koch) (pH 11, 25,000 ppm-day exposure)

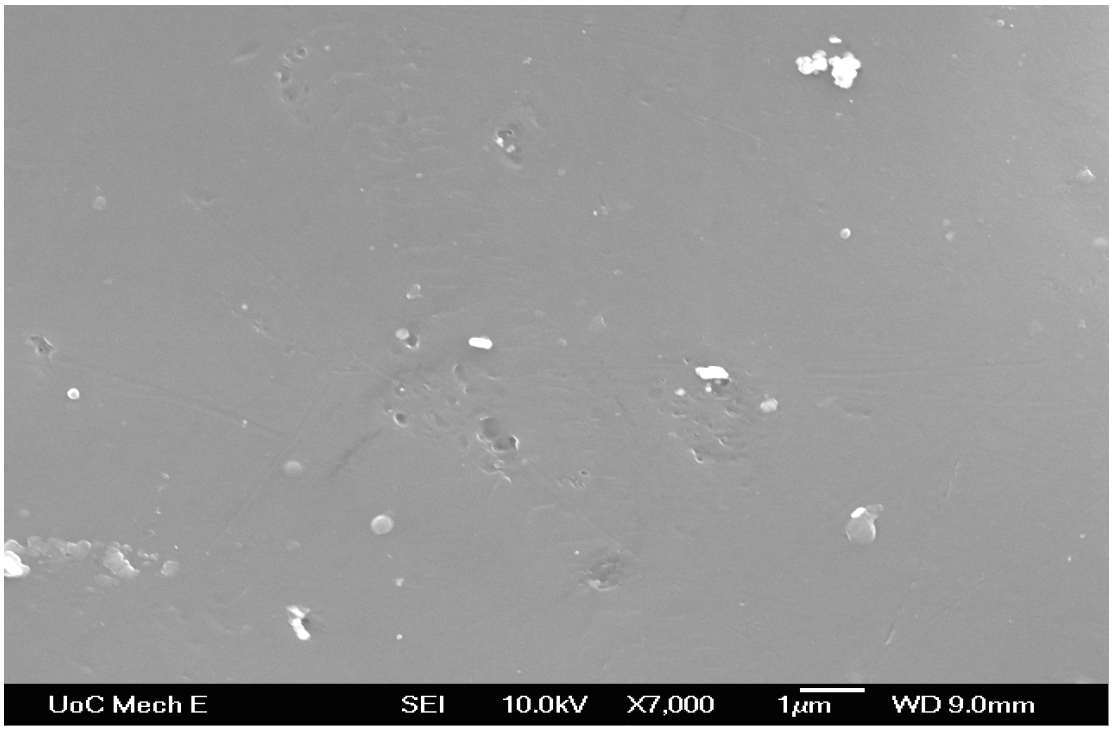

Figure 4.33 Hypochlorite degraded membrane (Koch) (pH 10, 10,000 ppm-day exposure)

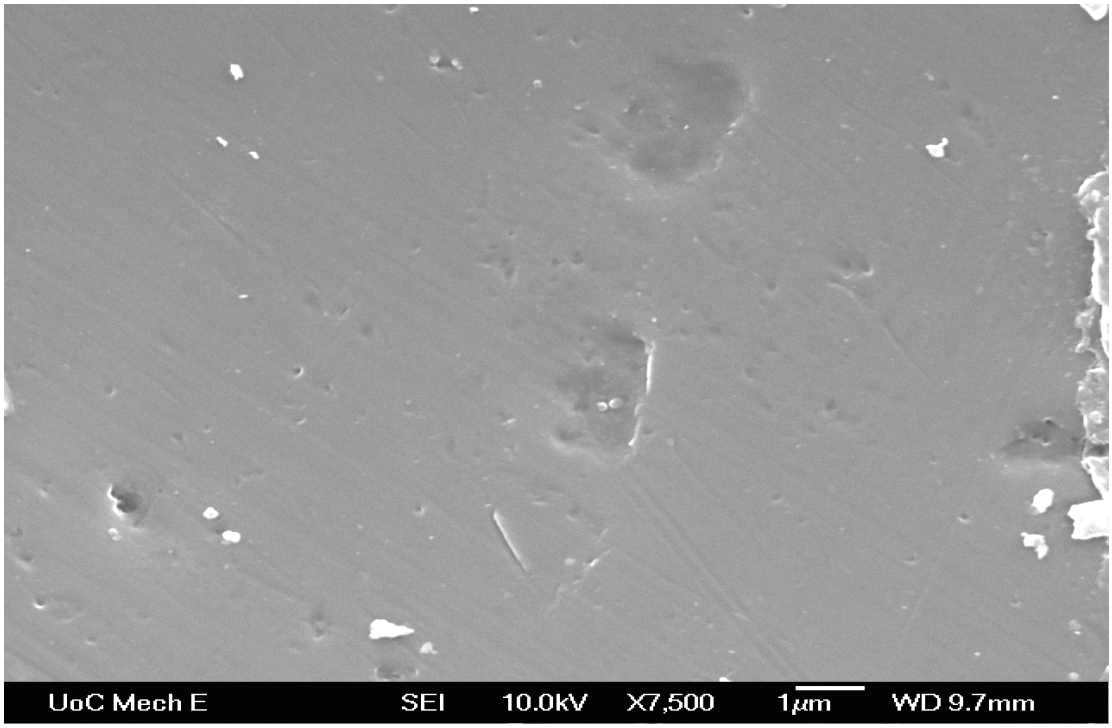

Figure 4.34 Hypochlorite degraded membrane (Koch) (pH 10, 15,000 ppm-day exposure)

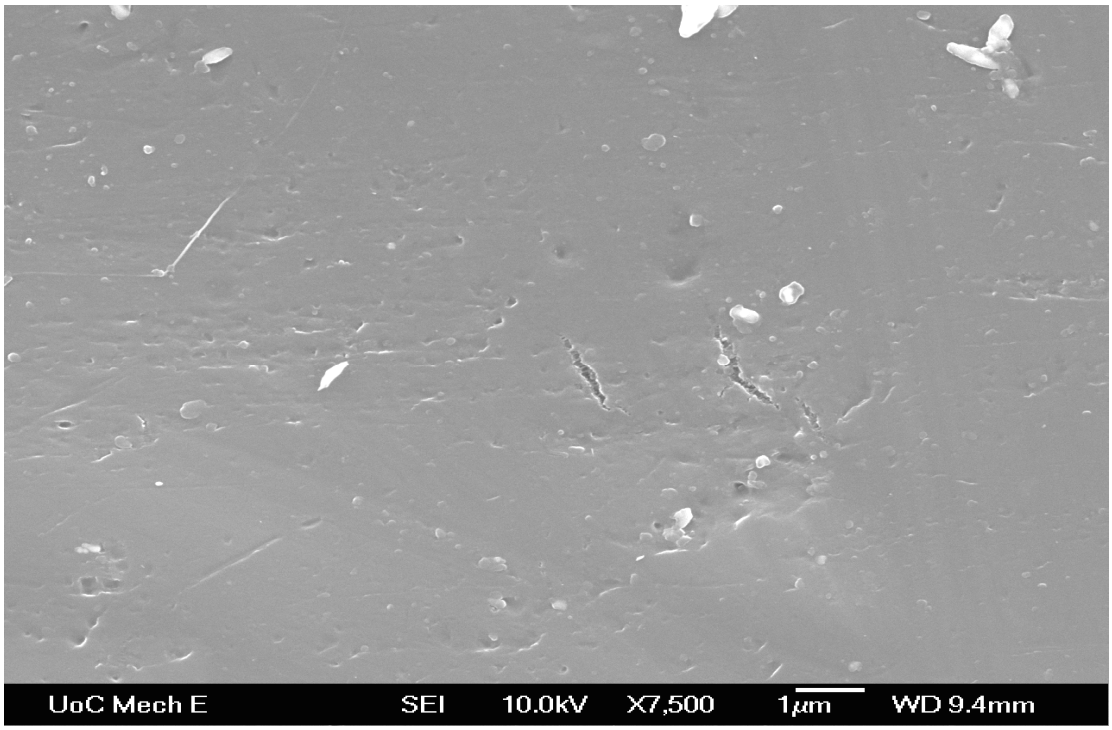

Figure 4.35 Hypochlorite degraded membrane (Koch) (pH 10, 20,000 ppm-day exposure)

For the 20,000 ppm-days hypochlorite degraded membrane the signs of degradation were more obvious. Cracking of the PES layer was observed throughout the surface which showed that the degradation effect of hypochlorite treatment on the PES surface was increasing with increase in exposure time (Figure 4.35).

Widespread cracking on PES layer was observed for the 25,000 ppm-days hypochlorite treated sample. A new kind of surface defect was also detected, i.e. surface pitting. Although surface pitting was not wide spread as compared to cracking, a significant number of pits were observed on the surface (Figure 4.36). The FESEM analysis on pH 10 hypochlorite treated membranes clearly indicated that the degradation severity was high in the case of pH 10 exposure as compared to pH 11 for the same exposure time. Also the degradation severity for pH 10 hypochlorite samples increased with increase in exposure time.

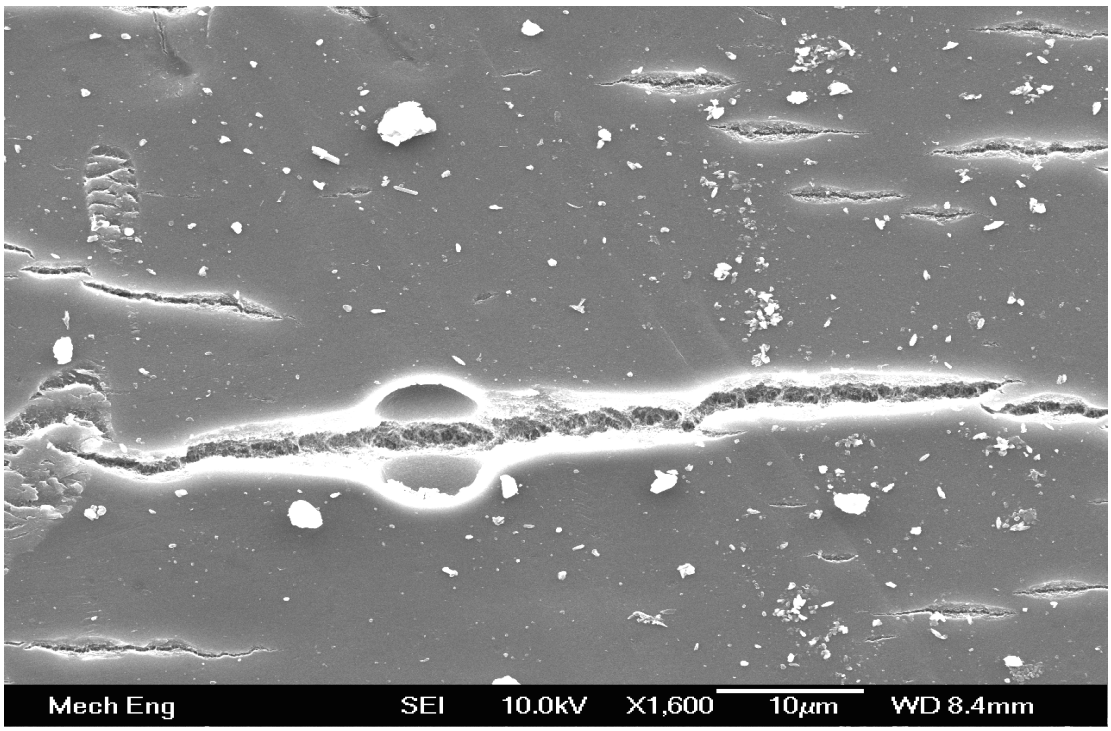

Figure 4.36 Hypochlorite degraded membrane (Koch) (pH 10, 25,000 ppm-days exposure)

Figures 4.37 to 4.40 shows the FESEM images of the PES layer surface for pH 9 hypochlorite exposed membranes (from 10,000 to 25,000 ppm-days exposure time). In the case of pH 9 hypochlorite treated samples surface cracking and surface pitting was observed for all the exposure times. The severity of surface cracking increased with increase in exposure time. 10,000 ppm-days exposed samples showed significant surface pitting visible at X3500 magnification. In the case of 25,000 ppm-days exposure the severity of pitting increased to a very high level and larger pits were detected at a lower magnification of X1000. A clear trend was observed for pH 9 hypochlorite treated membrane samples. The severity of surface cracking, the pit size and pit density increased with exposure time. It was also observed the surface cracks

tended to travel through the pits as the pits may have provided a weak surface for the crack to propagate. The surface pitting and crack formation may directly lead to complete loss of the integrity of the membranes.

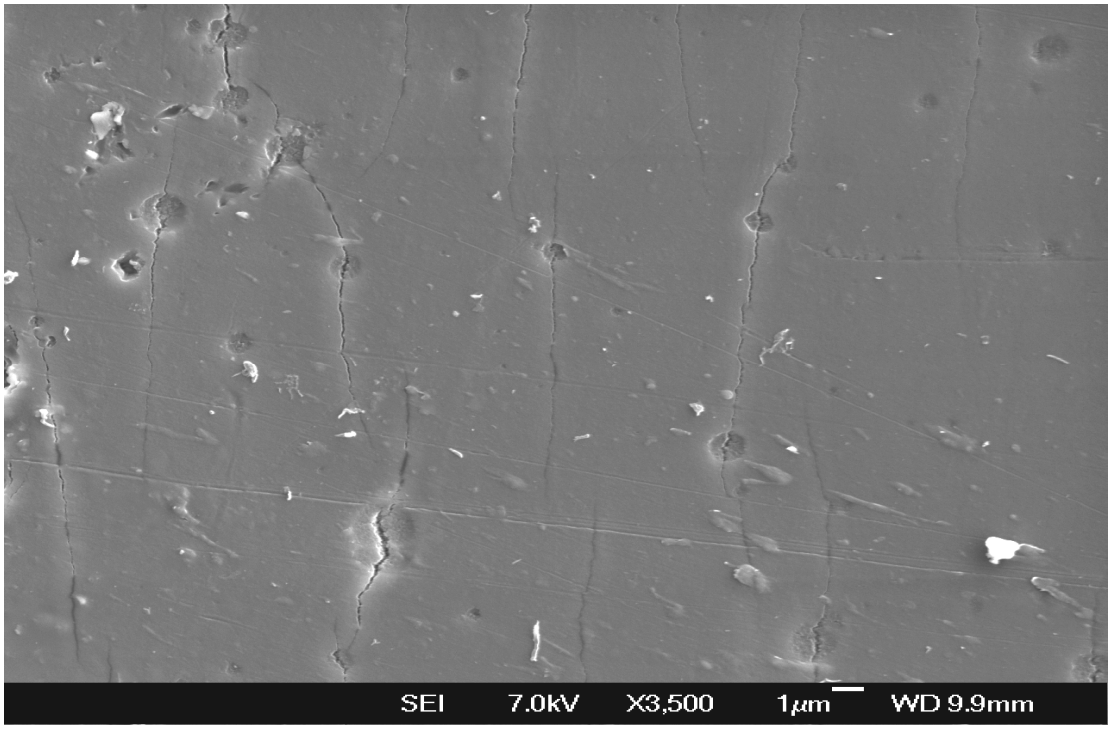

Figure 4.37 Hypochlorite degraded membrane (Koch) (pH 9, 10,000 ppm-day exposure)

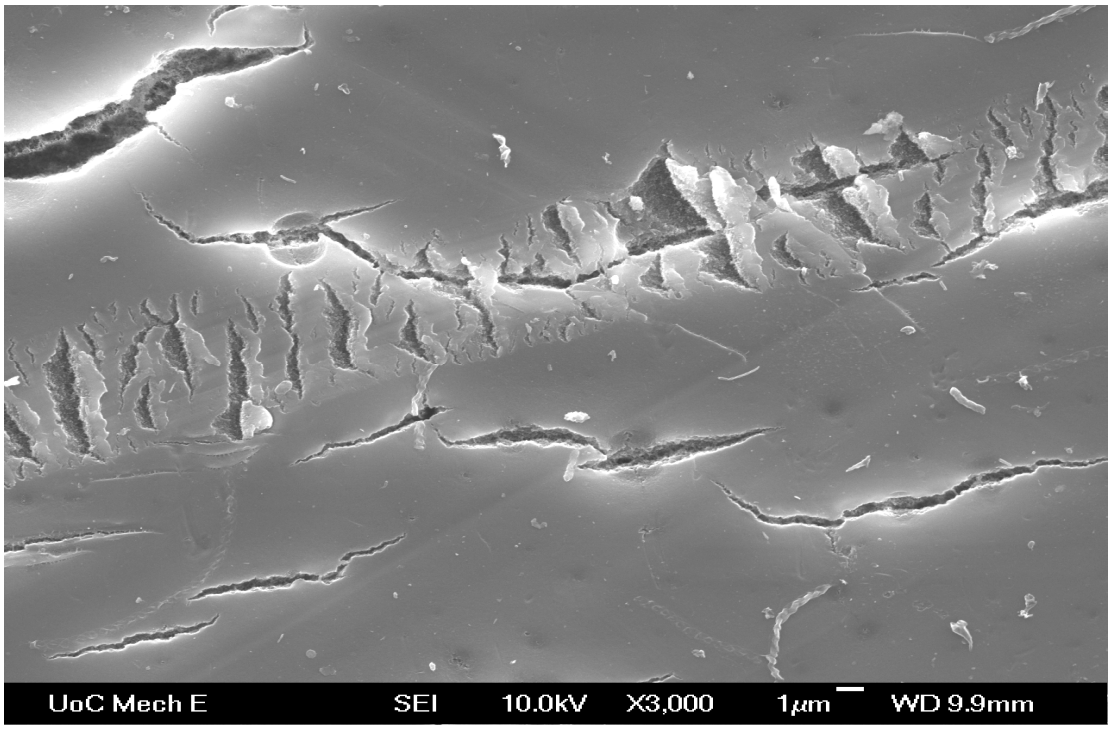

Figure 4.38 Hypochlorite degraded membrane (Koch) (pH 9, 15,000 ppm-day exposure)

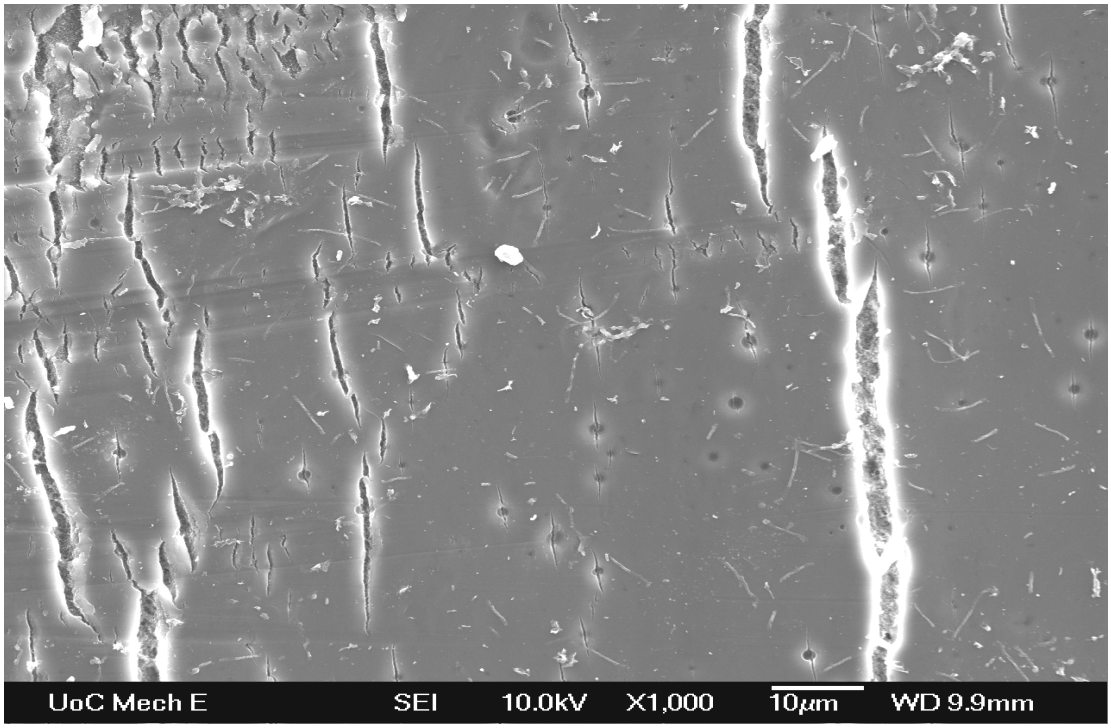

Figure 4.39 Hypochlorite degraded membrane (Koch) (pH 9, 20,000 ppm-day exposure)

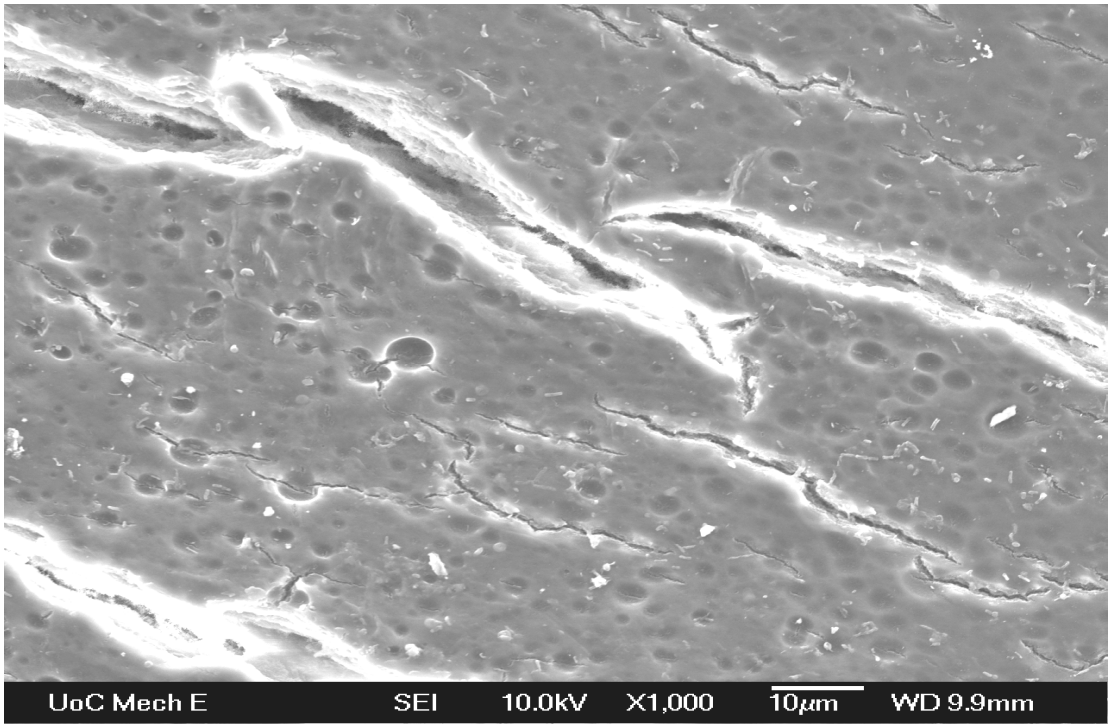

Figure 4.40 Hypochlorite degraded membrane (Koch) (pH 9, 25,000 ppm-day exposure)

The trends in surface defect formation observed in pH 9 treated samples were quite similar to pH 10 treated membranes. From FESEM imaging it was concluded that severity of degradation increased with decrease in pH of hypochlorite exposure. Also the severity of degradation increased with increase in exposure time for the same

hypochlorite pH. Pit formation was mainly observed in pH 9 treated samples and to some extent in pH 10 treated samples (only in 25,000 ppm-days exposure. It indicates that extreme degradation occurs at pH 10 or below which can directly lead to loss in separation properties of membrane.

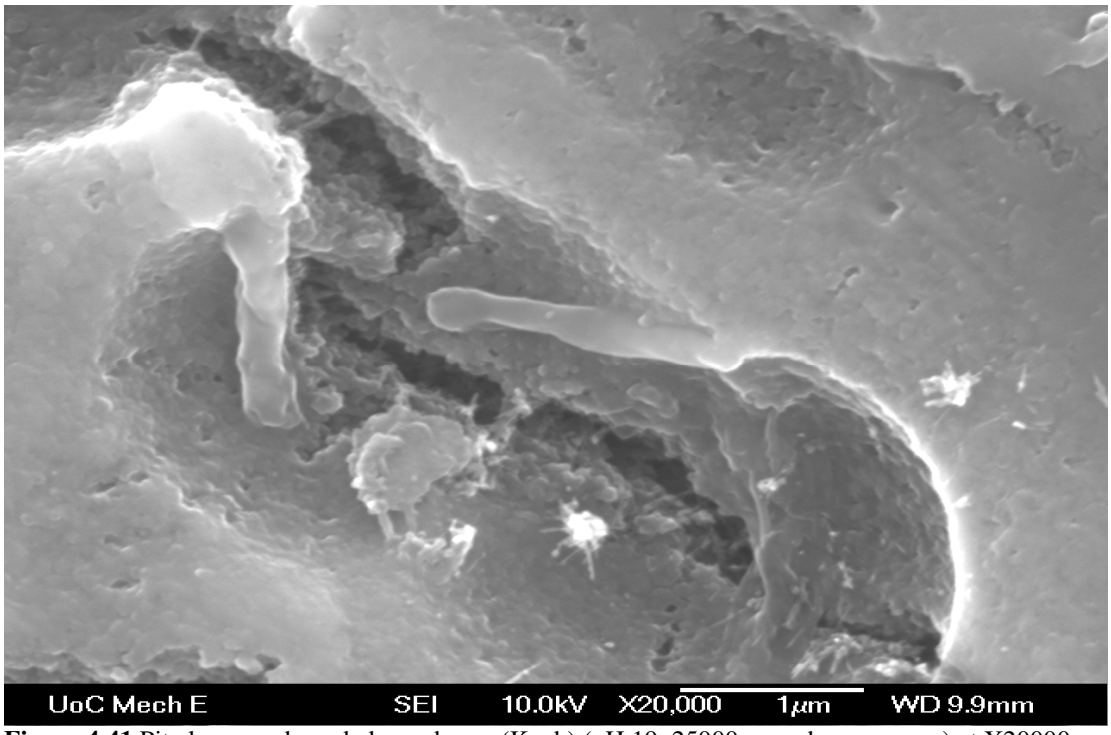

Figure 4.41 Pit close up, degraded membrane (Koch) (pH 19, 25000 ppm-day exposure) at X20000

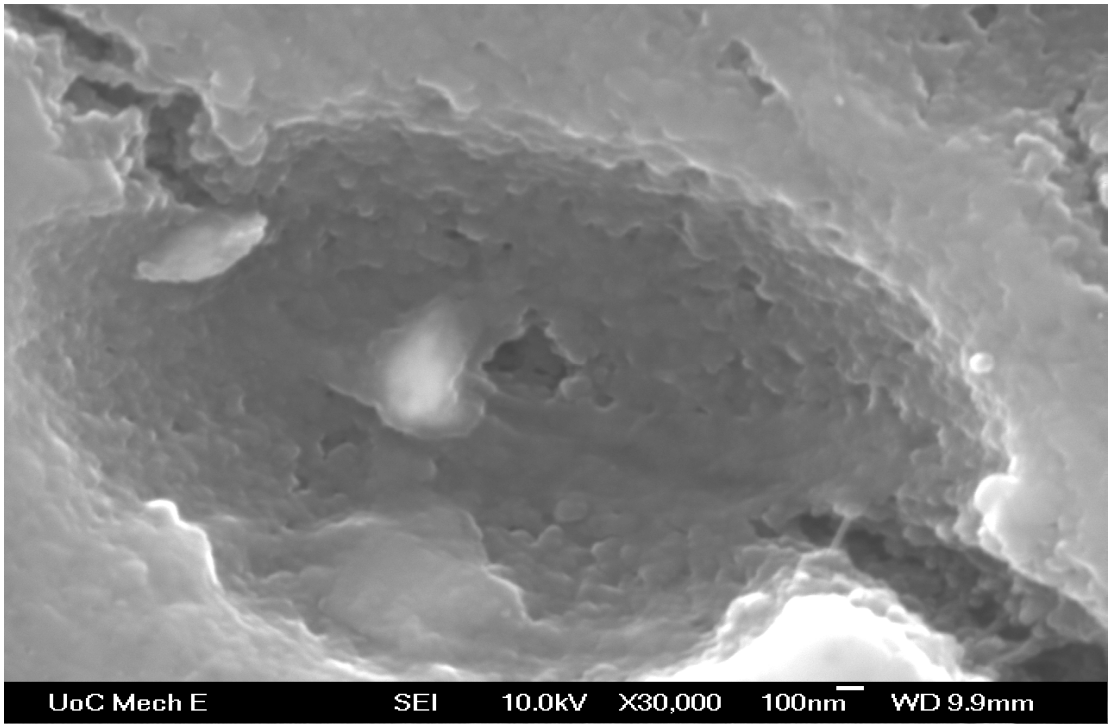

Figure 4.42 Pit close up, degraded membrane (Koch) (pH 19, 25000 ppm-day exposure) at X20000

Further analysis of surface pits formed for pH 9, 25,000 ppm-days hypochlorite treated membranes revealed a complete loss of the thin barrier layer in the pit area (Figure 4.41 and 14.42). Due to large pits in the surface of degraded membranes, during ultrafiltration a more porous under layer of PES will be exposed to any feed passed. It can directly cause leakage of higher molecular weight entities into the permeate stream and a loss in functional properties of the membrane. It was possible that pit formation also occurred on pH 11 and 12 hypochlorite degraded samples but the size may be too small to be detected by FESEM imaging.

FESEM imaging was also done on the polyolefin backing side of the membrane to check for any surface cracking or deformation due to hypochlorite exposure. Figure 4.43 shows the backing side of a pH 9, 25,000 ppm-days hypochlorite treated membrane. In all the exposures it was observed that polyolefin fibres were intact and did not show any sign of surface cracking or roughening with the exposure. It indicated that irrespective of pH or exposure time, hypochlorite exposure had no degradation effect on backing layer which could be detected by FESEM microscopy.

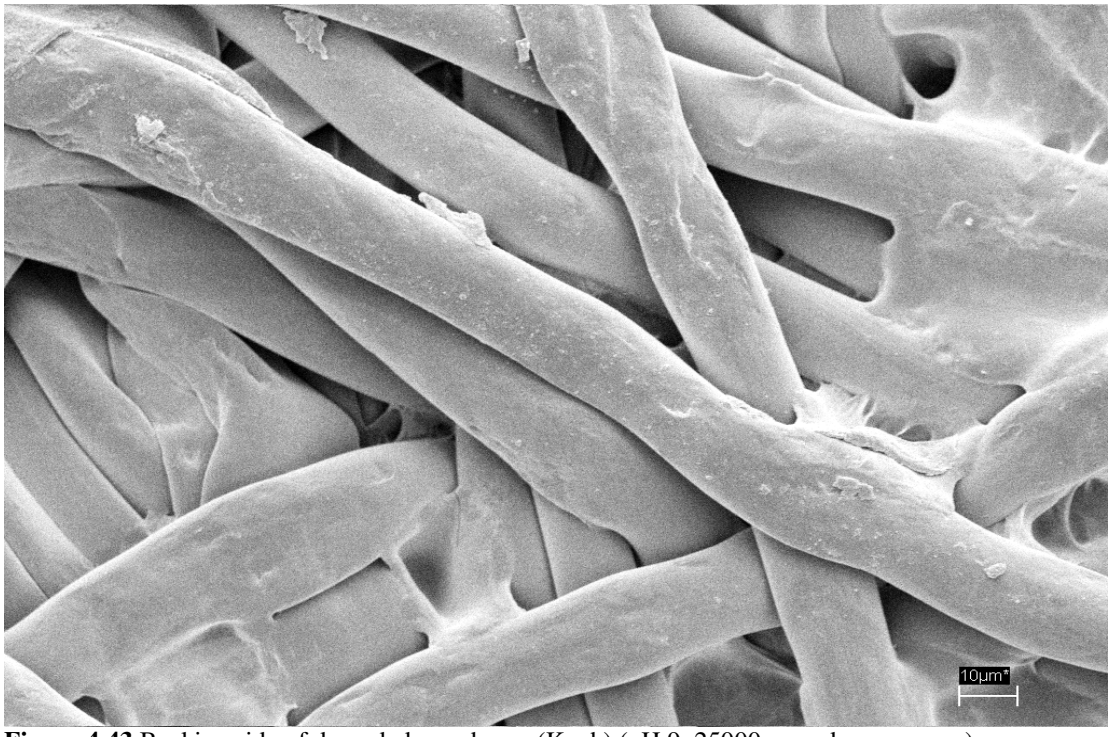

Figure 4.43 Backing side of degraded membrane (Koch) (pH 9, 25000 ppm-day exposure)

Sterlitech Microfiltration Membrane

Figure 4.45 and Figure 4.46 shows FESEM images of pH 9 and pH 12 (10,000 ppm-day) hypochlorite treated samples respectively.

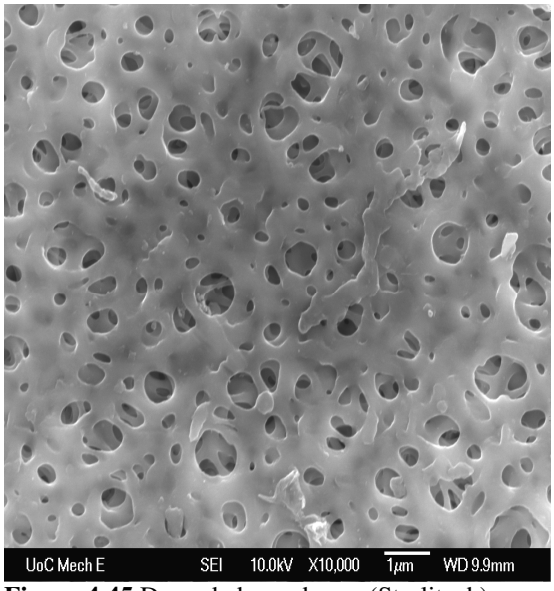

Figure 4.45 Degraded membrane (Sterlitech) (pH 9, 10000 ppm-days exposure)

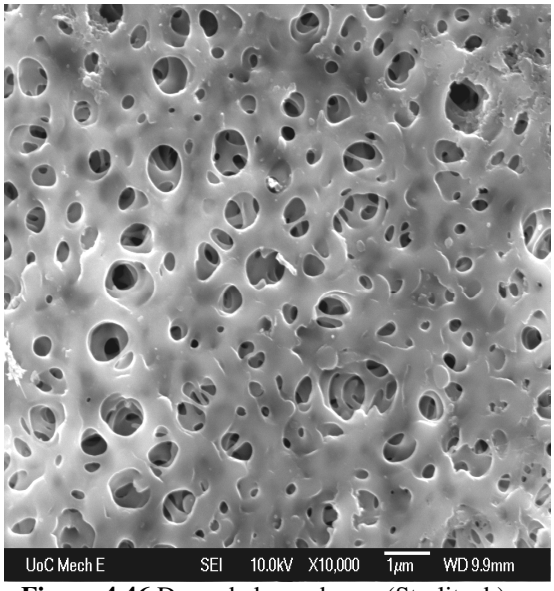

Figure 4.46 Degraded membrane (Sterlitech) (pH 12, 10000 ppm-days exposure)

Since the Sterlitech membrane had a highly porous structure it was difficult to locate any surface change in the membrane with hypochlorite treatment. Both pH 9 and pH 12 treated membranes looked similar to a new membrane. No surface cracking was observed for either sample. The double layer structure of commercial ultrafiltration membrane may be playing an important role in surface cracking. The flat sheets cut out from ultrafiltration membrane (Koch) tend to roll (during storage in water) when left freely which may be due to residual stress in between the backing and PES layer. This effect was absent in the Sterlitech microfiltration membranes as there was no backing layer. This residual stress may act as enhancer for crack formation in the PES layer of Koch membranes. The residual stresses seemed to be absent in Sterlitech membranes and no surface cracking was observed. Also the surface of the membrane was too porous to observe any surface pitting if it formed.

PES Foil (Good Fellow)

PES foil were also analysed for any surface defects produced by exposure to hypochlorite solution. Figure 4.47 and Figure 4.48 shows new foil and pH 9, 25,000 ppm-days hypochlorite exposed foil respectively.

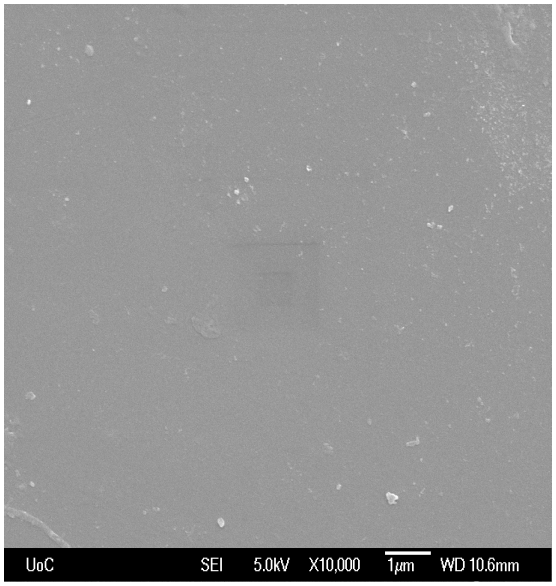

Figure 4.47 New PES foil (Good Fellow)

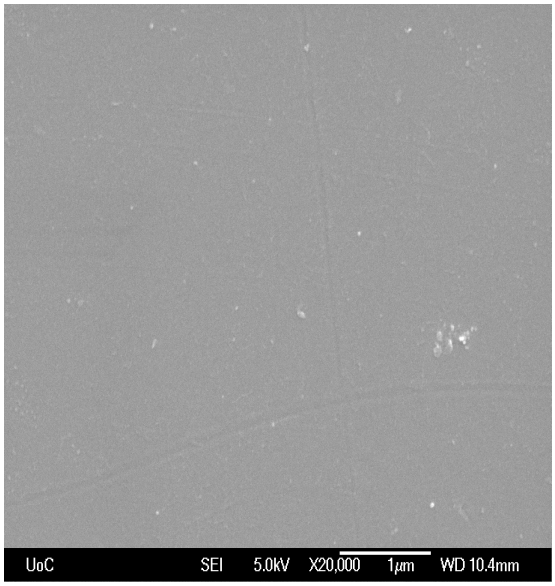

Figure 4.48 Degraded PES foil (Good Fellow) (pH 9, 25,000 ppm-days exposure)

No surface pitting or cracking was observed in any of the exposures. It demonstrates that surface porosity may here an important role in the degradation process. Maybe surface pores provided a weak area for hypochlorite to attack which was absent in case of PES foil.

4.5.3 EDS Analysis

EDS analysis was done on the Koch commercial UF membrane to find the amount of chlorine, bound to the surface of membrane samples. The surface composition was expressed as a ratio of each element to sulphur content.

EDS analysis indicated the presence of a significant amount chlorine on the surface of pH 9 treated samples without any trace of sodium. Since no trace of sodium was found on the surface of any of the samples analysed, it was understood that rinsing of membrane done after chlorine exposure was efficient and no residual chlorine or sodium was adhering to the surface. It was concluded that chlorine detected by EDS was chemically bound. EDS analysis demonstrated that the amount of chlorine increased with exposure time as shown in Figure 4.49. Although significant amount chlorine was detected on the surface of pH 10 exposed samples, it remained more or less constant even at higher exposure time. It may be because the amount of chlorine on surface was very low or near the detection limits of the EDS technique.

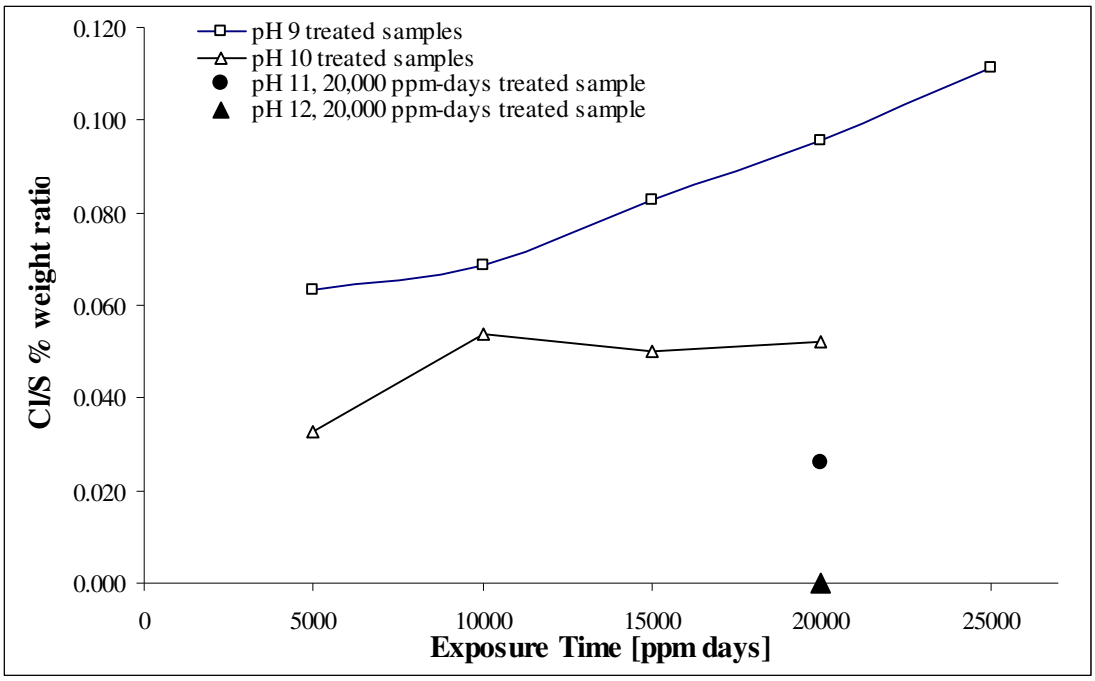

Figure 4.49 Chlorine/sulphur ratios for new and hypochlorite degraded Koch membrane samples (pH 9 to 12 hypochlorite solution for 5,000 ppm-days to 25,000 ppm-day exposure)

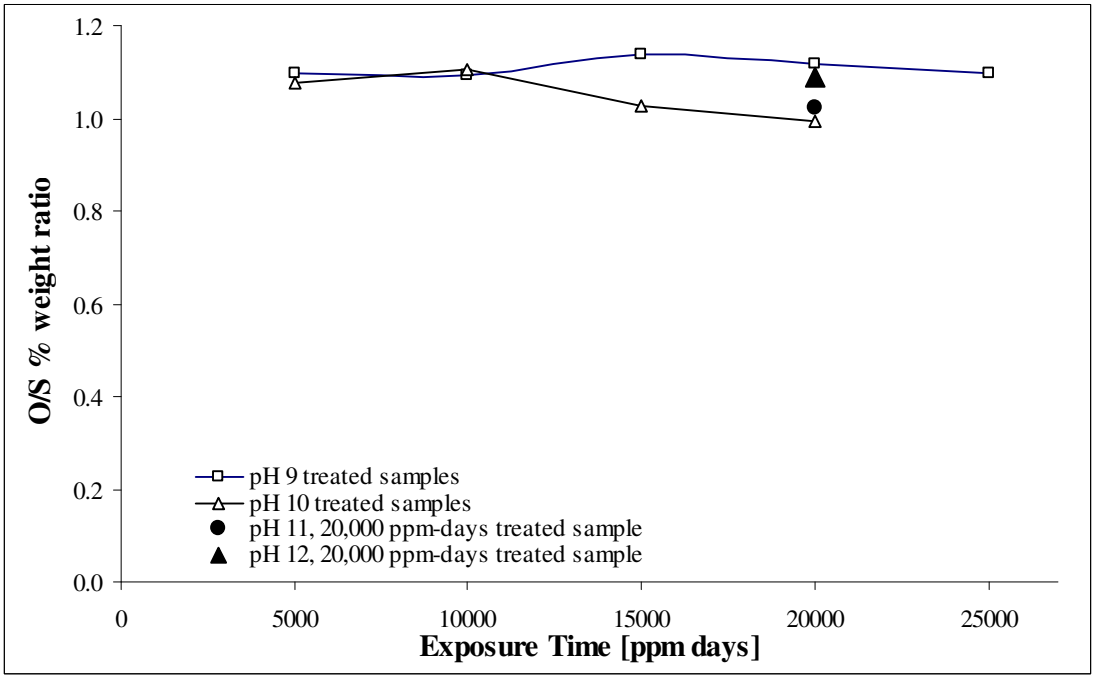

Figure 4.50 Oxygen/sulphur ratios for new and hypochlorite degraded Koch membrane samples (pH 9 to 12 hypochlorite solution for 5,000 ppm-days to 25,000 ppm-day exposure)

In the case of pH 11, chlorine was only detected for 20,000 ppm-day exposure and no chlorine was detected on the surface of any of the pH 12 hypochlorite degraded membrane samples. No significant change in oxygen/sulphur ratio was observed for any of the samples analysed (Figure 4.50). The ratio varied from 1 to 1.15 but it was hard to conclude that no change occurred in bound oxygen or sulphur with

hypochlorite treatment since the weight % measured by EDS technique were relative weights (for details of EDS analysis please refer to Appendix 2.3).

EDS analysis confirmed that chlorine bonds to the surface of membrane during hypochlorite exposure which gave an indication that a chemical reaction occurs on the surface which involves chlorine. These surface chemical reactions may lead to loss in membrane integrity as seen in FESEM imaging. Also EDS confirmed that the severity of degradation increased with increase in exposure time for pH 9 hypochlorite exposed samples. EDS analysis backs the finding of FESEM analysis that hypochlorite degradation is both pH and exposure time sensitive reaction.

4.6 FTIR-ATR

FTIR-ATR analysis was done on the Koch commercial UF membrane to find any change in functional groups on the surface of membrane with hypochlorite treatment. Figure 4.51 shows the FTIR-ATR spectra overlay for pH 9 to 12 hypochlorite degraded membrane for the highest exposure of 25,000 ppm-day. A significant fall in absorbance value was observed in all the samples analysed as compared to the new membrane. This effect was most prominent in pH 9 treated samples and least in pH 12. FTIR-ATR results showed that even pH 12 exposed membrane samples experienced a degradation of the PES surface though at a lower rate, which was not picked up FESEM-EDS analysis. The most probable reason of the loss in absorbance was increase in surface roughness of membranes with hypochlorite exposure. An increase in surface roughness may have caused scattering of infra red rays at membrane surface resulting in a weaker signal at detection end. Increased surface roughness was in accord with visual loss in surface gloss of the treated samples (Section 4.5.1). A depletion of PES polymer from the surface of membranes may have also occurred with hypochlorite exposure resulting in lower absorbance peaks in FTIR response. FTIR spectra were analysed for extinction of any existing peak or formation of new peaks which could indicate the chemical reaction mechanism involved in degradation of membranes with hypochlorite exposure. A new peak formation at 1034 cm^{-1} was observed for all the degraded samples in comparison to new membranes, as shown in Figure 4.52. This new peak formation was assigned to sulfonic acid which

may be formed by partial scission of the sulfonyl, phenol–S bond by hypochlorite exposure.

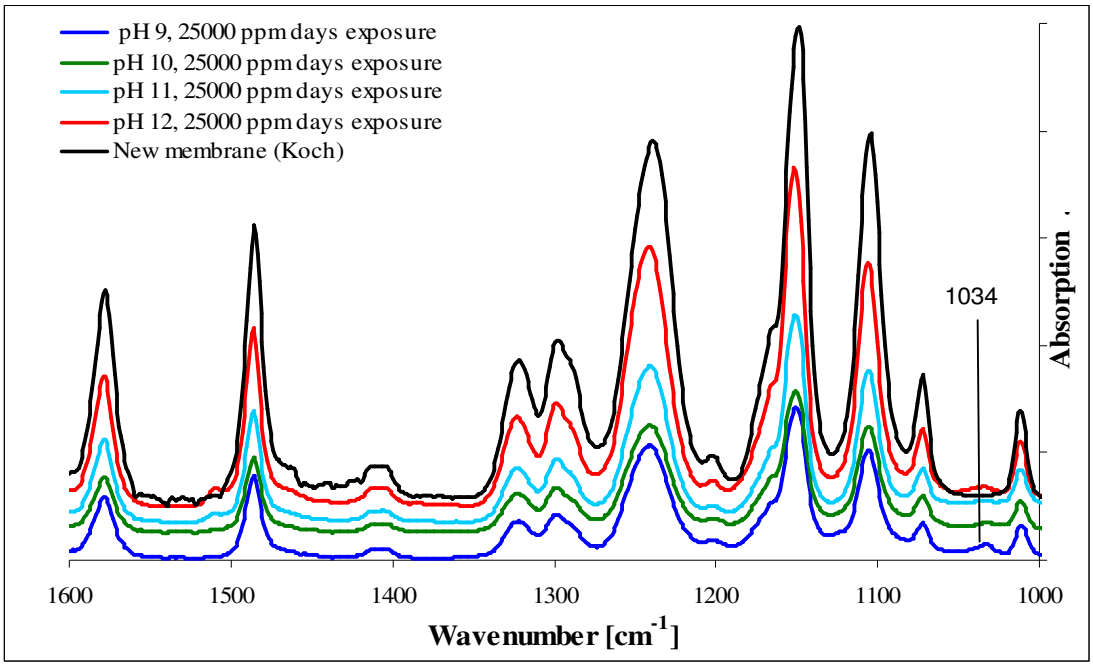

Figure 4.51 FTIR-ATR spectra overlay (displaced vertically to facilitate comparison) for Koch Membrane aged in different pH hypochlorite solution for 25000 ppm-day

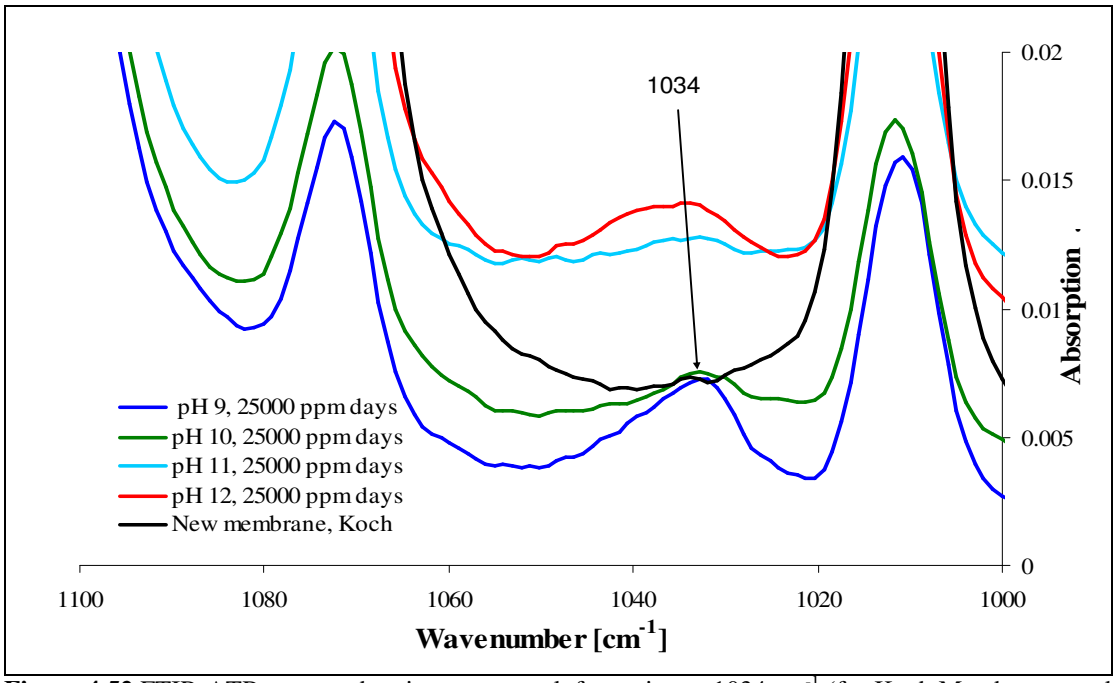

Figure 4.52 FTIR-ATR spectra showing a new peak formation at 1034 cm^{-1} (for Koch Membrane aged in different pH hypochlorite solution for 25,000 ppm-days)

It was also observed that the deteriorative effect of hypochlorite on the PES layer, i.e., in terms of loss in absorbance, increased with increase in exposure time for pH 9 hypochlorite exposure as shown in Figure 4.53. This might correspond to the increase

in pit formation observed using FESEM analysis. Further detailed analysis was done for each functional group to evaluate any change in absorbance with ageing.

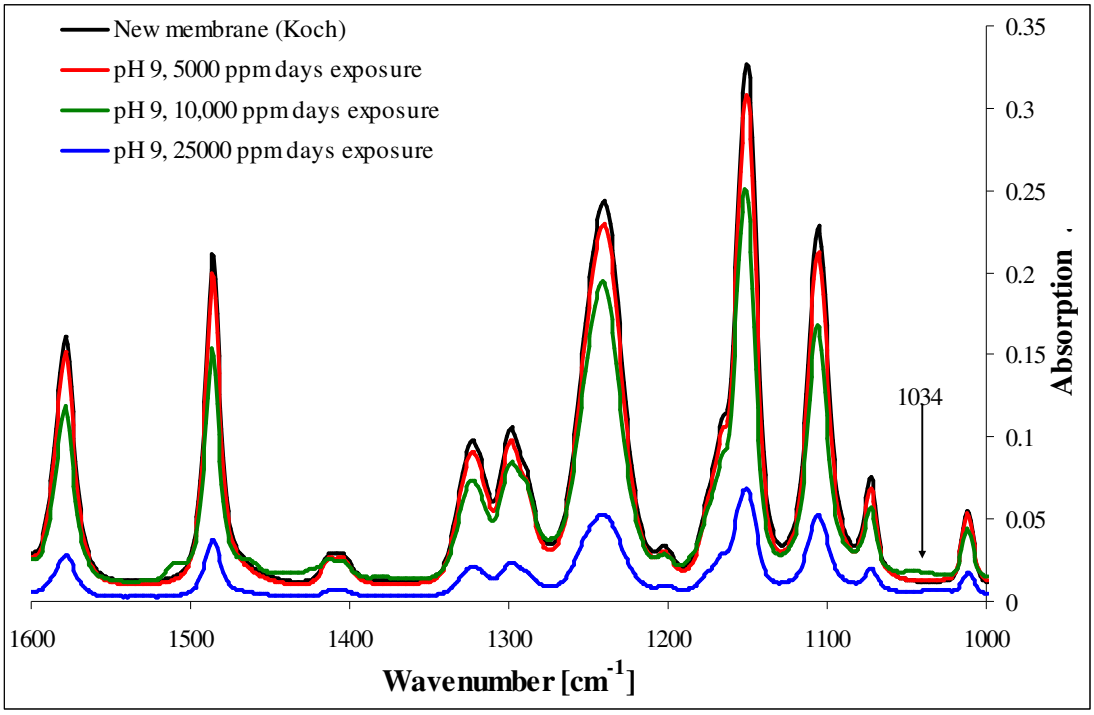

Figure 4.53 FTIR-ATR spectra overlay for Koch Membrane aged at pH 9 pH hypochlorite solution

Table 4.4 shows the percentage decrease in absorption values for pH 9 to pH 12 treated membranes with respect to a new membrane calculated as

$$\frac{A_{x\,(new)} - A_{x\,(treated)}}{A_{x\,(new)}} \times 100\ \%$$ where A_x is absorbance at wave number 'x' (1)

Table 4.4 Percentage decrease in absorption values for pH 9 to 12 (25,000 ppm-days exposed) Koch membrane samples with respect to new membrane for selected bands

Wave number cm^{-1}	Functional group	% Decrease in absorption with respect to new membrane (All sample had 25000 ppm-days exposure time)			
		Aged at pH 9	Aged at pH 10	Aged at pH 11	Aged at pH 12
1242	C-O ether	68.82	69.13	55.83	26.38
1105	Core aromatic	70.98	70.22	58.28	32.40
1484	C=C core	70.26	71.65	58.79	33.33
1576	C=C core	71.63	72.42	60.24	36.09
1147	SO_2 stretching	68.32	69.59	55.90	27.60
1296	SO_2	73.45	70.44	59.94	33.58
1320	SO_2	74.26	70.05	60.47	33.39
1034	Sulfonic acid	-2.46	-6.34	-79.86	-98.47

Analysis showed that pH 9 and 10 both observed a loss ~ 70% in absorption peaks while pH 11 experienced a loss ~ 58% and pH 12 sample experienced a loss ~33.5%.

The negative loss at wave number 1034 cm^{-1} shows formation of a new peak. Relatively the peaks at 1242 and 1147 cm^{-1} experienced the least drop in absorbance in both pH 12 and pH 9 treated samples.

Also the A_x / A_{1242} ratio was calculated to detect any change in particular functional group with respect to the C-O ether group within the spectra (as shown in Table 4.5). Going from left to right across the table it can be observed that the absorption ratio for a particular functional group remains more or less constant irrespective of hypochlorite exposure pH. It implies that within a sample spectrum the absorption for all the functional group decreased uniformly with respect to C-O ether linkage. This analysis verified that degradation reaction mechanism followed was independent of pH of hypochlorite exposure. The only difference in various hypochlorite pH exposures was of rate of degradation reaction. pH 9 experienced the highest rate of the degradation (70% loss in absorption) and pH 12 experienced the lowest degradation rate (33.5 % loss in absorption) for similar hypochlorite exposure time of 25,000 ppm-days.

Table 4.5 A_x / A_{1242} ratio of new pH 9 to pH 12 aged (25,000 ppm-days exposure), Koch membrane samples for selected bands

Wave number, cm^{-1}	**Functional Group assigned**	**Absorption ratio relative to wave number 1242 cm^{-1}**				
		New	**Aged at pH 9**	**Aged at pH 10**	**Aged at pH 11**	**Aged at pH 12**
1242	C-O ether	1.00	1.00	1.00	1.00	1.00
1105	Core aromatic	1.02	0.95	0.99	0.97	0.94
1484	C=C core	0.77	0.74	0.71	0.72	0.70
1576	C=C core	0.60	0.55	0.54	0.54	0.52
1147	SO2 stretching	1.32	1.34	1.30	1.31	1.29
1296	SO2	0.46	0.40	0.45	0.42	0.42
1320	SO2	0.41	0.34	0.40	0.37	0.37
1034	Sulfonic acid (assigned)	0.04	0.14	0.14	0.17	0.11

FTIR-ATR analysis was also done on Sterlitech, microfiltration membranes. The spectra collected for new and samples exposed to pH 9 and 12 sodium hypochlorite solution for 10,000 ppm-days are shown in Figure 4.54. Both pH 9 and 12 hypochlorite samples experienced a loss in absorption peak with hypochlorite treatment but to a very small extent as compared to the Koch membranes, i.e., around 10% for pH 9 and 5% loss for pH 12 hypochlorite treated membrane (Table 4.6). This

may be due to different pore size of the two membranes. Sterlitech had much larger pores as compared to Koch membrane and may have experienced a lower stress on the pores. Unlike Koch membrane, Sterlitech membrane did not have any backing layer and may not experience the stress due to adhesion of the two layers (i.e. PES layer and backing layer). A new peak formation was detected at 1034 cm^{-1} similar to the Koch membranes.

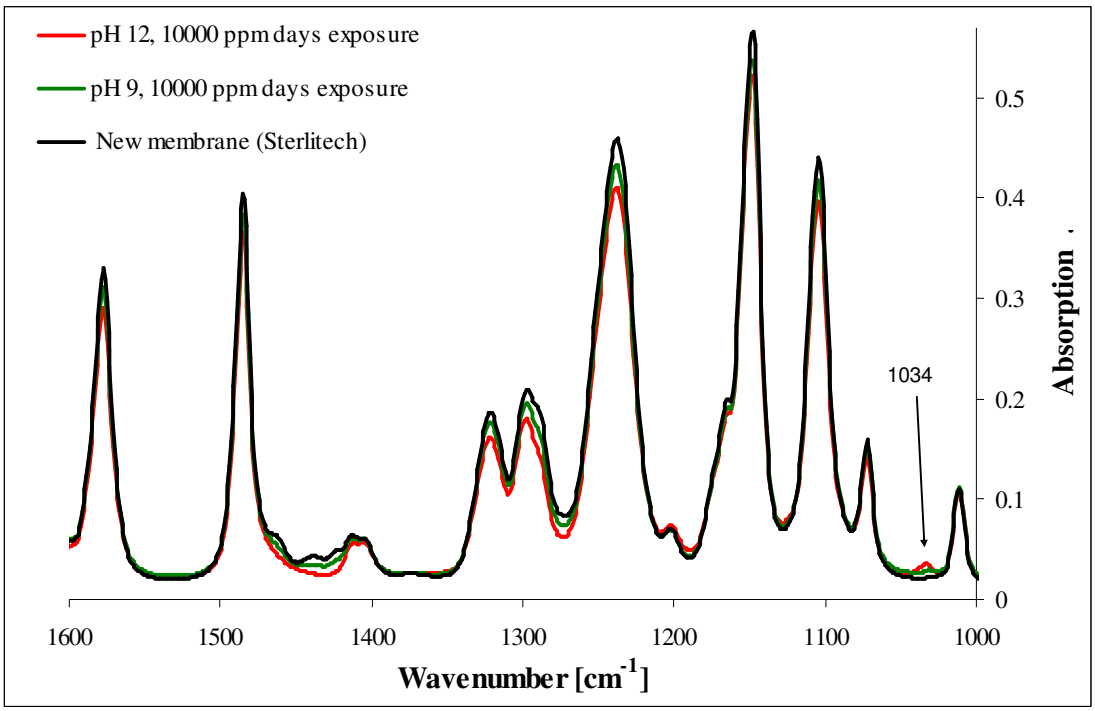

Figure 4.54 FTIR-ATR spectra for Sterlitech Membrane new and aged in pH 9 and 12 hypochlorite solution for 10000 ppm-day

Table 4.6 Percentage decrease in absorption values for pH 9 to 12 (10000 ppm-days exposed) Sterlitech membrane samples with respect to new membrane for selected bands

Wave number cm^{-1}	**Functional group**	**% Decrease in absorption with respect to new membrane (All sample had 10000 ppm-days exposure time)**	
		Aged at pH 9	**Aged at pH 12**
1242	C-O ether	9.44	4.76
1105	Core aromatic	9.97	5.36
1484	C=C core	9.41	5.01
1576	C=C core	11.51	5.43
1147	SO2 stretching	7.58	4.83
1296	SO2	13.31	5.78
1320	SO2	13.52	5.53
1034	Sulfonic acid (assigned)	-61.98	-32.11

Here, also irrespective of hypochlorite exposure pH, a constant A_x/A_{1242} ratio was observed to be constant for a given functional group (Table 4.7). It again confirmed

that all the samples analysed followed the same degradation reaction mechanism and the type of reaction mechanism followed is independent of exposure pH.

Table 4.7 A_x / A_{1242} ratio of new pH 9 and pH 12 aged (10000 ppm-days exposure), Sterlitech membrane samples for selected bands

Wave number, cm^{-1}	Functional Group assigned	Absorption ratio relative to wave number 1242 cm^{-1} (All sample had 10000 ppm-days exposure time)		
		New	Aged at pH 9	Aged at pH 12
1242	C-O ether	1.00	1.00	1.00
1105	Core aromatic	1.02	1.02	1.02
1484	C=C core	0.94	0.94	0.94
1576	C=C core	0.76	0.75	0.76
1147	SO2 stretching	1.31	1.34	1.31
1296	SO2	0.48	0.46	0.48
1320	SO2	0.43	0.41	0.43
1034	Sulfonic acid (assigned)	0.05	0.09	0.07

FTIR-ATR spectra were also obtained for the backing side of new and pH 9, 25000 ppm-days hypochlorite exposed samples (Figure 4.55). The samples showed no loss in absorption due to hypochlorite exposure. It was concluded that the FTIR-ATR could not detect the effect of hypochlorite exposure on the backing layer.

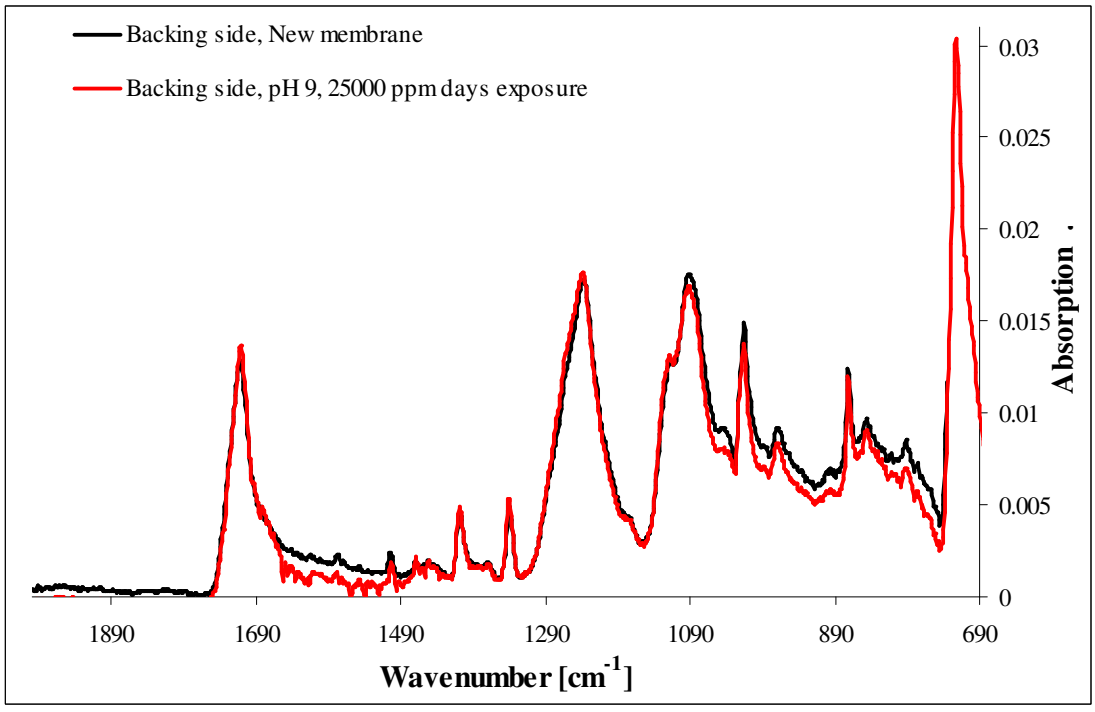

Figure 4.55 FTIR-ATR spectra of backing side for new, pH 9 Koch UF membrane (25000 ppm-days exposure)

4.7 Contact Angle

Contact angle was measured for both PES foil (Good Fellow) and commercial UF membrane (Koch). The experiment aimed to measure contact angle to detect changes in the surface with hypochlorite treatment. Contact angle results shown in Figures 4.56 to 4.58 are taken from the work of Thomas, 2008 as part of this research. In Thomas's work the contact angle for water, formamide, and methylene iodide were measured to enable calculation of the surface energy. For a new membrane water exhibited the highest contact angle of 85.7° followed by formamide (62°) and methylene iodide showed the least contact angle of 44°. In comparison to a new membrane, a significant decrease in contact angle was observed for all pH values for 10,000 ppm-days exposure, irrespective for contact liquid (Figure 4.56). However this observation was not repeated for 25,000 ppm-days exposure (Figure 4.57). Water and formamide both showed no significant change in contact angle for pH 9 hypochlorite degraded membranes in comparison to a new membrane. No clear trend was observed in both 10,000 and 25,000 ppm-days exposure which could link contact angle with hypochlorite degradation of membranes.

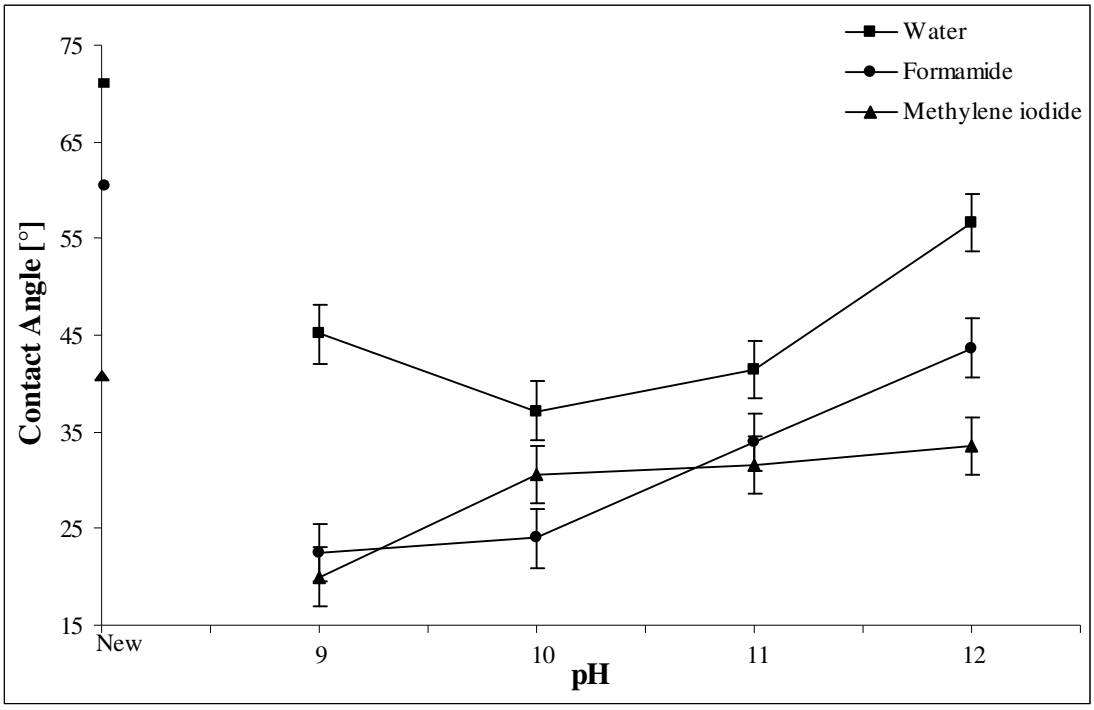

Figure 4.56 Contact angle for new and degraded Koch UF membrane (hypochlorite solution pH 9 -12, 10000 ppm-days exposure) (Thomas, 2008)

For all the membrane samples tested, liquid absorption through the membrane was observed for all the liquids tested. Absorption was quickest for pH 9 treated samples with 10,000 or 25,000 ppm-days exposure. Absorption was also observed on new membrane samples for all the liquids tested. The rate of absorption was slow but a significant difference in contact angle was seen after approximately 10 minutes.

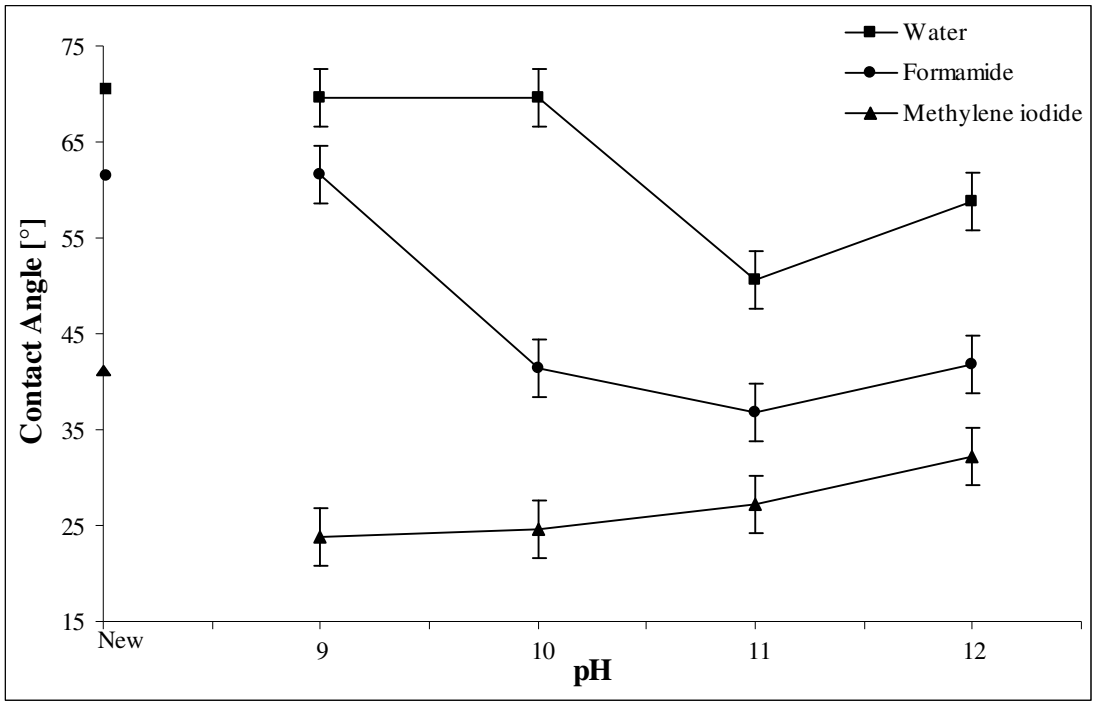

Figure 4.57 Contact angle for new and degraded Koch UF membrane (hypochlorite solution pH 9 -12, 25000 ppm-days exposure) (Thomas, 2008)

Although the absorption rate differed with hypochlorite pH and exposure time, significant absorption was observed which cannot be overlooked while measuring contact angle. Since pH 9 had the highest rate of liquid absorption, it was more likely that contact angle measured for pH 9 treated samples were most inaccurate. It was difficult to decide when the contact angle should be measured. If the contact angle was measured instantly the drop touched the surface, the drop was still in a dynamic adjustment stage and resulted in different left and right contact angle or a significantly higher contact angle than for later measurements. If the liquid drop was allowed to settle for few seconds, the liquid absorption through the surface resulted in lower value of contact angle measured. This combined phenomenon means that it is difficult to measure the contact angle of porous membranes and that it will have high uncertainty. To eliminate the uncertainty in measurement due to porosity, contact angle was measured on non-porous PES foil samples with pH 9 to 12, 10,000 ppm-

day exposure (Figure 4.58). No liquid absorption was observed for any of the samples treated. Water and formamide contact angle decreased significantly for all pH values as compared to the new membrane. For water, a decrease of 20-30° and for formamide a fall of around 20° was measured as compared to the new membrane. No significant change in contact angle for methylene iodide was observed. Also, no trend was noticed which can relate contact angle with pH of hypochlorite exposure and contact angle remained more or less constant for all the liquids tested.

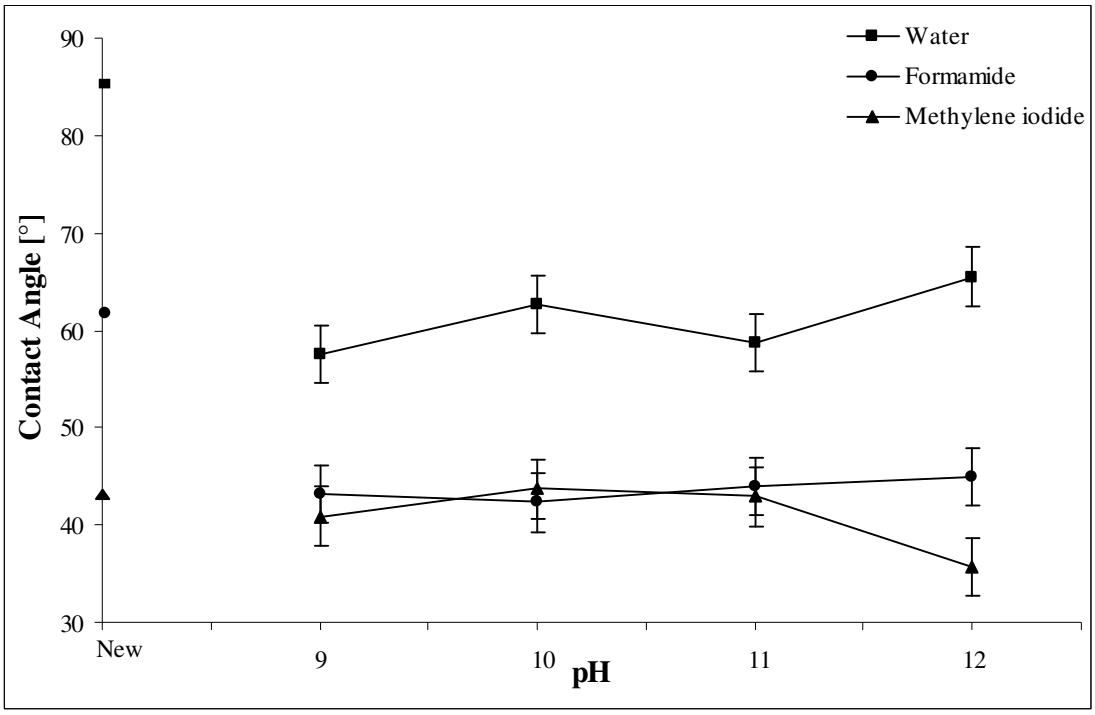

Figure 4.58 Contact angle for new and degraded PES foil (Good Fellow) (hypochlorite solution ph 9 - 12, 10000 ppm-days exposure) (Thomas, 2008)

Porosity played an important role in rate of hypochlorite degradation of sample as observed by FESEM analysis. Since the PES foil was non-porous so it was possible that not enough degradation was achieved to produce a significant relationship in between contact angle and hypochlorite exposure pH. It was concluded by Thomas that it was difficult to quantify the change on membrane surface due to hypochlorite exposure using the contact angle measurement technique. Thomas suggested that the rate of absorption of liquid through the membrane can provide useful information about the degradation of membrane. Based on this observation a new "Liquid absorption test" was designed for this current work.

4.8 Liquid Absorption Test

The liquid absorption test aimed to measure the absorption of a drop of test liquid on an ultrafiltration membrane (Koch) surface in terms of change in contact angle with time. It was important to choose a test liquid which can show measurable contact angle with time for the two extreme absorptions, i.e. pH 9 treated membranes and new membranes. For water on a new membrane, it took around 10 minutes to observe any significant change in contact angle and took around 20 minutes for the drop to completely disappear. So water was too slow to show a change in contact angle. In such a long time period evaporation of liquid will come into play and affect the contact angle measured. Methanol showed a very high absorption rate and it was immediately absorbed even on a new membrane but it also evaporates very quickly. So it was decided to test absorption of a low concentration methanol solution on new and pH 9 treated membranes. After series of absorption tests it was found that 20% (w/w) methanol in water was best suited for the liquid absorption test.

It was necessary not to confuse decrease in contact angle due to spreading with decrease due to absorption of liquid through the membrane surface. Figure 4.59 shows the contact angle measurement sequence for a new membrane.

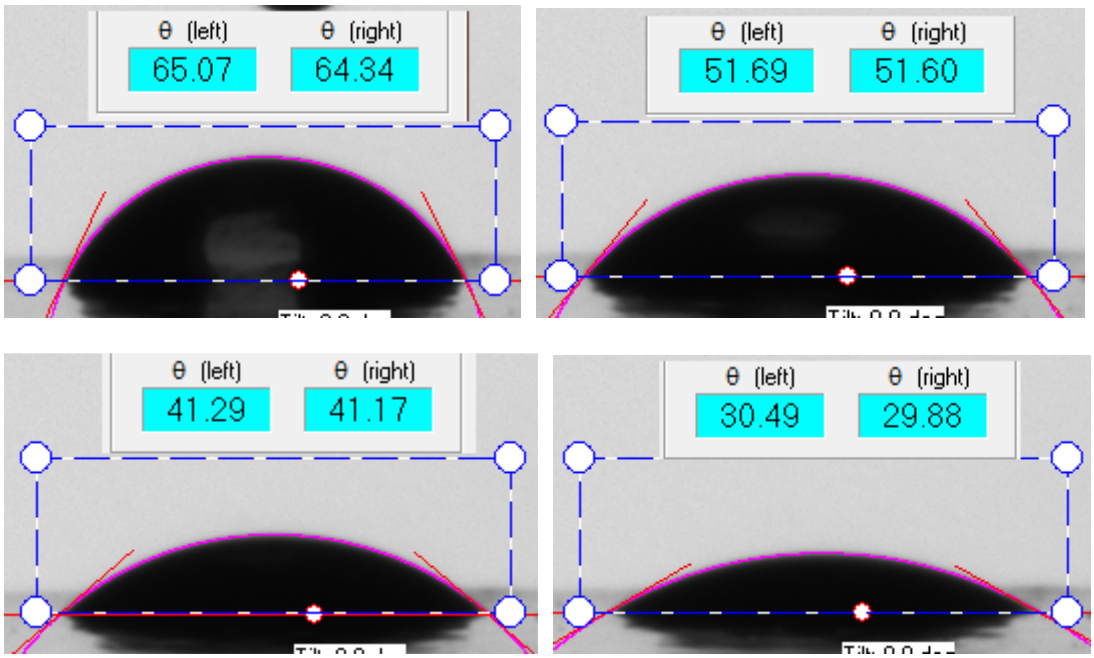

Figure 4.59 Measurement sequence of contact angle for new membrane by CAM200 software.

It can be noticed in Figure 4.59 that the change in contact angle is mainly due to the decrease in drop height. The boundaries of the drop remain more or less constant throughout the measurement. This effect was observed in all the membrane samples tested. It indicates that the change in contact angle is due to the absorption of liquid through the membrane surface rather than spreading of the liquid drop.

Figure 4.60 shows the contact angle measured with time for new and hypochlorite degraded membrane (pH 9-12, 20,000 ppm-days exposure). The graph shows a significant increase in absorption rate (i.e. change in contact angle per unit time) in all the hypochlorite treated samples which indicates degradation of the PES surface. Also a clear trend was visible with pH 12 showing the least and pH 9 showing the maximum severity of degradation.

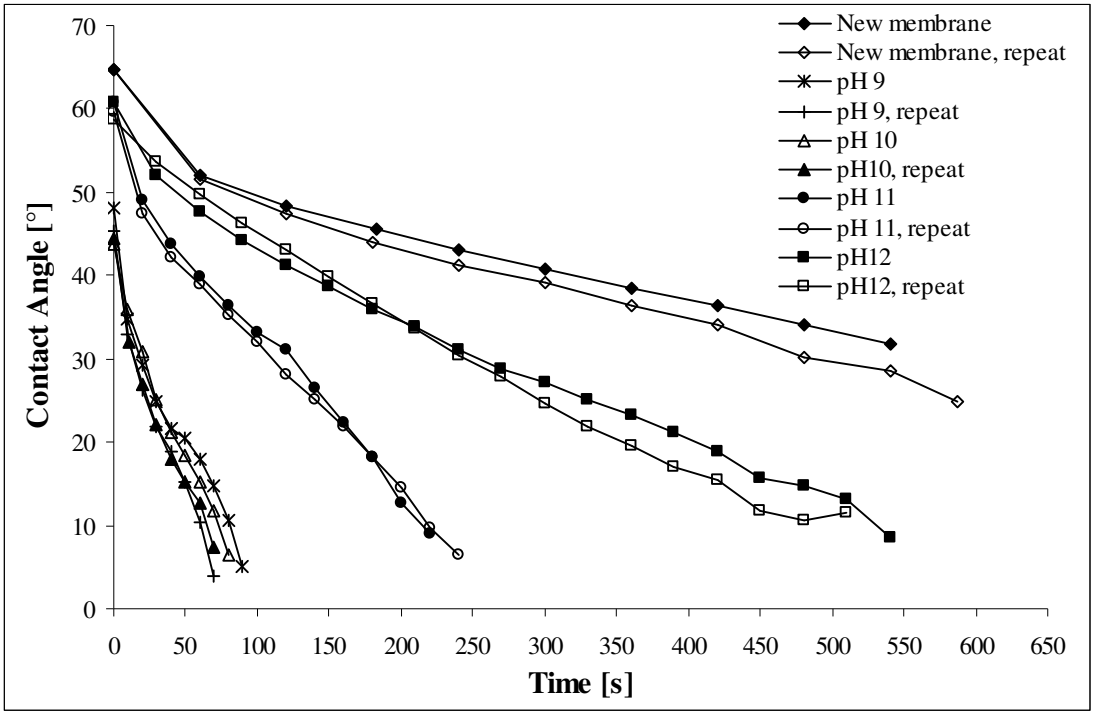

Figure 4.60 Contact angle measured with respect to time for new and degraded Koch ultrafiltration membrane (hypochlorite solution ph 9 -12, 20,000 ppm-days exposure)

The average decrease in contact angle with time is shown in Table 4.8. It was observed that even at pH 12 the rate of absorption was double that of the new membrane. It can be noticed that changes in absorption rate were significantly higher in the case of pH 9 and 10 as compared to pH 12 and 11. Also, the similar absorption rate for pH 9 and 10 indicates that the degradation reaction rate for these two hypochlorite exposures was quite similar. This matched the FESEM imaging results

where very high cracking and surface pitting was observed both in pH 9 and 10 (25,000 ppm-day) exposures. This microscopic pit formation might lead to a sudden increase in absorption rate for pH 9 and pH 10 hypochlorite degraded samples.

Table 4.8 Liquid absorption rate for Koch UF membrane (20,000 ppm-days exposure)

Sample	Rate of Contact Angle Decrease, °/s	Normalized Rate
New	-0.0461	1.0000
12.00	-0.1001	2.1707
11.00	-0.1804	3.9132
10.00	-0.4323	9.3774
9.00	-0.4479	9.7158

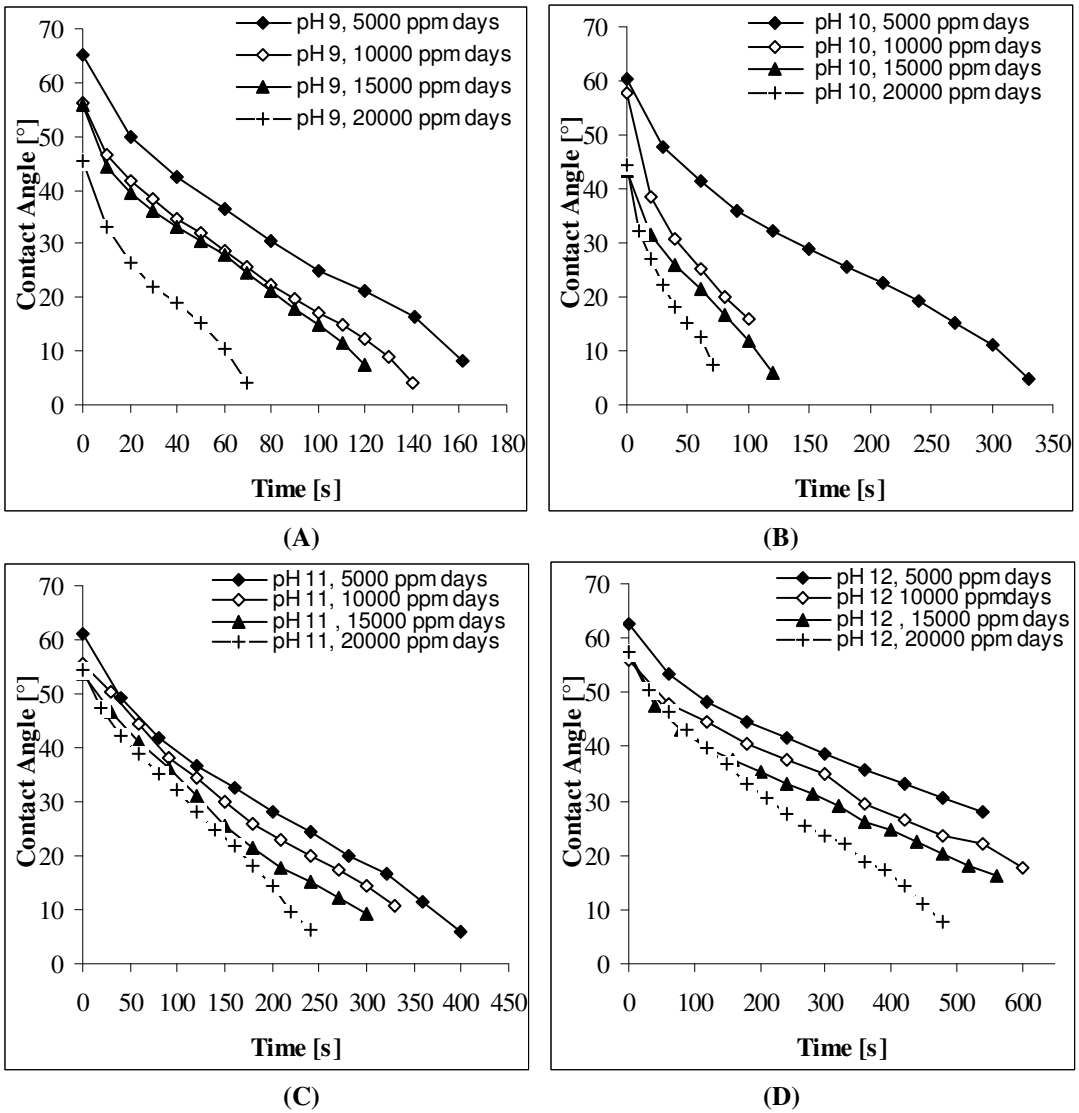

Figure 4.61 Change in contact angle with time for membranes degraded at (A) pH 9 (B) pH 10 (C) pH (D) pH 12, (5,000 to 20,000 ppm-day) (Note the different time scales)

Figure 4.61 shows the change in contact angle with exposure time for each pH. A common trend can be observed in all the graphs, i.e. the absorption rate increased

with increase in exposure time. It was concluded that liquid absorption promises to be an easy and non-destruction test which can differentiate between the samples degraded at various hypochlorite pH for a constant exposure time or vice versa.

Further analysis was done to compare hypochlorite degradation at various pH values. Contact angle values at 60 s time for 5,000 ppm-days and 20,000 ppm-days for each pH were plotted for each pH values (Figure 4.62), and accordingly a table of contact angle (from 12 to 45°) versus ppm-days versus was generated (Table 4.9)

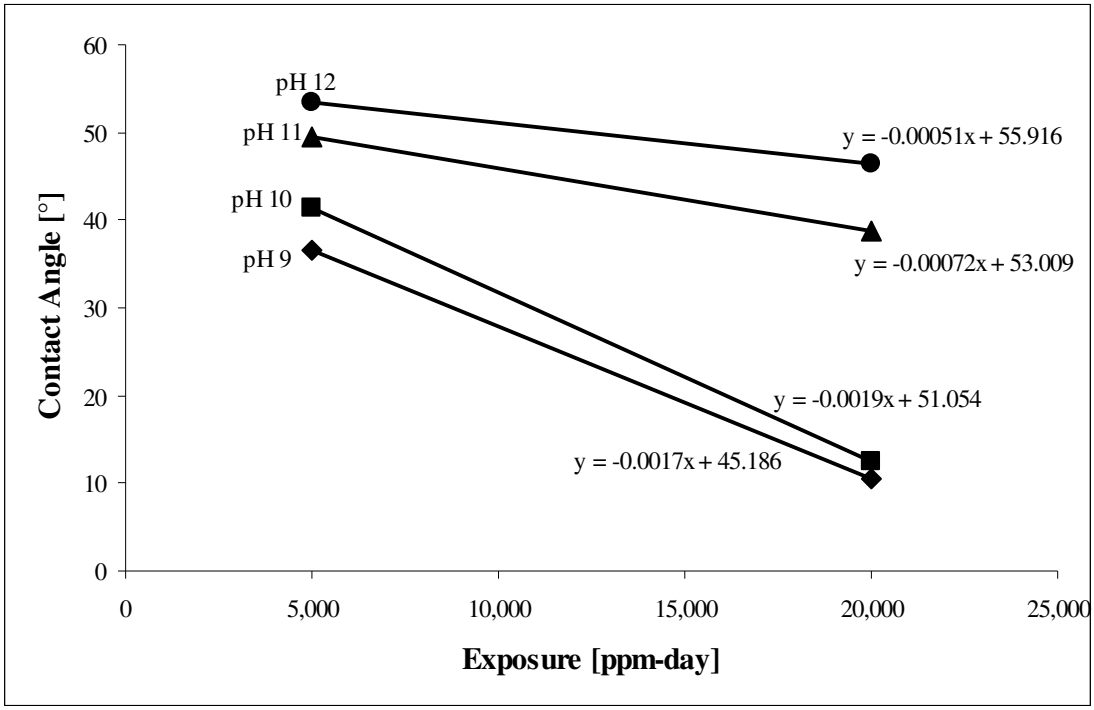

Figure 4.62 Contact angle versus exposure (ppm-day) measured at 60s after start of liquid drop absorption experiment for Koch membrane degraded by hypochlorite at pH 9, 10, 11, and 12

Table 4.9 gives a rough comparison for exposure times. It can be seen that just 109 ppm-days at pH 9 may be equivalent to 21404 ppm-days at pH 12. It can also be noted that degradation at pH 11 is twice than that at pH 12. It was concluded that the liquid dispersion test can give a rough overall mapping of degradation of ultrafiltration at various exposure pH values.

Table 4.9 Generated table for contact angle versus exposure (ppm-day) for Koch membrane degraded by hypochlorite at pH 9, 10, 11, and 12

Contact Angle, °	Exposure, ppm-days			
	pH 9	pH 10	pH 11	pH 12
12	19521	20555	56957	86110
15	17756	18976	52790	80227
18	15992	17397	48624	74345
21	14227	15818	44457	68463
24	12462	14239	40290	62580
27	10698	12660	36124	56698
30	8933	11081	31957	50816
33	7168	9502	27790	44933
36	5404	7923	23624	39051
39	3639	6344	19457	33169
42	1874	4765	15290	27286
45	109	3186	11124	21404

4.9 Zeta Potential

Because hypochlorite degradation is a surface phenomenon, it was expected that the measurement of zeta potential on a degraded membrane surface may be able to define the degradation age of the membrane. Zeta potential was measured in the pH range of 2 to 10. Figure 4.63 shows zeta potential curves generated for Koch UF membranes, for pH 9 to 12, 25,000 ppm-days hypochlorite treatments. It can be seen that PES new and degraded ultrafiltration membranes were negatively charged at neutral pH. The isoelectric point for a new membrane was found to be at pH 3.7. A significant decrease in isoelectric pH was observed for all degraded membrane samples but no clear trend in the zeta potential curves was observed which could be related to degradation of the membrane. Zeta potential was also measured for BASF PES sheets for same exposure conditions (Figure 4.64). Again a significant decrease in isoelectric pH was observed in all the degraded samples as compared to new PES sheet. Again no trend in zeta potential was observed which could define the hypochlorite degradation of membranes.

These experiments were conducted in the Department of Chemical Science and Engineering, UNSW, Sydney. Although all necessary precautions were taken for measuring zeta potential, the coating on Ag/AgCl electrodes was not stable and it had to be coated almost every third day of the experiment which was not normal. This problem may have aggravated the uncertainty in measurements. Time was a constraint

for this experiment; an improved experimental design could have enhanced the results obtained. However, it was decided that the trends were not clear enough to justify the time and expense of visiting the same department to develop the procedure further.

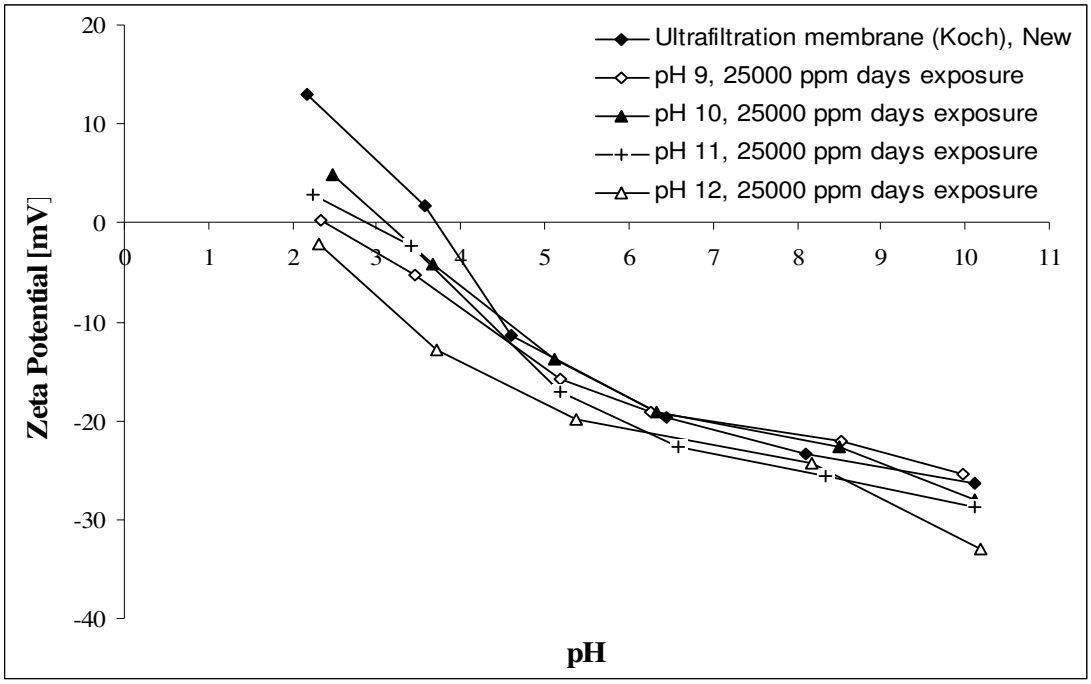

Figure 4.63 Zeta potential curves for new and degraded Koch UF membrane (pH 9 to 12, 25,000 ppm-days hypochlorite exposure)

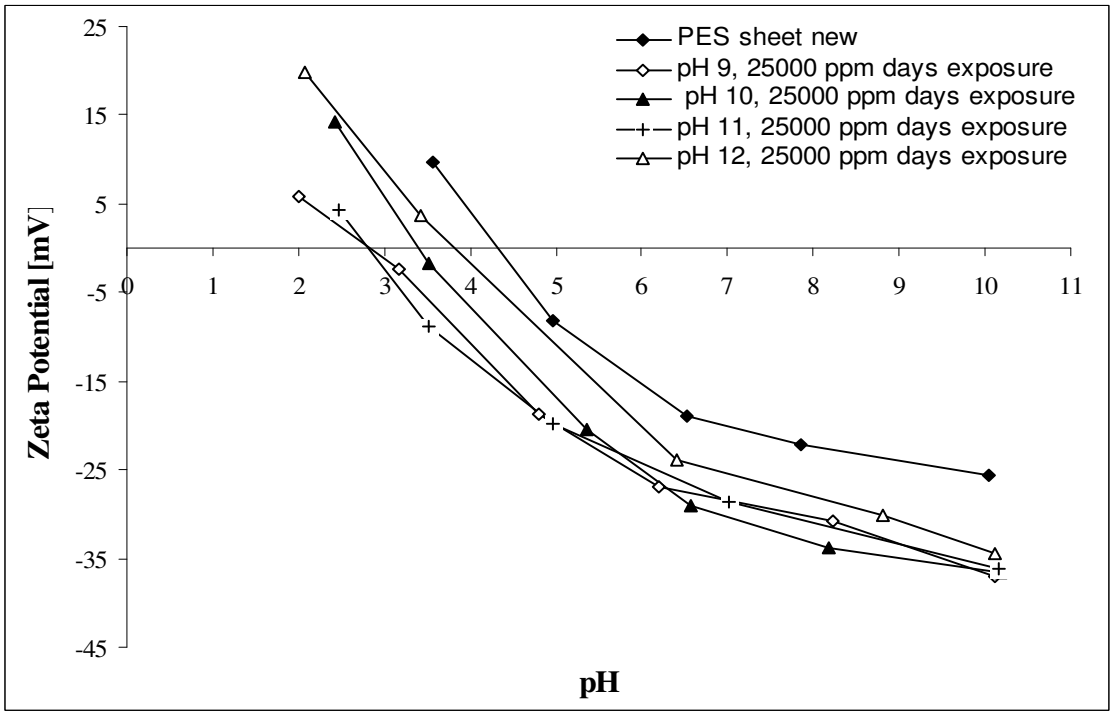

Figure 4.64 Zeta potential curves for new and degraded BASF PES sheets (pH 9 to 12, 25,000 ppm-days hypochlorite exposure)

4.10 Liquid-Liquid Displacement Porosimetery (LLDP)

4.10.1 Compression Study

Morison (2008) found that compression of membranes during testing would strongly affect the analysis of LLDP results. During the LLDP experiment, the membranes experienced a trans-membrane pressure (TMP) from 1 to 10 bar, so a compression study on a new Koch UF membrane was done to study the effect of TMP on permeance (permeate flux divided by TMP). Figure 4.65 shows water permeance of a new membrane from 1 to 10 bar, gauge. The pressure was released and brought back to atmospheric pressure and after 10 minutes another a permeance curve was generated for the same membrane. The graph shows that the permeance decreased from 25.8 to 22.3 g/m^{2}s bar (a fall of 13.5%) for the new membrane indicating that the membrane was being compressed. The compression seemed to be permanent (initial permeance gap of ~ 5 g/m^{2}s bar) as the subsequent run had significantly lower permeance which also decreased as TMP increased.

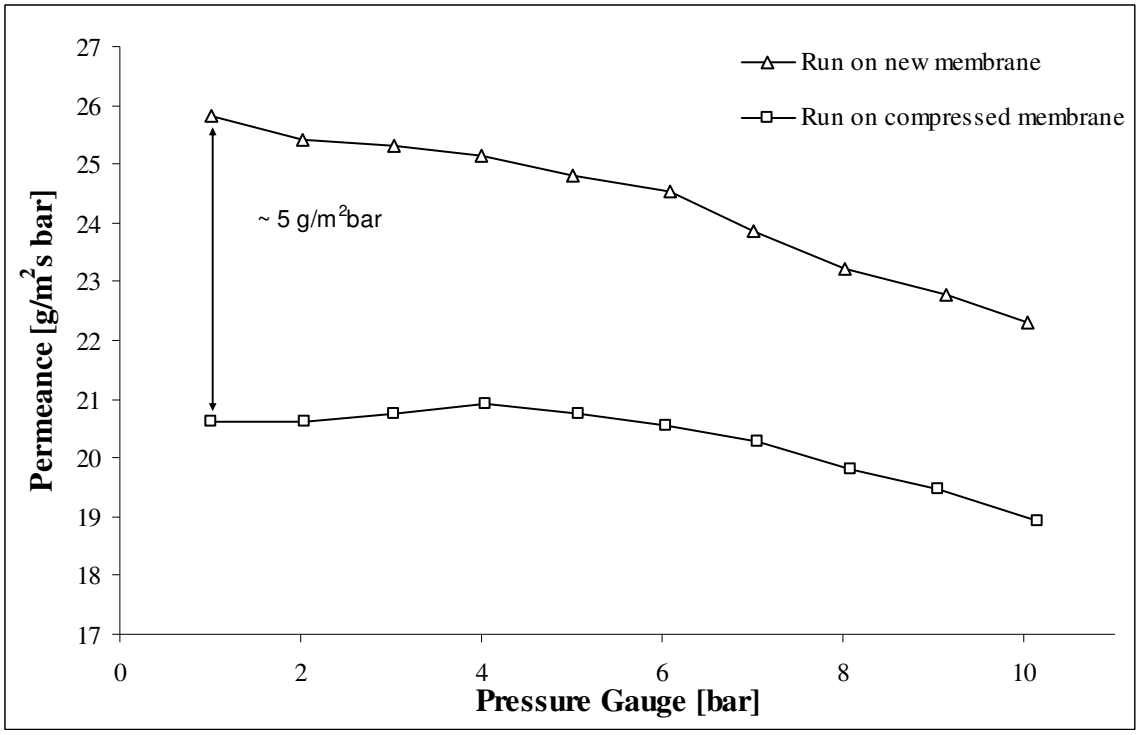

Figure 4.65 Compression test on new water wetted Koch ultrafiltration membrane

Because the LLDP test membrane was exposed to methanol, compression tests on a new membrane wetted by alcohol were thought to be more realistic. Figure 4.66 shows compression testing (from 1 to 10 bar, TMP) on a methanol wetted new

membrane. A high water permeance was observed after methanol wetting of the new membrane (for details on this effect please refer to Section 4.11). Membrane compression, i.e. a decrease in permeance from 44.0 to 33.7 g/m^{2}s bar (a fall of 23.4%), was noticed for the new wetted membrane. Again a permanent compression occurred which is indicated by initial permeance gap of ~ 5 g/m^{2}s bar.

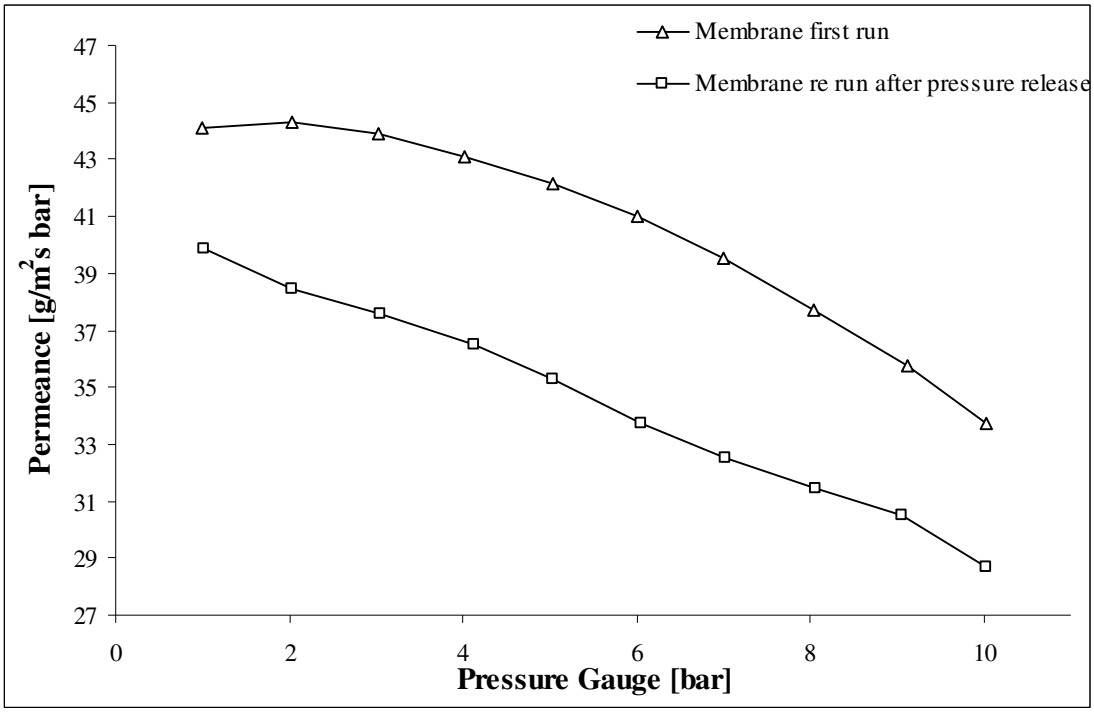

Figure 4.66 Compression test on a new methanol wetted Koch ultrafiltration membrane

The compression testing showed that the membrane wetted by methanol compressed 10% more than the membrane wetted with water for TMP 1-10 bar. It was concluded that LLDP permeance values must be corrected accordingly to compensate compression effect.

4.10.2 LLDP

The flux data for the alcohol rich phase as the displacement fluid in a new membrane is shown in Figure 4.67. This shows the classic shape expected with the flux values tending towards a straight line from the origin. The deviation from this line is very small and so the calculated pore size distribution will be very sensitive to the data. This data was smoothed using a cubic smoothing spline as discussed by Morison (2008). The change to the flux data after smoothing was a maximum of 2.2% for all data points.

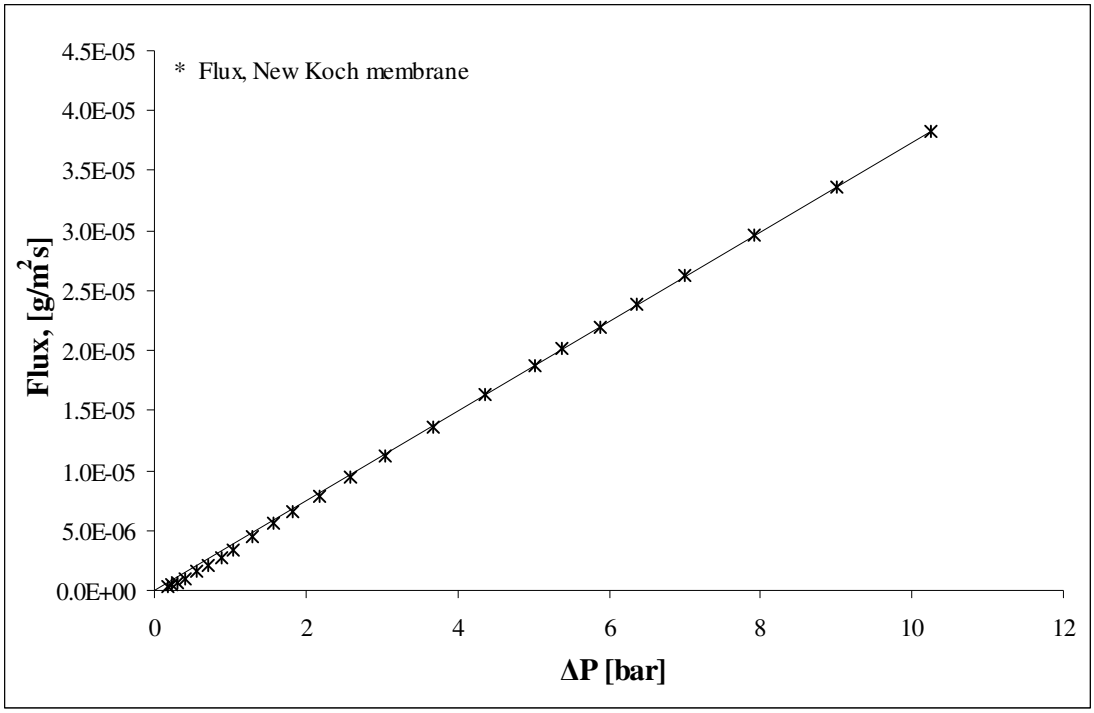

Figure 4.67 Flux data for the alcohol rich phase as the displacement fluid in a new membrane (without compression correction)

Initially no correction for compression was made, even knowing that a significant correction was required. Erbe's method (Morison, 2008) was used with the smoothed data to determine the pore size distribution for a new and a pH 9, 10,000 ppm-days degraded membranes. The results shown in Figure 4.68 suggest a reduction in the pore size with degradation, which is entirely contrary to the other results. Given the large uncertainties in this method it is unlikely that this result is real.

When a compression correction was applied, the flux curve as shown in Figure 4.69, does not have the classic shape. If this data was reliable, it would indicate that the pressure should be increased much more so that the curve would become tangent with a line through the origin. Higher pressure can not be applied without excessive compression. Already the applied pressure was excessive and produced a significant compression of the membrane. The maximum pressure used corresponds to a pore radius of 0.8 nm which seems very small. It is much more likely that the data are too sensitive to the experimental parameters to be meaningful. Also the effect of alcohols on the flux values is unknown and possibly not measureable in isolation from interfacial effects which puts uncertainty on the validity of the flux data obtained. Refer to Section 4.11 for details on effect of alcohols on water flux of the membranes.

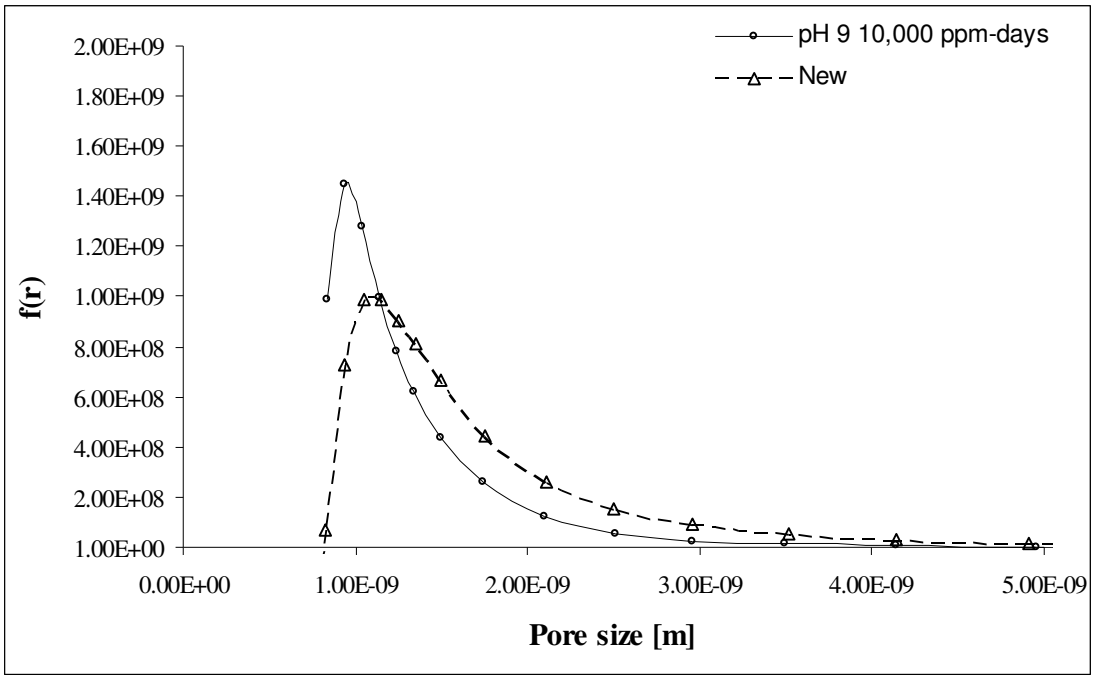

Figure 4.68 Pore size distribution for a new and pH 9, 10,000 ppm-days hypochlorite degraded Koch membrane.

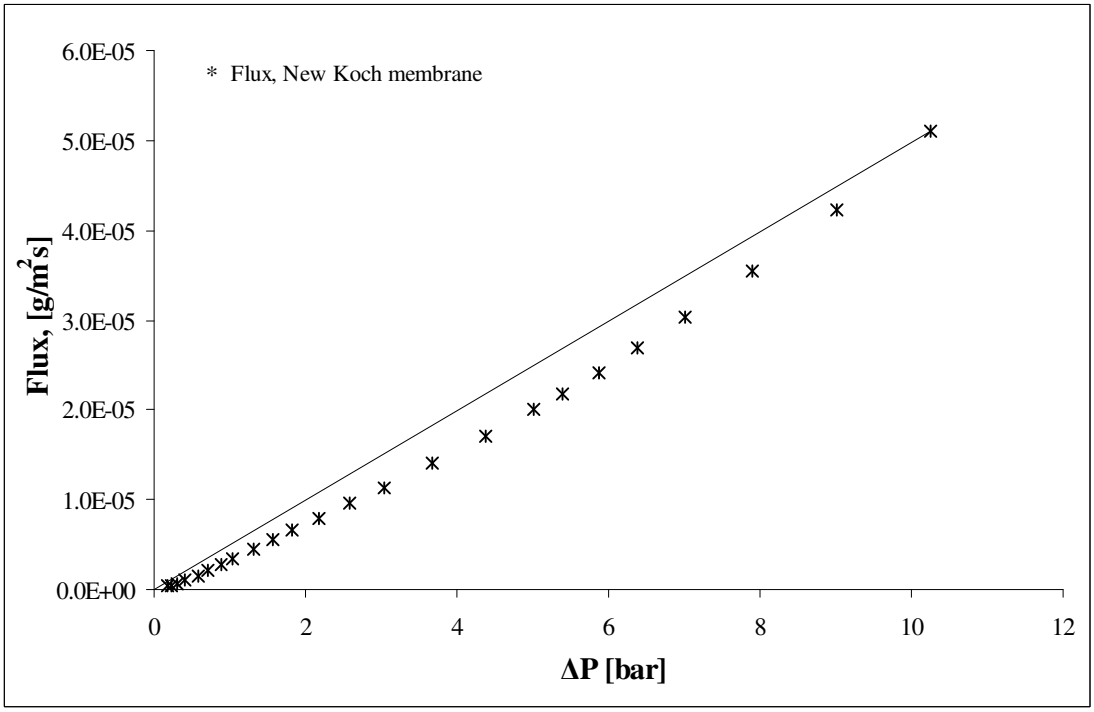

Figure 4.69 Flux data for the alcohol rich phase as the displacement fluid in a new membrane (with compression correction)

4.11 Cross-flow Flux Measurement

A sequential water flux and alcohol flux measurement was performed for new and degraded Koch ultrafiltration membrane. Methanol, ethanol and n-propanol were used as a pre-treatment of membrane. Clean water flux was measured before and after the pre-treatment step. Figure 4.70 shows sequential water-alcohol-water flux measurement on new membrane. Each liquid was run for at least 30 min and the flux was recorded. For each alcohol run a fresh clean new membrane was used.

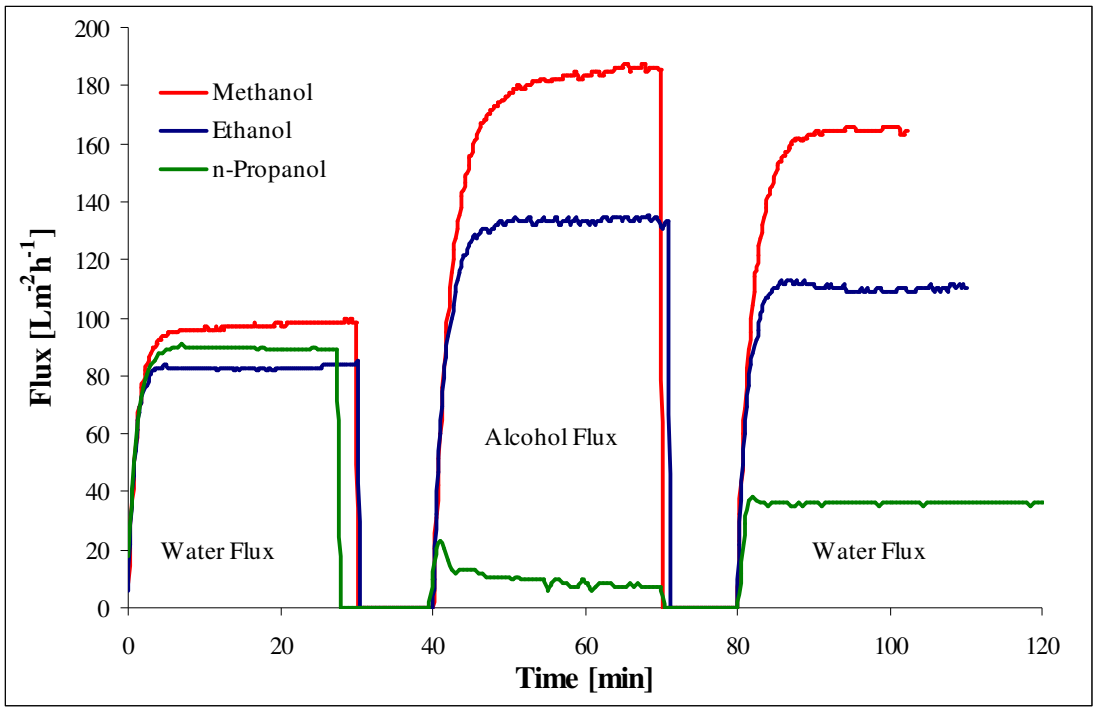

Figure 4.70 Run sequence of water-alcohol-water flux for new Koch membrane samples at 20°C, TMP: 1 bar, and feed flow: 50 mL/min

Table 4.10 Flux measurements for each liquid (measured after passing the liquid through membrane for at least 30 minutes)

Sample	Water W1	Alcohol W2	Water W3	Flux ratio W2/W1	W3/W1
Methanol	98.5	185.5	164.4	1.9	1.7
Ethanol	84.0	134.0	110.4	1.6	1.3
n-Propanol	88.8	7.2	36.0	0.1	0.4

Table 4.10 shows the flux measured for each water-alcohol-water run. Methanol exhibited a very high flux, i.e. 1.9 times that of the initial water flux. Ethanol also showed an increase in flux by 1.3 times but propanol experienced a 90% decrease in flux as compared to initial water flux. Methanol (Ageno and Frontali, 1967) had a lower viscosity followed by ethanol and n-propanol. Figure 4.70 clearly shows the

effect of alcohol viscosity on the corresponding flux values. After passing alcohol the membranes surface was thoroughly cleaned with water, and water was passed for 30 minutes (to make sure there is no more alcohol in the pores) before any water flux measurement was done. However the post-alcohol water flux measured retained the effect of alcohol passing and showed a flux value in accordance to the corresponding alcohol. For example post-alcohol water flux in the case of methanol remained 1.7 times higher than initial flux measurement and for post-propanol water flux remained low and was only 40% of initial water flux. A similar affect was noticed by Lindau *et al.* (1995) while studying the affect of octanoic acid on clean water flux of polysulfone membrane. This experiment showed that alcohols had a conditioning effect on membrane and the post-alcohol water flux depended on the alcohol passed. Subsequent measurements by a visiting research intern, Rob Hanson, has confirmed the methanol results but showed a higher post-propanol water flux.

Since methanol caused the highest increase in post-alcohol water flux, methanol conditioning was studied in detail. It was possible that some glycerol remained in the pores of new membrane and alcohol may have further cleaned the membranes. To verify this hypothesis clean membrane samples (for cleaning of membranes please refer to Section 3.1.1) were further cleaned with a different cleaning sequence and then water-alcohol-water flux test was performed. Figure 4.71 shows the cleaning sequence water – 0.1 M NaOH – water and then water-alcohol-water flux test was performed. Also an effort was made to bring back the flux to normal by passing 0.1 M NaOH. It was observed that cleaning with 0.1 M NaOH did not affect the water-alcohol-water flux results and again an increase in water flux was detected. Passing of 0.1 M NaOH after alcohol did not help to bring the water flux back to its original value. Figure 4.72 shows the flux sequence for the acid-water-base-water cleaning regime. Again a 50% increase in water flux was noted after methanol pre-treatment. It also showed that acid-base cleaning of membrane did not alter the effect of methanol on water flux. Figure 4.73 shows the water-alcohol-water test after the standard cleaning regime prescribed by the membrane manufacturer (Koch, International, USA). The cleaning regime followed was water (10 min); 2% alkali, at 10.5 pH (15 minutes); water (10 minutes); NaOCl, i.e. 200 ppm chlorine at 10.5 pH (15 minutes); water (10 minutes). The cleaning regime was followed at 50°C solution temperature at 1 bar TMP. A 90% increase in water flux was observed after methanol pre-

treatment. All the cleaning regimes showed similar results, i.e. a significant increase in water flux after methanol treatment so it was concluded that the increase in water flux was not due to cleaning of traces of glycerol but was related to interaction of membrane surface with methanol.

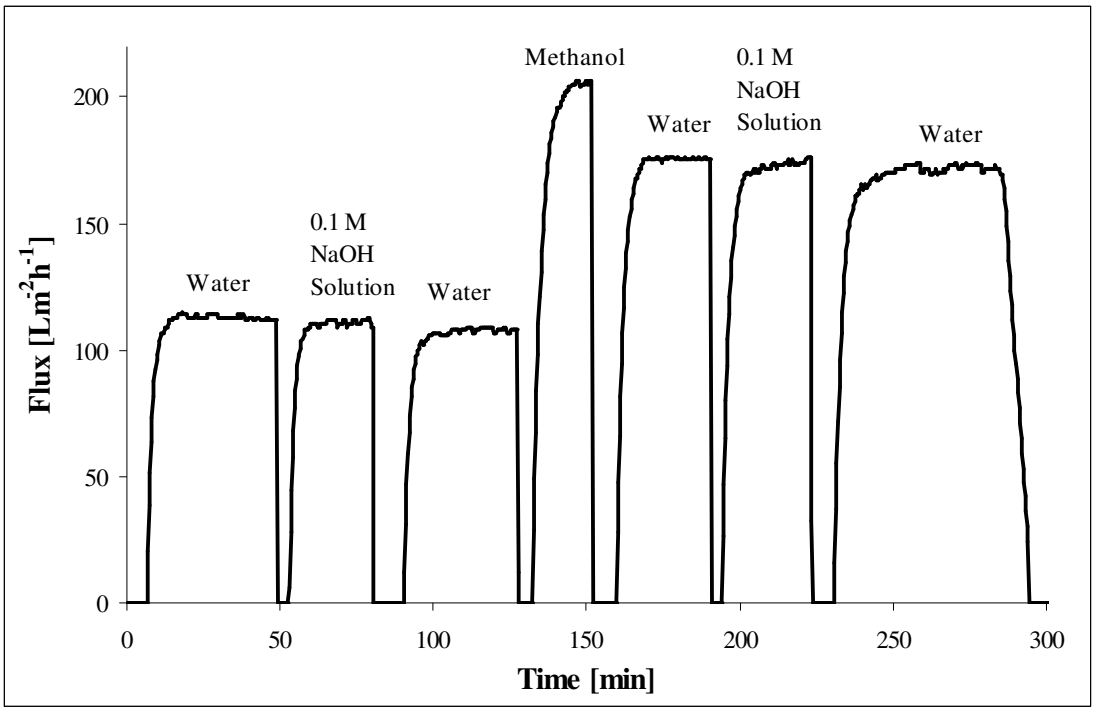

Figure 4.71 Cleaning sequence water-NaOH-water followed by water-methanol-water test on Koch membrane at 20°C, TMP: 1 bar, and feed flow: 50 mL/min

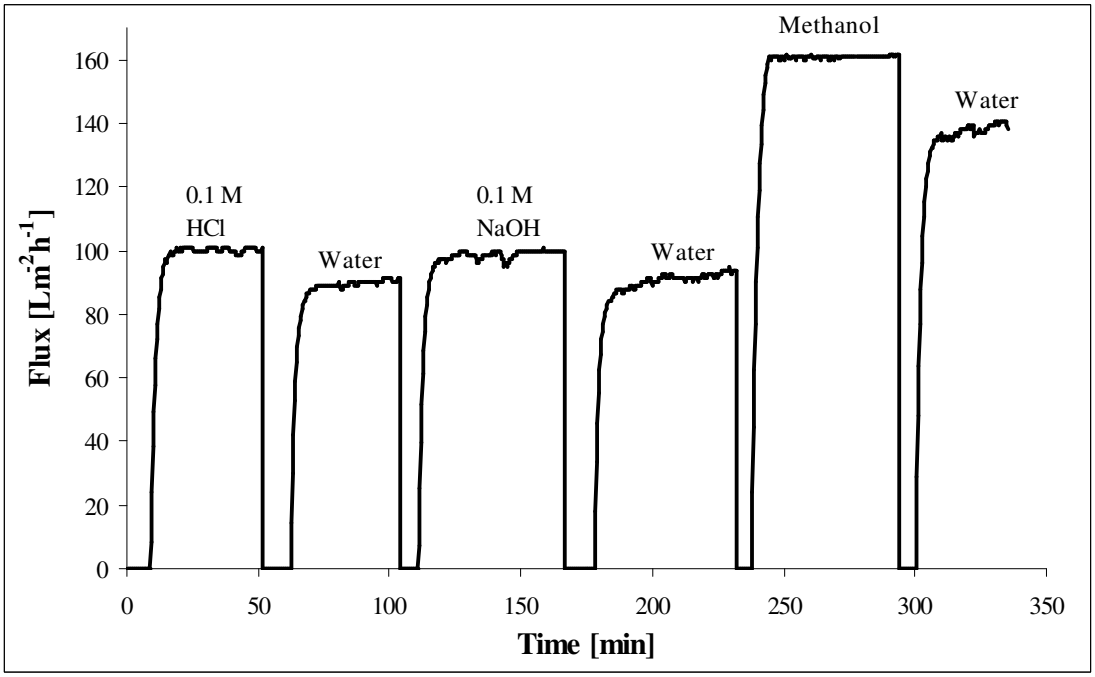

Figure 4.72 Cleaning sequence HCl-water-NaOH-water followed by water-methanol-water test on Koch membrane at 20°C, TMP: 1 bar, and feed flow: 50 mL/min

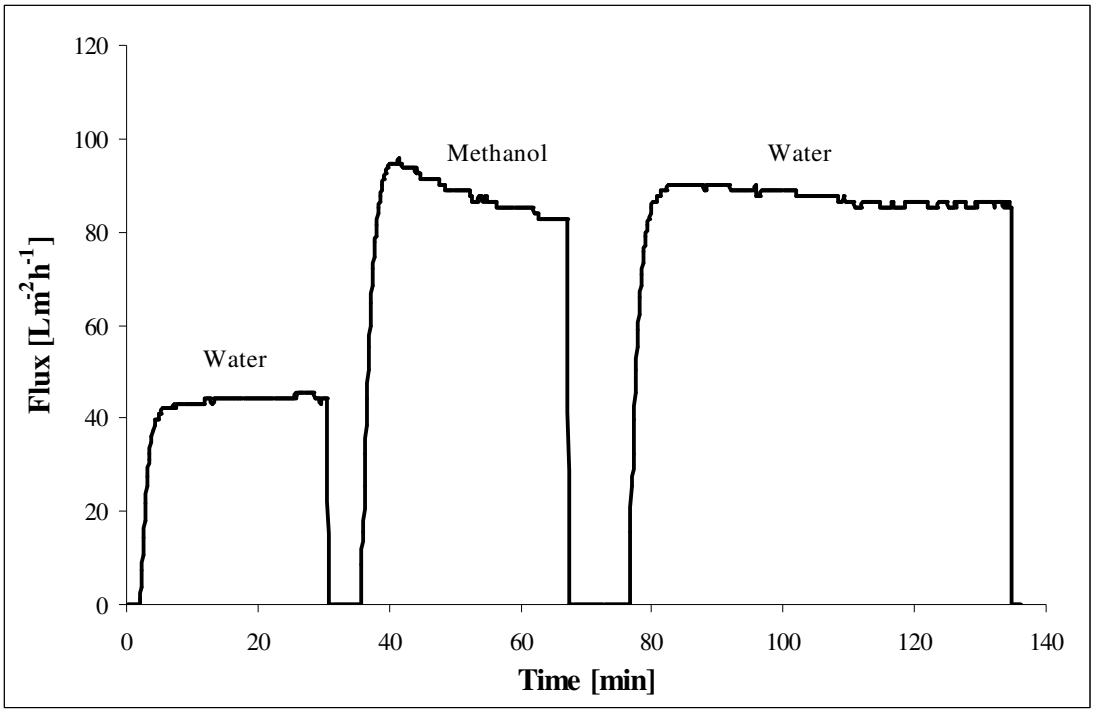

Figure 4.73 Water-methanol-water test after cleaning new membrane by standard procedure (specified by membrane manufacturer, Koch International) at 20°C , TMP: 1 bar, and feed flow: 50 mL/min

Trials were done to regain the original water flux by passing mild acid and base after the methanol pre-treatment. Figure 4.74 shows the flux values for methanol pre-treatment followed by 0.1 M HCl; water; 0.1 M NaOH; water cleaning. It can be noticed that passing acid and base after the methanol pre-treatment did not reduce the water flux to its initial values; again a net increase in water flux was recorded after completion of the cleaning regime.

It was difficult to understand and explain the water flux behaviour after methanol pre-treatment. A study by Gady (1996) on micro sized polystyrene particles showed that the surface charge of the particles decreased drastically by soaking in methanol. A similar effect may have occurred in the membrane pores leading to increase in water flux values. This may be due to formation of a layer by methanol which made a barrier between water and the membrane and shielded any interaction between PES and water. More study is needed to gain a better understanding of this effect. It was concluded that methanol was somehow interacting with the membrane surface which altered the clean water flux.

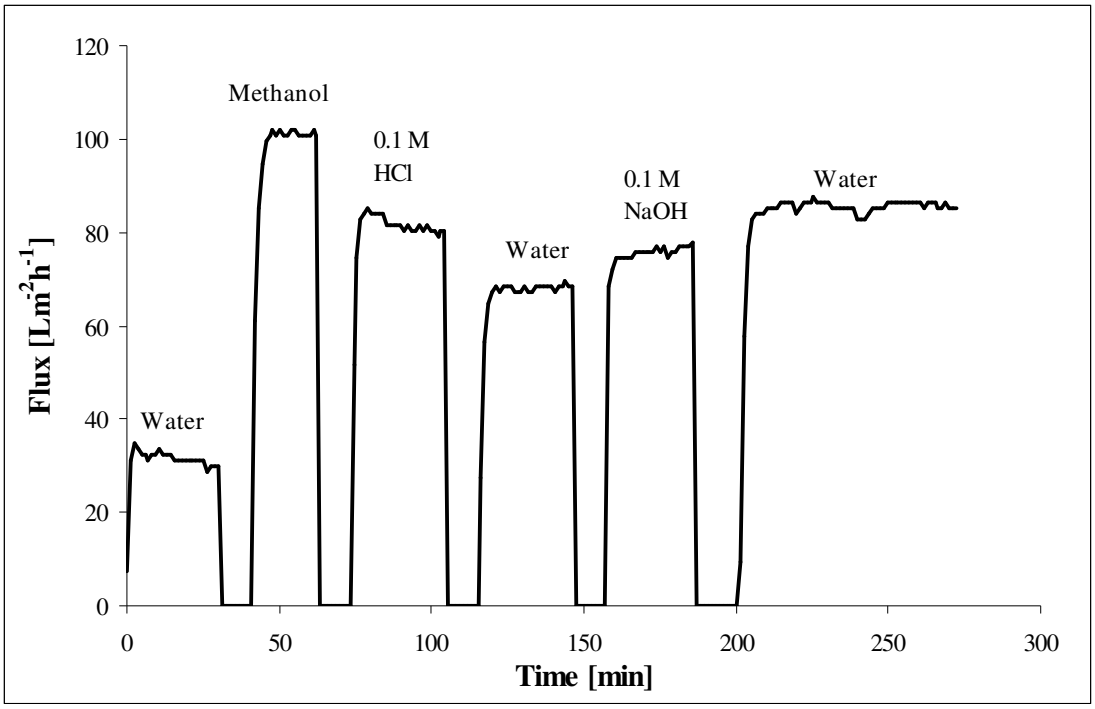

Figure 4.74 Methanol pre-treatment followed by HCl –water -NaOH-water cleaning sequence on Koch membrane at 20°C, TMP: 1 bar, and feed flow: 50 mL/min

In any case it was appealing to study water-methanol-water flux test on degraded membranes. It was expected that the degraded membranes will interact with methanol differently and the initial and post-alcohol water flux may tell something about surface change with degradation. Figure 4.75 show water-methanol-water flux test on new and degraded Koch ultrafiltration membranes (pH 9 and 12, 10,000 ppm-day hypochlorite exposures). Also the water-methanol-water flux test was done for a degraded membrane obtained from industry (taken out of a membrane plant after its useful life) and was compared to flux values for hypochlorite degraded membranes.

It can be noticed that the initial water flux for pH 9 degraded membranes was around 4 times that of the new membrane while pH 12 treated membrane showed flux around twice that of the new membrane (Table 4.11). The industrial degraded membrane showed an initial flux more than 3 times that of new membrane but less than pH 9 degraded membranes. The membrane obtained from industry may have had a higher level a degradation as compared to pH 9 samples but may have had blocked pores due to permanent fouling during its useful life resulting a lower initial water flux. The water flux was not affected by the methanol pre-treatment and showed no change after passing methanol.

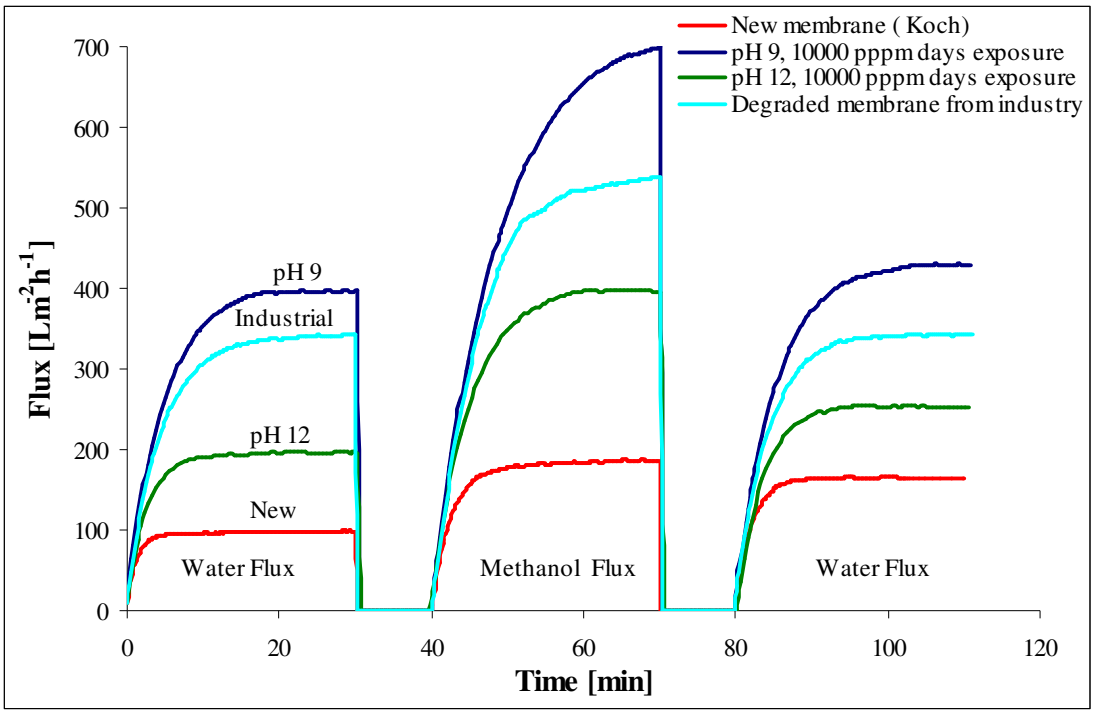

Figure 4.75 Run sequence of water-methanol-water flux for new and degraded Koch membrane samples at 20°C, TMP: 1 bar, and feed flow: 50 mL/min

Table 4.11 Flux ratios for run sequence of water-methanol-water flux for new and degraded Koch membrane samples

	Flux [LMH], After 30 min of run				
Sample	Water W1	Methanol W2	Water W3	Flux ratio W2/W1	W3/W1
New	98.5	185.5	164.4	1.9	1.7
pH 9	396.5	699.6	428.4	1.8	1.1
pH 12	195.6	396.0	253.2	2.0	1.3
Degraded	342.0	538.5	343.2	1.6	1.0

By looking at W2/W1 (Table 4.11) it can be noticed that for new or hypochlorite degraded membranes the methanol flux was almost 80-100% more than initial water flux as expected. A clear trend was visible in W3/W1. It was observed that in comparison to the initial water flux, the increase in post-alcohol water flux was only 10% for pH 9, 30% for pH 12 treated membrane and 70% in new membrane. It shows that the conditioning effect of methanol decreased with hypochlorite exposure. It was concluded that clean water flux gave a clear indication of extent of degradation by hypochlorite. Also W3/W1 values indicated that membrane-methanol interactions (which produced an increase in water flux) were decreasing with decrease in hypochlorite solution pH. It seemed that the more the membrane degraded, the less its surface interacted with methanol to produce changes in post-alcohol water flux. For extreme degradation conditions, methanol may not interact with the membrane

surface at all and producing no change in post-alcohol water flux as noted in case of membrane obtained from industry. The possibility exists that degraded membranes have a small number of very large pores which gives higher flux, but which are not affected by any methanol interaction.

4.12 Protein Separation Test

4.12.1 Membrane Throughput Test

In the membrane throughput test casein whey was passed through the membrane at a TMP of 3 bar. Both permeate flux and permeate UV absorbance were measured for new and hypochlorite degraded Koch membrane samples (pH 9-12, 5,000 to 20,000 ppm-days exposure). Figure 4.76 shows the UV absorbance for pH 9 5,000 to 20,000 ppm-days degraded samples. An increase in UV absorbance was noticed for all exposures as compared to the new membrane which indicates that more protein passed through the hypochlorite treated samples as compared to new membrane. It was also noticed that 15,000 ppm-days and 20,000 ppm-days exposure showed similar amounts of proteins passing through the membrane into the permeate stream.

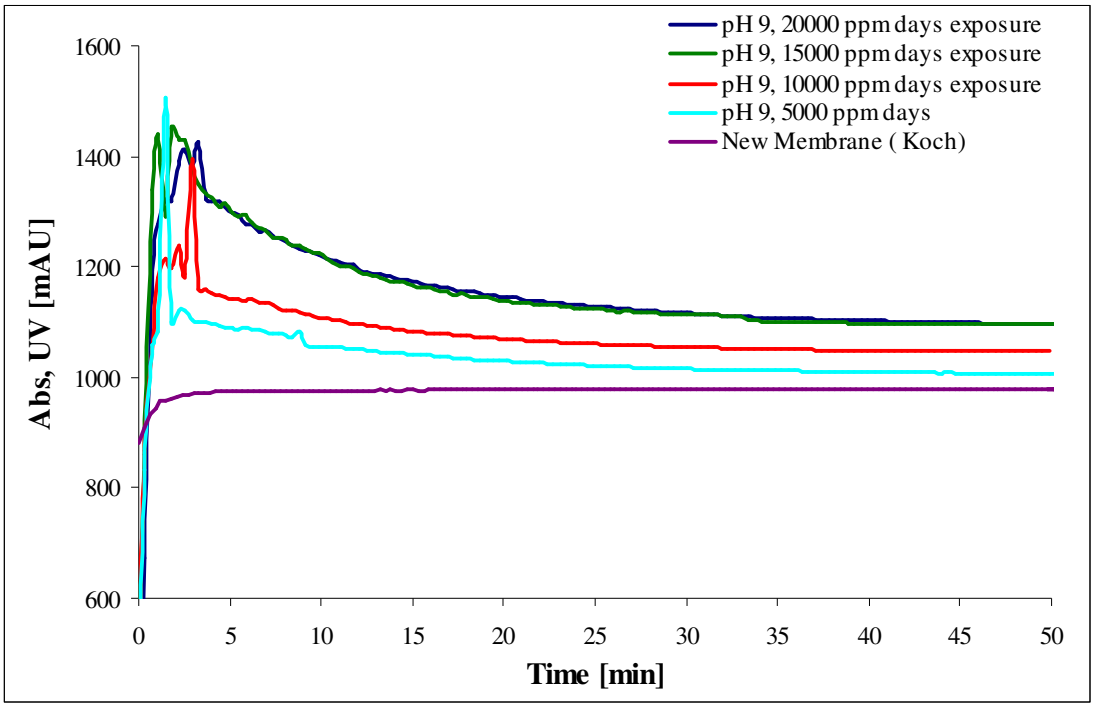

Figure 4.76 UV absorbance of permeate stream during ultrafiltration of casein whey through membrane samples exposed to pH 9 hypochlorite solution for different exposure time at 20°C, TMP: 3 bar, and feed flow: 200 mL/min

Figure 14.77 shows the permeate flux for pH 9 treated membranes for different exposure times. It can be noticed that permeate flux was significantly higher for the new membrane as compared to the pH 9 treated membrane. It may be due to hypochlorite treatment, which led to an increase in surface roughness and change in surface- liquid interactions which resulted in an increase in fouling of membrane. This high surface fouling may have caused the decrease in permeate flux.

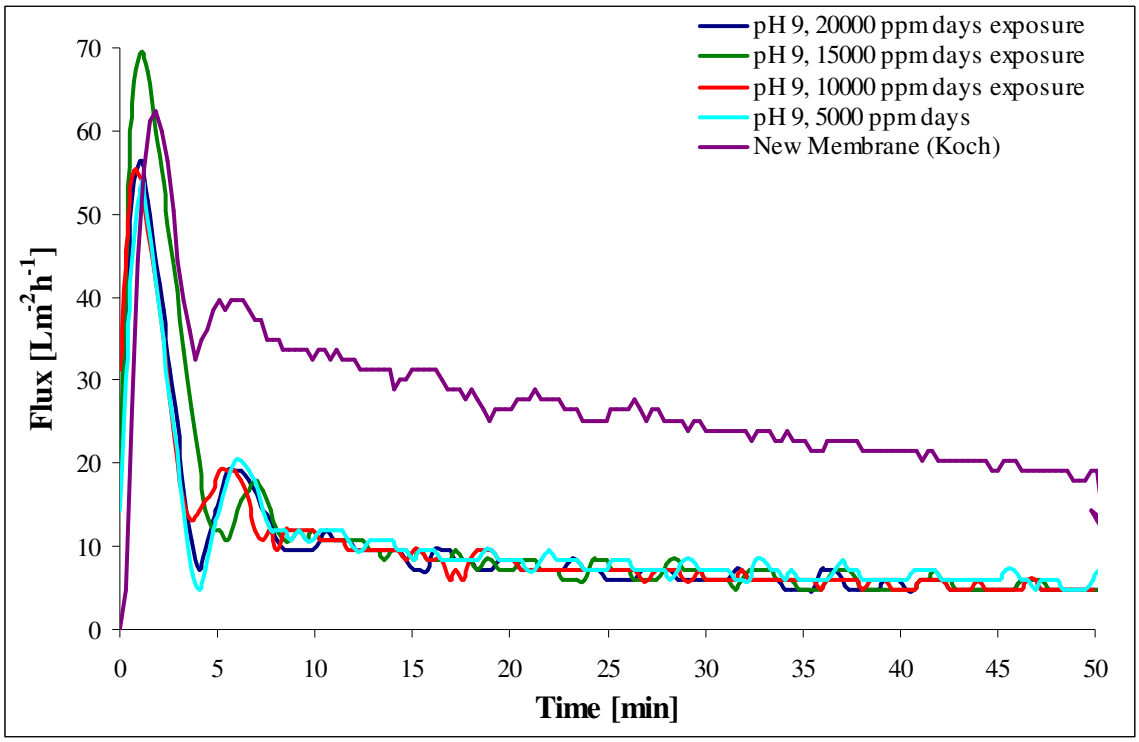

Figure 4.77 Permeate flux during ultrafiltration of casein whey through membrane samples exposed to pH 9 hypochlorite solution for different exposure time at 20°C, TMP: 3 bar, and feed flow: 200 mL/min

A similar trend was noticed for pH 10, 11 and 12 hypochlorite treated membrane (Figures 4.78 to 4.80) for UV absorbance. The UV absorbance gap between new and hypochlorite treated membrane decreased with increase in pH. A decrease in permeate flux was again registered for pH 10, 11 and 12 for all the exposures, which indicates that the surface fouling may have increased in all the hypochlorite treated membranes (Figures 4.81 to 4.83).

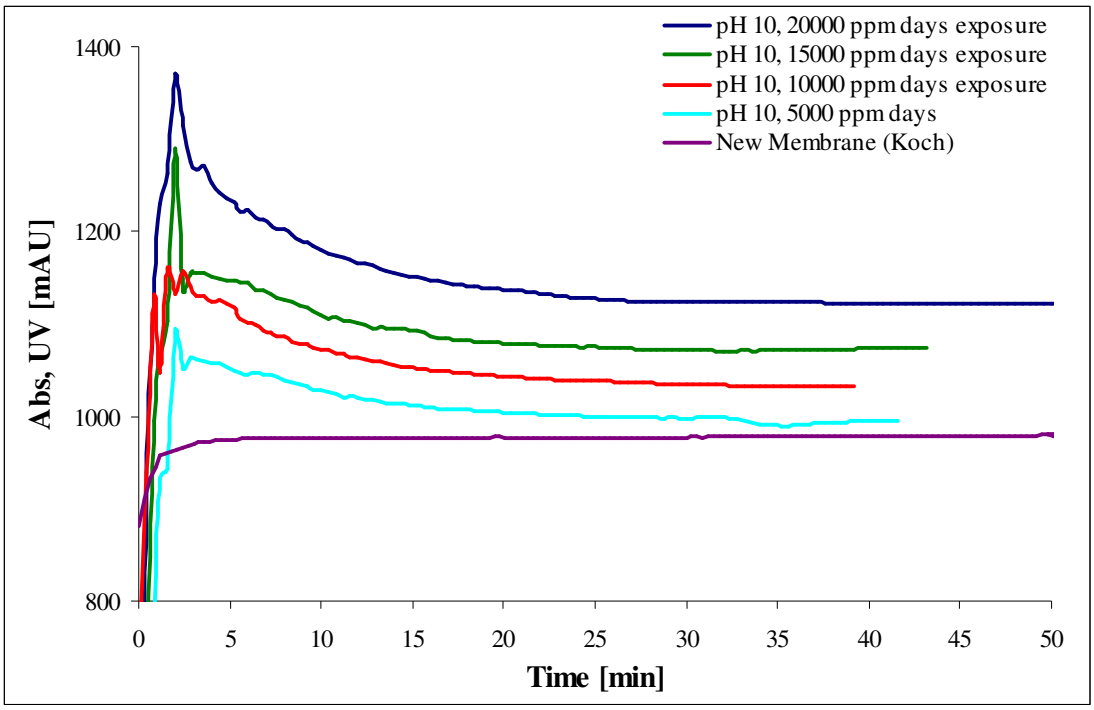

Figure 4.78 UV absorbance of permeate stream during ultrafiltration of casein whey through membrane samples exposed to pH 10 hypochlorite solution for different exposure times at 20°C, TMP: 3 bar, and feed flow: 200 mL/min

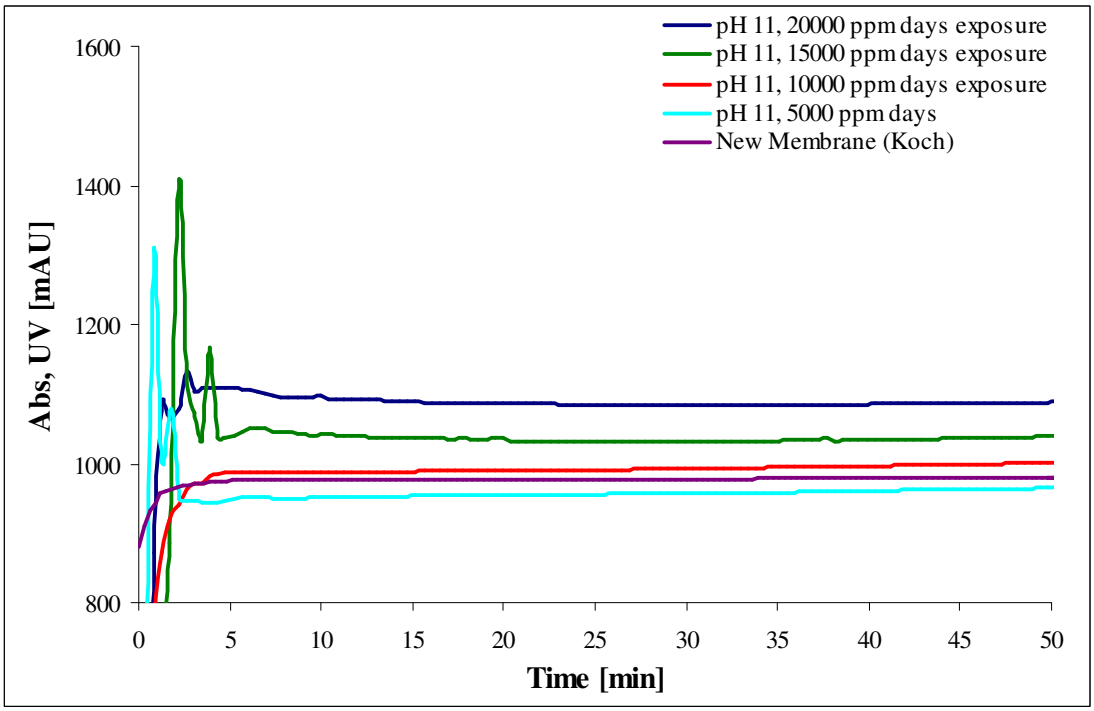

Figure 4.79 UV absorbance of permeate stream during ultrafiltration of casein whey through membrane samples exposed to pH 11 hypochlorite solution for different exposure times at 20°C, TMP: 3 bar, and feed flow: 200 mL/min

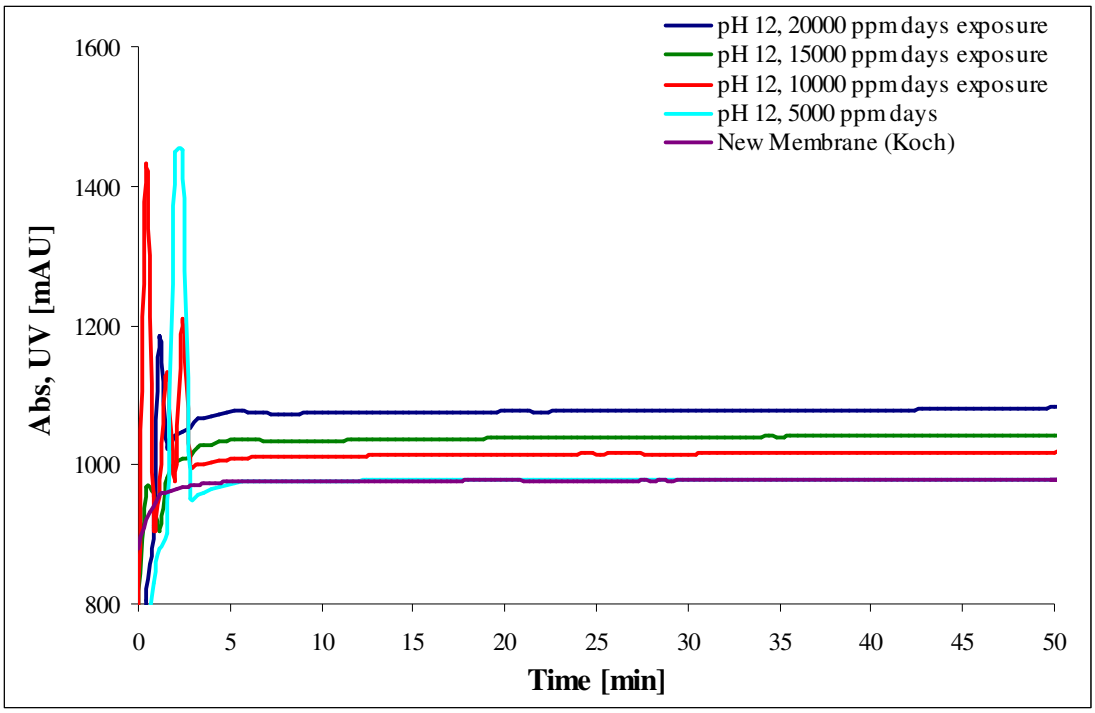

Figure 4.80 UV absorbance of permeate stream during ultrafiltration of casein whey through membrane samples exposed to pH 12 hypochlorite solution for different exposure times at 20°C, TMP: 3 bar, and feed flow: 200 mL/min

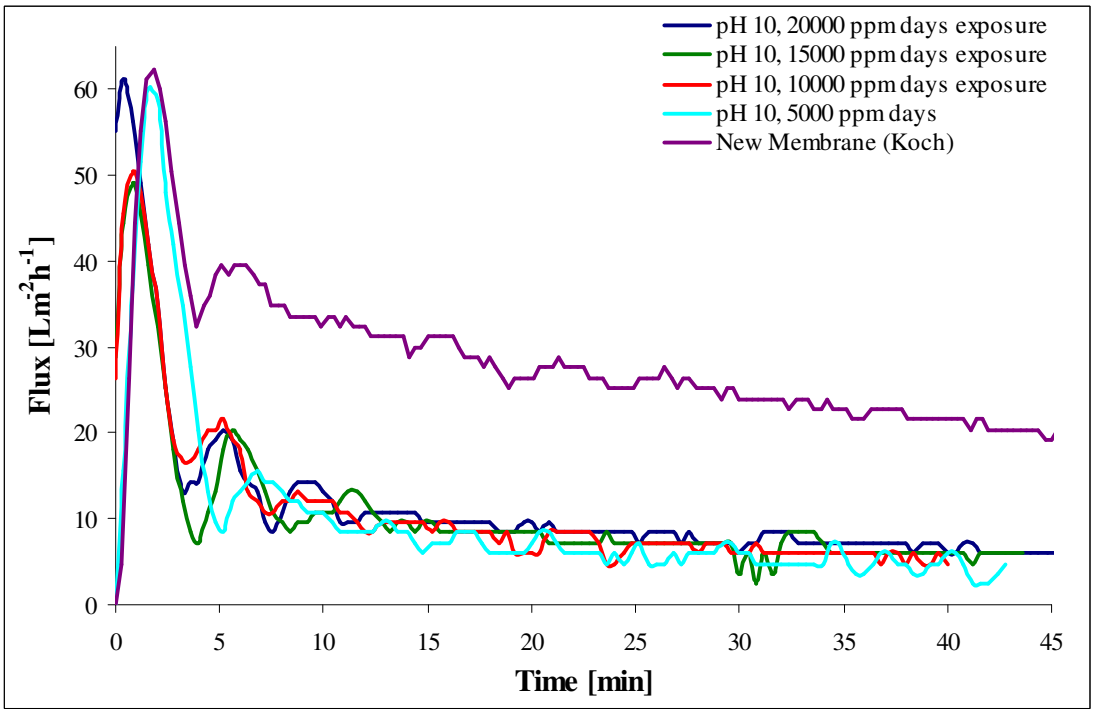

Figure 4.81 Permeate flux during ultrafiltration of casein whey through membrane samples exposed to pH 10 hypochlorite solution for different exposure times at 20°C, TMP: 3 bar, and feed flow: 200 mL/min

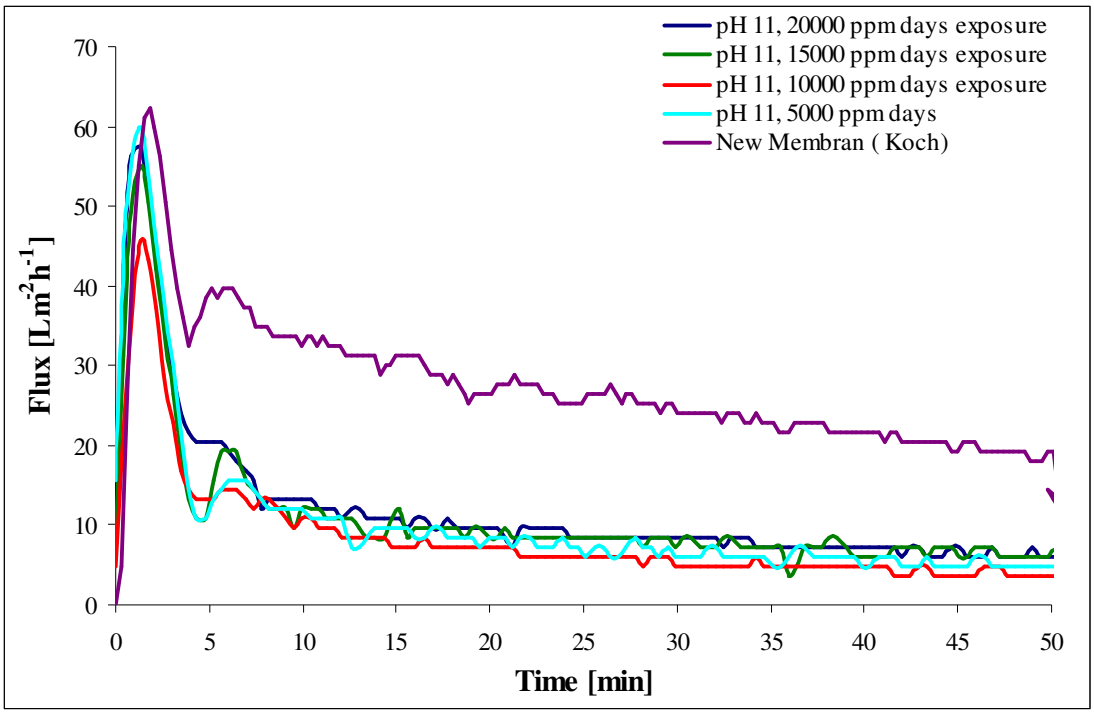

Figure 4.82 Permeate flux during ultrafiltration of casein whey through membrane samples exposed to pH 11 hypochlorite solution for different exposure times at 20°C, TMP: 3 bar, and feed flow: 200 mL/min

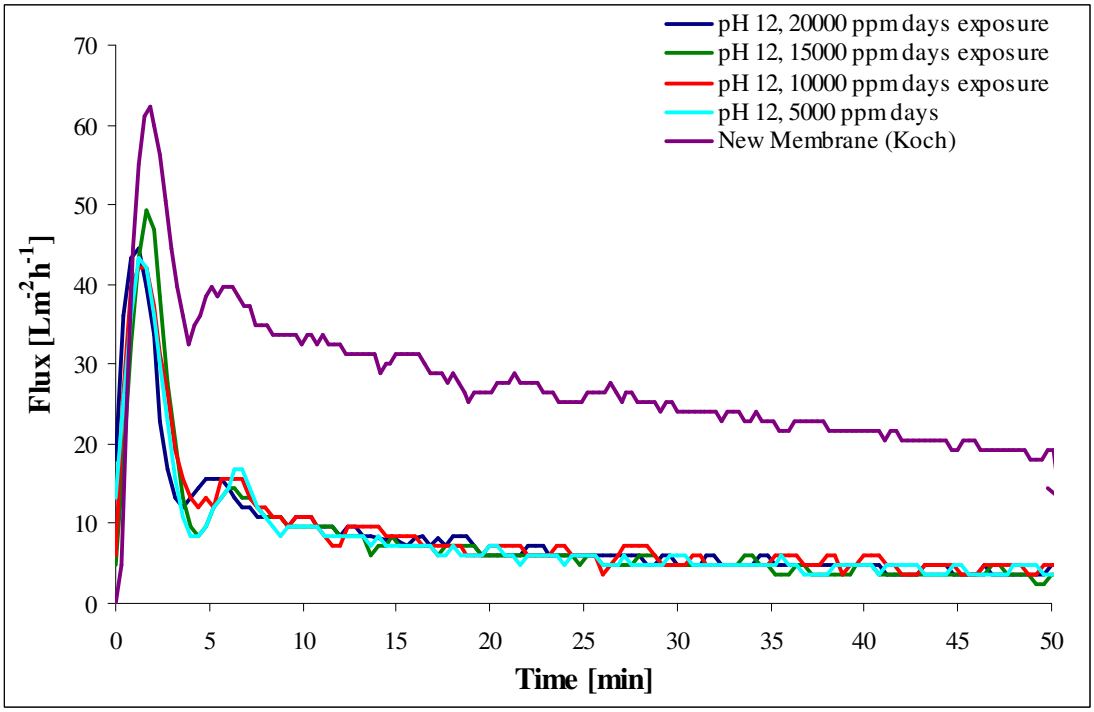

Figure 4.83 Permeate flux during ultrafiltration of casein whey through membrane samples exposed to pH 12 hypochlorite solution for different exposure times at 20°C, TMP: 3 bar, and feed flow: 200 mL/min

Figure 4.84 shows the comparison of UV absorbance and flux for the permeate stream after 30 minutes of the start of the ultrafiltration run. The permeate flux and UV

absorbance values in the graph are average values for a time period of 3 min (30 min to 33 min) from the start of the run. It can be clearly noticed that UV absorbance increased with increase in exposure time for all the four pH values, which indicates that amount of protein passing through membrane increased with increase in hypochlorite exposure time for same pH. Also the UV absorbance values increased with decrease in hypochlorite pH for same exposure time which indicated that the amount of protein passing through the membranes increased with decrease in exposure pH which was in accord to results obtained by other characterization techniques. However permeate flux did not show a clear trend for any of exposure pH or time. Surprisingly pH 9 treated membranes did not exhibit a high permeate flux as expected (FESEM imaging showed big pit formation on the surface and clean water flux also showed highest values for pH 9 treated membranes). It shows that whey permeate flux was not governed by surface pitting or pore size but possibly by surface PES-protein interactions resulting high surface fouling and low permeate flux. Also surface roughness may play a significant role in membrane fouling by providing favourable sites for fouling initiation (Bossu *et al*., 2006)

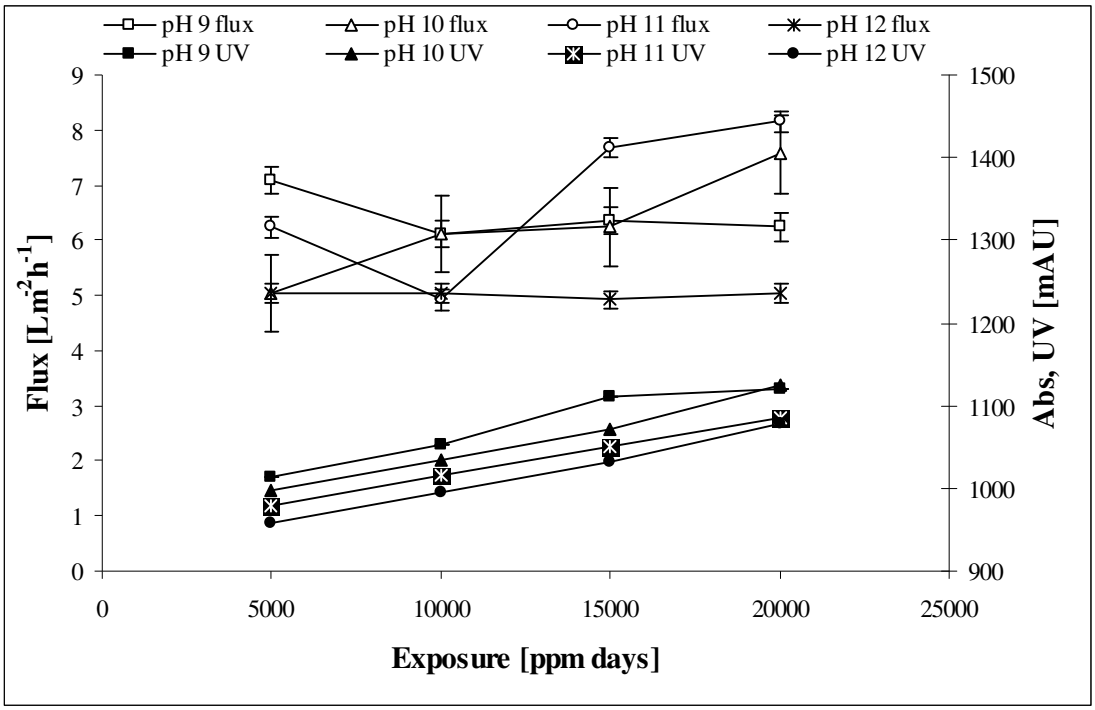

Figure 4.84 Permeate flux at 30 minutes and UV absorbance for ultrafiltration of casein whey through membrane samples exposed to pH 9 to 12 hypochlorite solution for different exposure time at 20°C, TMP: 3 bar, and feed flow: 200 mL/min

The membrane throughput experiment gave a clear understanding of the effect of hypochlorite degradation on performance of membranes in industry. It showed that hypochlorite degradation has two separate effects on membrane performance. Firstly the protein leakage through membrane increases with degradation leading to loss of product quality. Secondly hypochlorite exposure may also increase the fouling of membrane leading to a decrease in permeate flux which will result in reduced run lengths and lower overall throughput.

4.12.2 Size Exclusion Chromatography

The membrane throughput test only provided an indication of protein leakage in permeate, but it was not able to show the type or amount of protein passing through to the permeate stream. To have in depth knowledge of the protein leakage phenomena, SEC analysis was done on permeate, retentate and feed samples collected from the ultrafiltration of whey through new and hypochlorite degraded membranes. All the samples were collected after 30 min from the start of the ultrafiltration run. Figure 4.85 shows a typical SEC chromatograph of casein whey. The main focus was on α-lactalbumin and β-lactoglobulin protein since their molecular size (14.2 kDa and 18.3 kDa respectively, Neyestani *et al.*, 2003) were near to the membrane MWCO (10 kDa for the Koch ultrafiltration membrane). These proteins may leak into the permeate stream if there is any pitting or increase in membrane pore size. The chromatogram shows the α-lactalbumin peak at 17.2 ml retention and β-lactoglobulin at 16 ml. A sharp peak at 21.4 ml was registered which was assigned to small non-protein molecules having size less than 10 kDa.

Figure 4.86 shows chromatographs for the feed, permeate and retentate from ultrafiltration of whey through a new Koch membrane. It can be noticed that ultrafiltration of whey resulted in an increase of α-lactalbumin and β-lactoglobulin concentration in retentate stream. Only small non protein molecules were able to pass through the membrane into the permeate stream. No leakage of α-lactalbumin and β-lactoglobulin into the permeate stream was observed.

Figure 4.87 shows the SEC chromatograph for permeate and retentate samples obtained from ultrafiltration of whey through pH 9, 20,000 ppm-days hypochlorite

degraded samples. A significant leakage of α-lactalbumin and β-lactoglobulin into the permeate stream was observed.

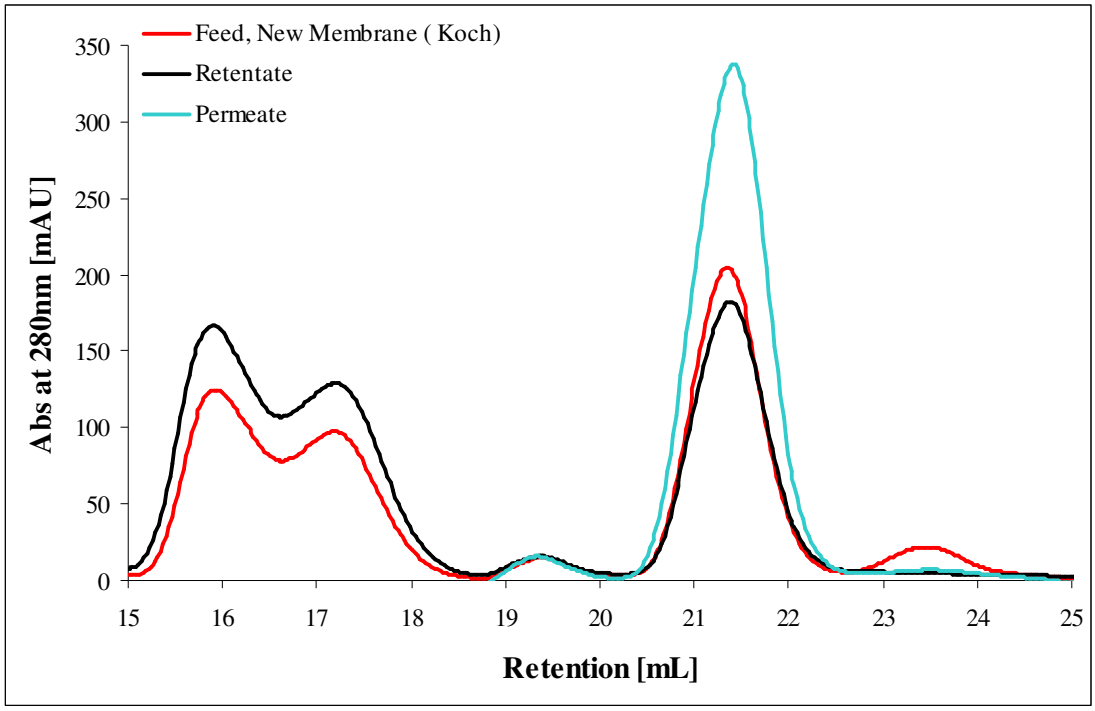

Figure 4.86 SEC chromatography comparison of whey protein isolated in different streams after ultrafiltration of whey through new membrane (Koch)

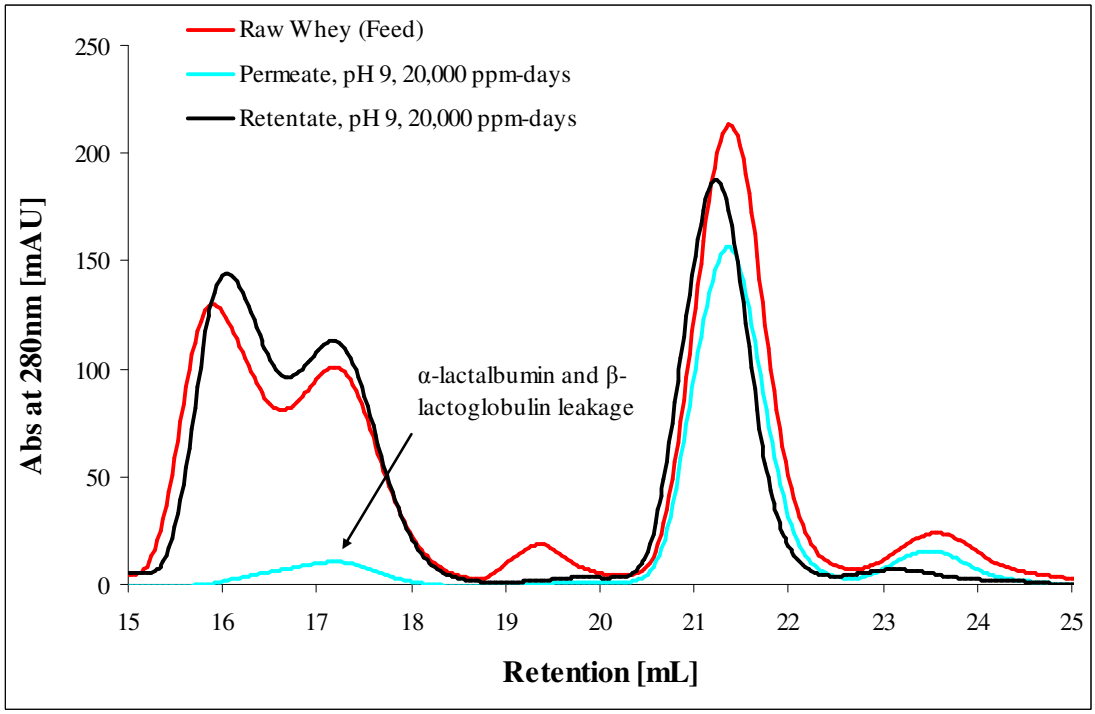

Figure 4.87 SEC chromatography comparison of whey protein isolated in different streams after ultrafiltration of whey through ph 9, 20000 ppm-days hypochlorite exposed Koch membrane

Figure 4.88 shows comparison of α-lactalbumin and β-lactoglobulin leakage in permeate stream for pH 9 hypochlorite exposure from 5,000 ppm-days to 20,000 ppm-day. The graph clearly shows α-lactalbumin leakage around 17.2 mL retention volume. A less prominent shoulder around 16.2 mL retention was observed which was designated to β-lactoglobulin leakage in permeate stream. The column used for this experiment was Superdex-200 HR 10/30 column which had optimal separation from 10 to 600 kDa. The α-lactalbumin and β-lactoglobulin molecular size (~14.15 kDa and ~18.3 kDa respectively) were near the lower detection limit of the column so it may be possible that the leakage was too small to be detected as clear peaks by the column used. The graph also shows that the total leakage (β-lactoglobulin + α-lactalbumin) increased with increase in exposure time for pH 9 hypochlorite degraded samples.

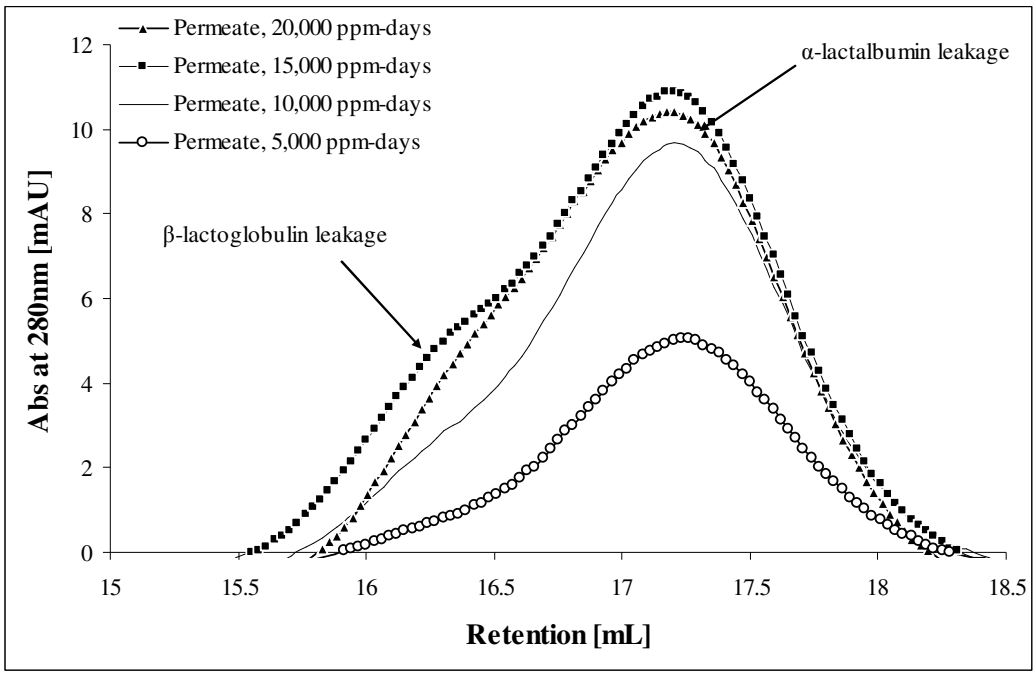

Figure 4.88 SEC chromatography comparison of β-lactoglobulin and α-lactalbumin leakage in permeate after ultrafiltration of whey through Koch membranes treated at various ppm-days exposure at pH 9

SEC analysis on membranes degraded at pH 9 to 12, for 20,000 ppm-days hypochlorite exposure (Figure 4.89) showed that total leakage of protein in permeate stream increased with decrease in hypochlorite exposure pH for same exposure time. No α-lactalbumin and β-lactoglobulin leakage was observed in case of pH 12, 20,000 ppm-days degraded samples.

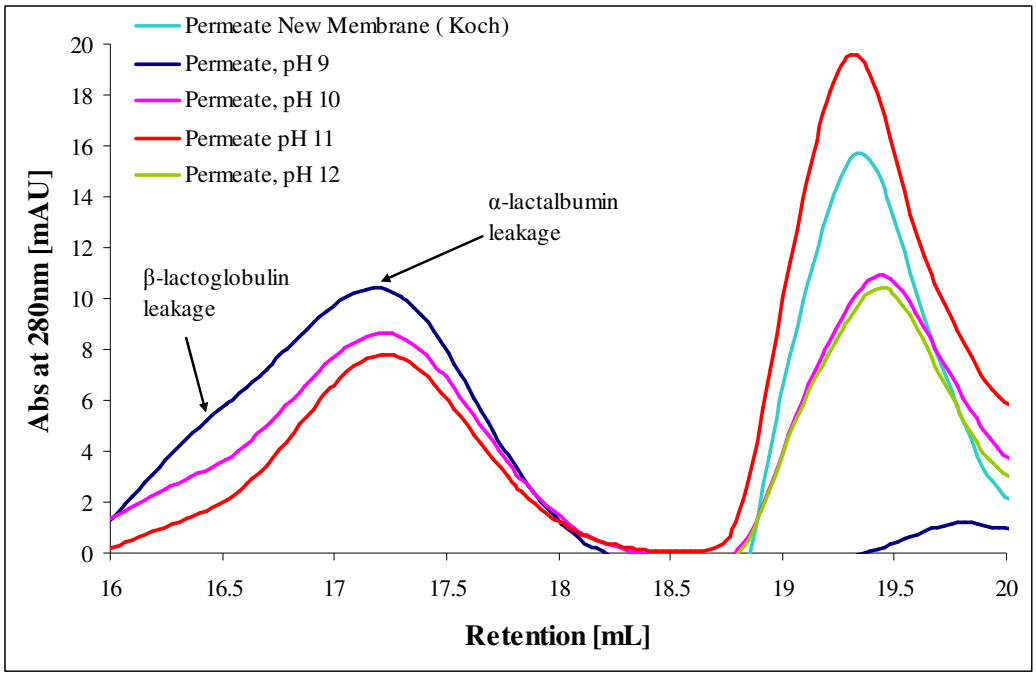

Figure 4.89 SEC chromatography comparison of whey protein isolated in permeate after ultrafiltration of whey through Koch new and hypochlorite treated membranes for 20,000 ppm-days at various hypochlorite solution pH

To calculate the concentration of α-lactalbumin and β-lactoglobulin in various streams a SEC analysis was done on standard bovine α-lactalbumin and β-lactoglobulin samples at various concentrations. The area under the curve for each sample was calculated and a standard curve was generated accordingly for both proteins as shown in Figure 4.90.

To calculate the individual concentration of α-lactalbumin and β-lactoglobulin, for each SEC run, a fit to the data was obtained by summing up to 10 different normal distributions. The mean, standard deviation and area of each distribution was optimised, using Excel Solver, to obtain the minimum of squared deviation between the data and the fitted curve over the range of retention volumes from 10 to 30 mL. The fit was always very good as indicated by Figure 4.91 (No statistics of the goodness of fit were obtained). The total areas under the individual protein peaks in the fitted curve were obtained (Figure 4.92) and the unknown concentration of α-lactalbumin and β-lactoglobulin in various streams was calculated by extrapolation of the area under the fitted curve for α-lactalbumin and β-lactoglobulin on the standard concentration curves obtained for each protein.

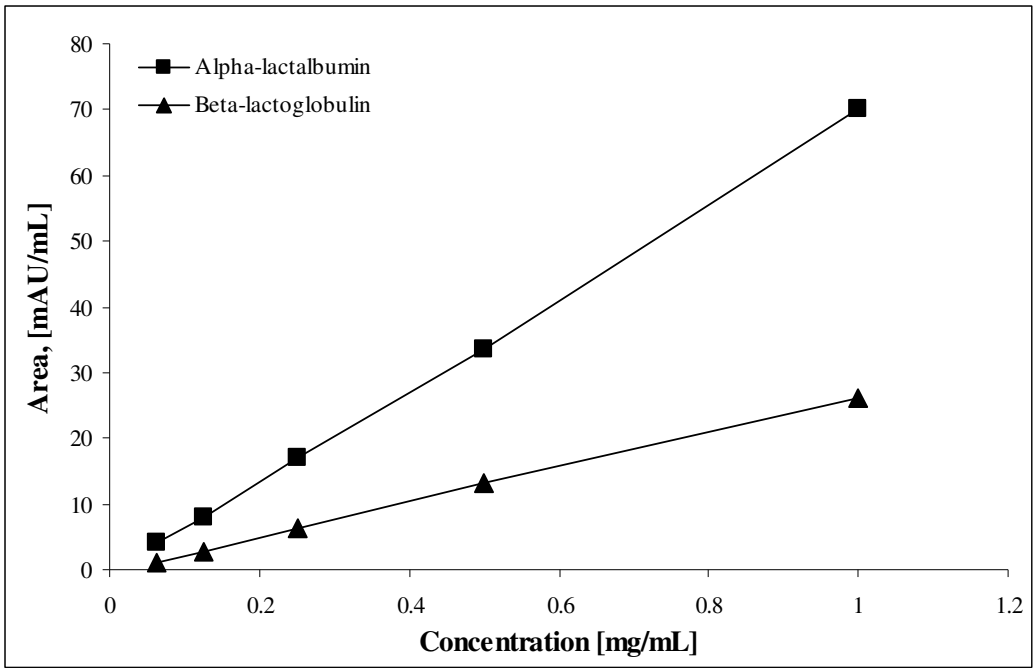

Figure 4.90 Standard concentration curves α-lactalbumin and β-lactoglobulin obtained by integrating area under the curve from SEC chromatograms
Standard proteins used:

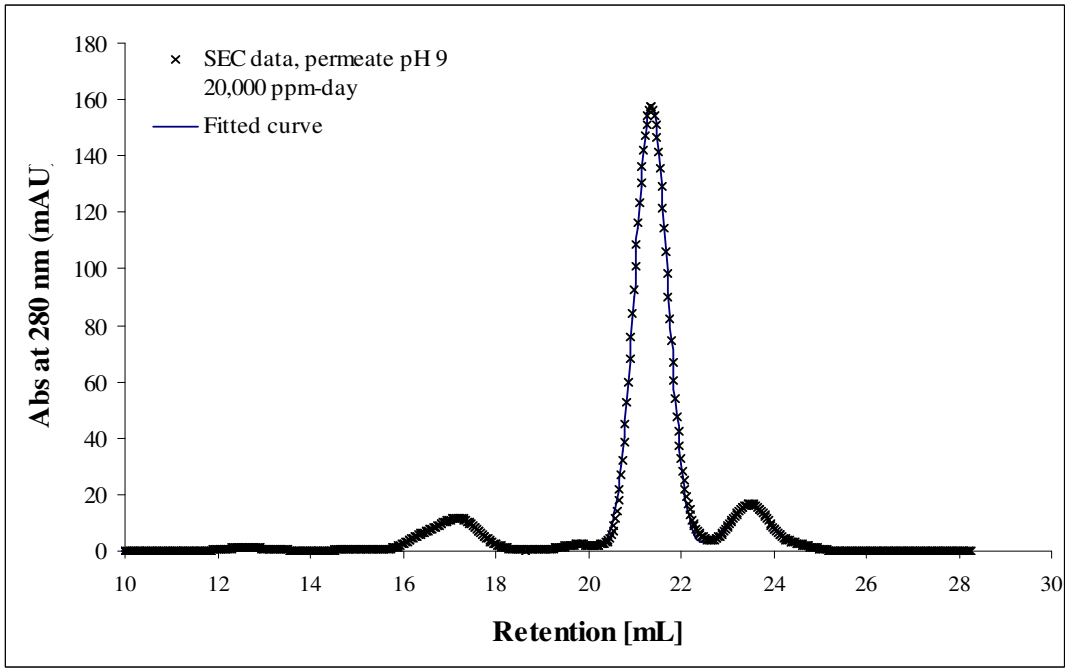

Figure 4.91 SEC curve and fitted curve for permeate sample obtained from ultrafiltration of whey through pH 9, 20,000 ppm-days hypochlorite treated Koch membrane.

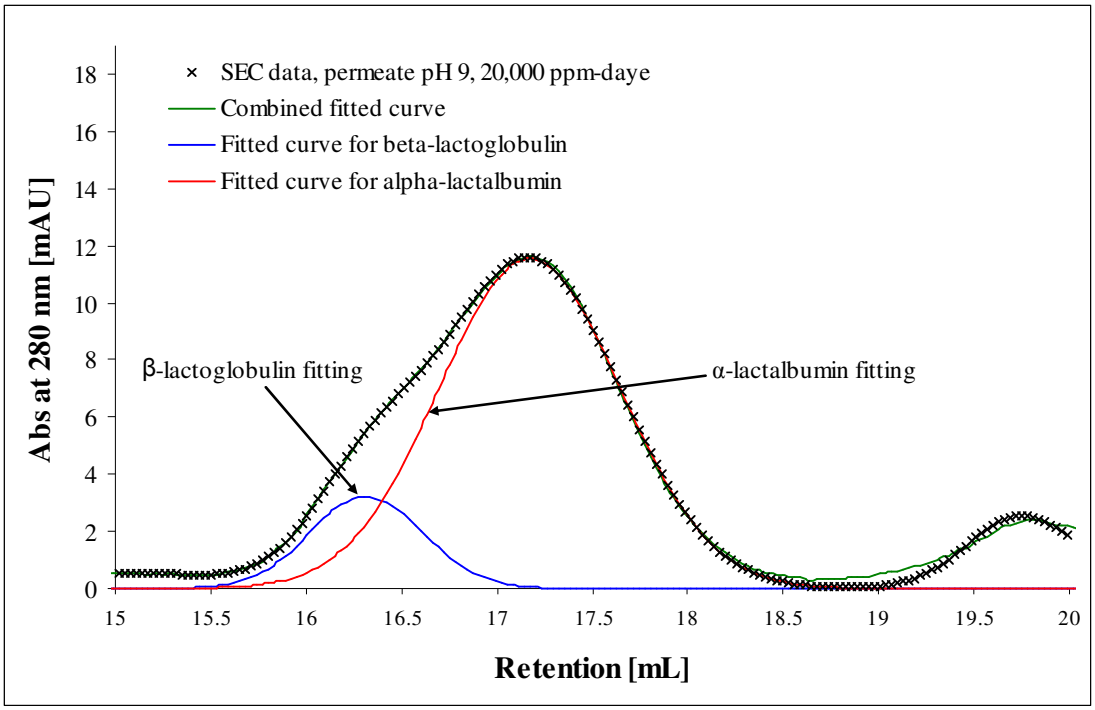

Figure 4.92 SEC curve and individual protein and combined fitted curve for permeate sample obtained from ultrafiltration of whey through pH 9, 20,000 ppm-days hypochlorite treated Koch membrane.

Table 4.12 shows the calculated concentration of α-lactalbumin and β-lactoglobulin in various streams for new and hypochlorite degraded membrane (pH 9 to 12, 5,000 to 20,000 ppm-days exposures). The feed contained 1.41 mg/mL of α-lactalbumin and 4.30 mg/mL of β-lactoglobulin. It can be seen that permeate stream from pH 9 20,000 ppm-days and 15,000 ppm-days degraded membranes showed similar amounts of total protein leakage. Similar observations were made for UV absorption of the permeate stream in the membrane throughput the experiment for pH 9 20,000 ppm-days and 15,000 ppm-days degraded membranes (Figure 4.85). This confirmed that the increase in UV concentration of permeate in the membrane throughput experiment was mainly due to α-lactalbumin and β-lactoglobulin leakage through the degraded membrane. No α-lactalbumin and β-lactoglobulin leakage was observed for pH 12 for any of the exposure time but UV absorption in membrane throughput experiment detected an increase in protein concentration in permeate stream for pH 12 treated membranes. It may be possible that the concentration in this case was extremely low and out of the SEC column detection limits. A smaller level of β-lactoglobulin leakage was observed as compared to α-lactalbumin for any exposure time, which may be due to the smaller molecular size of α-lactalbumin as compared to β-lactoglobulin.

Table 4.12 Concentration of α-lactalbumin and β-lactoglobulin leakage in permeate stream during ultrafiltration of whey through new and hypochlorite treated samples membrane samples.

Sample	pH	Exposure ppm-day	β -lactoalbumin mg/mL	α -lactglobulin mg/mL	Total leakage mg/mL
Permeate	9	5,000	0.04	0.10	0.13
		10,000	0.08	0.17	0.26
		15,000	0.14	0.20	0.33
		20,000	0.11	0.20	0.31
	10	5,000	0.05	0.20	0.25
		10,000	0.10	0.26	0.36
		15,000	0.07	0.14	0.21
		20,000	0.10	0.15	0.25
	11	20,000	0.04	0.14	0.18
	12	20,000	0.00	0.00	0.00
	New membrane		0.00	0.00	0.00
Retentate	New membrane		1.97	5.90	7.87
Feed	New membrane		1.41	4.30	5.71

(For the new membrane, the feed sample was taken in start of run and permeate and retentate sample were taken after 30 minutes from the start of ultrafiltration)

4.12.3 Gel Electrophoresis

An SDS-polyacrylamide gel electrophoresis (SDS-PAGE) test was conducted mainly on samples obtained from ultrafiltration of whey through pH 9 to 12, 20,000 ppm-days hypochlorite degraded membranes. Figure 4.93 shows the SDS gel and loading sequence followed. It clearly shows the leakage of α-lactalbumin in the permeate samples from all the hypochlorite degraded membrane samples. It also clearly detected β-lactoglobulin leakage in permeate for pH 9, 10 and 11 degraded membranes, which was detected just as a shoulder around 16.2 mL by SEC. No α-lactalbumin and β-lactoglobulin leakage was observed for new and pH 12 hypochlorite treated membranes. The intensity of the dye marks give a rough observation of the amount of each protein in the samples tested. It can be noted the colour intensity of dye marks for α-lactalbumin and β-lactoglobulin for permeate samples tested decreased with increase in pH. It can be interpreted as a decrease of α-lactalbumin and β-lactoglobulin amount in permeate stream with increase in hypochlorite pH for membrane degradation. SDS-PAGE gel electrophoresis not only

supported the results from membrane throughput and SEC but also clearly showed a presence of β-lactoglobulin in the permeate stream of degraded membranes (pH 9-11) but it can not give the concentration of α-lactalbumin and β-lactoglobulin in the leakage. It can be concluded from the SDS-PAGE electrophoresis experiment that both α-lactalbumin and β-lactoglobulin leakage occurred in pH 9 to 11, 20,000 ppm-days hypochlorite degraded membranes. This may be due to surface pit formation as seen in FESEM imaging. Further SEC study is needed with a column with smaller MWCO range (20 to 1 kDa) to give a better detection of β-lactoglobulin at a very low concentration as detected by SDS-PAGE electrophoresis.

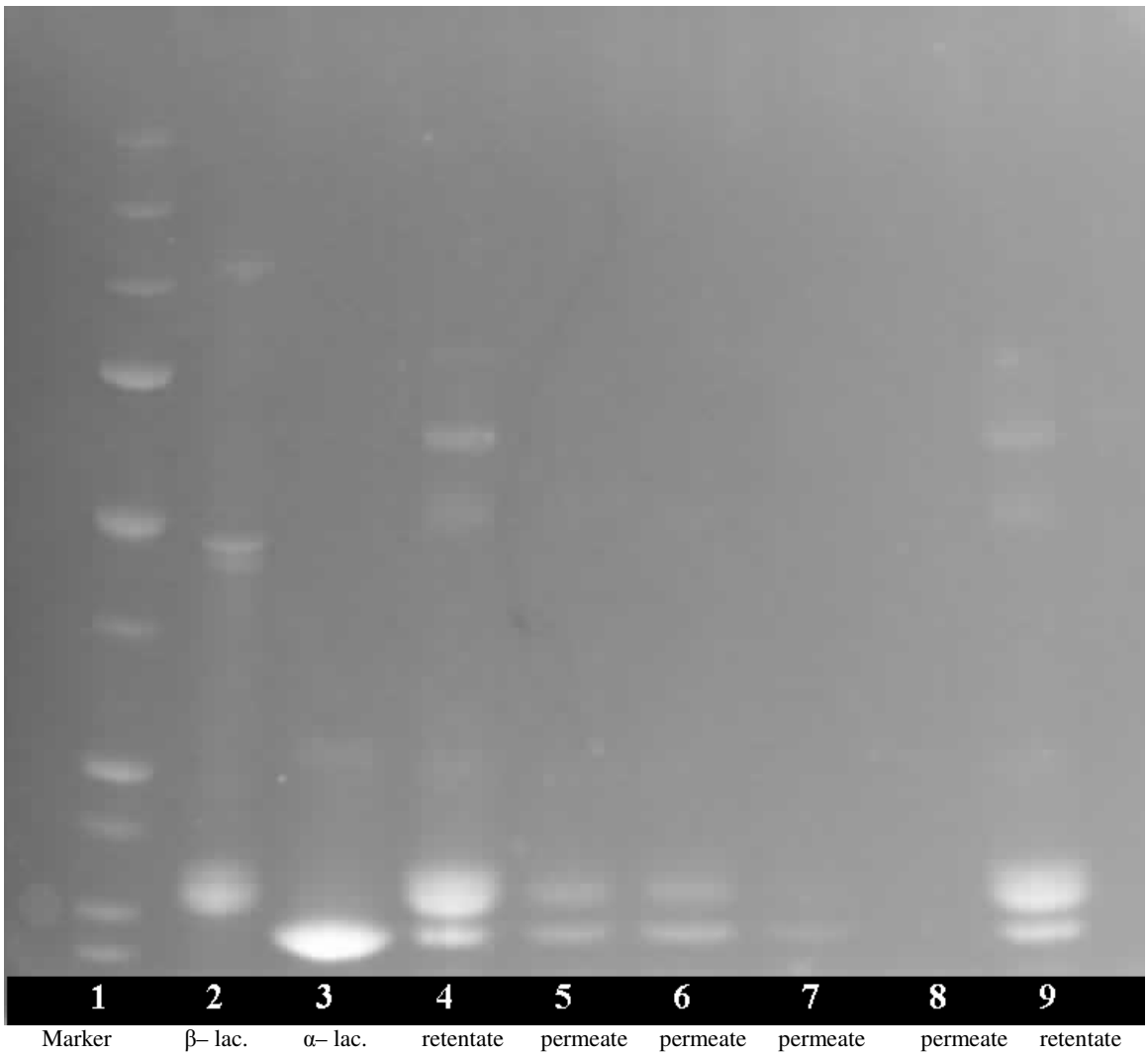

Figure 4.93 The SDS-PAGE of whey proteins in samples collected from ultrafiltration of whey through new and 20,000 ppm-days hypochlorite exposed Koch membranes.

4.13 Colour Measurement

During DMA analysis of Koch commercial UF membranes it was observed that the colour of the PES side of a membrane changed once the membrane was heated above the T_g of PES. The colour intensity differed with pH of hypochlorite exposure. It was decided to do a colour test in which new and degraded ultrafiltration membrane were heated just above glass transition temperature of PES and colour of the sample was measured (in Hunter LAB coordinates) once the sample had cooled down. New unheated membrane was used as control sample for all the colour comparisons. Figure 4.94 (A) shows the change in lightness of the samples tested. + ΔL means sample is lighter and -ΔL means sample is darker than the control sample.

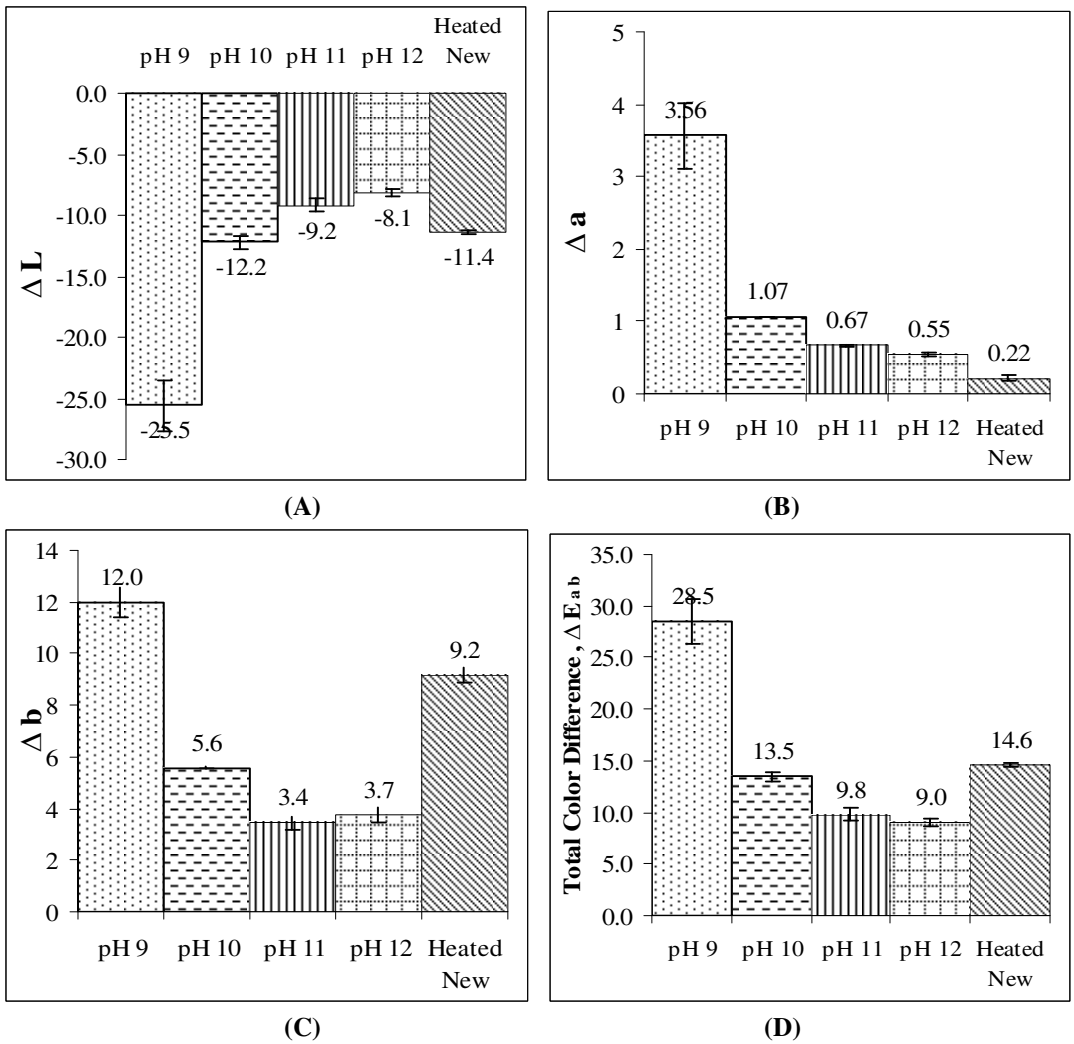

Figure 4.94 Colour measurements in Hunter LAB coordinates for new heated and hypochlorite degraded Koch membrane samples (pH 9 to 12, 25,000 ppm-days exposure). They are relative to an unheated new membrane.

Figure 4.94 (B) shows the change in colour intensity from green to red for each sample tested. +Δa means sample is redder than the control sample and -Δa means sample is greener than the control sample. Figure 4.94 (C) shows the change in colour intensity from yellow to blue for the sample tested. +Δb means sample is yellowier than the control sample and -Δb means sample is bluer than the control sample. Figure 4.94 (D) shows the total change in sample colour (E_{ab}) as compared to the control sample. Colour measurement was done on new-unheated (control), new-heated and heated hypochlorite degraded samples (pH 9 to 12, 25,000 ppm-days exposure).

It was observed that pH 9 samples were greyish black in colour showing a high -ΔL. pH 10 tested samples were also greyish black in colour but with lesser intensity, hence showing lower -ΔL as compared to pH 9 treated samples. pH 11 and 12 samples turned dull light yellow in colour after heating and hence exhibited a low value of Δa and Δb as compared to pH 10 and 9 treated samples. The heated new membrane was bright light yellow in colour after heating showing a high value of Δb as compared to pH 10, 11 and 12 treated samples. All the colour coordinates showed a clear trend which easily differentiated the samples treated at different hypochlorite pH.

The difference in colour with hypochlorite exposure pH may be because of changes in the surface chemical composition of the PES layer of the membranes, which on oxidation in air above the glass transition temperature produced a unique colour intensity typical of that exposure pH and time.

Colour comparison provided an easy and fast comparative technique to identify extent of degradation by hypochlorite degradation on membrane surface, but, being a destructive test, it would be hard to apply in industry and may only be used for laboratory scale studies. Further it gave no useful information about the cause of the difference.

4.14 Hypochlorite Disinfection Test

4.14.1 Disinfection Test on Membrane Surface

The disinfection test was done on a new Koch UF membrane (method in Section 3.4.13). The aim of this test was to mimic the disinfection condition in industry and analyse the effect of the hypochlorite solution pH on microbial load reduction. The aerobic plate count as APC/mL calculated for various exposures is given in Table 4.13

Table 4.13 APC/mL for membrane samples disinfected by hypochlorite solution at different pH, 55°C for 20 min.

Sample	APC/mL	APC/mL (duplicate)
Control	20	<10
pH 10.5 treated	10	<10
pH 11 treated	<10	<10
pH 11.5 treated	10	<10
pH 12 treated	10	<10

A very low level of microbial load was observed on all the samples. Against expectation, even the control samples did not show a high microbial load as compared to other samples. It may be due to a very low loading of microbes on the membrane surface even after a 12 hour run. Since the membrane was a flat sheet and microbial loading was done in a cross-flow module, it is possible that cross-flow velocity did not allow the accumulation of microbes. A new membrane may not be as rough as a used membrane, hence providing very few rough sites on the surface for microbial adhesion. Due to inadequate adhesion, the microbes may have just been washed away with water during the rinsing step after hypochlorite treatment. Overall this experiment failed to give an adequate microbial count even when no hypochlorite was added.

4.14.2 Disinfection Test directly on Microbial Culture

Due to failure of the first test, the disinfection test was directly done on a microbial culture which was then extracted by centrifugation. Table 4.14 shows the APC/ml for disinfection test done directly by adding sodium hypochlorite solutions at various pH values to a microbial culture. The results clearly indicate a significant reduction in

microbial load in all the hypochlorite disinfected samples as compared to control sample.

Table 4.14 APC/ml for extracted microbial culture disinfected by suspending in hypochlorite solution at different pH, 55°C for 20 min.

Sample	APC/mL	APC/mL (duplicate)	Log Reduction (from control)
Control	80,000	80,000	-
pH 10.5 treated	290	280	2.45
pH 11 treated	470	520	2.21
pH 11.5 treated	320	250	2.45
pH 12 treated	280	270	2.46

A similar log reduction was observed in all the hypochlorite disinfected samples irrespective of the pH of hypochlorite solution. The small variation in APC for the treated samples observed may be attributed to the variation in initial microbial load in the extracted microbial culture.

Sodium hypochlorite dissociates in water to form hypochlorous acid, HClO, which is a weak acid and further dissociates in aqueous solution to form hypochlorite ions, ClO^-.

$$NaOCl + H_2O \longleftrightarrow HClO + Na^+ + OH^-$$

$$HClO + OH^- \longleftrightarrow OCl^- + H_2O$$

The ratio of hypochlorous acid and hypochlorite ions in solution depends primarily on pH and somewhat on temperature (IC Controls, 2005). At pH higher than 10 predominantly OCl^- remains in the solution. So in the test pH range, i.e. 10.5 to 12 it may be possible that OCl^- was the only disinfection agent hence giving a similar range of load reduction for all the hypochlorite treatments. There is a need of detailed study on the effect of hypochlorite pH on microbial load reduction especially with a single target micro organism, instead of a crude culture, to confirm the results above.

Chapter 5 Comprehensive Discussion

This chapter aims at building links between the various characterization techniques used for studying long term hypochlorite degradation of commercial ultrafiltration membranes and to give a better understanding of the degradation mechanism. Also an effort has been made to propose characterization regimes for autopsy analysis and in-line monitoring of the health of membranes. A number of membrane characterization techniques were evaluated which can be broadly divided into:

1. Characterization in terms of change in bulk properties of membrane which included DMA, TGA, colour measurement and tensile testing.
2. Characterization of membrane surface properties which included FTIR-ATR, FESEM imaging, EDS analysis, contact angle, liquid absorption test and zeta potential.
3. Characterization of a membrane as a porous filter aid which included LLDP, cross-flow flux measurement, and protein separation.

5.1 Degradation Mechanism

5.1.2 Polymer Chain Scission

FTIR-ATR analysis showed that the surface PES layer became rough and a new peak was formed which was probably sulfonic acid. The TGA experiment showed a likely decrease in the molecular weight of PES. These two observations indicated the likelihood of PES polymer cleavage in presence of sodium hypochlorite. EDS experiments detected surface bound chlorine in pH 9 and 10 hypochlorite degraded membrane samples which further supported the finding of FTIR-ATR and TGA experiments. A chemical mechanism for PES cleavage was proposed by Gaudichet-Maurin and Thominette (2006) and again with similar steps by Arkhangelsky *et al.* (2007) which is as follow:

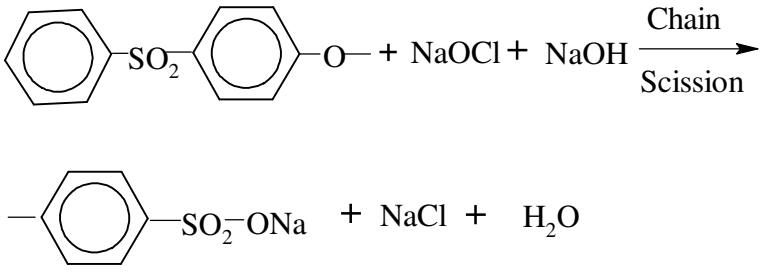

(5.1)

This mechanism shows formation of sodium sulfonate which is likely to be a highly unstable compound. EDS analysis detected the presence of chlorine along with sulphur, carbon, and oxygen and the absence of sodium on the surface of hypochlorite degraded membranes which can not be explained on the basis of above mechanism.

Since the sodium salt is likely to be unstable and highly susceptible to hydrolysis in presence of water (in subsequent water washing of membranes after hypochlorite exposure) sodium sulfonates converts into sulfonic acid terminal as

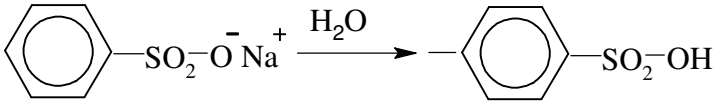

(5.2)

The new proposed reaction mechanism on the basis of findings of this research is as follows:

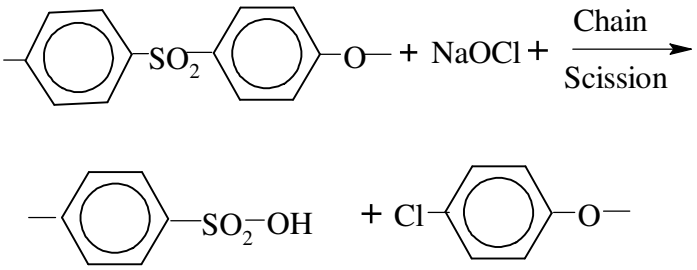

(5.3)

The proposed mechanism has chain scission of the PES polymeric backbone into two parts with one end terminated by a sulfonic acid group and other part terminated by a phenyl chloride group. This reaction mechanism explains the presence of chlorine and absence of sodium on the membrane surface. The formation of sulfonic acid group was detected as a new peak formation at 1034 cm^{-1} in the FTIR-ATR analysis.

5.1.2 Surface Pitting

The phenomenon of surface pitting is not unknown in polymers (Bershtein *et al.*, 1978; Sagripanti and Hughes-Dillon, 1996). A study on low temperature water plasma modification of polysulfone membranes showed that plasma introduced a visible pitting on the surface and increased the pore size of the membrane (Steen *et al.*, 2001). This was linked with surface oxidation of polysulfone which caused chain scission at methyl and sulphur positions causing surface pitting.

From FESEM imaging it was clear that surface pitting increased with decrease of hypochlorite pH. Although no surface pitting was observed for pH 11 and 12 hypochlorite treated Koch membrane samples, the protein separation experiment confirmed leakage of α-lactalbumin and β-lactoglobulin for membranes degraded at these pH values. It is likely that surface pits were formed on pH 11 and 12 degraded membranes but were too small to be detected by FESEM imaging. A clear dependence of surface pitting on exposure time was observed for same pH. Both the number and size of surface pits increased with increase in exposure time.

It is likely that localised surface oxidation at the sulphur position caused surface etching of the PES layer. The surface etching lead to the formation of rough surface pockets which was observed as an increase in surface roughness by FTIR-ATR experiment. FESEM images of pH 10 hypochlorite degraded ultrafiltration membranes (Section 4.5.2.2) also showed an increase in surface roughness with increase in hypochlorite exposure. It may be possible that these rough pockets on the surface may provide a favourable site for the degradation reaction leading to micro pit formation. With the progress of degradation, the barrier layer in the pit is depleted, exposing a more porous lower layer to hypochlorite solution and favourable condition inside an established pit may have increased the pit size with exposure time. Since the hypochlorite exposure occurred in non-stirred conditions, the degradation relied more on surface

diffusion so a local environment inside a pit may remain unchanged as compared to the surroundings.

It is likely that the pitting defect was not initiated by the membrane pores as, if this was true, it would have lead to uniform pit formation throughout the surface. The uneven and localised pit formation as observed at lower hypochlorite exposures, of 5,000 to 10,000 ppm-days indicates that the initiation of pitting occurs on the membrane surface rather than in membrane pores. It is clear that the degradation reaction is more favourable within an existing pit than elsewhere, but the number of pits increased with exposure time as new favourable sites may be formed with along exposure time.

Tensile testing showed a loss in tensile strength with hypochlorite exposure which can be linked to surface pitting and polymer cleavage. A loss in surface gloss and surface cracking of the PES layer coincided with a decrease in mechanical strength of the PES layer of the Koch membranes. It was concluded that surface degradation starts with surface etching leading to formation of microscopic pits. Consequently the size and density of these pits increases as the exposure time increases and ultimately leads to complete leakage of valuable α-lactalbumin and β-lactoglobulin proteins in permeate. On the other hand pitting also causes a loss in mechanical strength of PES layer leading to surface crack formation and complete breakdown of mechanical integrity of membrane. Figure 5.1 shows a schematic of the proposed mechanism for pit formation. While this gives an overview of the process, all the detail is not fully understood.

5.2 Links between Characterization Technique Results

The DMA experiment clearly showed that degradation is not a bulk phenomenon and does not affect the glass transition temperature of any of the polymers in the membrane. It indicated that the research should concentrate on surface characterization techniques rather than bulk properties measurements. All the bulk properties characterization techniques indicated that the backing was not much affected by hypochlorite degradation and this was further supported by

FTIR-ATR results. Tensile testing showed weakening of the PES layer leading to decrease in tensile strength of the membrane. FESEM imaging showed pit formation in the pH 9 and 10 hypochlorite degraded membranes clearly indicating high degradation of PES at these pH values. No pitting was observed for pH 11 and 12 degraded membranes but clean water flux test showed a significant increase in the water flux even for pH 12 degraded membranes as compared to new membrane. A similar effect was found with liquid absorption test which indicated that pH 11 and 12 degraded membranes were also affected by hypochlorite exposure for all the exposure of 10,000 to 20,000 ppm days. This observation was backed by membrane throughput experiment where an increase in UV absorption (protein) for the permeate stream was detected for all the degraded membranes as compared to a new membrane. SEC and gel electrophoresis also showed a leakage of α-lactalbumin and β-lactoglobulin in the permeate stream even in pH 11 and 12 degraded membranes. It was clear that degradation occurred at all pH values of hypochlorite exposure.

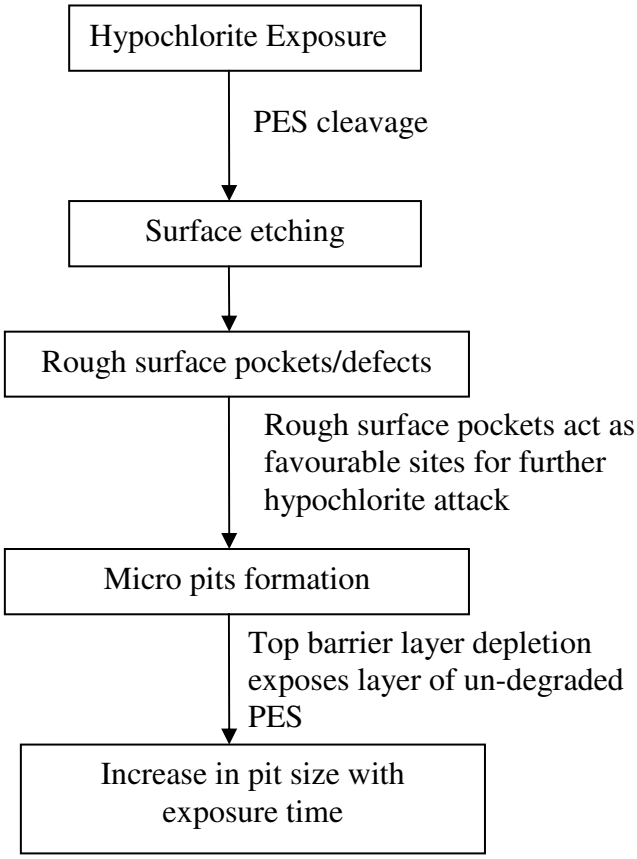

Figure 5.1 Proposed mechanism for pit formation on the surface of ultrafiltration membranes.

An important aspect of membrane processes in industry is trans-membrane pressure (TMP) control to maintain the permeate flux. The reduction of permeate flux with age of membrane is a serious problem in industry. To maintain a desirable flux, extensive cleaning is done but still a permanent decrease in flux occurs as the useful age of membrane decreases. To overcome the increase in resistance a higher TMP is applied and this balancing process continues till it is no longer possible to increase TMP or the membrane fails. Surface characterization of new and hypochlorite degraded membrane was helpful in explaining this phenomena. The membrane throughput experiment showed that the permeate flux during ultrafiltration of whey decreased for degraded membranes (in spite of an increase in pore size and pitting) as compared to new membranes. It indicated that the PES surface was modified in such a way that PES surface-liquid interactions resulted with an increase in affinity of membrane surface for organics, ultimately leading to an increase in surface fouling. The loss in mechanical strength of the PES layer due to pitting, coupled with the need to increase TMP to maintain a viable permeate flow, can multiply the effects of hypochlorite degradation. It aggravates the susceptibility of membrane failure and further decreases the useful life span of membrane.

Contact angle measurement showed that the hydrophilicity of the membrane changed with degradation (though it did not give a clear indication as the porous surface was a challenge for contact angle measurement). Zeta potential measurement showed that cleavage of PES decreased the isoelectric pH for the degraded samples. Similarly the water-methanol-water flux test indicated that the PES surface-methanol interaction decreased with increase in hypochlorite degradation. It was likely that methanol was able to interact with PES inside the membrane pores resulting in an increased post-alcohol water flux. Surface pitting of membrane caused large holes formation for which methanol will have little effect. All these techniques led to the conclusion that the surface of membrane was changed significantly with surface oxidation of the PES layer. A typical degradation map charted out for PES ultrafiltration membrane as per characterization techniques followed in this research is shown in Figure 5.2.

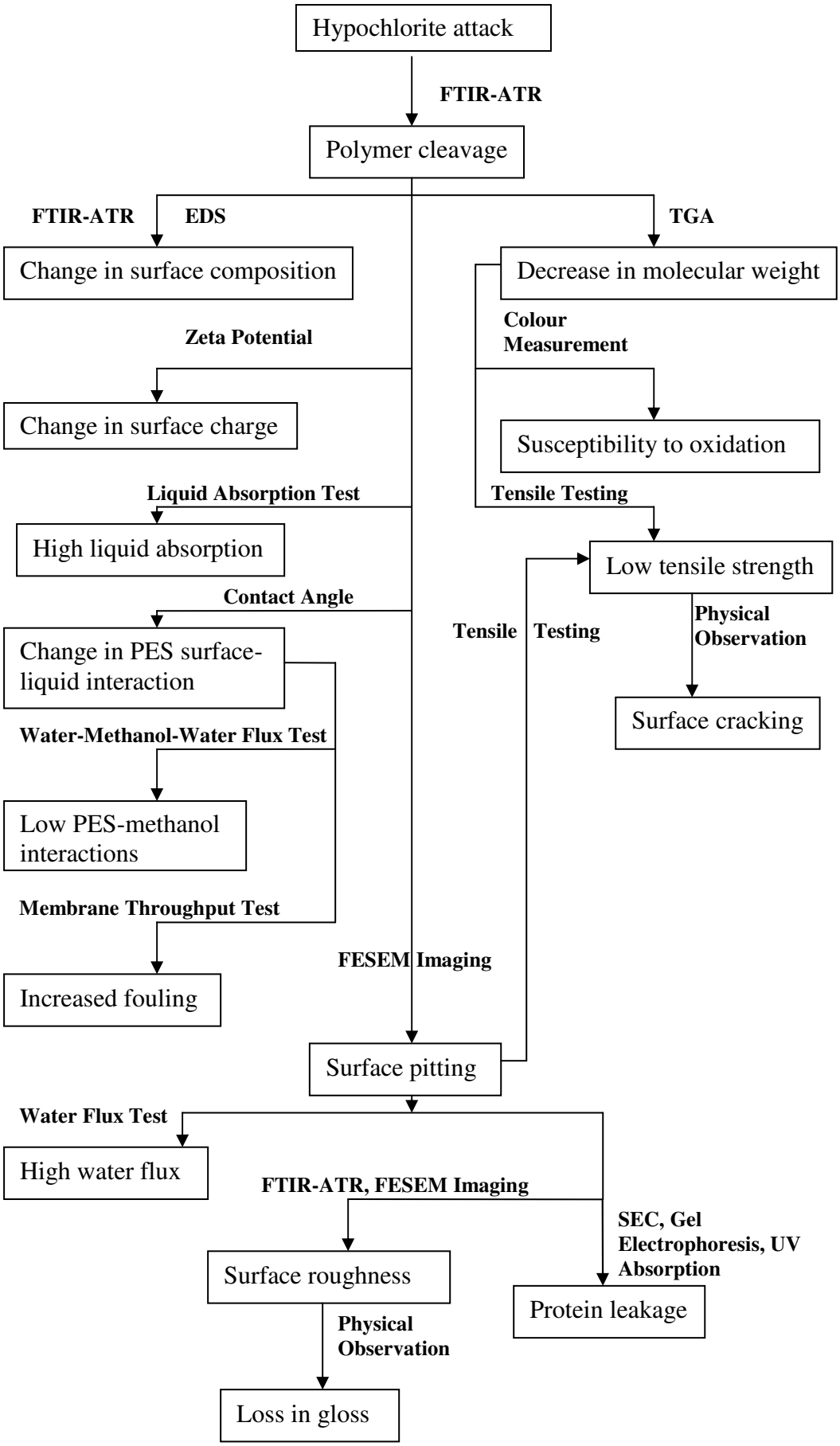

Figure 5.2 Degradation map for PES ultrafiltration membranes

5.3 Destructive Testing and In-line Testing

Destructive characterization methods include those tests in which the samples goes under a permanent irreversible modification during testing and the membrane can not be reused for ultrafiltration. These tests are suitable mainly for membrane autopsy analysis or laboratory scale study of membranes and can not be applied as in-line or as routine tests in industry to judge the health of membrane. The destructive testing performed in this research included DMA, TGA, tensile testing, colour measurement, FESEM imaging and EDS analysis, FTIR-ATR, LLDP, contact angle, liquid dispersion test, and zeta potential. Since these tests are done directly on membranes, the membrane element has to be opened to cut out membrane samples on which to perform the tests.

Only a handful of characterization tests can be practically used in industry as routine or online monitoring test. These tests do not involve direct testing on membrane. These tests include monitoring the flow or separation properties of membrane which can be done by flux measurements and feed, permeate, and retentate analysis. The tests performed in this research which can be used for in-line testing are clean water flux test, membrane throughput test, SEC and gel electrophoresis analysis.

The clean water flux test is routinely used in industry to judge the cleaning efficiency of the cleaning regime followed. It was noticed that the water flux increased with hypochlorite degradation but the experiment was performed on new membranes which were not fouled regularly by ultrafiltration of whey. In actual processes, clean water flux may depend on both degradation and permanent fouling of membranes. Being a compound effect of the two phenomena, the water flux test can not be used by its own as a routine test in industry to judge the degradation of the membrane. Online UV absorption monitoring of the permeate stream can give an indication of amount of protein passing through the membrane. Although it can not tell about the type or amount of each protein passing through the membrane, it can provide an easy online method which can give a fair indication of extent of degradation of membranes.

UV absorption monitoring can be coupled to routine SEC analysis on permeate and retentate stream with target proteins (e.g., α-lactalbumin and β-lactoglobulin in case of ultrafiltration of whey). Regular monitoring of the amount of target protein leakage through the membrane can give a good estimation of membrane life. Gel electrophoresis experiment can also be applied as a routine test to check the type of protein leakage and to support the SEC results.

There are few other characterization techniques possible, which can be used to gain better understanding of degradation of membrane. None of these techniques were used in this work. Atomic force microscopy (AFM) can be used to analyse the change in surface roughness with hypochlorite exposure. X-ray photoelectron spectroscopy (XPS) can be useful to examine PES polymer composition before and after hypochlorite exposure to identify and quantify surface changes. Gel permeation chromatography (GPC) can be used to investigate the change in molecular weight of PES with hypochlorite exposure. It may support the possibility of chain scission in the PES backbone causing a decrease in the molecular weight of PES. High-performance liquid chromatography (HPLC) can be another option, instead of SEC, to perform protein analysis on the permeate stream.

5.4 Characterization Regimes

On the basis of current research, the following characterization regime can be used in industry for judging the degradation condition of membrane.

1. Clean water flux as a regular monitoring test (a sudden increase in water flux can be a indication of the physical break down of membrane)
2. Online UV absorption measurement for the permeate stream (to give indication of total protein leaked through the membrane)
3. SEC/HPLC analysis of permeate and retentate streams as a routine test which can be performed after specific time period depending on the condition of membrane (to give amount of target protein leakage).

4. Gel electrophoresis test also as a routine test, which can be performed after a specific time period, to analyse the quality of protein leakage in the permeate stream.

An autopsy analysis should not only tell about physical and chemical condition of membrane but also give information about separation properties of the membrane to judge the overall working capabilities of the membrane. The following autopsy regime can be followed to gain a comprehensive knowledge of the membrane life (in terms of degradation).

1. Physical observation (check for surface cracks or roughness)
2. FESEM imaging with EDS (or XPS) analysis
3. Liquid absorption test
4. FTIR-ATR analysis
5. Water-methanol-water test
6. Membrane throughput experiment
7. SEC (or HPLC) analysis and gel electrophoresis of whey permeate.

Chapter 6 Conclusions and Future Work

A number of conclusions have been made in the last two chapters. This chapter presents the main conclusions drawn from this research work.

6.1 Stability of Hypochlorite Solution

The hypochlorite stability was directly related to the initial pH of the solution at a given temperature and chlorine concentration. Stability of the solution increased with increased initial pH of the solution. Solution stability of the solution for various pH values was as follow: pH 7< pH 8< pH 9< pH 10< pH 11< pH 12. pH 7 and 8 solutions were highly unstable and control of the chlorine concentration and pH was difficult so a range from initial pH 9 to 12 was used in the experiment.

6.2 Characterization Methods

6.2.1 Dynamic Mechanical Analysis

The dynamic mechanical analysis experiment was able to differentiate between the PES and polyolefin layers of the membrane in terms of glass transition temperature but failed to detect any change in visco-elastic properties of hypochlorite degraded membranes as compared to new membranes. The whole experiment indicated that the hypochlorite degradation is a surface phenomenon.

6.2.2 Thermo Gravimetric Analysis

Thermo gravimetric analysis confirmed that the hypochlorite degradation affected the thermal degradation behaviour of the PES layer in the membrane. No change in the thermal degradation properties of the backing layer was noticed. This effect was only detected at the high exposure time of 25,000 ppm days. No change was detected in 10,000 ppm-day hypochlorite exposed ultrafiltration membrane samples which indicated that degradation increased with exposure

time. The lowering of the thermal degradation temperature for the PES layer was linked to decrease in the molecular mass of PES by chain scission during the ageing process. TGA also showed that pH 12 hypochlorite treated membranes experienced a smaller change in thermal degradation behaviour as compared to pH 9 hypochlorite treated samples. It indicated that pH plays an important role in hypochlorite degradation behaviour of membrane. This effect was further confirmed by the colour measurement experiment which showed that hypochlorite degradation leads to formation of products (on the surface of membrane) which are more susceptible to thermal oxidation.

6.2.3 Tensile Testing

Tensile testing of ultrafiltration membranes (Koch) and their backing layer revealed that the tensile properties of the ultrafiltration membrane were dominated by the backing layer due and it was difficult to detect any change in the tensile properties of PES layer. Tensile testing of Sterlitech membranes showed a significant decrease in tensile strength and yield strength (in comparison to new membranes) for pH 12 and 9, 10,000 ppm-day hypochlorite degraded samples. The decrease in tensile properties was higher in pH 9 treated samples as compared to pH 12 treated samples which confirmed that degradation rate depends directly on hypochlorite solution pH.

6.2.4 FESEM Imaging and EDS Analysis

FESEM imaging showed surface pit formation and cracking for pH 9 and 10 hypochlorite treated ultrafiltration membrane samples. Pits were observed in pH 9 samples for exposure times of 5,000 ppm-days to 25,000 ppm-days. No pits were detected in pH 11 and 12 degraded samples even at the high exposure time of 25,000 ppm-days which indicated that the hypochlorite degradation rate increased with decrease in hypochlorite pH. The pit formation was thought to be linked to surface oxidation of PES layer which increased the surface roughness and produced surface defects which ultimately led to formation of localised pits. The size and density of pits formed increased with increase in exposure time.

FESEM imaging did not detect any change in the backing layer of the membrane. It showed that degradation increased with increase in exposure time. EDS analysis detected presence of chlorine on the surface without any trace of sodium for all the hypochlorite degraded samples. This indicated that degradation reaction is a surface bound reaction involving chemical bonding of the chlorine on the surface of PES layer.

6.2.5 FTIR-ATR

FTIR-ATR experiments showed an increase in the surface roughness of the PES layer (detected as decreases in absorption peaks) for all the hypochlorite degraded ultrafiltration membrane samples. The surface roughness showed a clear trend as follows: pH 9 ≥ pH 10 ≥ pH 11 ≥ pH 12. Also for the same pH the surface roughness increased with exposure time. FTIR-ATR was able to differentiate samples on the basis of both hypochlorite pH and exposure time. From further peak analysis it was concluded that, at all the hypochlorite pH values, the degradation followed the same degradation mechanism and the difference was only of degradation rate. A new peak formation at 1034 cm^{-1} was detected which assigned to sulfonic acid group. This new peak confirmed that, during hypochlorite exposure, PES experienced a chain scission at the sulphur position leading to product which has sulfonic acid terminal.

6.2.6 Contact Angle and Liquid Absorption Test

The contact angle experiment indicated that the surface-liquid interaction changed with hypochlorite degradation but failed to detect any trend which could be linked to pH or exposure time for hypochlorite treatment. The rough and highly porous surface of new and degraded membranes limited the accuracy of contact angle measurement. The absorption of 20% w/w methanol solution (aq) was significantly increased with decrease in hypochlorite pH. It was attributed to changes in membrane surface-liquid interactions and formation of surface pits as observed in FESEM analysis. An increase in absorption for pH 11 and 12 treated

samples was observed as compared to a new membrane which indicated that membrane was not immune to degradation even at the higher pH of 12.

6.2.7 Zeta Potential

Zeta potential measurement showed that the ultrafiltration membrane was negatively charged at neutral pH. It also detected a drop in the isoelectric pH with hypochlorite degradation but was not able to detect a clear trend which could explain the effect of hypochlorite pH on the surface charge of the membrane.

6.2.8 LLDP

Compression testing confirmed that membranes compressed significantly in the pressure range used for LLDP testing (1-10 bar) and LLDP permeance values must be corrected to compensate for the compression effect. The LLDP experiment failed to give any meaning full pore size distribution within tested pressure range. Also the effect of alcohols on the flux values is unknown (as observed in water-alcohol-water flux measurements) and possibly not measureable in isolation from interfacial effects which puts uncertainty on the validity of the flux data obtained for LLDP.

6.2.9 Cross-flow Flux Measurements

The clean water flux experiment showed a significant increase in water flux in hypochlorite degraded samples as compared to new membranes. The increase in water flux was more for pH 9 as compared to pH 12 hypochlorite degraded samples. It was believed to be directly linked to increase in porosity of degraded membrane due to surface pitting. The water-methanol-water flux test indicated that the effect of PES-methanol interaction decreased with increase in hypochlorite degradation. It may be linked to a change in surface-methanol interaction inside the pores, due to PES cleavage. At extreme degradation it was found that methanol treatment did not produce any change post water flux. Surface pitting of membrane produced large holes minimising the effect of methanol-PES interactions. It was concluded that the water-alcohol-water flux

test can be a unique non-destructive test which could provide a good indication of degradation of a membrane.

6.2.10 Protein Separation Test

The membrane throughput test showed that protein leakage through membranes increased with an increase in exposure time and/or decrease in hypochlorite exposure pH. The flux values measured for ultrafiltration of whey using degraded membranes indicated that fouling of the membrane increased in degraded samples as compared to new membranes resulting a significant fall in permeate flux. It was concluded that the increase in surface fouling of membranes was due to a change in membrane surface-liquid interactions caused by hypochlorite exposure. Size exclusion chromatography analysis confirmed that protein leakage was mainly α-lactalbumin. Also β-lactoglobulin leakage was also detected more clearly by SDS-PAGE gel electrophoresis. Protein separation test gave a clear picture that hypochlorite degradation of membrane results in loss of valuable proteins in permeate stream and an increase in surface fouling. This test also confirmed that α-lactalbumin and β-lactoglobulin leakage was directly linked with hypochlorite pH and exposure time.

6.3 Hypochlorite Disinfection Experiment

The hypochlorite disinfection experiment carried out directly on the membrane surface failed to show a significant number of microbial colonies by the plate count method which indicated poor microbial loading for all the samples. It was concluded that the disinfection test should be done directly on concentrated microbial cultures rather than on microbes loaded onto a flat membrane. The disinfection test done directly on microbial culture showed ~2.5 log reduction in microbial population for all the hypochlorite exposure pH values. Though it showed the disinfection effect, it was not able to show the difference between different hypochlorite exposure pH values. It was concluded that, above pH 10, hypochlorite solution pH does not play a significant role in the disinfection rate

and resulted in a similar log reduction for all the exposure pH values, i.e. 10.5, 11, 11.5 and 12. Further studies are required to confirm this effect.

6.4 Future Work

6.4.1 Chemistry of Degradation Mechanism

To confirm the proposed degradation mechanism a detailed chemical study of the reaction mechanism is needed. This study might include reacting hypochlorite solution at a fixed pH and chlorine concentration with simpler compounds, e.g., diphenyl sulfonates which resemble the basic unit of PES in structure. After completion of the reaction separation, identification and quantification of products will be required and accordingly the reaction mechanism can be confirmed. Further study of the reaction rate with change in hypochlorite pH is also essential for a complete degradation study.

6.4.2 Testing of Proposed Characterization Regimes

The study was mainly done on new membranes which did not experience the separation conditions and regular fouling of the surface that the membranes would face in industry. It would be interesting to do autopsy analysis on membranes degraded in an industrial separation process. The experiments will include autopsy analysis of membrane (as per proposed characterization regime) on membrane samples obtained from industry after a fixed time period of use to try to judge the degradation age of the membrane accordingly.

A characterization regime has been proposed which could be applied for online evaluation of membrane condition (in terms of degradation) in industry (Section 5.3). An industrial study can be done by online routine testing as specified in proposed regime over a specific time period, e.g., a milk season. Analysis of the data may give a mapping of degradation of the membranes.

6.4.3 Effect of Hypochlorite pH on Microbial Disinfection

The disinfection test on centrifuged microbial culture was able to produce a reasonable log reduction. A more detailed study is needed with a broad range of hypochlorite pH from pH 7 to 12. Broad pH range may differentiate the disinfection effect of hypochlorous acid and hypochlorite ions on microbes. Also the disinfection study could be done on a target microorganism rather than mixed culture which will provide better control of microbial growth and detection by plate count method.

6.4.4 Industrial Scale Optimization of Hypochlorite Dosing Process

In industry, hypochlorite is dosed into the alkali rinse which requires a dosing time that depends on the size of ultrafiltration unit. Also, in the initial stage of dosing, a fall in hypochlorite concentration is experienced due to the chlorine demand of the system and more hypochlorite is dosed until a constant target concentration is attained. Once the target concentration is achieved the membranes are further exposed to hypochlorite for 20 minutes to achieve the desired sterility level. The whole disinfection cycle, from the start of dosing to discharge of hypochlorite, results in 2-3 times higher hypochlorite exposure of the membranes than actually needed. An industrial study is needed for more efficient hypochlorite dosing with the aim of reducing the disinfection cycle time while maintaining the sterility level required.

References

Abaticchio P., Bottino A., Camera Roda G., Capannelli G., Munari S., Characterisation of ultrafiltration polymeric membranes, Desalination 78 (1990) 235-255.

Ageno M., Frontali C., Viscosity Measurements of Alcohol-Water Mixtures and the Structure of Water, in: Proceedings of the National Academy of Sciences of the United States of America, 57 (4) (1967) 856-860

Allie Z., Jacobs E.P., Maartens A., Swart P., Enzymatic cleaning of ultrafiltration membranes fouled by abattoir effluent, Journal of Membrane Science 218 (2003) 107–116.

Almécija M. C., Ibáñez R., Guadix A., Guadix E. M., Effect of pH on the fractionation of whey proteins with a ceramic ultrafiltration membrane, Journal of Membrane Science 288 (1-2) (2007) 28-35.

Amy G. L., Cho J., NOM Rejection by, and Fouling of, NF and UF membranes, AWWA Research Foundation, American Water Works Association, USA, (2001) 9-10.

Annual Review, Fonterra Co-operative Group Limited, NZ, (2008) 21.

Arkhangelsky E., Kuzmenko D., Gitis V., Impact of chemical cleaning on properties and functioning of polyethersulfone membranes, Journal of Membrane Science 305 (2007) 176–184.

Atra R., Vatai G., Bekassy-Molnar E., Balint A., Investigation of ultra- and nanofiltration for utilization of whey protein and lactose, Journal of Food Engineering 67 (3) (2005) 325-332.

Baker R. W., Membrane Technology and Applications, 2nd ed., John Wiley and Sons Ltd, England, 2004.

Bartlett M., Bird M. R., Howell J. A., An experimental study for the development of a qualitative membrane cleaning model, Journal of Membrane Science 105 (1-2) (1995) 147-157.

Bartnikas R., Engineering Dielectrics, Electrical Properties of Solid Insulating Materials: Measurement Techniques, ASTM International, Baltimore, Md, USA, II B (1987) 373.

Bégoin L., Rabiller-Baudry M., Chaufera B., Hautbois Marie-Christine, Doneva T., Ageing of PES industrial spiral-wound membranes in acid whey ultrafiltration, Desalination 192 (2006a) 25–39.

Bégoin L., Rabiller-Baudry M., Chaufera B., Hautbois Marie-Christine, Doneva T., Methodology of analysis of a spiral-wound module: Application to PES membrane for ultrafiltration of skimmed milk, Desalination 192 (1-3) (2006b) 40-53.

Belfer S., Fainchtain R., Purinson Y., Kedem O., Surface characterization by FTIR-ATR spectroscopy of polyethersulfone membranes-unmodified, modified and protein fouled, Journal of Membrane Science 172 (1-2) (2000) 113-124.

Belfort, G., Davis, R. H., Zydney, A., Journal of Membrane. Science 96 (1-2) (1994) 1-58.

Bershtein V. A., Pogodina T.Ye., Yegorova L.M., Nikitin V.V., Defects in the surface layer and the strength of stretched polyamide, Polymer Science U.S.S.R., 20 (3) (1978) 654-660.

Birley A. W., Scott M. J., Plastics Materials: Properties and Applications, Leonard Hill, Glasgow, UK, (1982) 38.

Black J., Hastings G. W., Handbook of biomaterial properties, Chapman and Hall, London, UK, (1998) 283-84.

Blanpain-Avet P., Fillaudeau L., Lalande M., Investigation of mechanisms governing membrane fouling and protein rejection in the sterile microfiltration of beer with an organic membrane, Transactions of the Institution of Chemical Engineers 77 (C) (1999) 75-89.

Bohner H. F., Bradley Jr. R. L.**,** Effective cleaning and sanitizing of polysulfone ultrafiltration membrane systems , Journal of Dairy Science 75 (3) (1992) 718-724 .

Bolong N., Ismail A.F., Salim M.R, Rana D., Matsuura T., Development and characterization of novel charged surface modification macromolecule to polyethersulfone hollow fiber membrane with polyvinylpyrrolidone and water, Journal of Membrane Science, 331 (1-2) (2009) 40-49.

Boufford, T., Making the Right Choice –Sanitizers, Ecolab, Inc., Food & Beverage Div., St. Paul, MN., USA, 1996.

Boussu K., Belpaire A., Volodin A., Van Haesendonck C., Van der Meeren P., Vandecasteele C., Van der Bruggen B., Influence of membrane and colloid characteristics on fouling of nanofiltration membranes, Journal of Membrane Science 289 (1-2) (2007) 220-230.

Boussu K., Van der Bruggen B., Volodin A., Van Haesendonck C., Delcour J. A., Van der Meeren P., Vandecasteele C. , Characterization of commercial nanofiltration membranes and comparison with self-made polyethersulfone membranes, Desalination 191 (1-3) (2006) 245-253.

Brydson J. A., Plastics materials, 6th ed., Butterworth-Heinemann, Oxford, UK, (1995) 580.

Calvo J. I, Bottino A., Capannelli G., Hernández A., Pore size distribution of ceramic UF membranes by liquid–liquid displacement porosimetry, Journal of Membrane Science 310 (2008) 531–538.

Calvo J. I, Bottino A., Capannelli G., Hernández A., Comparison of liquid–liquid displacement porosimetry and scanning electron microscopy image analysis to characterise ultrafiltration track-etched membranes, Journal of Membrane Science 239 (2004) 189–197.

Capannelli G., Becchi I., Bottino A., Moretti P., Munari S., Computer driven porosimeter for ultrafiltration membranes, Studies in Surface Science and Catalysis 39 (1988) 283-294.

Capannelli G., Vigo F. and Munari S., Ultrafiltration membranes – characterisation methods, Journal of Membrane Science 15 (1983) 289-313.

Causserand C., Rouaix S., Lafaille J.P., Aimar P., Ageing of polysulfone membranes in contact with bleach solution: Role of radical oxidation and of some dissolved metal ions, Chemical Engineering and Processing 47 (2008) 48–56.

Charrier J. M., Polymeric Materials and Processing: Plastics, Elastomers, and Composites, Hanser Publishers; New York, USA, (1991) 127.

Chen V., Fane A. G., Fell C. J. D., The use of anionic surfactants for the reducing fouling of ultrafiltration membranes: their effects and optimization, Journal of Membrane Science 67 (1992) 249–261.

Cheryan M., Ultrafiltration and Microfiltration Handbook, Technomic Pub. Company, Pennsylvania, USA, 1998.

Choo K.-H., Lee, C.-H. , Understanding membrane fouling in terms of surface free energy changes, Journal of Colloid and Interface Science 226 (2) (2000) 367-370.

Choo K.-H., Lee, C.-H. , Membrane fouling mechanisms in the membrane-coupled anaerobic bioreactor, Water Research 30 (8) (1996) 1771–1780.

Chung T. S., Teoh S. K., The ageing phenomenon of polyethersulphone hollow fibre membranes for gas separation and their characteristics, Journal of Membrane Science 152 (1999) 175-188.

Clark W. M., Bansal A., Sontakke M., Ma Y. H., Protein adsorption and fouling in ceramic ultrafiltration membranes Journal of Membrane Science 55 (1-2) (1991) 21-38.

Clescerl LS, Greenberg AE, Eaton AD (eds.), Standard Methods for Examination of Water and Wastewater, 20th ed., American Public Health Association, 1999.

Cohen N. S., Odlyha M., Foster G.M., Measurement of shrinkage behaviour in leather and parchment by dynamic mechanical thermal analysis, Thermochimica Acta 365 (2000) 111-117.

D'Souza N.M., Mawson A. J., Membrane cleaning in the dairy industry: A review, Critical Reviews in Food Science and Nutrition 45 (2005) 125–134.

Dairy Management Inc, Opportunities of membrane filtration of milk, Innovations in Dairy: Dairy Industry Technology Review, (2000) 1-6.

Daufin G., Escudier J.P., Carrére H., Béarot S., Fillaudeau L. and Decloux M., Recent and emerging applications of membrane processes in the food and dairy industry, Trans IChemE 79 (C) (2001) 89-102.

Daufin G., Merin U., Kerherve F. L., Labbe J. P., Quemerais A., Bousser C., Efficiency of cleaning agents for an inorganic membrane after milk ultrafiltration, Journal of Dairy Research 59 (1) (1992) 29-38.

Delgado A.V., González-Caballero F., Hunter R.J., Koopal L.K., Lyklema J., Measurement and interpretation of electrokinetic phenomena, Journal of Colloid and Interface Science 309 (2) (2007) 194-224.

Ehrenstein G. W., Riedel G., Trawiel P., Thermal Analysis of Plastics: Theory and Practice, Hanser Verlag, Munich, Germany, 2004

Elias Hans-G., Macromolecules, 2nd ed., Plenum Press, New York, USA, (1984) 959.

Erbe F., The determination of pore distributions according to sizes in filters and ultrafilters, Kolloid-Z 63 (1933) 277-285.

Evan P. J., Bird M. R., Solute-membrane fouling interactions during the ultrafiltration of black liquor tea, Food and Bioproducts Processing 84 (4) (2006) 292-301

Fane, A.G., An overview of the use of microfiltration for drinking water and waste water treatment. Proc., Microfiltration for Water Treatment Symposium '94, 25–26 August, Irvine, Califonia, (1994) 3.

Fariaa R., Duncan J. C. and Brereton R. G., Dynamic mechanical analysis and chemometrics for polymer identification, Polymer Testing 26 (2007) 402–412.

Fernández-Blázquez J. P., Bello A. and Pérez E., Dynamic mechanical analysis of the two glass transitions in a thermotropic polymer, Polymer 46 (2005) 10004–10010.

Gady B. L., Measurement of Interaction Forces between Micrometer-Sized Particles and Flat Surfaces using an Atomic Force Microscope, PhD thesis, Purdue University, USA, (1996) 90-99.

Gaudichet-Maurin E., Thominette F., Ageing of polysulfone ultrafiltration membranes in contact with bleach solutions, Journal of Membrane Science 282 (2006) 198–204.

Gauthier, S. F., Pouliot, Y., Maubois, J. L., Growth factors from bovine milk and colostrum: composition, extraction and biological activities. Lait 86 (2006) 99–125.

Ghosh R., Protein bioseparation using ultrafiltration: theory, applications and new developments, Imperial College Press, London, UK, (2003) 33.

Gijsbertsen-Abrahamse A.J., Boom R. M., van der Padt A., Why liquid displacement methods are sometimes wrong in estimating the pore-size distribution. AIChE Journal 50 (7) (2004) 1364-1371.

Groleau, P. E., Lapointe, J. F., Gauthier, S. F., Pouliot, Y., Fractionation of whey protein hydrolysates using nanofiltration membranes, in: Advances in fractionation and separation: Processes for novel dairy applications:

Bulletin 389, Brussels, Belgium: International Dairy Federation (2004) 85–91.

Guan R., Zou H., Lu D., Gong C., Liu Y. , Polyethersulfone sulfonated by chlorosulfonic acid and its membrane characteristics, European Polymer Journal 41 (7) (2005) 1554-1560.

Hall, G. M., Membrane filtration, Fish Processing Technology, Blackie Academic and Professional, New York, USA, (1992) 230– 233.

Harper C. A., Handbook of Plastics, Elastomers, and Composites, McGraw-Hill Professional, USA, (2002) 61.

Harper C. A., Petrie E. M., Plastics Materials and Processes: A Concise Encyclopedia, John Wiley and Sons, Hoboken, New Jersey, USA, (2003) 447.

Henis, J. M. S., Tripodi, M. K., Composite hollow fiber membranes for gas separation: the resistance model approach, Journal of Membrane Science 8 (1981) 233.

Henkel Corporation, The Loctite Design Guide for Bonding Plastics-Supplier Design Guide (LT2197), 3 (2005) 48.

Henning, D. R., Baer, R. J., Hassan, A. N., Dave, R., Major advances in concentrated and dry milk products, cheese and milk fat-based concepts, Journal of Dairy Science 89 (2001) 179–1188.

Hobman, P. G., Ultrafiltration and manufacture of whey protein concentrates, in: Zadow J. G. (Ed.), Whey and Lactose Processing, Elsevier Applied Science, NY, USA, (1992) 195–230.

Horton, B. S., Commercial utilization of minor milk components in the health and food industry. Journal of Dairy Science 78 (1995) 2584–2589.

Hubbard A. T., Encyclopedia of surface and colloid science, CRC Press, NY, USA, 1 (2002) 1213-1216.

IC Controls, Chlorine theory and measurement, Technical notes 8 (2) (2005) 1-2. [Online accessed on 30th April 2009, http://www.iccontrols.com/files/8-2.pdf].

Ionics Inc, Membrane technology benefits the food processing industry, Filtration & Separation 41 (8) (2004) 32-33.

Jucker C., Clark M., Adsorption of aquatic humic substance on hydrophobic ultrafiltration membranes, Journal of Membrane science 97 (1994) 37-52.

Jung Y-J, Kiso Y., Yamada T., Shibata T., Lee T-G., Chemical cleaning of reverse osmosis membranes used for treating wastewater from a rolling mill process, Desalination 190 (1-3) (2006) 181-188.

Kazemimoghadam M., Mohammadi T., Chemical cleaning of ultrafiltration membranes in the milk industry, Desalination 204 (2007) 213–218.

Kelly P. M., Horton B.S., Burling H., in: IDF Special issue - New Applications of Membrane Processes, International Dairy Federation, Bulletin No. 9201, Brussels, Belguim, (1992) 130-140.

Keusch S., Haessler R., Influence of surface treatment of glass fibre on the dynamic mechanical properties of epoxy resin composites, Composites: Part A 30 (1999) 997–1002.

Kim K. J., Fane A.G., Ben Aim R., Liu M. G., Jonsson G., Tessaro I. C., Broek A. P., Bargeman D., A comparative study of techniques used for porous membrane characterization: pore characterization, Journal of Membrane Science 87 (1994) 35-46.

Kim S., Park N., Lee S., Cho J., Membrane characterizations for mitigation of organic fouling during desalination and wastewater reclamation, Desalination 238 (1-3) (2009) 70-77.

Kricheldorf H. R., Nuyken O., Swift H., Handbook of Polymer Synthesis, 2nd ed., CRC Press, NY, USA, (2004) 146.

Kroschwitz J. I., Concise Encyclopedia of Polymer Science and Engineering, John Wiley and Sons, NY, USA, (1990) 886.

Kwon Y-K., Leckie J. O., Hypochlorite degradation of cross linked polyamide membranes: Changes in chemical/morphological properties, Journal of Membrane Science 283 (1) (2006) 21-26.

Lemanski J., Lipscomb G. G., Effect of fiber variation on the performance of countercurrent hollow fiber gas separation modules, Journal of Membrane Science 167 (2000) 241–252.

Li N. N., Fane A. G., Ho W. S. W., Matsuura T., Advanced Membrane Technology and Applications, Wiley-Interscience, Hoboken, New Jersey, USA, (2008) 324.

Liang M., Chen V. Y. T., Chen H-L., Chen W., A simple and direct isolation of whey components from raw milk by gel filtration chromatography and structural characterization by Fourier transform Raman spectroscopy, Talanta 69 (5) (2006) 1269-1277.

Lin Li, Chung D.D.L., Electrical and mechanical properties of electrically conductive polyethersulfone composites, Composites 25 (3) (1994) 215-224.

Lindau J., Jönsson A. –S., Wimmerstedt R., The influence of a low-molecular hydrophobic solute on the flux of polysulphone ultrafiltration membranes with different cut-off, Journal of Membrane Science 106 (1-2) (1995) 9-16.

Lindau J., Jönsson A-S., Cleaning of ultrafiltration membranes after treatment of oily waste water, Journal of Membrane Science, 87 (1-2) (1994) 71-78.

Loeb S., Sourirajan S., Sea water Demineralisation by means of an Osmotic Membrane, Saline Water Conversion – II, Advances Chemistry Series 38, American Chemical Society, Washington DC, USA, (1963) 117-132.

Luss, G., Fouling and cleaning in membrane processes involved in dairy applications, Proceedings of the Whey Products Conference, Chicago, IL, US, 1984.

Ma Z., Kotaki M., Ramakrishna S., Surface modified nonwoven polysulphone (PSU) fiber mesh by electrospinning: A novel affinity membrane, Journal of Membrane Science 272 (2006) 179–187.

Maartens A., Swart P, Jacobs E. P., Membrane pre-treatment: A method for reducing fouling by natural organic matter, Journal of Colloid and Interface Science 221 (2000) 137–142.

Maartens A., Swart P, Jacobs E. P., Feed-water pre-treatment: methods to reduce membrane fouling by natural organic matter, Journal of Membrane Science 163 (1999) 51–62.

Maillart, P., Ribadeau Dumas, B., Preparation of β-lactoglobulin and β-lactoglobulin-free proteins from whey retentate by NaCl salting out at low pH, Journal of Food Science 53 (1988) 743.

Marcilla A., Gómez-Siurana A., Odjo A. O., Navarro R., Berenguer D., Characterization of vacuum gas oil–low density polyethylene blends by thermogravimetric analysis, Polymer Degradation and Stability 93 (3) (2008) 723-730.

Mathew Aji P., Packirisamy S., Thomas S., Studies on the thermal stability of natural rubber/polystyrene interpenetrating polymer networks: thermogravimetric analysis, Polymer Degradation and Stability 72 (3) (2001) 423-439.

Matthiasson E., The role of macromolecular adsorption in fouling of ultrafiltration membranes, Journal of Membrane Science 16 (1983) 23-36.

Maubois, J. L., Oliver, G., IDF special issue -New applications of membrane processes, International Dairy Federation, Brussels, Bulletin 9201, Belgium, (1992) 15-22.

Mayank Omprakash, Nigam M. O., Bansal B., Chen X. D, Fouling and cleaning of whey protein concentrate fouled ultrafiltration membranes, Desalination 218 (2008) 313–322.

McDonough, F.E. and Hargrove, R.E., Sanitation of reverse osmosis/ ultrafiltration equipment, Journal of Milk and Food Technology, 35 (2) (1973) 102–106.

Mehra, R. K., Donnely, W. J., Fractionation of whey protein components through a large pore size, hydrophilic, cellulosic membrane, Journal of Dairy Research, 60 (1993) 89-97.

Mehra, R., Kelly, P. M, Whey protein fractionation using cascade membrane filtration, in Processes for Novel Dairy Applications, Advances in Fractionation and Separation: Bulletin 389, International Dairy Federation, Brussels, Belgium (2004) 40–44.

Menard K. P., Dynamic Mechanical Analysis: A Practical Introduction, CRC Press, Boca Raton, FL, 2008.

Mittelman, M.W., Biological fouling of purified-water systems: part 3, treatment, Microcontamination 4 (1) (1986) 30-40.

Morel G., Ouazzani N., Graciaa A., Lachaise J., Surfactant modified ultrafiltration of nitrate ion removal, Journal of Membrane Science 134 (1997) 47–57.

Morison K.R., A comparison of liquid–liquid porosimetry equations for evaluation of pore size distribution, Journal of Membrane Science 325 (1) (2008) 301-310.

Mossoba M. M., Spectral Methods in Food Analysis: Instrumentation and Applications, CRC Press, Boca Raton, Florida, USA, (1999) 399.

Mueller P., Paulson D., Microbial control and sanitization of membrane-based pure water treatment systems, Filtration News, 1997.

Mufioz-Aguado M.J., Wiley D.E., Fane A.G., Enzymatic and detergent cleaning of a polysulfone ultrafiltration membrane fouled with BSA and whey, Journal of Membrane Science 117 (1996) 175-187.

Mulder M., Basic Principle of Membrane Technology, Kluwer Academic Publishers, Dordrecft, Netherlands, 1997.

Munari S., Bottino A., Moretti, Capannelli G., Becchi I., Permoporometric study on ultrafiltration membranes, Journal of Membrane Science 41 (1989) 69-86.

Muthukumaran S., Yang K., Seuren A., Kentish S., Kumar A. M., Stevens G. W., Grieser F., The use of ultrasonic cleaning for ultrafiltration membranes in the dairy industry, Separation and Purification Technology 39 (2004) 99–107.

Nakatsuka S., Michaels A. S., Transport and separation of proteins by ultrafiltration through sorptive and non-sorptive membranes, Journal of Membrane Science 69 (3) (1992) 189-211.

New Zealand Dairy and Products Annual Dairy Industry Report 2008, Gain report number: NZ8026, USDA Foreign Agricultural Service, USA, (2008) 3-4.

Neyestani T. R., Djalali M., Pezeshki M., Isolation of α-lactalbumin, β-lactoglobulin, and bovine serum albumin from cow's milk using gel filtration and anion-exchange chromatography including evaluation of their antigenicity, Protein Expression and Purification 29 (2) (2003) 202-208.

Nigam M. P., Bansal B., Chen X. D., Fouling and cleaning of whey protein concentrate fouled ultrafiltration membranes, Desalination 218 (1-3) (2008) 313-322.

Nunes S. P., Peinemann K. V., Membrane Technology: In the Chemical Industry, Wiley-VCH, Weinheim, Germany, (2006) 25.

Nyström M., Pihlajamäki A., Ehsani N., Characterization of ultrafiltration membranes by simultaneous streaming potential and flux measurements, Journal of Membrane Science 87 (3) (1994) 245-256.

Nyström M., Zhu H., Characterization of cleaning results using combined flux and streaming potential methods, Journal of Membrane Science 131 (1-2) (1997) 195-205.

Pavlova S., Study on the cleaning of new ultrafiltration spiral-wound modules to prevent membrane fouling (including biological fouling), Desalination 172 (2005) 267-270.

Perkin Elmer, Chapter 1, DMA Measurement and Analysis, Pyris Diamond DMA, Dynamic Mechanical Analyser, Measurement Procedure, Perkin Elmer, Massachusetts, USA, (2002) 1-12.

Persson A., Jönsson A. –S., Zacchi G., Transmission of BSA during cross-flow microfiltration: influence of pH and salt concentration, Journal of Membrane Science 223 (1-2) (2003) 11-21

Pieracci J., Crivello J. V., Belfort G., Photochemical modification of 10 kDa polyethersulfone ultrafiltration membranes for reduction of biofouling, Journal of Membrane Science 156 (2) (1999) 223-240.

Pouliot Y., Membrane processes in dairy technology—From a simple idea to worldwide panacea, International Dairy Journal 18 (2008) 735– 740.

Porter, M. C., Handbook of Industrial Membrane Technology, Noyes Publication, New Jersey, USA, 1990.

Puhan, Z., Standardization of milk protein content by membrane processes for product manufacture, New applications of membrane processes, International Dairy Federation, Bulletin 9201, Brussels, Belgium, (1991) 23–32.

Qin J. J., Oo M. H., Li Y., Development of high flux polyethersulfone hollow fibre ultrafiltration membranes from a low critical solution temperature dope via hypochlorite treatment, Journal of Membrane Science 247 (1-2) (2005) 137-142.

Qin J. J., Wong F. S., Li Y., Liu Y. T., A high flux ultrafiltration membrane spun from PSU/PVP (K90)/DMF/1, 2-propandiol, Journal of Membrane Science 211 (1) (2003) 139-147.

Rabiller-Baudry M, Le Maux M, Chaufer B and Bégoin L, Characterisation of cleaned and fouled membrane by ATR-FTIR and EDX analysis coupled with SEM: application to UF of skimmed milk with a PES membrane, Desalination 146 (2002) 123–128.

Radel, Resins Design Guide, Solvay Advanced polymers, LLC, GA USA, (2004) 23.

Raghi S. E., Zahran R.R, Gebril B.E., Effect of weathering on some properties of polyvinyl chloriderlignin blends, Materials Letters 46 (2000) 332–342.

Ramaswamy S., Alan R. Greenberg A. R., L. Peterson M. L., Non-invasive measurement of membrane morphology via UFDR: pore-size characterization, Journal of Membrane Science 239 (1) (2004) 143-154.

Ratner B. D., Hoffman A .S., Schoen F. J., Lemons J. E., Biomaterials Science: An Introduction to Materials in Medicine, Elsevier Academic Press, California, USA, (2004) 270-271.

Reddy A.V.R., Patel H. R., Chemically treated polyethersulfone / polyacrylonitrile blend ultrafiltration membranes for better fouling resistance, Desalination 221 (1-3) (2008) 318-323.

Ricketts R. T., Lebherz III W. B., Klein F., Gustafson M. E., Flickinger M. C., Application, sterilization and decontamination of ultrafiltration systems for large-scale production of biologocals, in: LeRoith D., Shiloach J., Leahy T. J. (Ed.), Purification of Fermentation Products, ACS Symposium series, American Chemical Society, Washington DC, USA, (1985) 21.

Ricq L., Pierre A., Bayle S., Reggiani J. C., Electrokinetic characterization of polyethersulfone UF membranes, Desalination 109 (3) (1997) 253-261.

Riga A., Collins R., Mlachak G., Oxidative behaviour of polymers by thermogravimetric analysis, differential thermal analysis and pressure differential scanning calorimetry, Thermochimica Acta 324 (1-2) (1998) 135-149.

Robert J. C., Engineering Plastics: A Handbook of Polyarylethers, Taylor & Francis Group, Boca Raton, FL, (1995) 2.

Robinson J. W., Frame G. M., Undergraduate Instrumental Analysis, 6th ed., CRC Press, NY, USA, (2005) 255-256.

Rosenberg M., Current and future application for membrane processes in the dairy industry, Trends in Food Science & Technology 6 (1995) 12-19.

Rouaix S., Causserand C., Aimar P., Experimental study of the effects of hypochlorite on polysulfone membrane properties. Journal of Membrane Science, 277 (2006) 137–147.

Roux S.P., Jacobs E.P., van Reenen A.J., Morkel, Meincken M., Hydrophilisation of polysulphone ultrafiltration membranes by incorporation of branched PEO-block-PSU copolymers, Journal of Membrane Science 276 (2006) 8-15.

Sagripanti J. L., Hughes-Dillon M. K., Stability of five plastics used in medical devices to oxidation produced by copper or iron ions and reducing agents Polymer Degradation and Stability 46 (2) (1994) 241-246.

Salamone J. C., Concise polymeric materials encyclopedia, CRC Press, Boca Raton, Florida, USA, (1998) 841

Sandler S. R., Karo W., X Bonesteel J. A., Pearce E. M., Experiment 15-Thermogravimetric analysis, Polymer Synthesis and Characterization- a Laboratory Manual, Academic Press, San Diego, USA, (1998) 108-119.

Sandy te Poele , van der Graaf J., Enzymatic cleaning in ultrafiltration of wastewater treatment plant effluent, Desalination 179 (1-3) (2005) 73-81.

Sasuga T., Kudoh H., Seguchi T. , High energy ion irradiation effects on polymer materials–Changes in mechanical properties of PE, PSF and PES, Polymer 40 (18) (1999) 5095-5102 .

Scott K., Handbook of Industrial Membrane, Elsevier Advanced Technology, Oxford, U.K., 1995.

Siebert J. W, Lalor A., and Kim S. Y., The Commercial Potential of New Dairy Products from Membrane Technology, Journal of Food Distribution Research 32 (2001) 24-33.

Somasundaram P., Encyclopedia of Surface and Colloid Science, 2nd ed., Taylor and Francis Groups, 5 (2006) 3574.

Song L., Flux decline in cross-flow microfiltration and ultrafiltration: mechanisms and modelling of membrane fouling. Journal of Membrane Science 139 (1998) 183–200.

Sperling L. H., Introduction to physical polymer science, John Wiley and Sons, Hoboken, New Jersey, USA, (2006) 564.

Steen M. L., Hymas L., Havey E. D., Capps N. E., Castner D. G., Fisher E. R., Low temperature plasma treatment of asymmetric polysulfone membranes for permanent hydrophilic surface modification, Journal of Membrane Science 188 (2001) 97–114.

Stropnik Č., Kaiser V., Polymeric membranes preparation by wet phase separation: mechanisms and elementary processes, Desalination 145 (1-3) 2002 1-10.

Susanto H., Balakrishnan M., Ulbricht M., Via surface functionalization by photograft copolymerization to low-fouling polyethersulfone-based ultrafiltration membranes, Journal of Membrane Science 288 (1) (2007) 157-167.

Susanto H., Franzka S., Ulbricht M., Dextran fouling of polyethersulfone ultrafiltration membranes-causes, extent and consequences, Journal of Membrane Science 296 (1-2) (2007) 147-155.

Susanto H., Ulbricht M., Characteristics, performance and stability of polyethersulfone ultrafiltration membranes prepared by phase separation method using different macromolecular additives, Journal of Membrane Science 327 (2009) 125-135.

Susanto H., Ulbricht M., Influence of ultrafiltration membrane characteristics on adsorptive fouling with dextrans, Journal of Membrane Science 266 (1-2) (2005) 132-142.

Sutherland K., Filters and Filtration Handbook 5th ed., Elsevier Ltd, Oxford, U.K., (2008) 184.

Tanimoto, M., Kawasaki, Y.V.N., Shinmoto, H., Dosako, S., Tomizawa, A., European Patent EP 0393 850 A2, 1990.

Thomas G. E., Effect of Sodium Hypochlorite (NaOCl) on the surface energy of UF PES membranes, Dissertation report, Department of Chemical and Process Engineering, University of Canterbury, Christchurch, NZ, 2008.

Thominette F., Farnault O., Gaudichet-Maurin E., Machinal C., Schrotter J. C. , Ageing of polyethersulfone ultrafiltration membranes in hypochlorite treatment, Desalination 200 (2006) 7–8.

Trägårdh, G., Membrane Cleaning, Desalination 71 (1989) 325–335.

Tran-Ha M. H., Wiley D. E. ,The relationship between membrane cleaning efficiency and water quality, Journal of Membrane Science 145 (1) (1998) 99-110.

Ultrason E® and S Luvitec® K, Versatile materials for the production of tailor-made membranes, BASF Aktiengesellschaft, Germany, (2004) 5. URL: http://www.iccontrols.com/files/8-2.pdf

Van der Horst H. C., Timmer J. M. K., Robbertsen T., Leenders J., Use of nanofiltration for concentration and demineralization in the dairy industry: Model for mass transport, Journal of Membrane Science 104 (1995) 205-218.

Wagner J., Practical tips and hints, in: Membrane Filtration Handbook, 2nd ed. Revision 2, Osmonics, Minnetonka, MN, USA, 2001.

Walsra P., Wouters J. T. M., Grurts T. J., Dairy Science and Technology, 2nd ed., CRC Press, Boca Raton, FL, (2006) 431.

Wang L. K., Pereira N. C., Hung Y. T., Handbook of Environmental Engineering, Humana Press, Totowa, New Jersey, USA, (2007) 228.

Wang M., Wu L-G., Zheng X-C., Mo J-X., Gao C-J., Surface modification of phenolphthalein poly(ether sulfone) ultrafiltration membranes by blending with acrylonitrile-based copolymer containing ionic groups for imparting surface electrical properties, Journal of Colloid and Interface Science 300 (1) (2006) 286-292.

Weis A., Bird M. R., Nyström M., The chemical cleaning of polymeric UF membranes fouled with spent sulphite liquor over multiple operational cycles, Journal of Membrane Science 216 (1-2) (2003) 67-79.

Weis A., Bird M. R., Nyström M., Wright C., The influence of morphology, hydrophobicity and charge upon the long-term performance of ultrafiltration membranes fouled with spent sulphite liquor, Desalination 175 (2005) 73-85.

Wenten I. G., Application of crossflow membrane filtration for processing industrial suspensions, PhD thesis, The Technical University of Denmark, 1994.

Wienk I. M., Folkers B., van den Boomgaard T., Smolders C.A., Critical factors in the determination of the pore size distribution of ultrafiltration membranes using the liquid displacement method, Separation Science and Technology 29 (11) (1994) 1433–1440.

Wolff S.H., Zydney A.L., Effect of bleach on the transport characteristics of polysulfone hemodialyzers, Journal of Membrane Science 243 (1-2) (2004) 389–399.

Zall, R. R., On-farm ultrafiltration of milk: The California experience, Milchwissenschaft 42 (1987b) 3–7.

Zator M., Warczok J., Ferrando M., López F., Güell C., Chemical cleaning of polycarbonate membranes fouled by BSA/dextran mixtures, Journal of Membrane Science 327 (1-2) (2009) 59-68.

Zeman L. J., Zydney A. L., Microfiltration and ultrafiltration: principles and applications, M. Dekker, New York, USA, 1996.

Zhu H., Nystrom M., Cleaning results characterized by flux, streaming potential and FTIR measurements, Colloids and Surfaces A: Physicochemical and Engineering Aspects 138 (1998) 309–321.

Zhu L. P., Zhu B K., Xu L., Feng Y. X., Fu Liu, Xu Y. Y., Corona-induced graft polymerization for surface modification of porous polyethersulfone membranes, Applied Surface Science 253 (14) (2007) 6052-6059.

Zularisam A.W., Ismail A.F., Salim M.R., Mimi Sakinah, Hiroaki O., Fabrication, fouling and foulant analyses of asymmetric polysulfone (PSF) ultrafiltration membrane fouled with natural organic matter (NOM) source waters, Journal of Membrane Science 299 (1-2) (2007) 97-113.

Zydney, A. L., Protein separations using membrane filtration: New opportunities for whey fractionation. International Dairy Journal 8 (1998) 243–250

Appendix 1
Testing Procedures for Various Characterization Experiments

Appendix 1.1 DMA Testing Procedure

The following method sequence was followed to test samples on the DMA instrument

1. Turn on the DMA and start the measurement software. There should be no sample in the tension fixture before any further steps.
2. Before each test, run the initialization step which resets load and probe position. For performing DMA under tension mode, the probe position should be set at 0 mm.

Generating Temperature Pre-calibration File

Steps 3 to 8 are for generating pre-calibration file for a specific temperature range in which sample is to be tested

3. Select Pre-calibration if doing a pre-calibration for a temperature program.
4. Insert the radiation shield into the slit of the tension base.
5. Close the furnace and turn on the nitrogen.
6. Click the "Start" button in the software window to start the pre-calibration run.
7. Save the pre-calibration as a method file which can be used each time the sample is tested within the pre-calibrated temperature range.
8. Repeat step 2 before doing sample testing.
9. Set the temperature control to "Normal control mode". Enter the desired temperature program from the saved method file.

Sample Testing Procedure

10. Enter the "Sample condition", i.e. the length, width and thickness of the sample. The standard length of sample in tension mode is 20 mm for a

probe position of 0 mm. The test length can be decreased if the sample is soft or fragile.

11. Enter the name and location of the test file to be saved.
12. Position the sample in the tension attachment as per procedure given in operation manual Perkin Elmer (2002) Sample is clamped at top and bottom, and subjected to an underlying tensile stress to prevent it from buckling during dynamic loading as shown in Figure A1.1

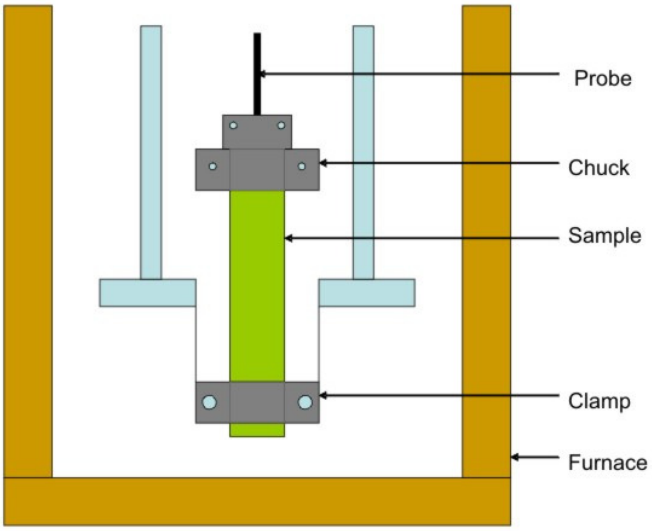

Figure A1.1 Schematic diagram of tension measurement attachment used in DMA

13. Insert the radiation shield into the slit of the tension base.
14. Close the furnace and turn on the nitrogen.
15. Click the “test” button in software window to check the sample is within measurement range. The dot which signifies the sample should be within the two parallel green lines in the “measurement range” window
16. Start the run by clicking “run” button on software window. DMA will automatically record the data and save it into a file. Convert the file into Excel file for data analysis.
17. Turn off the nitrogen and open the furnace for the sample and furnace to cool down. Once the furnace has cooled down remove the sample carefully without disturbing the probe.

Appendix 1.2 TGA Q600 Instructions

Following are the instructions to perform TGA.

1. Wake TGA from sleep mode by pressing touch screen of Q 600.
2. Select AIR or NITROGEN as a purge gas and turn cylinder on half a turn. Make sure there is enough pressure for a run.
3. Computer set-up: open Instrument Explorer, and then click on Q 600 icon to open Thermal Advantage.
4. On the 'Summary " tab, set mode, pan type, sample name and comments. Make a folder in C:\TA\Data\SDT with Operator name (e.g., your initials). Save data into this folder.
5. On the 'Procedure' tab set TEST. It is recommended to use CUSTOM and then use EDITOR to set up the method. Use the 'Post' tab to control cooling features at the end of the run.
6. On the 'Notes' tab, set the operator and the extended text. Set purge gas flow rate to 100 ml/min.
7. Open the furnace using touch screen control panel.
8. Decide to use either platinum or ceramic pans. Carefully place pans on the balance beams. Use tweezers and rest your arm on the support bar. Don't jar the beam arms.
9. Close the furnace using touch screen controls.
10. 'Tare' balance on touch screen.
11. Open furnace and fill the closest pan with sample. Use 10 mg or less. Don't fill pan more than half full. Make sure nothing is hanging over the sides.
12. Close the furnace.
13. Commence experiment using Green button on touch screen.
14. When experiment is finished use "Universal Analysis" to give onset points, weight changes etc.
15. When temp is back to approx 30 ºC, turn off gas supply.
16. Leave Q600 and computer on.

Appendix 1.3 Method for Casting Membranes by Wet Phase Inversion Method

(adapted from Stropnik and Kaiser, 2002; Roux *et al*., 2006)

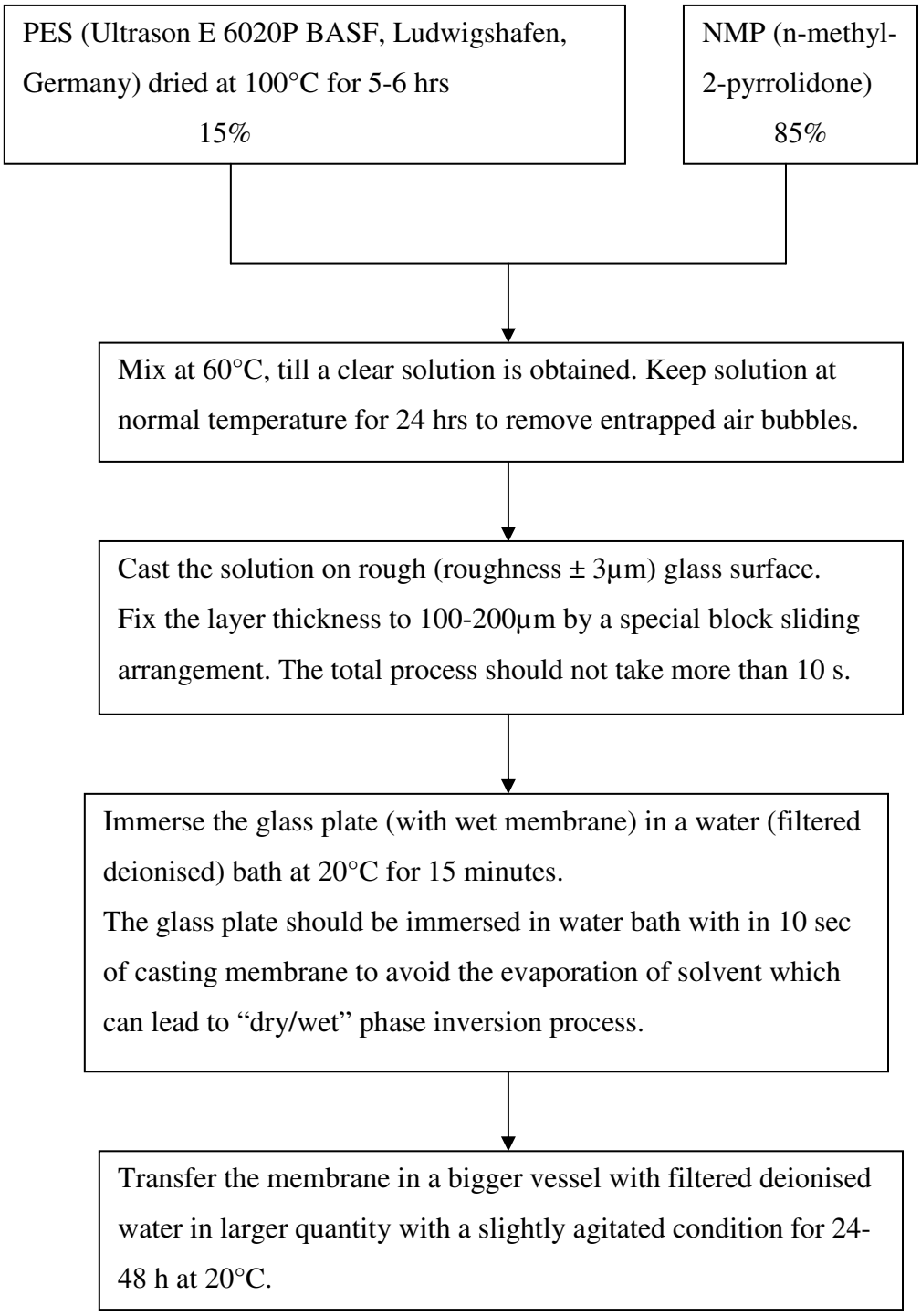

Appendix 1.4 Jeol 7000 FESEM Operating Instructions

Inserting a Specimen

1. Use gloves to handle specimens and holders
2. Check GUN VALVE CLOSE button is lit (front panel column unit).
3. Check exchange chamber buttons
   - HLDR should be off (otherwise you need to remove a specimen)
   - EXCH POSN should be on (otherwise you need to move the stage to the exchange position)
   - If the VENT button is not lit, press and hold briefly.
4. Once the VENT button is lit, open the exchange chamber.
5. Insert the specimen holder into the spring loaded exchange holder – note how much the specimen sticks up above the top of the holder.
6. Close the chamber and press EVAC.
7. Wait for the EVAC light to remain on.
8. The exchange rod is not particularly strong, handle it carefully. Lift the exchange rod slightly and move to the horizontal position. Gently push the rod through the o-ring until the specimen holder engages on the stage. The rod should be nearly fully inserted and the HLDR light should be on.
9. Remove the rod, pulling it fully out before raising to the vertical position.
10. Click on the Stage Specimen Holder Exchange icon. Select the holder type from the following: 12.5 mm, 32 mm, 3WH (SM71040), SM71270
11. Enter the specimen surface offset, i.e. how much the specimen sticks up above the holder if at all.
12. If not tilting the sample, click HOME to move the holder to the normal starting position.
13. Close the Specimen Exchange window.
14. Click on the PVG icon if the Penning Gauge is not already active.
15. Select the instrument control icon.
16. Set the accelerating voltage to 15 kV
17. Click the Instrument Maintenance icon and enter the microscope condition details in the log book.
18. Close the Maintenance window.

19. Set the accelerating voltage.
20. Set probe current to 7 for imaging or 9-13 for EDS.
21. Wait for the vacuum to reach at least 5.14 x 10^{-4} Pa.
22. Press GUN VALVE CLOSE to open the gun valve and turn on the high voltage.
23. Click SEI DETECTOR ON (secondary electron detector).
24. Check scan rotate is off.
25. Check the FREEZE button is off.
26. Press ACB – auto contrast and brightness.
27. Focus the image at low magnification.
28. TIP: If it is hard to locate your specimen, click on WD and set to 40 mm, leave unfocused, you can then reduce the magnification to 10x. It may be useful to note the x and y coordinates of areas of interest. Click on WD and set back to 10 mm.

Moving the Sample

There are several ways to move the sample and keep track of its location.

1. X, Y, Z coordinates and rotation and tilt are indicated at the lower left of the screen. The specimen can be moved by entering new values into the boxes. Care needs to be taken not to enter coordinates that will cause the sample to collide with the final lens or back-scattered electron detector.
2. Use the joystick, rotation can be carried out by twisting the stick.
3. Right click on a feature to move it to the screen centre.
4. Click on arrows which appear when the cursor is positioned near the edge of the screen.

Removing a Specimen

1. Press GUN VALVE CLOSE so that the light comes on.
2. Click the Stage Specimen Holder Exchange icon.
3. Click on EXCHANGE.
4. Once the EXCH POSN is lit, checks EVAC is on and insert the exchange rod to remove the specimen.
5. Withdraw the rod and the HLDR light should go off.
6. Press VENT and wait for the light to stay on.

7. The specimen chamber can now be opened and the holder removed. Remember gloves and that the holder is spring loaded!
8. Close chamber and press EVAC.
9. Record total hours used in the log book

EDS Operation

1. Check the liquid nitrogen dewar is filled and that 1 hour has elapsed since it was filled.
2. If the ready light is not ON, press the START button
3. Click on Analyser Manager and click on Analyser Station
4. Click on the SSM dead-time icon, select monitoring window
5. Click on the SSM BIAS icon set to on.
6. Select a suitable accelerating voltage – over voltage 3 x peak energy.
7. Set probe current 9- 13 so that when collecting a spectrum or mapping, the dead-time is about 30%. Note: The detector time constant is different for mapping and analysis so the probe current depends on whether you are analysing or mapping
8. Select the area to be analysed, adjust focus and brightness/contrast.
9. Click on IMAGE. Once the image is completed, right click on the title and rename.
10. Click Spectrum icon to analyse the whole area or SEQ icon to select areas. Allow the spectrum to grow and then right click Auto Identification. Check all the peaks have been properly identified. The timer indicates when the analysis is complete.
11. If necessary select the file then click on QUANT then OK.
12. Select PRINT PREVIEW and select your preferred options – you can PRINT or EXPORT to word or power point.
13. File SAVE AS to save work.
14. When finished, File/save as.

Appendix 1.5 Design Aspects of LLDP Apparatus

A1.5.1 Membrane Holder

It was decided to design a circular membrane holder as membrane cell to house circular membrane disc of 50 mm in diameter which can handle small volumes of fluids. Although the membrane holder may be used for ultrafiltration of milk and milk products, the main consideration was LLDP characterization. The membrane cell consists of two metal circular plates in which membrane can be sandwiched. Each plate had six equi-distance holes to screw down the bolts. The two plates were to be sealed with an o-ring and pressure necessary for sealing was applied by tightening six bolts with help of torque wrench (40 ft-lbf)

A1.5.1.1 Materials of Construction

Material of Construction for Membrane Holder

Following test conditions were known prior to design of the apparatus

1. Temperature at which experiment was to be conducted: 20°C
2. Internal pressure on membrane holder and sample cylinder: Maximum 50 bar
3. Fluids in contact
    - Water
    - Isobutanol
    - Methanol

On the basis of the experiment conditions stainless steel – grade 316 (UNS 31600) was selected as material for constructing membrane holder and sample cylinders due its good mechanical strength, corrosion resistance and food product compatibility.

Material of Construction for O-ring Sealing

Ethylene – propylene, EPDM was selected as o-ring material due to its compatibility with alcohols and food products. Also it has wide working temperature range of -60 to 150ºC

A1.5.1.2 Design Parameters

Table A1.1 shows the parameters fixed for the design calculation and Table A1.2 shows the parameters calculated. This calculations were done on base of formula obtained from Case 2e, Table 11.2, Formulas for flat circular plate of constant thickness Chapter 11, "Roarks's Formulas for Stress and Strain", ed 7, Young W. C., Budynas R.G., McGraw-Hill, NY, USA, 2002; Page 465.

Table A1.1 Fixed parameter

Internal pressure	Q	5,000,000 Pa
Effective plate radius	R	0.0443 m
Desired whole radius	B	1 mm
Stainless Steel (316) properties		
Maximum Allowable Stress for plates below 38ºC	σ_m	137,900,000 Pa
Poison ratio	v	0.28

Table A1.2 Calculated parameters

Desired plate thickness	t	25 mm
Maximum bending stress	σ_b	11773518 Pa
Safety factor		11.71

A1.5.2 Bolts for Tightening Plates of the Membrane holder

6 bolt design with stainless steel bolts of 12.5 mm in diameter were chosen for tightening the two plates of the membrane holder. An initial bolt load was calculated to check the load applied on the bolts during pressurising the rig is within the safety limits. For the calculations it was assumed that the area under pressure to be just near the outer dimension of bolts. Hence the radius under pressure design was estimated to be 44.3 mm. The design parameters for checking safety of using the bolts are given in Table A1.3.

Table A1.3 Design parameters for calculating bolt load and safety factor

Radius of Bolt	0.00625 m
Working Pressure	50 bar
Minimum height of the bolt	0.025 m
Area under pressure	0.0064468 m2
Total force acting on single bolt	5372.3591 N
Total shear in single bolt	43.78 MPa
Allowable bolt Stress for 0-38ºC (SS-316)	129.6 MPa
SS316 bolt Materials, ASME Boiler and Pressure Vessel Code, 2004 Section II- Division 4	
Safety Factor	2.96

A1.5.3 O-ring Design

A1.5.3.1 Minimum Thickness of Steel between Bore and O-ring

To calculate the internal radius of O-ring it was necessary to calculate the minimum thickness of the shell needed to bear the pressure of 50 bar. It was calculated as per ASME boiler and pressure vessel code UG-27: Thickness of Shells under Internal Pressure, UG-27, ASME Boiler and Pressure Vessel Code, 2004 Section VIII- Division 1, Page No: 23-24.

Thickness of shell, t calculated from circumferential stress (longitudinal joints) is given by

$$t = \frac{P \times R}{(S \times E) - 0.6P} \sim 3 \text{ mm}$$

Where

- Inner radius of shell (membrane holder), R = 0.025 m
- So design pressure for calculation, P = working pressure x safety factor, i.e. 15,000 kPa (with working pressure = 50 bar or 5,000 kPa and safety factor selected = 3)
- Maximum allowable stress for SS Plates, S = 137900 kPa (as per Table-1A, Line No 37 ASME Boiler and Pressure Vessel Code, 2004, Section II- Division 4, page: 66)
- Efficiency of joint, E =1 (The contact was considered to be a full butt joint)

  As per UW-12, maximum allowable joint efficiency for arc and gas welded joints, ASME Boiler and Pressure Vessel Code, 2004 Section VIII- Division 1 page: 102

The minimum thickness of the pressure shell calculated was considered as the minimum thickness of the steel between the bore and the o-ring.

A1.5.3.2 Groove Diameter (G_d)

The internal diameter at which groove for O-ring was to be made from calculated was

G_d = 2 (minimum thickness of the steel between the bore and the o-ring + inner radius of shell, R) = 2 x (3 + 25) = 56 mm

A1.5.3.3 Internal Diameter for O-ring

The O-ring inner diameter $ID_{o\text{-}ring}$ can be found from the recommended stretch S_{rec} (2%) and the groove diameter G_d, as

$ID_{o\text{-}ring} = (1 - S_{rec}) \times G_d = 0.98 \times 56 = 54.88$ mm

Nearest standard available O-ring size available had the dimensions of ID: 56.74 mm, CS 3.53 mm (Code: AS568+ BS 1806). Therefore thickness between O-ring and grove was increased to 4 mm to suits the available o-ring size. Since the working pressure is less than 100 bar, no back up rings were required.

The application of O-ring is "static" since no internal movement occur at O-ring so a standard imperial cross sectional diameter of 3.53 mm was chosen (as per O-ring Size Reference Guide, 2005, Engineering Plastic Limited page: 8) with O-ring groove design dimensions shown in Table A1.4 and the schematics of O-ring groove is shown in Figure A1.2

Table A1.4 Design dimensions for O-ring groove

Cross Section	Groove Depth, D	Groove Width, W	Radius, R
3.53 mm	2.70 mm	4.80 mm	1 mm

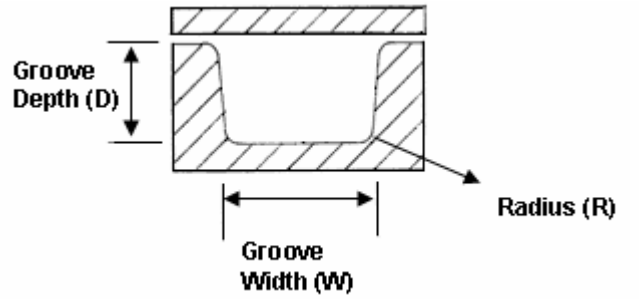

Table A1.2 Schematics of an O-ring groove

The O-ring used in the design had following features:

- Material of Construction: EPDM 90
- Internal Diameter: 56.74 mm
- Cross Section Diameter: 3.53 mm

Figures A1.3-A1.5 shows the plate drawn in Solid Works software according to calculated design dimensions.

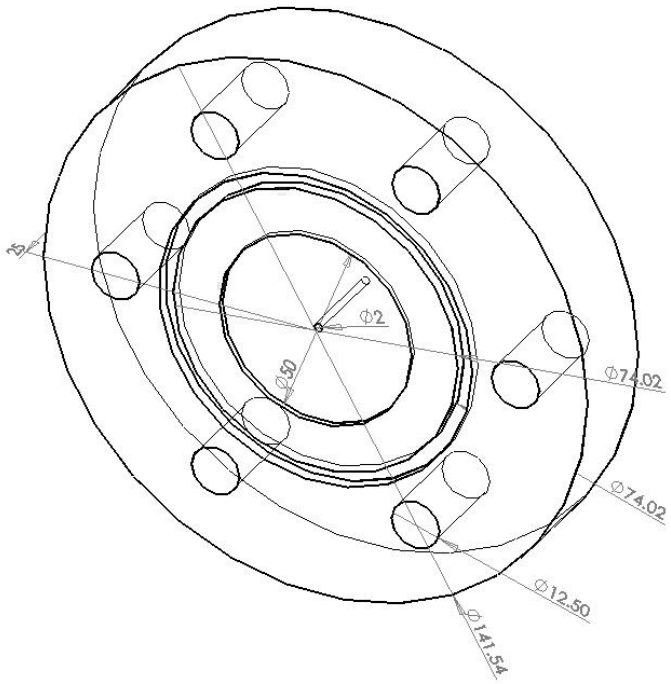

Figure A1.3 Trimetric view of permeate side/bottom plate (The permeate side plate had only one hole in the centre for permeate outlet)

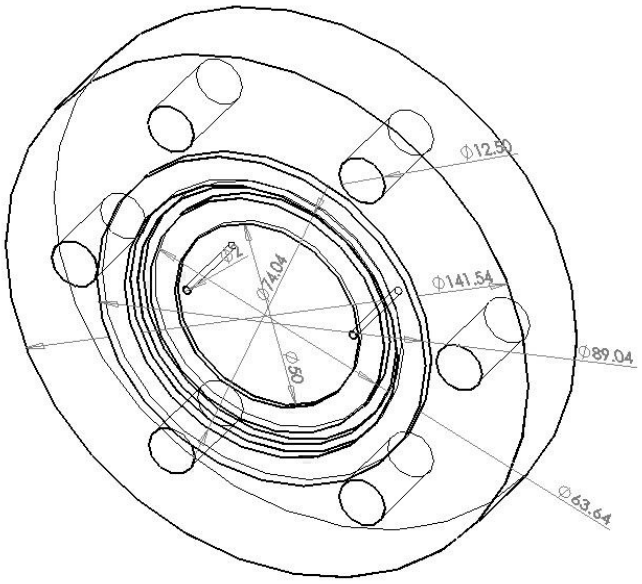

Figure A1.4 Trimetric view of the feed/retentate side plate of the membrane holder (The feed side plate had two equidistant holes, one for feed to enter and other to be used for feed rejection during air bubble removal)

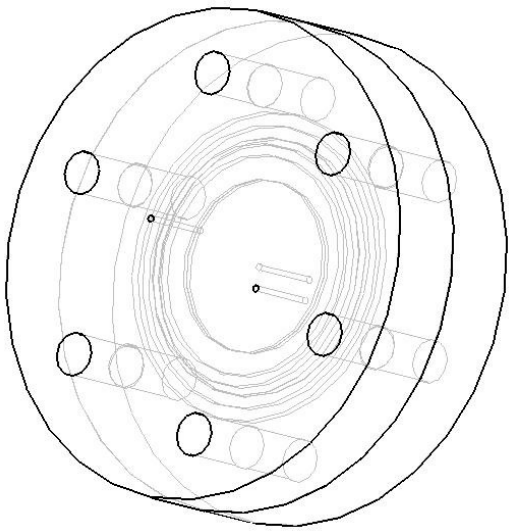

Figure A1.5 Coupling of the two plates to form the membrane holder

A stress analysis was also done on membrane cell to counter check the calculation and the safety factor. Static nodal stress plot for each plate of membrane rig was obtained by COSMOSXpress stress analysis tool present in Solid Works package. Figure A1.6 shows an example of stress analysis window run on permeate plate. The colour blue to red shows the increase in stress over different region of the plate under applied pressure, i.e. 50 bar.

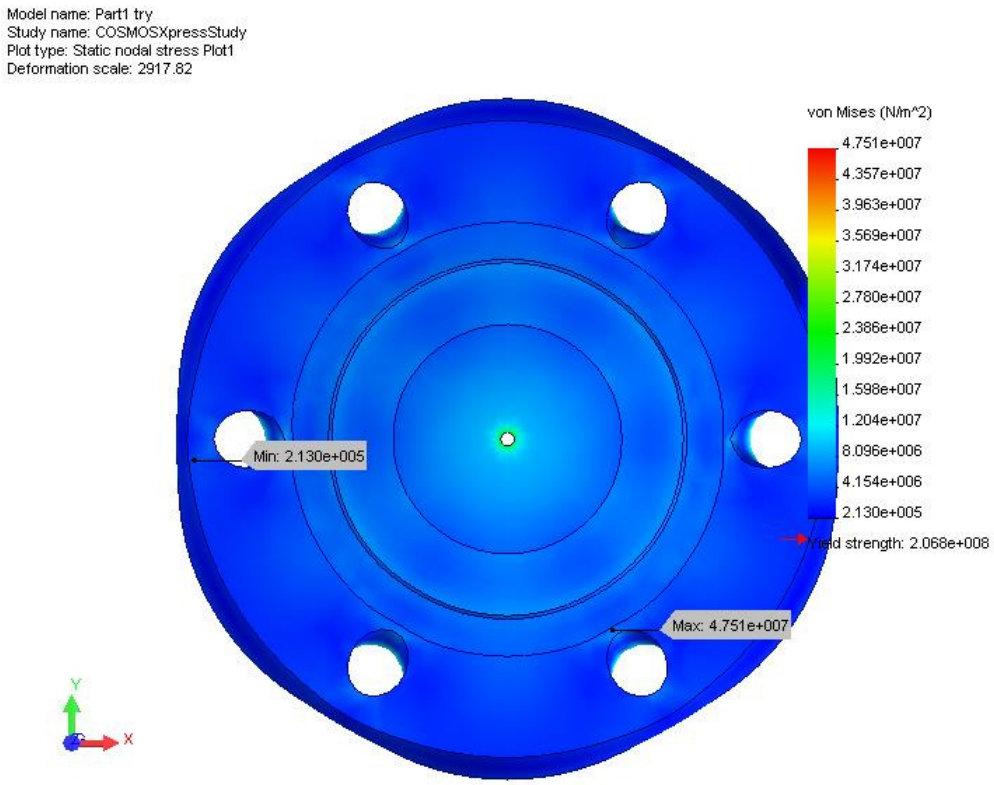

Figure A1.6 Stress analysis window for permeate plate of the membrane holder

Appendix 2 Extended Results

Appendix 2.1 Dynamic Mechanical Analysis

Appendix 2.1.1 DMA, Commercial Ultrafiltration Membrane (10,000 ppm-days Exposure)

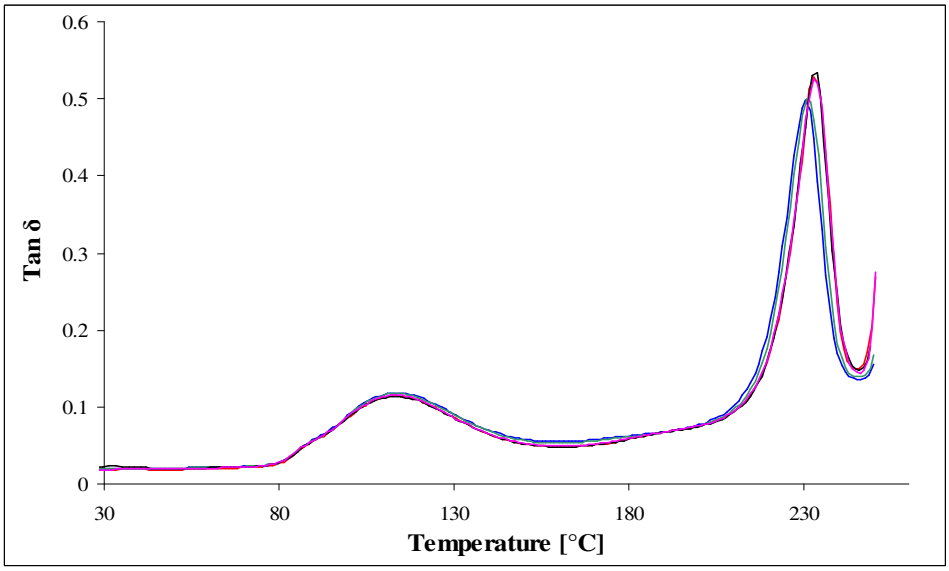

Figure A2.1 Tan δ curve for Koch membrane, pH 9, 10000 ppm-days exposure (5 repeats), at 1 Hz

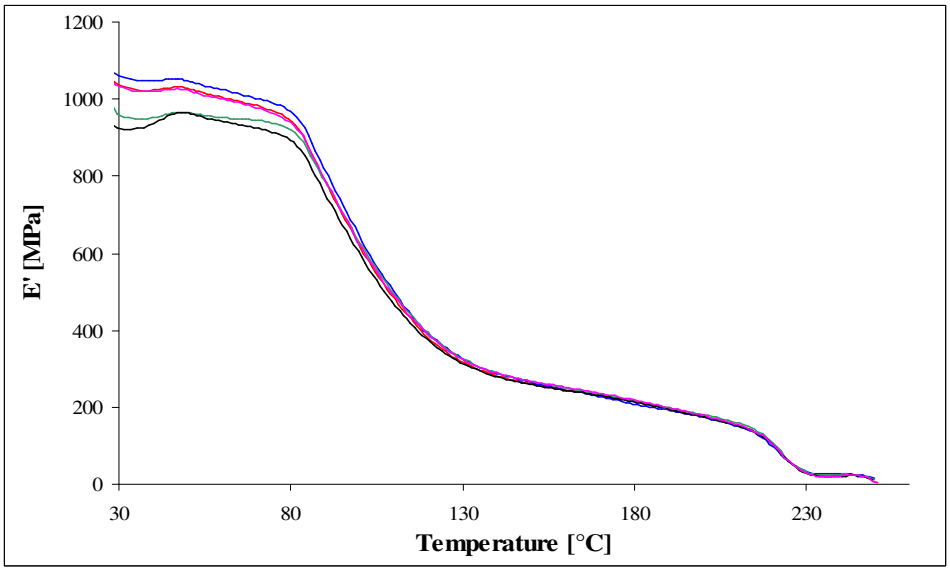

Figure A2.2 E' curve for Koch membrane, pH 9, 10000 ppm-days exposure (5 repeats), at 1 Hz

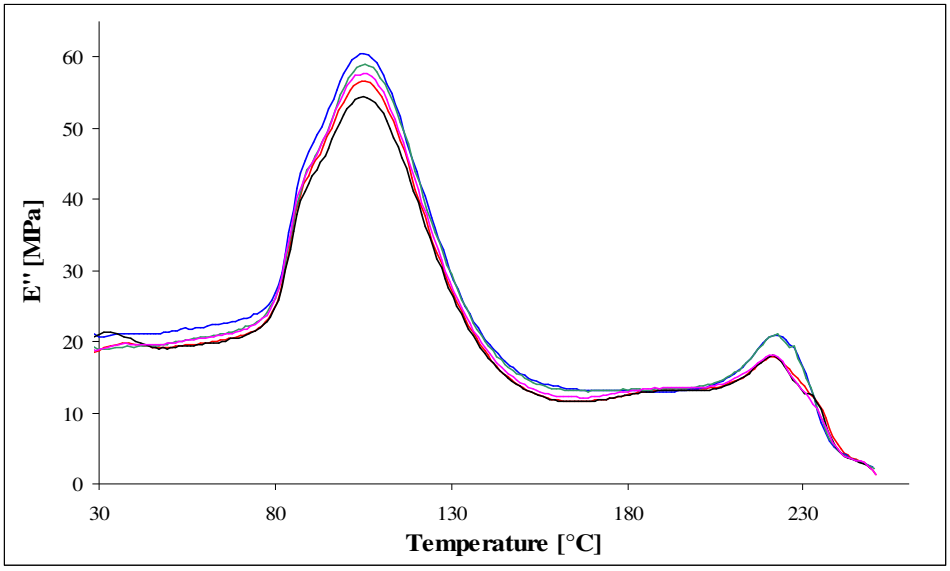

Figure A2.3 E" curve for Koch membrane, pH 9, 10000 ppm-days exposure (5 repeats), at 1 Hz

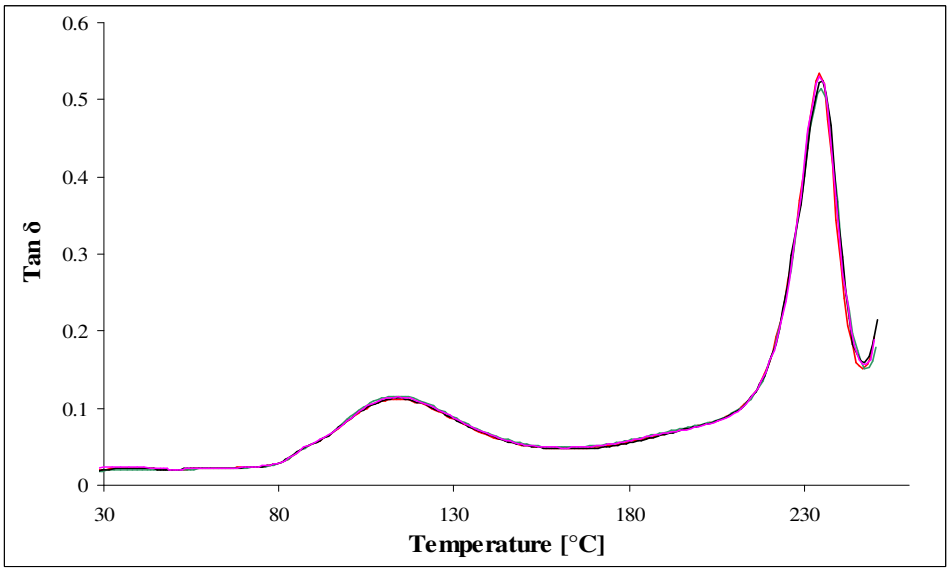

Figure A2.4 Tan δ curve for Koch membrane, pH 12, 10000 ppm-days exposure (5 repeats), at 1 Hz

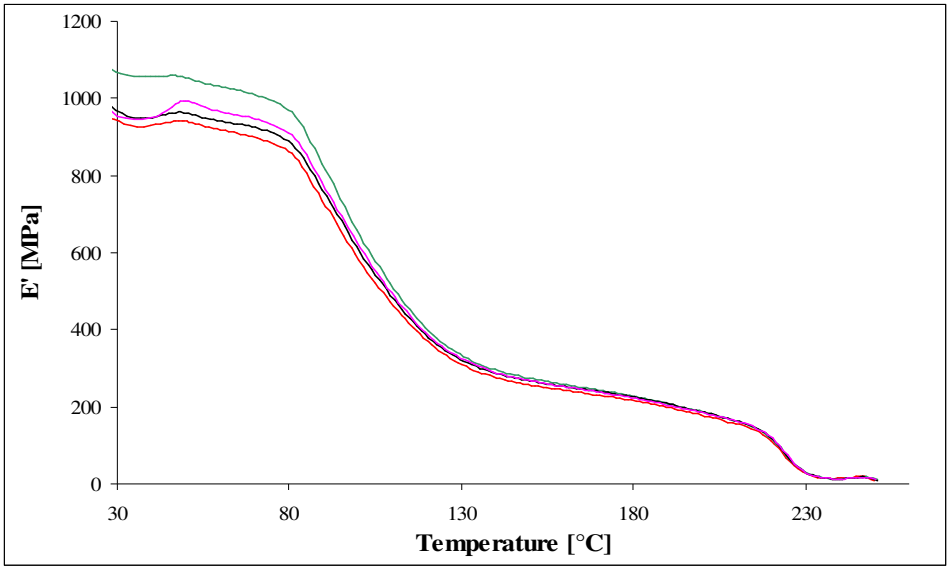

Figure A2.5 E' curve for Koch membrane, pH 12, 10000 ppm-days exposure (5 repeats), at 1 Hz

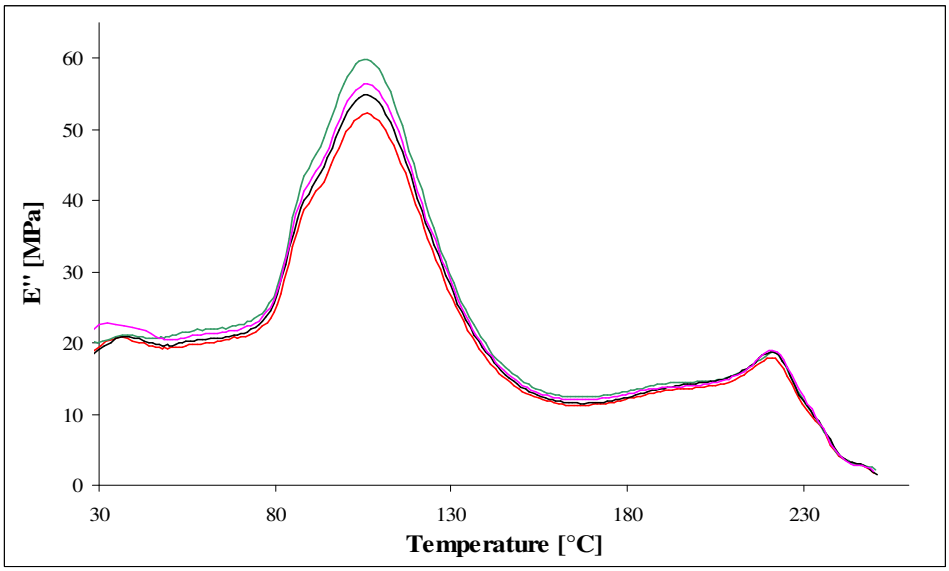

Figure A2.6 E'' curve for Koch membrane, pH 12, 10000 ppm-days exposure (5 repeats), at 1 Hz

Appendix 2.1.2 DMA, Commercial Ultrafiltration Membrane (25,000 ppm-days Exposure)

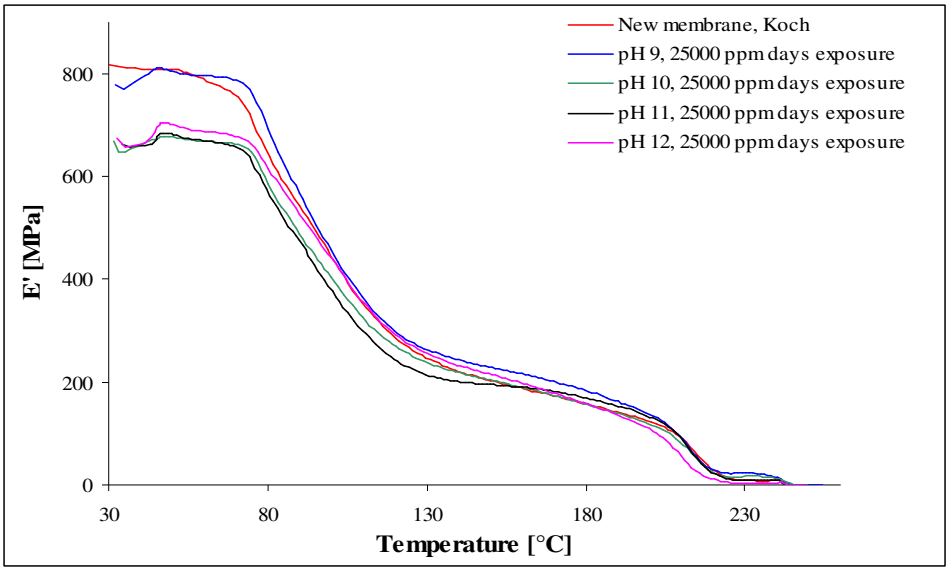

Figure A2.7 E" curve for new and hypochlorite degraded Koch membranes (pH 9-12, 25,000 ppm-days exposure), at 1 Hz

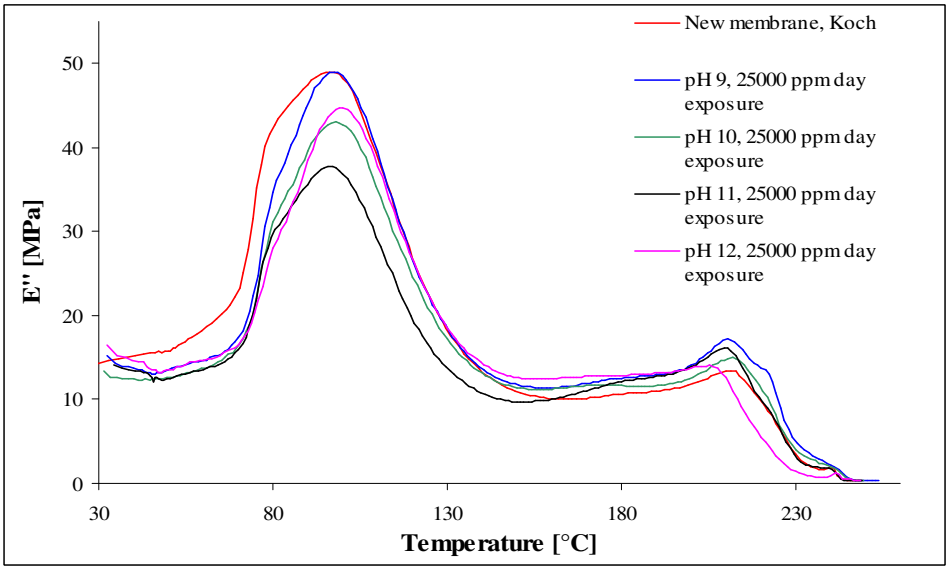

Figure A2.8 E" curve for new and hypochlorite degraded Koch membranes (pH 9-12, 25,000 ppm-days exposure), at 1 Hz

Appendix 2.1.3 DMA, Backing Layer Commercial Ultrafiltration Membrane (10,000 ppm-days Exposure)

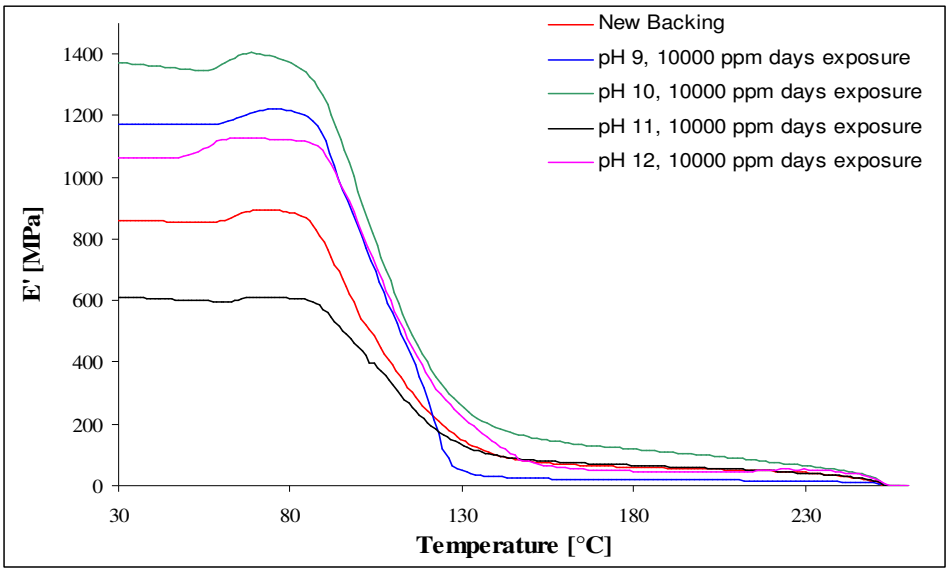

Figure A2.9 E' curve for new and hypochlorite degraded Backing from Koch membranes (pH 9-12, 10,000 ppm-days exposure), at 1 Hz

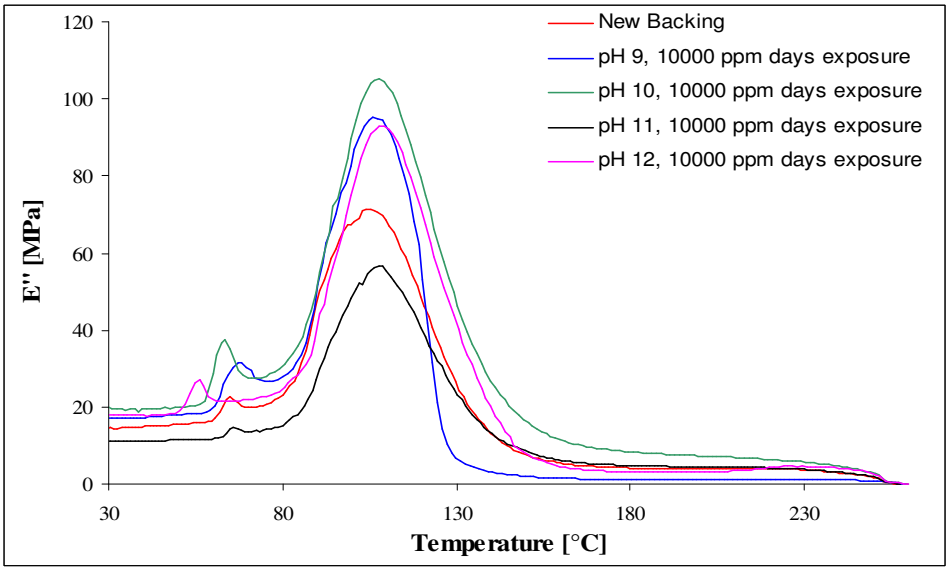

Figure A.2.10 E" curve for new and hypochlorite degraded Backing from Koch membranes (pH 9-12, 10,000 ppm-days exposure), at 1 Hz

Appendix 2.1.4 DMA, Sterlitech Membrane (10,000 ppm-days Exposure)

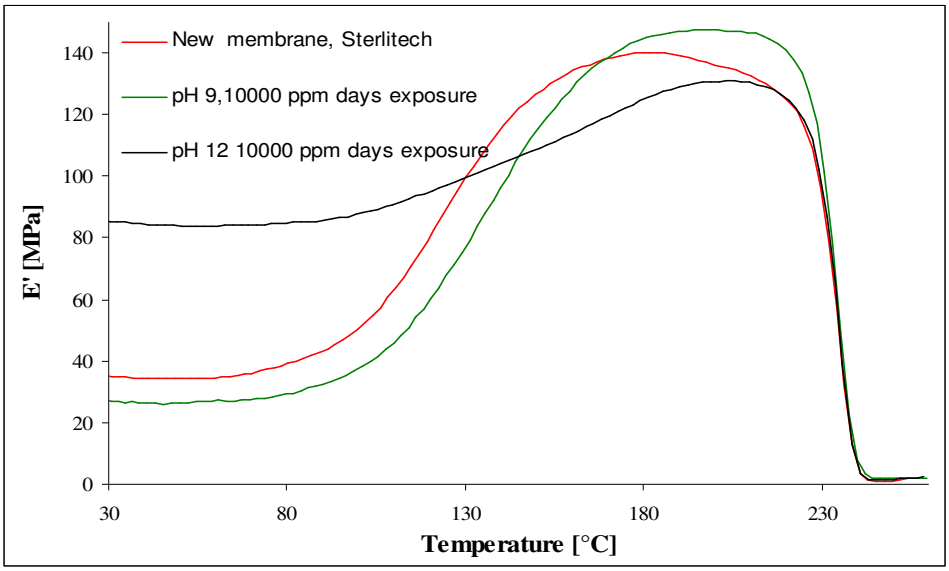

Figure A2.11 E' curve for new and hypochlorite degraded Sterlitech membrane (pH 9-12, 10,000 ppm-days exposure), at 1 Hz

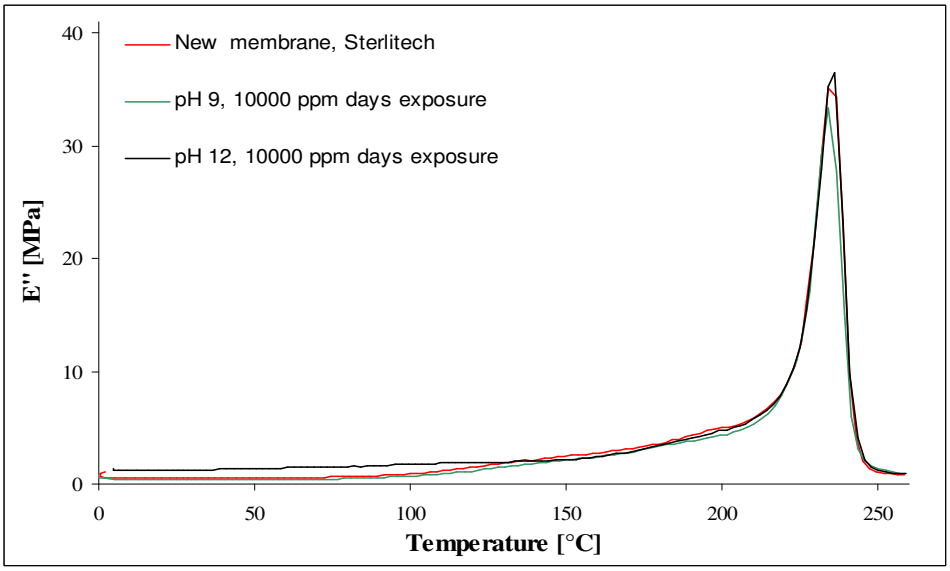

Figure A2.12 E" curve for new and hypochlorite degraded Sterlitech membrane (pH 9-12, 10,000 ppm-days exposure), at 1 Hz

Appendix 2.1.5 DMA, PES Foil, Good Fellow (25,000 ppm-days Exposure)

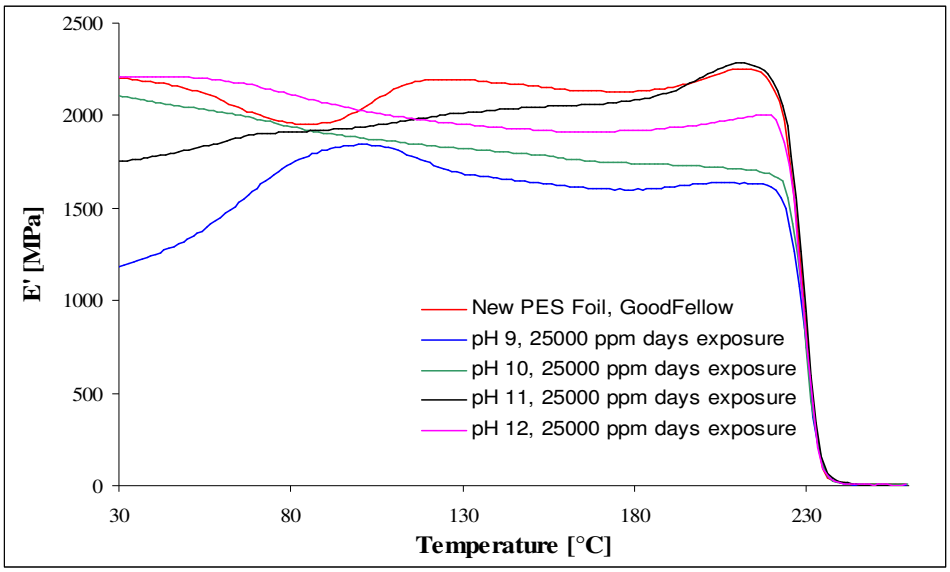

Figure A2.13 E' curve for new and hypochlorite degraded PES foil (Good Fellow) (pH 9-12, 25,000 ppm-days exposure), at 1 Hz

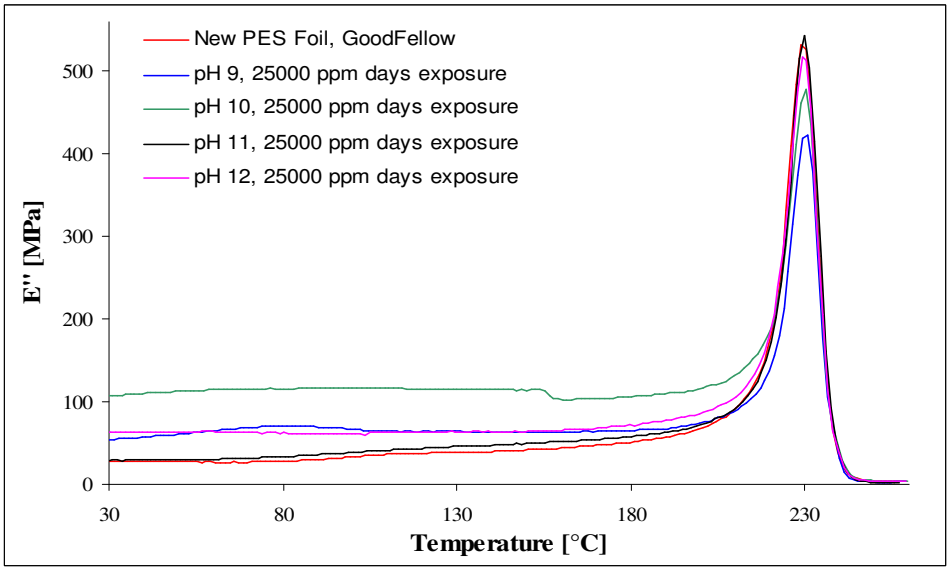

Figure A2.14 E" curve for new and hypochlorite degraded PES foil (Good Fellow) (pH 9-12, 25,000 ppm-days exposure), at 1 Hz

Appendix 2.1.6 DMA, PES Sheet, BASF (25,000 ppm-days Exposure)

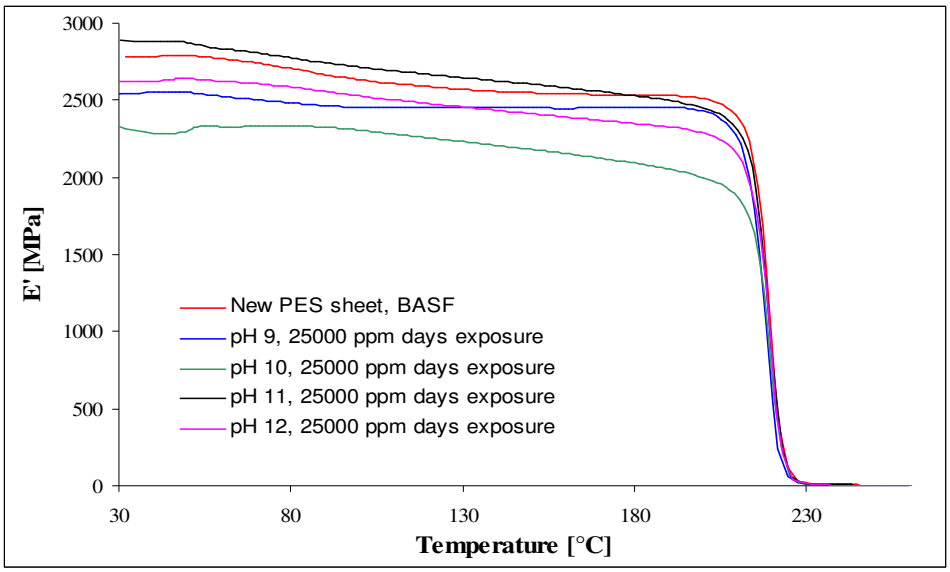

Figure A2.15 E' curve for new and hypochlorite degraded PES sheet (BASF) (pH 9-12, 25,000 ppm-days exposure), at 1 Hz

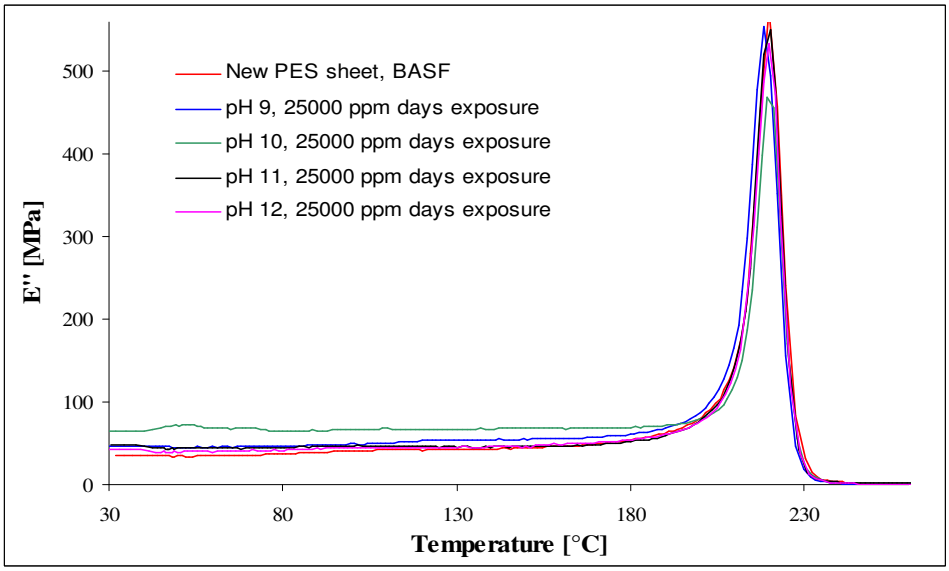

Figure A2.16 E" curve for new and hypochlorite degraded PES sheet (BASF) (pH 9-12, 25,000 ppm-days exposure), at 1 Hz

Appendix 2.2 Detailed Analysis for Tensile Testing

Table A2.2.1 Details of calculated properties from stress strain data obtained from tensile testing

Sample	Tensile Strength MPa	% Decrease in Tensile strength	Yield Strength MPa	% Decrease in Yield Strength	Elastic Modulus MPa	% Decrease in Elastic Modulus
Koch membrane, New	38.95±0.60	0.00	22.44±0.33	0.00	1127.07±19.91	0.00
Koch membrane, pH 9	29.20±0.82	25.04	19.74±0.18	12.03	875.91±7.47	22.28
Koch membrane, pH12	34.51±0.48	11.40	20.16±0.13	10.16	863.62±3.64	23.37
Koch backing, New	38.16±0.55	0.00	24.26±0.35	0.00	1135.46±21.76	0.00
Koch backing, pH 9	28.04±0.40	26.51	20.24±0.28	16.57	864.43±13.03	23.87
Koch backing, pH12	35.27±0.47	7.57	24.24±0.24	0.10	1158.58±20.98	-2.04
Sterlitech membrane, New	4.92±0.05	0.00	3.35±0.08	0.00	108.77±3.19	0.00
Sterlitech membrane, pH 9	3.65±0.11	25.86	2.87±0.14	14.45	89.43±1.78	17.78
Sterlitech membrane, pH 12	4.37±0.10	11.24	3.15±0.06	5.96	113.18±7.38	-4.05

Appendix 2.3 Detailed EDS Analysis

Table A2.3.1 EDS analysis done on commercial ultrafiltration membranes, Koch samples (pH 9 to pH 12, 5000 to 25,000 ppm-days of hypochlorite exposure)

pH	Exposure, ppm-days	% Weight, O	% Error	% Weight Cl	% Error	% Weight S	% Error	O/S	Cl/S
9	5000	50.81	3.12	2.18	5.75	46.26	3.91	1.098	0.063
	10000	50.58	3.2	2.43	5.88	46.24	4	1.094	0.069
	15000	51.25	2.9	2.97	5.35	45.03	3.65	1.138	0.083
	20000	50.51	2.76	3.57	5.03	45.17	3.43	1.118	0.096
	25000	49.72	2.63	4.28	4.75	45.25	3.24	1.099	0.111
10	5000	51.08	3	0.8	5.58	47.38	3.78	1.078	0.033
	10000	51.18	2.9	1.75	5.37	46.32	3.65	1.105	0.054
	15000	49.44	3.03	1.67	5.53	48.14	3.74	1.027	0.050
	20000	48.62	2.98	1.8	5.4	48.83	3.65	0.996	0.052
11	20000	49.88	3.15	0.52	5.8	48.85	3.92	1.021	0.026
12	20000	52.76	3.35	0	0	47.24	4.32	1.117	0.000

The EDS results were obtained only O, S and Cl so the total weight was expressed as % weight of these three elements (i.e. % Cl + % O +% S =100% weight). A peak value of 0.75% weight (average values for 5 repeats) was observed at chlorine peak position for a new membrane. This peak value was declared as background noise. So 0.75% weight was subtracted from chlorine % weight readings obtained for all the samples, to negate the error due to background noise.